A STUDY OF DIFFUSION IN POLYMERS

USING C-14 LABELLED MOLECULES

by

H. K. TOH

Supervisors: Dr. R. E. Wetton; Dr. A. R. Ware

Submitted as partial fulfilment for the

Degree of Doctor of Philosophy

of Loughborough University of Technology

Department of Chemistry

October, 1970

CERTIFICATE OF ORIGINALITY

The experimental work presented in this thesis is the original work performed by the author, and no part of this thesis has previously been submitted for any degree award from any institution.

ACKNOWLEDGEMENTS

The author wishes to thank Dr. R. E. Wetton and Dr. A. R. Ware, for supervising this work and for their help and encouragement throughout; Professor R. F. Phillips for providing the facilities; Mr. G. Oldham for the use of the Radiochemistry Laboratory; the Natural Rubber Producers' Research Association for the award of a research studentship; Mr. D. W. Southwart of the Dunlop Rubber Company for supplying the silicone rubber samples, and members of the University laboratory staff, especially Messrs. I. Lawrence and E. Miller, for their technical assistance.

ABSTRACT

A novel method of measuring the self-diffusion coefficient of a penetrant molecule in various polymers was devised. This method makes use of a permeation experiment, where the radioactively labelled molecules exchange with the chemically identical but non-radioactive molecules through the polymer membrane specimen. The rate of permeation is measured by the excitation of the non-radioactive molecules which act as the solvent in a liquid scintillation mixture, with subsequent excitation and fluorescence of the dissolved scintillator solutes. By maintaining the concentrations of the radioactive and non-radioactive molecules in the vapour phase at the same level, a self-diffusion coefficient D^* at one precise penetrant concentration level can be determined.

The diffusion coefficients measured were compared to those obtained from conventional sorption-desorption methods, and the comparison was discussed in terms of the basic definitions of the different diffusion coefficients.

The diffusional behaviour in silicone rubber and S-B-S block copolymer was discussed mainly with reference to the free volume theory and the activated zone theory, with particular emphasis on chain mobility. Dynamic mechanical studies were also obtained in these polymers and related to the diffusion characteristics through chain mobility and free volume concepts.

Diffusion in filled systems and the two-phase S-B-S copolymers was discussed with the help of mathematical models derived for analogous electrical conductivity through hetereogeneous medium, and a certain order of polystyrene domain distribution was indicated in the latter. Silica-silicone rubber interaction was considered and some conclusions were made.

CONTENTS

LIST OF FIGURES.

CHAPTER I

INTRODUCTION

1.1. General.

The diffusion of molecules, both large and small, in high polymers is a widely studied subject not only because of its commercial importance, but also because of its connection with the structural study of the polymers themselves.

Industrially the high flexibility and physical toughness of polymer films have made them ideal materials for the packaging of foodstuffs and other industrial items, such as cosmetics, detergents, etc. However, one important requirement for such applications is that the package should prevent the loss of volatile constituents from the contents, or prevent the ingress of gases and vapours, particularly water vapour. In the case of liquid mixtures, the partial loss of contents by permeation through the container walls may lead not only to changes in chemical composition of the contents, but also the collapse or deformation of the packages themselves. The storage of foodstuffs in plastic containers may lead to sorption of undesirable flavours and odours through the package. Similarly, the sorption of odours and flavours from the previous contents into the walls of the container may discourage its use for other materials. In the manufacture of inflatable items, such as rubber tyre inner tubes, the permeability to gases of the polymer used is of obvious importance. The resistance of polymers to chemicals and water is also vital in such applications as paints, coatings and electrical insulants. Furthermore, the property of selective transmission of gases has made it possible to employ a polymer as part of biological system where, for instance, simple gases such

as oxygen, are transmitted to the exclusion of larger molecules like water. By careful selection of the polymers, compounding ingredients, and processing conditions, it is possible to meet the practical requirements of physical adaptability and low permeability. However, some of the means used to achieve this end have been costly and therefore uneconomical, and it is the continual aim of industrial research to find a material which satisfies all the requirements.

The use of fillers in polymers has been well known to increase the mechanical durability and elastic properties, and since in most cases it also reduces the permeability of the polymer to gases (1), it would seem a reasonable proposition in some applications such as rubber hoses and plastic containers. The mechanism of filler-polymer interaction is not a clearly understood subject, as the filler particles if not entirely "wetted" by the polymer may provide large surface areas for the absorption of the gas or the vapour involved. The concept of "bound rubber" (2), where the filler particles and the rubber form strong, possibly chemical bonds (3), is especially evident in the case of silica-reinforced silicone rubber (4), and it is hoped that this work will throw more light on the matter.

Apart from the technological importance, diffusion of molecules in polymers can also be used to study the behaviour of the polymer chains themselves; since the thermal motions of polymer chain segments is one of the controlling influences on the rate by which a diffusing molecule can translate through the polymer. This is similar to the molecular theory advanced for the dynamic mechanical relaxation in polymers, where the displaced polymer chains after the removal of the external stress tend to diffuse back to their undisturbed equilibrium position by Brownian motion at a rate which

depends on the displacement and the nature of the polymer (5). When very small diffusant molecules are used, their thermal motions are rapid compared with those of the polymer chains, their rate of permeation will therefore depend entirely on the latter. Molecules comparable in size with the polymer segments involved in thermal motion of the polymer diffuse by more complicated mechanisms which are dependent on both the diffusant and the polymer. By using varying sizes of the diffusant, it is therefore possible to study in some detail the mechanisms involved in polymer segmental motions.

1.2. Major features of diffusion through polymeric systems.

The permeation of gases and vapours through polymeric systems can occur by two entirely different processes. In the case of porous media, such as paper, fabrics and glass-like substances, the main form of transfer is by capillary flow or convective flow. If no porosity is present, as in homogeneous amorphous polymeric materials, the transmission mechanism is of the activated diffusion type, i.e. a process in which the gas or vapour dissolves into the polymer at the inflow surface and diffuses through the polymer under a concentration gradient, and evaporates from the surface at the lower concentration. Whereas capillary flow shows a slightly negative temperature dependence, (due mainly to changes in gas viscosity), activated diffusion is characterised by a large positive temperature dependence. Also, in capillary flow, the transmission rate is not dependent upon the nature of the diffusant molecule, but in the case of activated diffusion, both the solubility and diffusivity are highly dependent on the nature of the diffusant molecule. In most investigations of diffusion of gases and vapours in polymers, the polymers are assumed to be structurally homogeneous and diffusion occurs by an activated mechanism; however, evidence has been advanced for the presence of microporous structures in certain amorphous polymers below or near their glass transition temperatures, in semi-crystalline polymers above the glass temperature, and in filled polymers. In these cases it is necessary to assume a combination of these mechanisms.

In the absence of porosity, the diffusion of a molecule through the polymer can be regarded as the movement of the molecule through the free volumes formed between adjacent polymer molecules by thermal motion. In elastomers the kinetic motion of the segments is comparable to that of molecules in a normal liquid, in short-range

respects, and the energy required to form such "holes" is low. Thus diffusion is a fast process. In other polymers with high glass transition temperature, such as polystyrene, much higher energy is required for the formation of free volumes large enough to accommodate the diffusing molecule, and diffusion is a relatively much slower process. This is because on approaching the glass temperature the movements of the polymer segments become more and more restricted, and more energy is required to displace the polymer chains. It is generally true that raising the glass transition temperature of a polymer will lead to a slower diffusion process.

1.3. The Diffusion of small molecules as a means of evaluating chain mobility.

In the molecular theories of polymer viscoelasticity (Chapter 2.8), it is assumed that polymer chains, if free to do so, undergo translational diffusion through their surroundings. This movement occurs as a result of random translations of sub-chain units (segments). Co-operation of several neighbouring segments is necessary for the re-arrangement process to occur. A term, monomeric friction coefficient, may be defined as the force on a chain monomer unit due to viscous resistance when travelling at 1 cm/sec. through its surroundings at rest. Thus $n\zeta_o$ is the friction coefficient governing the motion of the segment of n monomer units. ζ_o is usually calculated from the viscoelastic relaxation spectrum, H, or the retardation spectrum, L. (6).

There have been attempts to measure ζ_o from self-diffusion experiments of the polymer by using radioactively labelled polymers (7) and spin-echo nuclear magnetic resonance methods (8). But in these cases the friction coefficient of the entire molecule is measured.

The use of small molecules (each comparable in size to a re-arranging segment) in trace amounts as penetrant in a diffusion experiment may be interpreted more meaningfully. These molecules diffusing down a concentration gradient may be regarded as pushing their way individually past the polymer segments. The frictional resistance they encounter will be closely related to that experienced by the polymer segments themselves, in their random thermal motions, (i.e. ζ_o). Under these conditions the friction coefficient of the penetrant, ζ_1, may be expressed by the relationship (See Chapter 2.8):-

$$\zeta_1 = kT/D_o \qquad 1.1$$

where D_o is the diffusion coefficient of the penetrant extrapolated to zero concentration, and k is the Boltzmann constant.

The variation of ζ_1 with the size of the penetrant has been investigated by several workers (9-12). It was found that for large molecules there was marked dependence, and for smaller molecules (C4, C5 hydrocarbous) the dependence was less (12).

By comparing the friction coefficient of a penetrant of suitable size in the polymer medium with the monomeric friction coefficient (13), the latter may be evaluated from a diffusion experiment, which is usually quicker and easier to perform than a viscoelastic experiment.

Following the same logical argument the activation energy of viscoelastic relaxation, ΔH_a, should also correspond to the activation energy of diffusion, ΔH_D, of a foreign molecule at temperatures above the glass transition point, Tg, since the activated processes involved in both cases can be similarly interpreted (See Chapter 2.4 and 2.8).

1.4. Present Study.

Silicone rubber and styrene-butadiene-styrene three-block copolymer are the polymers chosen for study in this work.

The very mobile silicone rubber chain segments make this polymer highly permeable to gases and vapours (14). The study of the concentration dependence of the diffusion coefficient of a penetrant, of a size comparable to that of a polymer segment, would be interesting because of the possibility that the polymer chains may be even more mobile than the penetrant. High mobility of chain segments also means low activation energy for chain rearrangement, and diffusion and viscoelastic processes in this polymer should not be too temperature dependent. Also silicone rubber has been known to have special interaction with silica fillers, with the formation of "bound rubber" as mentioned previously. The proportion of this "bound" rubber is known to increase on storage (4). It is hoped that the present study will explain some of the intriguing behaviour of this polymer.

Three block copolymers, such as the most commonly known styrene-butadiene-styrene copolymer, are a recent addition to the list of commercially available polymers. These polymers possess rubbery properties at normal ambient temperature, but at elevated temperatures become thermoplastic. Therefore, they require no vulcanization, and processing operations can be carried out automatically at highly economic speeds.

The requirements of a A-B-A type three block copolymer are that A is a thermoplastic block [illegible] (with a high Tg value), and B is an elastomeric block [illegible]. A two-phase system is formed, with the middle-block phase constituting a continuous three-dimensional elastomeric network and the dispersed end block phase serving as multi-junction points for the ends of the middle blocks. This is diagramatically illustrated in Fig.1. A good balance between

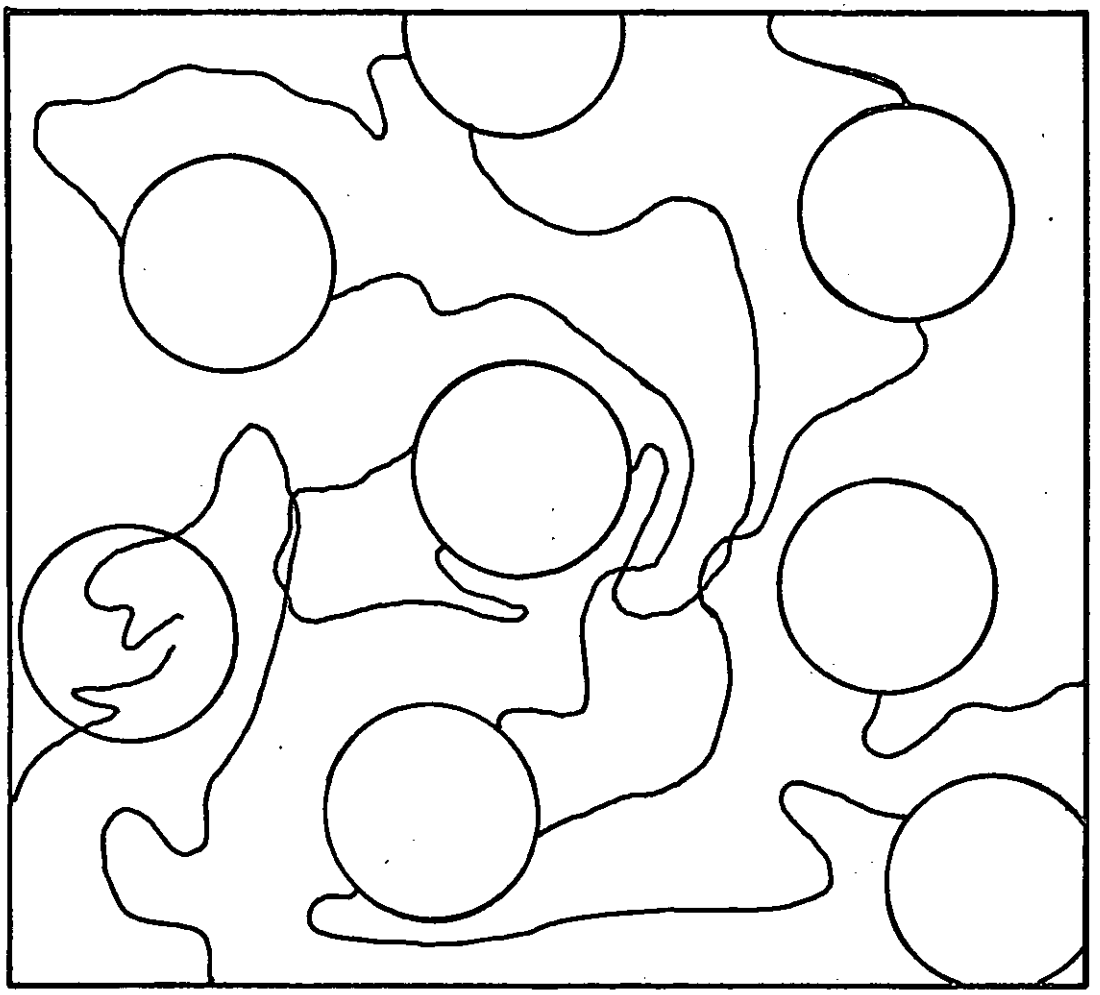

FIG. 1 S-B-S BLOCK COPOLYMER MORPHOLOGY

processing performance and elastomeric character can be obtained at a range of selected molecular weights for A and B. It is desirable to have a discreet thermoplastic phase and a continuous elastic phase. Considering a styrene-butadiene-styrene (S-B-S) copolymer, the styrene domains as illustrated in Fig.1. serve both as multiple cross-links and as filler particles. The diffusion of gases and vapours in this polymer has not been well studied up to date by other workers. It is worth noting that the morphology of the styrene domains actually vary with the way by which the polymer film is prepared (15). Casting the film from "good" and "bad" solvents has a considerable influence on the structure of these polymers, and this should be reflected in the diffusion studies.

The design of the experiment in this work enables a self-diffusion coefficient of the penetrant in the polymer to be measured. This is clearer in interpretation than, for instance, a normal permeation experiment where the mutual diffusion coefficient is measured. A mutual diffusion coefficient involves mass flow as well as true diffusion (see 2.1), and although it is of great practical significance (because it enables the actual amount transferred to be calculated), it does not describe fully the movement of the penetrant in the polymer. A self-diffusion coefficient of the penetrant in the polymer indicates exactly the frictional resistance it experiences in the circumstances.

CHAPTER 2

THEORETICAL

2.1. Definition of diffusion coefficients.

Diffusion is defined as the process by which molecules are transported from one part of the system to another as a result of random motions. Fick (16) analysed the diffusion of isotropic substances by comparing it with the mathematical treatment of heat conduction earlier derived by Fourier (17). According to this theory, the rate of transfer of the diffusing substance across unit area of a section is proportional to the concentration gradient measured normal to the section, i.e.

$$F = -D \frac{d c}{d x} \qquad 2.1.$$

where F is the rate of transfer per unit area of section per second,

c is the concentration of the diffusing substance

x is the space coordinate measured normal to the section,

and D is called the diffusion coefficient.

The differential form of Eqn. 2.1 can easily be derived as (18):-

$$\frac{dc}{dt} = D \frac{d^2c}{dx^2} \qquad 2.2$$

Equations 2.1 and 2.2 are popularly known as Fick's first and second laws of diffusion.

In cases where the diffusion coefficient is itself a function of concentration, as in many cases of organic vapours in polymers,

$$\frac{dc}{dt} = \frac{d}{dx} \left(D \frac{dc}{dx}\right) \qquad 2.3$$

For a two component system, i.e. a mixture of substances A and B, the diffusion coefficient relating to the movement of A and B must be defined with a certain frame of reference. A few important

definitions of different diffusion coefficients are listed below:-

Volume-fixed reference.

The section across which the rates of transfer of A and B are measured is so chosen that the total volume on either side of it remains constant.

The volume transfer of A and B per unit time across unit area of the section are, respectively:

$$- D_A^v \quad V_A \frac{d C_A}{d x} \qquad 2.4$$

and $$- D_B^v \quad V_B \frac{d C_B}{d x} \qquad 2.5$$

where V_A is the partial specific volume of A

V_B is the partial specific volume of B

By definition of the frame of reference

$$D_A^v V_A \frac{d C_A}{d x} + D_B^v V_B \frac{d C_B}{d x} = 0 \qquad 2.6$$

Since only A and B are present

$$V_A C_A + V_B C_B = 1 \qquad 2.7$$

or differentiating

$$V_A \frac{dC_A}{d x} + V_B \frac{dC_B}{d x} = 0 \qquad 2.8$$

In order that both Eqn. 2.6 and Eqn. 2.7 be satisfied, it must follow that

$$D_A^v \equiv D_B^v \qquad 2.9$$

Thus the behaviour of two components on mixing with no volume change may be defined by a single diffusion coefficient, referred to conveniently as the mutual diffusion coefficient and denoted by D_{AB}^v.

Mass-fixed reference.

By defining the section across which transfer of A and B are measured as one where there is no change in mass on either side of it, we can define a mass-fixed mutual diffusion coefficient D_{AB}^m in a similar manner.

One component-fixed reference.

If a section fixed with respect to one component, say the polymer component, B, is used, then clearly $D_B^b = 0$. Only one diffusion coefficient D_A^b is then needed to describe the behaviour.

Relations between D_A^v, D_A^m, and D_A^b.

The three diffusion coefficients as defined above are related to each other as follows (19):-

$$D_A^b = D_A^m (V_B^o C_B^m)^2 \qquad 2.10$$

where V_B^o is an arbitrary specific volume of B, depending on the reference used for its definition.

$$D_A^b = D_A^v (V_B C_B^v)^2 \qquad 2.11$$

i.e. $$D_A^b = D_A^v (\text{volume fraction of B})^2 \qquad 2.12$$

and $$D_A^m = D_A^v (C_B^v/C_B^m)^2$$

$$= D_A^v (\text{basic total volume/true total volume})^2 \qquad 2.13$$

Intrinsic diffusion coefficients.

When the components A and B as discussed above in the volume-fixed frame of reference are of different mass and size, the rates of transfer of A by random motions may then become greater or less than that of B. To compensate for this, so that the volumes on either side of the section are equal, a whole solution of A and B will flow together in the appropriate direction (20). This effect has been observed in polymer-solvent systems by Robinson (21). Since the polymer molecules diffuse much more slowly in this case than the solvent molecules, the movement of the polymer measured from the mutual diffusion coefficient is mostly mass-flow. Thus the overall rate of transfer of either component across a volume-fixed section is a combination of mass-flow and true diffusion resulting from random molecular motions. The mutual diffusion coefficient D_{AB}^v is

therefore unnecessarily complicated by the presence of this mass-flow, hence arises the necessity of defining a new coefficient known as the intrinsic diffusion coefficient. The reference section is defined as one so fixed that no mass flow occurs through it, and it must move with the mass-flow to maintain this condition.

When the partial volumes of A and B are constant, the intrinsic diffusion coefficients $\underline{D_A}$ and $\underline{D_B}$ can be related to the mutual diffusion coefficient D^b_{AB} in a polymer-solvent system by the following expression (22):-

$$\underline{D_A} = D^v_{AB}/(1-V_A C_A)$$
$$= D^v_{AB}/(V_B C_B)$$
$$= D^v_{AB}/(\text{volume fraction of B}) \qquad 2.14$$

$$\underline{D_B} = 0 \qquad 2.15$$

(if B is sluggish compared to A)

$$\text{and } \underline{D_A} = D^b_A/(\text{Volume fraction of B})^3 \qquad 2.16$$

It is evident from Eqn.2.14 that at low penetrant concentration the mutual diffusion coefficient approaches the same value as the intrinsic diffusion coefficient of the penetrant.

Self-diffusion coefficient.

By using radioactively labelled molecules it is possible to observe the rate of diffusion of one component in a two component system of uniform chemical composition. This involves the interchange of labelled and unlabelled molecules which are otherwise identical and so no mass flow occurs. However, these "self-diffusion coefficients", although involving no mass flow, are different from the intrinsic diffusion coefficients if the thermodynamic activity of component A is not equal to its concentration. Johnson (23) has demonstrated this point experimentally for metal systems.

A relationship between the intrinsic diffusion coefficient $\underline{D_A}$, and the self-diffusion coefficient - denoted by D_A^* exists as follows (24):-

$$\underline{D_A} = D_A^* \frac{d \ln a_A}{d \ln C_A} \qquad 2.17$$

where a_A is the thermodynamic activity of component A

and C_A is the concentration of component A.

D_A^* is also related to the thermodynamic mobility, m_d, by the expression

$$D_A^* = RT\, m_d \qquad 2.18$$

$$\text{Therefore } \underline{D_A} = RTm_d \frac{d \ln a_A}{d \ln C_A} \qquad 2.19$$

2.2. Steady state permeation through a plane sheet.

A thin membrane approximates to an infinite plane sheet across which diffusion occurs in a linear direction X. After a certain time a steady state is reached when the concentration remains constant at all points in the membrane. Fick's "second law" (Eqn.2.2) then reduces to: (if D is constant)

$$\frac{d^2C}{dx^2} = 0 \qquad 2.20$$

The frame of reference is:-

$$x = o,\ t = t,\ c = c_1$$

$$x = l \quad t = t,\ c = c_2 \qquad 2.21$$

where l is the thickness of the membrane,

C_1 and C_2 are the concentrations of the penetrant at the two faces respectively,

t is the time.

On integrating Eqn. 2.20 with respect to x, we have

$$\frac{dc}{dx} = \text{constant} \qquad 2.22$$

On further integration, and applying the reference frame 2.21,

$$\frac{C - C_1}{C_2 - C_1} = \frac{x}{l} \qquad 2.23$$

Since (Eqn. 2.1) $F = -D\frac{dc}{dx}$

$$\therefore\ F = D(C_1 - C_2)/l \qquad 2.24$$

Thus, if the thickness l, and the surface concentrations C_1, C_2 are known, D can be clearly deduced from a single observation of the flow rate, F.

In deriving Eqn. 2.24 an assumption has been made that D does not vary with concentration. Thus the concentration varies linearly with distance from C_1 to C_2 through the sheet. In the case of concentration dependent diffusion coefficients, as is indeed the case

in most polymer-organic vapour systems (Chapter 2.4), the simple value of D deduced from a measurement of the steady state of flow is some kind of mean value over the range of concentrations involved. If D is a function of C, Eqn. 2.20 must be replaced by

$$\frac{d}{dx}\left(D\frac{dc}{dx}\right) = 0 \qquad 2.25$$

Hence

$$F = -D\frac{dc}{dx} = \text{constant} \qquad 2.26$$

still holds, as is expected in the steady state.

Integrating Eqn. 2.26 between C_1 and C_2

$$F = \frac{1}{l}\int_{C_1}^{C_2} D\,dC = \bar{D}\,(C_1 - C_2)/l$$

$$\text{where } \bar{D} = \frac{1}{C_1 - C_2}\int_{C_2}^{C_1} D\,dC \qquad 2.28$$

and this is the mean value deduced from a measurement of F. It follows from 2.26 that if D varies with concentration, the concentration will not vary linearly with distance in the membrane.

The concentration dependence of D can be obtained experimentally by measuring F for a series of C_1 values with C_2 fixed at a low value which may be zero. Differentiating the curve relating F and C_1 will show this dependence. If $C_2 = 0$, a relationship (25)

$$D_{C=C_1} = \bar{D} + C_1\frac{d\bar{D}}{dC_1} \qquad 2.29$$

can be conveniently used.

Barrer (26) obtained a series of typical steady-state concentration distribution curves across a membrane by deriving a solution for Eqn. 2.25, applying the right boundary conditions, and evaluating the flow rate F (C) at different concentrations. Knowing the concentration distribution through the membrane, the concentration dependence of D can be deduced from a single experiment using Eqn. 2.26, since $\frac{dC}{dx}$ at different concentrations can be measured from the slopes of the concentration distribution curves.

The Concept of 'Permeability Constant' or 'Permeability Coefficient'.

In some systems the actual concentrations C_1 and C_2 are not known, but only the vapour or gas pressures p_1 and p_2 on two sides of the membrane. It is then possible to define a term, P, referred to as the permeability constant, as the amount of gas or vapour at some standard temperature and pressure, passing per unit time through unit area of a membrane of unit thickness, when the pressure difference across the membrane is of a unit measure (say 1 cm Hg). The rate of transfer then can be expressed as:

$$F = \frac{P(p_1 - p_2)}{1} \qquad 2.30$$

If the external vapour pressure is linearly proportional to the equilibrium concentration within the membrane, i.e. if Henry's law is obeyed, then

$$C = Sp \qquad 2.31$$

where C is the concentration within the material of the membrane in equilibrium with an external pressure p, and S is the solubility.

Substituting Eqn. 2.31 into Eqn. 2.24,

$$F = \frac{DS\ (p_1 - p_2)}{1} \qquad 2.32$$

Combining Eqn. 2.30 and Eqn. 2.32

$$P = DS \qquad 2.33$$

Thus for a system where the diffusion coefficient does not vary with concentration, and Henry's linear sorption isotherm is obeyed, the diffusion coefficient may be determined by measuring the permeability constant and the solubility. This is known as the steady state permeation method of obtaining diffusion coefficient.

Diffusion coefficients may also be obtained from the "time-lag" method and the "early time" method. (27-30). These methods also involve permeation through a polymer membrane and are therefore included here.

The time-lag method:-

From the moment the diffusant is admitted to one side of the sheet and prior to the establishment of a steady state, both the rate of flow and concentration at any point of the sheet vary with time. If the diffusion coefficient is constant, the amount of diffusant which emerges from the low concentration side of the membrane, (actually $C_2 = 0$), per unit time, Q_t is given by the expression (31):-

$$\frac{Q_t}{lC_1} = \frac{Dt}{l^2} - \frac{1}{6} - \frac{2}{\pi^2} \sum_{1}^{\infty} \frac{(-1)^n}{n^2} \exp. \left(\frac{-Dn^2\pi^2 t}{l^2}\right) \qquad 2.34$$

As $t \longrightarrow \infty$, the steady state is approached, and the exponential terms become negligibly small, so that the graph of Q_t against t tends to the asymptote

$$Q_t = \frac{DC_1}{l}\left(t - \frac{l^2}{6D}\right) \qquad 2.35$$

which has an intercept, L, on the time (t) axis given by

$$L = \frac{l^2}{6D} \qquad 2.36$$

Thus the diffusion coefficient can be easily calculated from the time lag L, l being the thickness of the membrane.

By measuring the time-lag and the steady-state rate of permeation, or permeation constant, in one experiment, it is possible to obtain all the three parameters P, D and S by using equations 2.33 and 2.36 (32, 33). This is subjected to the conditions stated earlier of constant D (with respect to time and concentration) and Henry's linear sorption isotherm.

The early-time method (27-30).

An alternative expression for the solution of Eqn. 2.34 is (27)

$$\frac{dp}{dt} = \left(\frac{2AS_R}{v}\right)\left(\frac{D}{\pi}\right)^{1/2} \sum_{m=0}^{\infty} \exp\left[-\left(\frac{l^2}{4Dt}\right)(2m+1)^2\right] \qquad 2.37.$$

where S is the solubility,

$\frac{dp}{dt}$ is the rate of increase of pressure in an initially evacuated vessel of volume V due to vapour leaving one face of a plane sheet of area A and thickness l. The other face is in contact with a vapour at pressure p_1.

When t is small, Eqn. 2.37 approximates to:-

$$\ln (t^{1/2} \frac{dp}{dt}) = \ln \left[\left(\frac{2AS p_1}{V} \right) \left(\frac{D}{\pi} \right)^{1/2} \right] - \frac{l^2}{4Dt} \qquad 2.38$$

Therefore a graph of $\ln (t^{1/2} \frac{dp}{dt})$ against $\frac{1}{t}$ should be a straight line of slope $(-l^2/4D)$ from which the value of D is obtained. Again this method applies strictly to a constant D.

The attraction of this method lies in the fact that since the extrapolution is towards t = o, a value of $D_c \rightarrow o$ is obtained. Thus the diffusion coefficient at zero concentration can be obtained from one experiment instead of the lengthy extrapolation to zero concentration, otherwise needed.

Meares (30) obtained all the parameters involved in the relationship $D = D_o e^{\beta C}$ 2.39

by first determining D_o using the early time method and then using Frisch's equation for time-lag (34, 35) to obtain the term βC, from which β may be determined. The early-time method, though not very widely practised, is seen as a very flexible and fast method of extracting substantial information on diffusion of small molecules at very low concentrations in a polymer system unperturbed.

An interesting comparison of three diffusion coefficients obtained from steady-state permeation, time-lag, and early time for the same penetrant-polymer system was made by Barrer and Chio (36). The three procedures for measuring D refer to different time intervals. The steady-state measurements give the coefficient appropriate for time = ∞, the time-lag method gives a mean value over a time interval comparing with the time-lag, L. The early time

procedure gives an average value over a still shorter period. If the diffusion coefficient is time dependent, the three coefficients would, therefore, be expected to differ. Barrer and Chio, however, did not find any significant difference between these diffusion coefficients for n-butane in silicone rubber.

2.3. Sorption and desorption in a plane sheet.

The steady-state permeation method as described previously can be very time-consuming, as the diffusion coefficients of some vapours in polymers can be as low as 10^{-10} cm^2 $sec.^{-1}$ This perhaps was the reason for the search of transient methods which would give rapid results. The kinetic study of the sorption and desorption of gases and vapours can be made both simple and rapid.

The polymer membrane is maintained initially at a uniform concentration C_o (C_o may be zero). At the start of the experiment, both sides of the membrane are simultaneously exposed to a vapour of fixed pressure, at a constant temperature. Assuming that the surfaces of the polymer exposed to the vapour immediately attain a concentration value equal to the equilibrium concentration value, the mass uptake of the vapour by the polymer can be expressed as (37):-

$$\frac{Mt}{M_\infty} = 1 - \frac{8}{\pi^2} \sum_{m=0}^{\infty} \frac{1}{(2m+1)^2} \exp.\left[-D(2m+1)^2 \pi^2 t/l^2\right] \qquad 2.40$$

where M_t is the total amount of the vapour sorbed by the sheet at time t, and M_∞ is the equilibrium sorption attained theoretically after infinite time.

The same equation holds also for desorption if M_∞ is the amount desorbed at infinite time, and M_t is the amount lost up to time t.

Eqn. 2.40 for short times approximates to

$$\frac{Mt}{M_\infty} = \frac{4}{l}\left(\frac{Dt}{\pi}\right)^{1/2} \qquad 2.41$$

Therefore, a plot of $\frac{Mt}{M}$ against $t^{1/2}$ is initially linear and has a slope of $\frac{4}{l}\left(\frac{D}{\pi}\right)^{1/2}$ from which D may be calculated.

If the "half-time" i.e. the time, $t_{0.5}$, at which $M_t/M_\infty = 0.5$ is measured, then

$$D = \pi l^2/(64\ t_{0.5}) \qquad 2.42$$

The equations 2.40, 2.41, 2.42 apply to systems where the diffusion coefficient, D, remains constant with respect to concentration and time. In cases where D is a function of concentration, the value of D obtained from these equations is a mean value over the concentration range involved.

Prager et al (42) have shown that the "integral diffusion coefficient", $\bar{D}$, over the range 0 to C, is given to a good approximation by the average of the values of D obtained from absorption to, and desorption from, the same equilibrium amount sorbed, M_∞. Thus,

$$\bar{D} = \frac{1}{2} (\overline{Da} + \overline{Dd}) \qquad 2.43$$

where $\overline{Da}$ is the mean absorption value

$\overline{Dd}$ is the mean desorption value

A series of sorption and desorption experiments for different values of M enables $\bar{D}$ to be determined as a function of C_1. $\bar{D}$ is related to $D_{C = C_1}$ by a relationship (see Eqn. 2.29).

$$D_{C = C_1} = \bar{D} + C_1 \frac{d\bar{D}}{dC_1} \qquad 2.44$$

Hence $D_{C = C_1}$ can be evaluated.

Crank and Park (39) have derived a method to determine the quantitative dependence of diffusion coefficient upon concentration from sorption data by the use of successive approximations. They assumed the relationship:

$$\bar{D} \simeq \frac{1}{C_1} \int_0^{C_1} D\,dC \qquad 2.45$$

Thus if $\bar{D}\, C_1$ is plotted against C_1, the gradient of the tangent at a point corresponding to a certain value of C_1 will give a first approximation of the value of D at that concentration. Using this first approximation value of D, a theoretical sorption-time curve can be constructed, and a value of $\bar{D}$ from the calculated curve is then obtained according to Eqn. 2.42, and compared with the experimental

value of $\bar{D}$. There will be a difference because Eqn. 2.45 is not exactly correct. Thus a second approximation is carried out by plotting $\bar{D}\ C_1$ ($\bar{D}$ is now the value obtained from the first approximation) against C_1 again, and differentiating. By repeating the procedure until the value of $\bar{D}$ from the theoretical curve is almost equal to the experimental one, a real D - C relationship can be obtained.

This method is applicable no matter what the D - C relationship is, but it is tedious and lengthy.

Other methods of determining concentration dependence include Kokes' (40) method of approximation from $\bar{D}_a$ and $\bar{D}_d$ over small concentration ranges; Barrer and Brooks' (41) method of using successively smaller concentration intervals in a series of sorption experiments; Prager's (42) step-function approximation; Fujita and Kishimotos' (43) method of moments, Huang's (44) polynomial approximation; and Crank's (45) weighted-mean diffusion coefficient approximations.

These methods will not be dealt with in detail here as they are of no direct bearing to the main work described in this thesis, where the diffusion coefficient is obtained from permeation experiments. Sorption experiments were carried out mainly to determine the vapour pressure-concentration isotherms.

Summary.

In sections 2.1, 2.2 and 2.3, the definitions of the diffusion coefficients, and the methods of obtaining diffusion coefficients from permeation and sorption experiments have been discussed. However, it is essential to understand which of the numerous diffusion coefficients defined in 2.1 are the ones measured experimentally. The presence of the penetrant in the polymer causes a change in the position of local volume centre,

and local mass centre, as well as causing a mass flow of the solution. These effects give rise, therefore, to differences in the various diffusion coefficients defined by different reference frames.

In a permeation experiment where the gas or vapour is allowed to diffuse from a high concentration to a lower concentration across the polymer membrane, a mutual diffusion coefficient, with a fixed-volume reference (if there is no volume change on mixing), D^{v}_{AB}, is measured.

In an absorption-desorption type of experiment, a polymer fixed mutual diffusion coefficient is measured.

The diffusion coefficient obtained from the exchange of labelled and unlabelled molecules in the polymer, as is the case in this work, is a self-diffusion coefficient, D^{*}_{A}, as defined before (Eqn. 2.17).

It is obvious from the relationships (derived in Section 2.1) between these coefficients, that at zero penetrant concentration, they should all have the same value. If only limiting behaviour is required, it is advisable, in experiments of this kind, to keep the penetrant concentration as low as possible and to extrapolate to zero concentration.

2.4. The free-volume theory as applied to solvent diffusion in polymers.

The dependence of diffusion coefficients of organic solvent in polymers on concentration has been found to be very pronounced in many cases (46-51). Many authors have attempted to explain this phenomenon; early suggestions included explanations of thermodynamic non-ideality in polymer-diluent mixtures (52), and of immobilization of penetrant molecules in the polymer network (53). These theories have later been found to be insufficient to account for the actual data. The zone theories of Barrer (24) and Brandt (54) which will be discussed, are also not useful in the temperature range just above the glass transition temperature because of the rapid variation of activation energy with temperature, and the consequently large number of degrees of freedom, g, involved in the calculation (see section 2.5). The free volume approach (49, 51, 55, 56) is a useful quantitative treatment which explains both the temperature and concentration dependence of D.

The origin of the free volume concept was the equation derived by Doolittle (57, 58) to explain the dependence of viscosity of simple liquids on temperature. A liquid is pictured as a mixture of free volume and occupied volume. The larger the free volume, the easier it is for molecular motion to occur (59, 60). Simply, it can be expressed as

$$\eta = A \exp. (B / f) \qquad 2.46$$

where A and B are constants independent of temperature, and f is the fractional free volume which increases with temperature, η is the viscosity.

Williams, Landell, and Ferry (61) have derived, from the Doolittle concept, a similar expression, (WLF expression), for the dependence of viscosity of a bulk polymer on temperature.

With the presence of a diluent, the viscosity of the subsequent concentrated solution has been shown to be dependent on the diluent concentration, if the fractional free volume is assumed to be proportional to the diluent concentration (62). Further work by Ferry and Stratton (63), on the dependence of viscosity on pressure and tensile strain analysed in the free volume concept, indicate that the polymer segmental mobility (bulk viscosity) depends on the free volume in a manner suggested by Doolittle.

Fujita, Kishimoto and Matsumoto (49) considered that the mobility of the diluent molecules (hence the diffusion coefficient of the diluent-polymer system) should also be controlled by the free volume of the system, and derived an expression for the dependence of D on concentration.

It is best to begin the derivation of an expression for the diffusion coefficient in terms of the fractional free volume by using Cohen and Turnbulls' concept of identical molecules (64). A liquid is envisaged as consisting of "hard spheres" where molecules reside within cages bound by their neighbours. Occasionally a void is opened up because of thermal fluctuations to allow a considerable displacement of the molecule. Diffusion occurs as a result of redistribution of the free volume within the liquid. The total probability, $P(v^*)$ of finding a free volume exceeding a given volume v^* is represented by

$$P(v^*) = \exp(-bv^*/\bar{v}) \qquad 2.47$$

where b is a numerical factor near unity, introduced to correct for overlap of free volume,

and $\bar{v}$ is the average free volume of one molecule,

i.e. the total free volume divided by the total number of molecules.

To apply Eqn. 2.47 to polymer systems the various parameters need to be re-interpreted. Thus following Fujita (55) $\bar{v}$ is regarded as the average free volume per unit volume of the system, and designated by the symbol f; the product bv* is written as B and is interpreted as the measure of the hole size.

Then we have, for polymer systems,

$$P(B) = \exp(-B/f) \qquad 2.48$$

Now the mobility of a diluent in the polymer medium should depend upon the probability of its finding a hole in its neighbourhood large enough to allow its displacement. If the minimum hole size for a particular diluent displacement is B_d, then

$$m_d = A_d \exp(-B_d/f) \qquad 2.49$$

where m_d is the mobility of the diluent molecule,

A_d is a constant depending upon the size and shape of the diluent.

A_d and B_d, by their definitions, should be independent of temperature and diluent concentration, thus the mobility of a diluent is primarily determined by the average fractional free volume of the system. It is interesting to note that by comparing Eqn.2.49 to Eqn. 2.46, the viscosity (although a simple liquid is referred to in Eqn. 2.46), an expression for a polymer system can be similarly derived (65)) is found to be inversely proportional to the mobility.

The thermodynamic diffusion coefficient, D_{th}, (66), of the diluent is related to the molar mobility m_d by the expression (67):

$$D_{th} = RT\, m_d \qquad 2.50$$

where R is the gas constant, and T is the absolute temperature of the system.

Combining equations 2.49 and 2.50, therefore

$$D_{th} = A_d RT \exp(-B_d/f) \qquad 2.51$$

f, the fractional free volume, is dependent on the temperature

and diluent concentration, and is hence written as $f(v_1,T)$, v_1, being the volume fraction of the diluent.

Fujita and Kishimoto (65) have established that if the increase in free volume of the system is proportional to the volume of the added diluent, then $f(v_1,T)$ turns out to be a linear function of v_1, given by the expression:-

$$f(v_1,T) = f(o,T) + \beta(T)\, v_1 \qquad 2.52$$

where $$\beta(T) = \gamma(T) - f(o,T) \qquad 2.53$$

and $\gamma(T)$ is the proportionality factor between the free volume increase and the volume of added diluent; and $f(o,T)$ is the value of f at zero diluent concentration.

Substituting Eqn. 2.52 into Eqn. 2.51, we obtain

$$\ln\left(D_{th}/D_o\right) = B_d \beta(T)\, v_1 \Big/ \left\{ [f(o,T)]^2 + \beta(T) f(o,T) v_1 \right\} \qquad 2.54.$$

Note D_{th} tends to D_o at zero diluent concentration.

At a fixed temperature, B_d, $\beta(T)$, $f(0,T)$ are all constants,

$$\therefore \quad \ln (D_{th}/D_o) = K' v_1 / (K'' + K''' v_1) \qquad 2.55$$

where K', K'', and K''' are constants.

Since v_1 is small in practice, the term $K''' v_1$ in the denominator is negligible compared with K'',

$$\therefore \quad \ln (D_{th}/D_o) = \frac{K'}{K''} v_1 \qquad 2.56$$

$$\text{i.e.} \quad D_{th} = D_o \exp \left(\frac{K'}{K''} v_1 \right) \qquad 2.57$$

This represents the concentration dependence of diffusion coefficient often observed in practice.

Eqn. 2.54 can also be expressed reciprocally as

$$\frac{1}{\ln(D_{th}/D_o)} = \frac{f(0,T)}{B_d} + \frac{[f(0,T)]^2}{B_d \beta(T)} \frac{1}{v_1} \qquad 2.58$$

Experimentally a plot of $1/\left[\ln(D_{th}/D_o)\right]$ against $1/v_1$, should give a straight line. From the intercept at $1/v_1 = 0$ and the slope, respectively, values of $f(0,T)/B_d$ and $\left[f(0,T)\right]^2/B_d \beta(T)$ can be

obtained. Thus knowing either $f(0,T)$ or B_d from other experiments, all the three parameters may be evaluated. $f(0,T)$ should be independent of the diluent species.

It should be noted that the thermodynamic diffusion coefficient, D_{th}, as defined by Eqn. 2.50 is equivalent to the self-diffusion coefficient D_A^* as defined in section 2.1. At low concentrations, therefore, D_{th} approximates to the intrinsic diffusion coefficient $\underline{D_A}$, since

$$D_{th} = \underline{D_A} \left(\frac{d \ln C_A}{d \ln a_A} \right) \qquad 2.59$$

where C_A and a_A are the concentration and activity of component A (diluent) respectively in the polymer-diluent mixture (See section 2.1)

Temperature dependence.

For amorphous polymers above the glass transition temperature (61, 68),

$$f(0,T) = f(0,0) + \alpha_f (T-To) \qquad 2.60$$

where $f(0,T)$ and $f(0,0)$ are the fractional free volumes at temperature T and the reference temperature To; α_f is the thermal expansion coefficient of the free volume and is roughly equal to the difference between its liquid-like and glass-like thermal expansion coefficients.

Eqn. 2.51 becomes (writing D for D_{th}),

$$D = A_d RT \exp\left\{ -B_d / \left[f(o,o) + \alpha_f (T-To) \right] \right\} \qquad 2.61$$

at reference temperature To,

$$D_o = A_d RTo \exp\left\{ -B_d / f(o,o) \right\} \qquad 2.62$$

Assuming $A_d RT$ and $A_d RT_o$ to be almost equal and combining Eqn. 2.61 and 2.62, we have

$$(T-To)/\ln(D/D_o) = \frac{f(o,o)^2}{B_d \alpha_f} + \frac{f(o,o)(T-To)}{B_d} \qquad 2.63$$

Therefore $(T-To)/\ln(D/D_o)$ is linearly related to $(T-To)$.

Since f(o,o), B_d, α_f are independent of temperature,

$$(T-To)/\ln(D/D_o) = K_1 + K_2 (T-To)$$

$$\therefore \quad \ln(D/D_o) = \frac{T-To}{K1 + K2(T-To)} \qquad 2.64$$

where K_1 and K_2 are constants.

Eqn. 2.64 resembles the WLF equation derived from viscosity considerations (61), and it has been shown to be experimentally valid in various diluent-polymer systems (9).

Relation of D_o with Tg.

Newns and Park (69) have recently derived an expression linking Tg with the diffusion coefficient of benzene at zero concentration in various elastomers by using the free volume concept. Substituting Tg for the reference temperature To, Eqn. 2.61 can be written

$$D = A_d RT \exp\left\{-B_d / \left[f(0,Tg) + \alpha_f (T-Tg)\right]\right\} \qquad 2.65$$

$$\text{Rearranging } \ln D = \ln(A_d RT) - \frac{B_d}{\left[f(o,Tg) + \quad (T-Tg)\right]} \qquad 2.66$$

at a constant temperature T,

A_d, B_d, α_f, R and f (O,Tg) are constant,

therefore,

$$Tg = C_1 + C_2 / (C_3 + \log D) \qquad 2.67$$

C_3 is small in magnitude compared to logD. For polymethylacrylate-benzene system, C_3 was found to be only 0.53 (70). A linear plot was obtained, using ten different polymers, of Tg against $(C_3 + \log D)^{-1}$, where D is the diffusion coefficient of benzene at zero concentration. Polyisobutene did show a rather large deviation and this was explained by the large B_d value in this polymer caused by the steric hindrance of the two methyl groups.

It is seen, therefore, that the free volume theory can be applied successfully to explain the concentration and temperature dependence of diffusion of organic diluents in polymers, and possibly

to predict the diffusion coefficient from a knowledge of the glass transition temperature, or vice versa.

2.5. The activated zone theory.

This theory is due to Barrer (71-78), according to which transport of a molecule in a polymer medium takes place when local conditions are favourable, i.e. when the concentration of thermal energy is sufficient to enable the localized chain environment to acquire the transition (activated) state necessary for any rearrangement of molecules.

Suppose the assembly of hydrocarbon chains in the rubber contain N_1 degrees of freedom (oscillators and restricted rotators require two squared terms each to specify the vibrational or rotational degres of freedom).

The chance of an energy $>$ E being distributed among g degrees of freedom, is (78):-

$$e^{-E/RT}\left[\frac{E}{RT}\right]^{g-1}\frac{1}{(g-1)!} \qquad 2.68$$

Since there are N_1 possible places where the zone centre may be located, the chance of these g degrees of freedom being together in a group $=(\frac{1}{N_1})^{g} N_1$

Number of such groups which may be chosen from N_1 degrees of freedom is $\frac{N_1}{g}$

Therefore, the number of these activated groups

$$= N_1\left[\left(\frac{E}{RT}\right)^{g-1}\frac{1}{g!}\ \frac{1}{(N_1)^{g-1}}\right]e^{-E/RT} \qquad 2.69$$

Since g may vary from 1 to N_1, total number of activated zones $= \sum N_1$

$$= N_1 e^{-E/RT}\sum_{f=1}^{N_1}\left(\frac{E}{RT}\right)^{g-1}\frac{1}{g!}\ \frac{1}{(N_1)^{g-1}} \qquad 2.70$$

However, the above derived equation tends to give a "clustering" picture of the process, as it is evident from Eqn. 2.70 that only zones of 1 degree of freedom are present in large numbers. If one assumes that an average region contains n degrees of freedom and

then replacing $(\frac{1}{N_1})^{g-1}$ in Eqn. 2.70 by $(\frac{n}{N_1})^{g-1}$, one can then shift the pattern closer to experimentally extrapolated ones where the largest number present are zones containing 10 - 20 degrees of freedom (76).

However, size n $\ll N_1$ the same difficulty remains.

Thus a segmental behaviour of polymer is next assumed where the rubber is divided into small regions (or quasi-molecules) whose identity may change, but whose number N_E is constant.

Then the number of zones activated becomes:

$$\sum N = N_E \, e^{-E/RT} \sum_{i=1}^{n} \left(\frac{E}{RT}\right)^{g-1} \frac{1}{(g-1)!} \qquad 2.71$$

The activated quasi-molecules may then undergo internal reorientation processes. Eqn. 2.71 has the correct form to explain the experimental data. The terms of the summation lead to a maximum value for an intermediate value of g. (See Fig.2). The most likely number of degrees of freedom as indicated by the peak increases the larger the activation energy term E/RT. This suggests firstly that the motion of many polymer segments is involved in the diffusion process, and secondly more degrees of freedom are excited the higher the activation energy. The average energy in the chosen g degrees of freedom, represented by $\bar{E} = gRT$, varies with g as shown by the locus of maxima in Fig.2. Zones which are "hotter" than average in total energy content ($E > gRT$) and zones which are "colder" than average ($E < gRT$) are both less probable than zones containing average total energy ($E = gRT$).

In an activated region, many sets of librations of $-CH_2$ units are possible, but only a fraction, α, may be successful in producing net transport of a solute molecule in one direction. The chance of a translation in the x-direction, in the absence

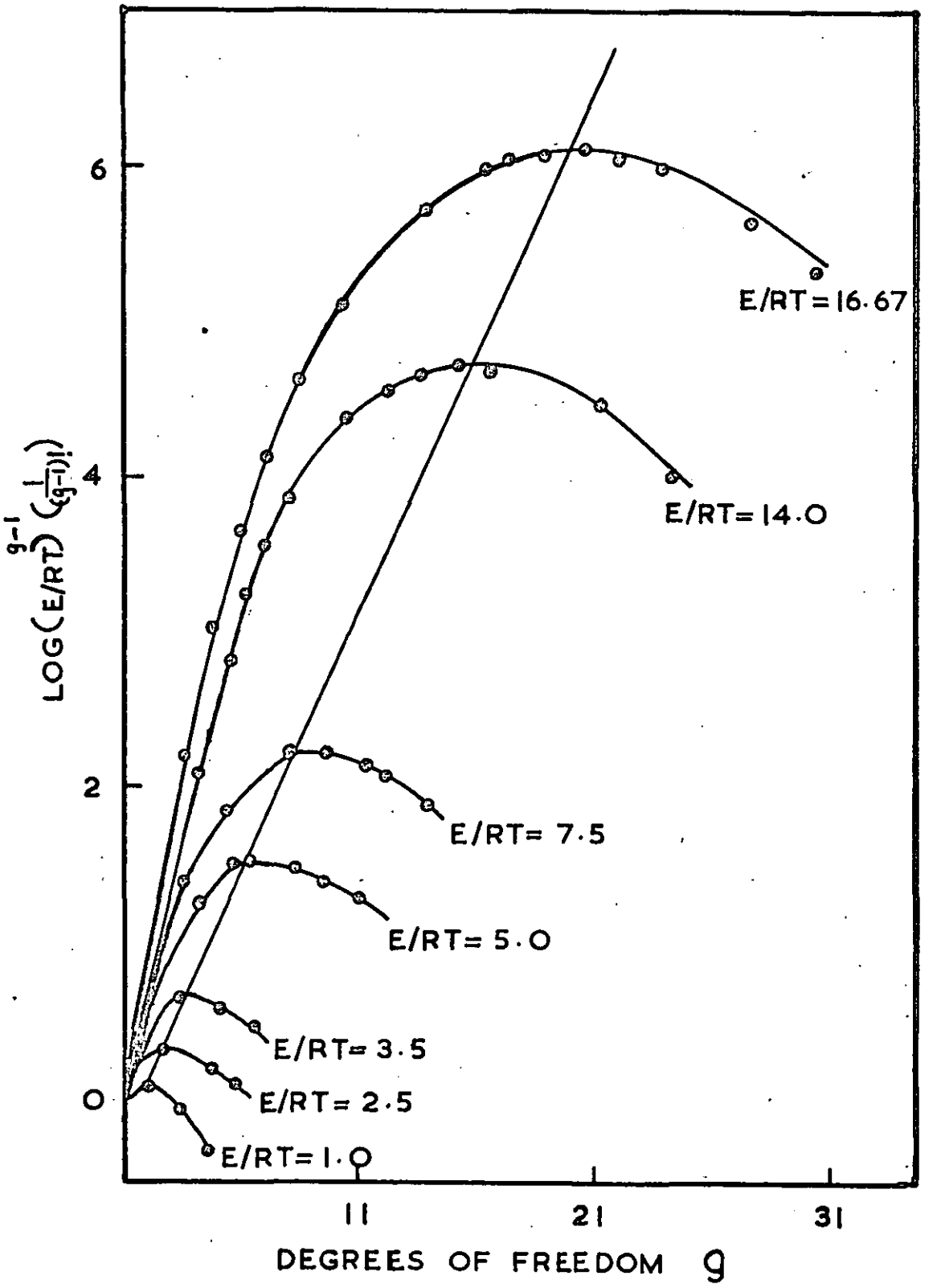
6
4
2
0
LOG $(E/RT)^{g-1} \left(\frac{1}{(g-1)!}\right)$
E/RT = 16.67
E/RT = 14.0
E/RT = 7.5
E/RT = 5.0
E/RT = 3.5
E/RT = 2.5
E/RT = 1.0
11
21
31
DEGREES OF FREEDOM g

FIG. 2

of external forces, is 1/2. Also, however, α may include the possibility that for a successful translation there must be a synchronisation with time and direction of sets of librations. Such synchronisation is an improbable event and the value of α would therefore be reduced This is corrected by multiplying each summation term by ρ, where $\rho < 1$ but remains to be determined.

If the mean lifetime of the activated state is τ, and the period of a libration is τ_o, the number of sets of libration during the period of activation is $\frac{\alpha\tau}{\tau_o}$ per zone. The total number of sets of successful librations in the activated regions involving N_1 solute molecules is then, (from Eqn. 2.71),

$$N_2 = N_1 e^{-E/RT} \sum_{g=1}^{n} \frac{\tau\alpha}{\tau_o} \left(\frac{E}{RT}\right)^{g-1} \frac{1}{(g-1)!} \qquad 2.72$$

In each second this becomes

$$N_2 = N_1 e^{-E/RT} \sum_{g=1}^{n} \frac{\alpha}{\tau_o} \left(\frac{E}{RT}\right)^{g-1} \frac{1}{(g-1)!} \qquad 2.73$$

The diffusion coefficient (78) then becomes

$$D = \lambda^2 e^{-E/RT} \sum_{g=1}^{n} \frac{\alpha}{\tau_o} \left(\frac{E}{RT}\right)^{g-1} \frac{1}{(g-1)!} \qquad 2.74$$

where λ is the average distance moved in the x-direction by the solute per unit act of diffusion.

If the mean value of λ is 3×10^{-9} cm. $\tau_o \sim 10^{-12}$ sec., and $\alpha = 1/2$,

$$D \simeq 4.8 \times 10^{-4} e^{-E/RT} \sum_{g=1}^{n} \left(\frac{E}{RT}\right)^{g-1} \frac{1}{(g-1)!} \text{ cm}^2 \text{ sec.}^{-1} \qquad 2.75$$

Barrer (71) considered only a few terms in the summation are likely to make contributions to D, and without serious errors a single term in g will suffice.

A similar expression can be derived for the self-diffusion coefficient in rubber (71), thus

$$D_s \simeq 6 \times 10^{-4} \; e^{-E/RT} \sum_{g=1}^{\infty} \left(\frac{E}{R\,T}\right)^{g-1} \frac{1}{(g-1)!} \text{ cm}^2 \text{ sec.}^{-1} \qquad 2.76$$

Thus the diffusion coefficient is derived for penetrant-fubber and rubber-rubber systems from considering the statistical probability of finding an activated zone involving several segmental motions.

Barrer and Skirrow (77) have fitted experimental values of D_o in the expression

$$D = D_o \; e^{-E/RT} \qquad 2.77$$

into Eqn. 2.75 and found for hydrocarbons diffusing in rubber the degrees of freedom vary around 20, increasing with decreasing temperature.

It is apparent that an appreciable zone of activation is necessary in order for a unit diffusion to take place. This view is supported by the large energies and entropies of activation for diffusion and flow in elastomers observed (71) as compared with monomeric liquids even when cohesive energy densities of polymer and liquid are similar.

2.6. Brandt's Theory.

Brandt (54) proposed a molecular model for the diffusion of small molecules in high polymers, and obtained from it an activation energy term. Although the value of his calculated activation energy turned out to be too low compared with the experimentally determined one, it is nevertheless interesting to consider his theory in some detail as it gives an insight into the molecular movements involved in the polymer segments during diffusion.

Basically Brandt agreed with Barrer's zone theory, but whereas Barrer assumed one of the summation terms in Eqn.2.75 was large enough so that the others could be neglected without substantial error (as mentioned in section 2.5), Brandt considered this an unwarranted assumption, and actually evaluated Eqn. 2.75 numerically by substituting mathematically derived values for the parameters involved in the equation.

The assumptions made can be summarised as follows:-

1. The activated state is considered as the case in which two polymer chains, originally approximately parallel, have moved apart to accommodate the passage of a penetrant molecule (Fig.3).
2. The activation energy is thought to consist of two contributions (a and b):-
   (a) An intermolecular term due to the repulsion which the chains experience from their neighbours on making room for the penetrant molecule. This energy term can be taken as the product of the internal pressure and the volume that has to be swept out by the chains to allow the penetrant molecule to pass through.

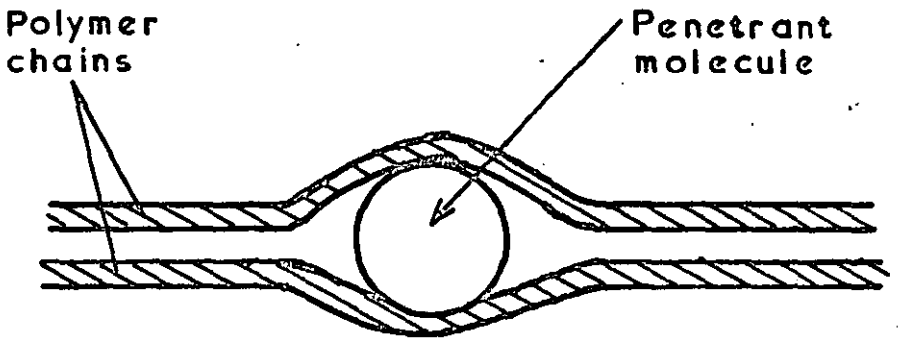

(a) Symmetrical model used in calculation

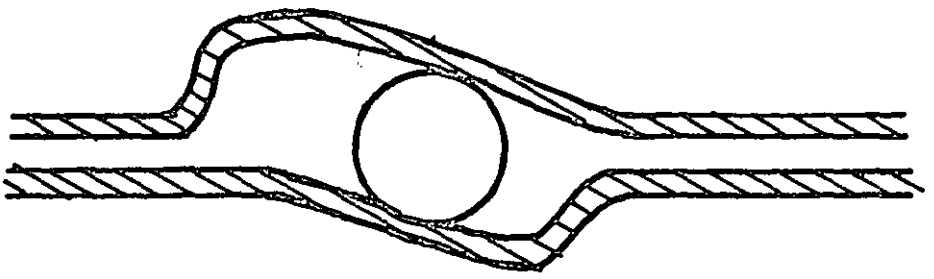

(b) Unsymmetrical model

FIG. 3

(b) An intramolecular term due to the resistance of the chains themselves to "bending." It is assumed that the bending of the chains involves a partial rotation of chain units out of their equilibrium position against a hindering potential of internal rotation.

3. The activated state as shown in Fig.3 is formed by the partial rotation of each backbone chain unit against the hindering potential, such that the total torsional strain is distributed evenly over the whole segment.

4. The number of degrees of freedom in a segment is proportional to the segmental length.

5. The probability that the g degrees of freedom contained in a segment will co-operate in a diffusion step is

$$Pg = \left(\frac{1}{m}\right)^{g} \qquad 2.78$$

where m is a term corresponding to the number of different directions of motion, and in this case is taken to be two, since a rotation against a hindering potential may proceed in only two different directions (24).

The total energy found with g degrees of freedom in the activated state can be expressed as:-

$$E = E_i + E_b + E_{th} \qquad 2.79$$

where E_i is the intermolecular term

E_b is the intramolecular term

E_{th} is the thermal energy which is not part of the activation energy but of the total energy.

Now,

$$E_i = P_i \Delta V \qquad 2.80$$

where P_i is the internal pressure,

ΔV is the volume swept out by chains to accommodate the penetrant molecule.

$$E_b = \frac{2s}{\lambda} \quad \psi \qquad 2.81$$

where S is the length of the segment

λ is the length of one back bone chain bond measured along the chain axis,

ψ is the potential of hindered rotations for an angular displacement.

$$E_{th} = g\,RT \qquad 2.82$$

Since the number of degrees of freedom available to a segment is proportional to the length of that chain (assumption 4 above)

$$g = \frac{2s}{\lambda} Z \qquad 2.83$$

where Z is the proportionality factor which represents the number of degrees of freedom associated with one backbone chain. Brandt has justifi ably used Z = 1 for most of his calculations (79).

Furthermore, the term ΔV may be represented by

$$\Delta V = \frac{1}{2} (\sigma_p - \phi^{\frac{1}{2}}/2)^2 \left[s^2/(\sigma_p - \phi^{\frac{1}{2}}/2)^2 - 1 \right]^{\frac{1}{2}} \sigma_c N \qquad 2.84$$

where σ_p is the diameter of the penetrant molecule

σ_c is the average diameter of the polymer molecule

ϕ is the free volume per unit length of the polymer.

The potential of hindered angular rotation

$$\psi = 9 \psi \lambda^2 \bar{s}^2 \left[s^2/(\sigma_p - \phi^{1/2}/2)^2 - 1 \right]^{-1} \qquad 2.85$$

Substituting Eqn. 2.83, 2.84, 2.85 into 2.80, 2.81, 2.82,

$$E = E_i + E_b + E_{th}$$

$$= \frac{1}{2} (\sigma_p - \phi^{\frac{1}{2}}/2)^2 \left\{ \left[g \lambda / 2 Z (\sigma_p - \phi^{\frac{1}{2}}/2) \right]^2 - 1 \right\}^{\frac{1}{2}} \sigma_c N P_i$$

$$+ 36 \psi_c Z g^{-1} \left\{ \left[g \lambda / 2 Z (\sigma_p - \phi^{\frac{1}{2}}/2) \right]^2 - 1 \right\}^{-1}$$

$$+ g\,RT \qquad 2.86$$

From Eqn. 2.86 it is possible to plot the energy factors against the numbers of degrees of freedom g. Brandt found that E_i and E_{th} increased linearly with increasing degrees of freedom, but E_b varied from a high value for small g, to a much diminished value at higher g's. Consequently E has a distinct minimum value at an intermediate number of degrees of freedom, g min.

By substituting different values of g, and therefore E, into the right hand side of the Barrer equation (Eqn.2.75), value of D at a fixed temperature can be obtained. The activation energy term can be evaluated from the Arrhenius relationship

$$D = D_0 \, e^{-E_D/RT}$$

Brandt also proceeded to prove his point that more than one term in the summation series in Eqn. 2.75 give equally large contributions to the diffusion coefficient, D. He plotted $\log\left[\left(\frac{E}{RT}\right)^{g-1}\frac{1}{(g-1)!}\right]$, $\log(\alpha)^g$ and $\log e^{-E/RT}$ against the number of degrees of freedom g, and then adding the three terms to give a sum plot against g. This is shown in Fig.4. It is evident from the sum plot that several terms of the series in Eqn.2.75 are of nearly the same magnitude.

An interesting observation is made by the author in comparing Brandt's and Barrer's respective plots of $\log\left[\left(\frac{E}{RT}\right)^{g-1}\frac{1}{(g-1)!}\right]$ against g. Barrer assumed constant E/RT with respect to g, and obtained a maximum as shown previously in Fig.2. Brandt, however, assumed E/RT to be itself a function of g, and his plot showed a minimum (Fig.4). If Barrer's $\log\left[\left(\frac{E}{RT}\right)^{g-1}\frac{1}{(g-1)!}\right]$ against g plot is used in Brandt's addition (Fig.4), a sharp peak in the sum will be observed, thus illustrating Barrer's assumption that only a few terms in the summation are significant contributors.

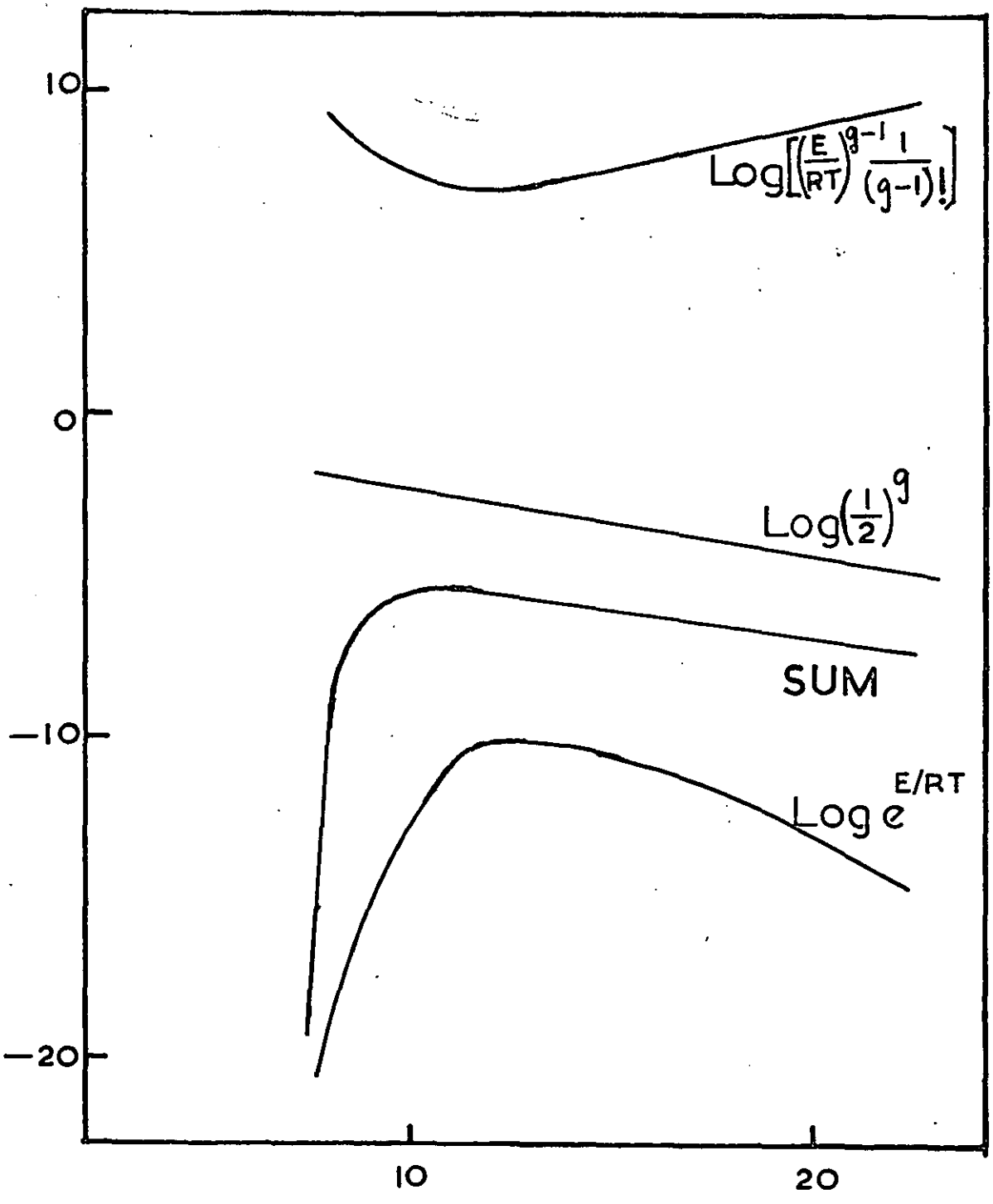

FIG. 4 BRANDT'S "SUM" PLOT

Another point of arbitration is Brandt's assumption (Assumption 3 listed above) that the activated state is formed by the partial rotation of the backbone chain. This may be the case when very small penetrant molecules are involved. With larger molecules complete rotational transition may occur, and the energy required is much higher. This may account for the lower evaluated activation energy from Brandt's model, compared to the experimental value.

2.7. Theory of Paul and Di Benedetto (80,81).

In their approach the polymer is pictured as consisting of cell models which contain polymer segments arranged more or less parallel to each other, i.e. some kind of short range order is assumed. As the chains fluctuate, due to thermal motions, a volume is swept out, and the intermolecular forces, or van der Waals bond energies, will be altered. The variation in this intermolecular energy, which is taken as the average potential energy of molecular interaction which accompanies a volume change, is related to the activation energy of diffusion. The process of diffusion of a small molecule in the polymer may be visualised as follows. A gas molecule is originally trapped by parallel bundles of n-centre segments, each centre being a back-bone carbon atom. The gas molecule has a collision diameter r_g, and it is undergoing vibration. After some time a unit cell right next to the trapped gas molecule slowly, with respect to the vibrational motion of the gas molecule, will increase in volume due to normal thermal motion. Once the unit cell's volume has increased by enough to accommodate the gas molecule the latter can pass through the unit cell. The volume of the unit cell that will just permit this unit diffusional jump is taken as a cylinder whose diameter is r_g and whose length is $2n\lambda$ (82). (2λ is the distance of the effective carbon-to-carbon bond).

$$\text{i.e. } \delta(nv) = \frac{\pi}{4} r_g^2 \; 2\lambda n \qquad 2.87$$

The amount of excess energy required to produce this volume fluctuation is the activation energy for the fluctuation. This activation energy is related to the variation in the average potential energy of molecular interaction which accompanies a volume change of $2\lambda n \left(\frac{\pi}{4}\right) r_g^2$.

Paul and Di Benedetto assumed that a Lennard-Jones (6-12) potential function describes the potential energy of interaction ϕ

Thus $$\phi = \varepsilon^* \left[\left(\frac{\rho^*}{\rho'} \right)^{12} - 2 \left(\frac{\rho^*}{\rho'} \right)^{6} \right] \qquad 2.88$$

where ε^* and ρ^* are energy and distance parameters, and ρ' is the distance apart between centres.

By assuming a picture mode for chain interaction, Fig. 5, it is clear that

$$\rho_i^{\,2} = \rho_o^2 + i^2 (2\lambda)^2 \qquad 2.89$$

where ρ_o is the nearest neighbour distance, and ρ_i is the distance between centres.

Substituting Eqn. 2.89 into 2.88, and arbitrarily summing up for 10 centres on either side of the centre in question, the total interaction energy

$$\phi_c = \varepsilon^* \left[C \left(\frac{\rho^*}{\rho_o'} \right)^{12} - 2D \left(\frac{\rho^*}{\rho_o'} \right)^{6} \right] \qquad 2.90$$

where C and D are terms linear in $\rho_o/2\lambda$

Eventually,

$$\phi_C = \left(\frac{\varepsilon^* \rho^*}{2\lambda} \right) \left[0.77 \left(\frac{V^*}{V} \right)^{11/2} - 2.32 \left(\frac{V^*}{V} \right)^{5/2} \right] \qquad 2.91$$

where $V^* = 2\lambda \rho^{*2}$ 2.92

the activation energy ΔE_d is given by

$$\Delta E_d = N_o (\Delta \phi) \qquad 2.93$$

where $\Delta\phi$ is the additional energy required to create a void whose excess volume is $2\lambda n \left(\frac{\pi}{4}\right) r_g^2$, and N_o is the Avogadro's number.

The unit cell volume in the activated state V_a is related to the average effective volume (nv) by the equation

$$V_a = V \left(1 + r_g^{*\,2} \right) \qquad 2.94$$

Combining equations 2.91, 2.93, and 2.94

$$\Delta E_d = \frac{4\pi N \varepsilon^*}{2\lambda} \rho^* \left\{ 0.77 \left[\left(\frac{V^*}{V_a} \right)^{11/2} - \left(\frac{V^*}{V} \right)^{11/2} \right] - 2.32 \left[\left(\frac{V^*}{V_a} \right)^{5/2} - \left(\frac{V^*}{V} \right)^{5/2} \right] \right\} \qquad 2.95$$

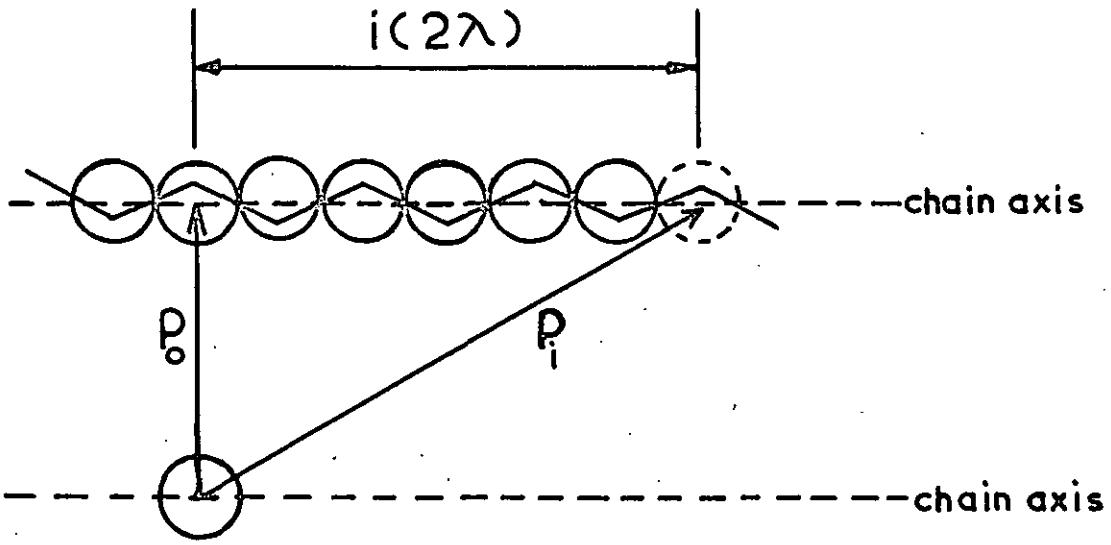

FIG. 5

By plotting E_d values against $(r_g^*)^2$ for each polymer system for various gases whose $r_g^{*\,2}$ values have been calculated, and then superimposing plots of Eqn.2.95 with V_a substituted from Eqn. 2.94, and with appropriately substituted values for the other parameters, the theory may be validated. This has indeed been done by Di Benedetto and Paul (83) for polyvinyl acetate.

Again the assumptions made in this model approach does not allow for complete segmental rotation which is necessary for large diffusing molecules. However this, and Brandt's theory, show that it is possible to work out an energy term for diffusion purely by using molecular models, and applying the right values to the parameters involved.

2.8. Some aspects of viscoelastic behaviour in polymers.

When a polymer molecule is subjected to an external force, it will assume a new equilibrium state in which segments occupy new positions with respect to the centre of gravity of the molecule. When the stress is removed, the segments diffuse back to their unstressed positions, (which are positions of minimum free energy and maximum entropy), with reference to the centre of gravity of the molecule, which in the meantime may have moved as a result of viscous flow. The ability of the segments to return to their previous configuration is referred to as the elastic property. The readiness of the segments to flow past each other is related to the viscous property. In high polymers, both these properties are inherent, hence the behaviour is referred to as viscoelastic.

In the phenomenological description of viscoelasticity (6, 84-90), which will not be dealt with here in detail, mathematical models are made which consist of perfectly elastic, "Hookean," springs, and perfectly viscous, "Newtonian" dashpots, to represent the combination of elastic and viscous responses exhibited by polymers. From these models it is possible to work out values for relaxation and retardation times, which are respectively, the time taken for the stress in the polymer to relax to $^1/_e$ its initial value when the polymer is held under constant strain, and the time taken for the strain to "decay" to an equilibrium value when the polymer is held under constant stress. The viscoelastic behaviour of a polymer is too complex to be represented by a single model, and can be described by a large number of these models either in series or in parallel. Thus, a generalised model has a distribution of relaxation times, instead of a single relaxation time.

For a single model under a sinusoidal strain, the stress is also sinusoidal but lags behind the strain because energy is dissipated. A sinusoidal strain may be written:

$$e = e_o \exp(iwt) \qquad 2.96$$

where w is the angular frequency which equals $2\pi f$ (f is the frequency). The relationship between stress and strain when the strain is alternating is

$$F = G^*(w)\, e \qquad 2.97$$

where F is the force

$G^*(w)$ is a complex shear modulus, or complex rigidity.

$G^*(w)$ in turn may be expressed as

$$G^*(w) = G'(w) + i\, G''(w) \qquad 2.98$$

where $G'(w)$ is the component of shear stress that is in phase with the strain, divided by the strain, and

$G''(w)$ is the component of shear stress that is 90° out of phase with the strain, divided by the strain.

$G'(w)$ is a measure of energy storage,

$G''(w)$ is a measure of energy dissipation.

If τ is the relaxation time, as defined before, of the single model (the model used here contains a spring and a dashpot in series - called a Maxwell element), then the real and imaginary parts of the complex rigidity may be represented as:-

$$G'(w) = (G\, w^2 \tau^2) / (1 + w^2 \tau^2) \qquad 2.99$$

$$G''(w) = (G\, w \tau) / (1 + w^2 \tau^2) \qquad 2.100$$

where G is the spring rigidity.

For a generalized model containing an array of Maxwell elements in parallel, the corresponding equations are

$$G'(w) = \sum_i (G_i\, w^2 \tau_i^2) / (1 + w^2 \tau_i^2) \qquad 2.101$$

$$G''(w) = \sum_i (G_i\, w \tau_i) / (1 + w^2 \tau_i^2) \qquad 2.102$$

Thus the behaviour of the system in static or dynamic strain experiments may be calculated, once the distribution functions G'(w) and G''(w) are known, and conversely, the possibility arises of determining the distribution function from the observed mechanical behaviour.

This latter problem is a difficult one as it is complicated by the very wide range of relaxation times which have to be taken into account when dealing with most polymers. Experiments are necessary whose time-scales cover a range comparable with the relaxation times. Since no single experimental method is capable of covering the time range of the order of 10^{-5} sec to 10^{5} sec, a combination of methods is required.

In the longest time range (10^{1} - 10^{5} seconds) the study of creep under static load or stress relaxation at constant strain has proved most useful. For shorter times methods employing alternating stresses or strains are almost invariably used. For very short times (10^{-4} second) wave propagation methods and mechanical impedence methods are employed. Ferry (6) has given an excellent review of all the experimental methods used in these time scales. In an apparatus used by the author (87) a dynamic mechanical instrument is employed which measures the stress response, in-phase and out-of-phase, when a sinusoidal stress input in the frequency range 10^{3} - 10^{-1} cycles per second, (time range 10^{-3} - 10^{1} seconds), is applied. In all experiments accurate thermostating is essential, as the visco-elastic behaviour of polymers is strongly dependent on temperature (see later section). One of the advantages of methods which make use of electro-mechanical transducers like the one employed by the author is that the sample is subjected to only very small stresses and strains so that the conditions of linear visco-

elasticity (88), on which are based the stated equations 2.99 - 2.102, are fully satisfied.

Temperature dependence of viscoelastic properties.

It is a well known observation that visco-elastic parameters like G'(w) when plotted against log w and log t separately, show similar shapes (t is the absolute temperature). They can be superimposed by shifting them along the log w or log t axis. This is known as the time-temperature super position principle, and it can be applied to curves of stress relaxation (89), creep (90), G'(w) and G"(w) (91,92), as well as the relaxation time spectra derived therefrom. The superposition principle is important practically because it enables data obtained at different temperatures to be translated into those at corresponding frequencies, and vice versa. Therefore if experimental conditions limit the frequency applicable to a narrow range, the viscoelastic behaviour can be measured within this frequency range over several temperatures, and the data converted to a fixed reference temperature, and combined to give a master curve (93).

The kinetic theory of rubber elasticity (94) showed that the modulus of the polymer network at equilibrium was proportional to the density ρ, and the absolute temperature T. Therefore to convert the complex moduli obtained at T to a reference temperature To, it is necessary to apply a "vertical shift", i.e. for instance, G'(t) must be multiplied by a factor $\frac{To\,\rho o}{T\,\rho}$, before the "Horizontal shift" of $\pm \log a_T$ is added, where a_T is known as the shift factor, and is measured by the horizontal distance apart between the reference temperature curve and the curve at temperature T.

William, Landell, and Ferry (61) in their important work published in 1955 have found that for a variety of polymers, and also for polymer solutions and some non-polymeric substances, a_T can be expressed in the form:-

$$\log a_T = \frac{-17.44\ (T-Tg)}{(51.6 + T - Tg)} \qquad 2.103$$

where Tg was chosen as the reference Temperature, To, This equation fits well over the range from Tg to (Tg + 100)°C.

A physical significance may be given to the numerical coefficients in Eqn. 2.103 by making use of Doolittle's free volume equation for viscosity (57, 58) (see section 2.4). Doolittle's equation may be modified to express a_T in the form:-

$$\log a_T = \frac{(T - Tg)}{2.303\ fg\left[fg/(\alpha_l - \alpha_g) + (T-Tg)\right]} \qquad 2.104$$

where fg is the fractional free volume at Tg

and $(\alpha_l - \alpha_g)$ is the difference between the coefficients of thermal expansions above and below Tg. Comparison between Eqn. 2.103 and Eqn. 2.104 gives fg = 0.025 and $(\alpha_l - \alpha_g) = 4.8 \times 10^{-4}$ deg.$^{-1}$ The latter is close to the observed value for many polymers, and the former is certainly of the right order of magnitude.

A theoretical justification of the superposition principle can be shown in Bueche's molecular theory of viscoelasticity (95).

Molecular interpretation.

Earlier theory by Kirkwood (96) assumes a molecular model in which the chain atoms lie on a cubic lattice of James and Guth (97), containing n bonds of length b. If there are ν chains per unit cross section area, and an alternating tensile stress $[\sigma_0 \exp(i\omega t)]$ is applied to the terminal planes of the cubic network, each chain in the direction of stress will experience a force given by:

$$F = \frac{\sigma_o}{\vartheta} \exp(iwt) \qquad 2.105$$

Brownian motion of the chains allows a strain to develop in the direction of the stress. It is assumed that this is accompanied by a contraction of half the longitudinal strain in chain perpendicular to the stress.

By postulating a probability distribution of a chain, a generalized diffusion equation of Brownian motion was derived (98), and this is

$$\nabla \cdot D\left(\nabla \cdot j + j \cdot \nabla \vartheta / kT \right) = \frac{\partial j}{\partial t} \qquad 2.106$$

where j is the probability distribution function

t is the time

D is the internal rotatory diffusion tensor given by

$$D = kT/\xi \qquad 2.107$$

where ξ is the resistance tensor.

Kirkwood and Fuoss (98) derived a rotatory diffusion tensor D_S, about bond S, to replace the general diffusion tensor, D, in Eqn. 2.106. Kirkwood's final expression for the retardation time is

$$L(\tau) = \frac{Mc}{8\rho RT} \cdot \frac{\tau/\tau_m}{(1 + \tau/\tau_m)^2} \qquad 2.108$$

where M_c is the molecular weight between junction points,

ρ is the density

τ_m is the retardation time of maximum loss compliance.

In the theory of Rouse (99), a polymer chain is regarded as a succession of 'submolecules', each long enough to obey the Gaussian distribution function for random chain configurations (94). In the presence of a shearing force, the unstressed equilibrium configuration is disturbed, and the free energy is increased. Thus by co-ordinated Brownian motion of chain segments,

the molecules continually drift back towards their most probable distribution of configuration at a rate proportional to their displacement from equilibrium . Rouse has obtained expressions for the complex viscosity of a polymer solution by calculating the free energy stored in the distorted molecules according to Gaussian distribution of the chains. The shearing force was considered to vary sinusoidally with time. From his expressions the relaxation spectrum of the molecules may be derived. It was assumed by Ferry (100) that for an undiluted polymer above its Tg, Rouse's Theory might be obeyed over a useful range of relaxation times. The relaxation and retardation time spectra can then be expressed as:-

$$H(\tau) = \frac{\rho N}{2\sqrt{\pi} M} \left(\frac{\overline{r_o}^2 \, n \, k T \, \zeta_o}{6}\right)^{1/2} \tau^{-1/2} \qquad 2.109$$

$$L(\tau) = \frac{2M}{\pi \rho N} \left(\frac{6}{\overline{r_o^2} \, n \, k T \, \zeta_o}\right)^{1/2} \tau^{1/2} \qquad 2.110$$

where $\overline{r_o^2}$ is the unperturbed mean square displacement length of n monomer units,

ζ_o is the monomer friction coefficient which is equal to the force (in dynes) on a chain monomer unit due to the viscous resistance when travelling at 1 cm/sec through its surroundings at rest. (ζ_o is therefore characteristic of the particular polymer and temperature),

M is the monomeric molecular weight

N is the Avogadro's number.

Over the frequency range where the theory is applicable, a plot of $\ln H(\tau)$ against $\ln \tau$ should be linear with a slope of $-1/2$. Erom comparison with experimental curves over this region, the monomeric friction ζ_o can be evaluated provided

ρ , M, and $\overline{r_o^2}$ are known. ($\overline{r_o^2}$ may be obtained from the intrinsic viscosity in a Θ solvent).

The theory of Bueche (95) was formulated directly to apply to solid polymers. Brownian motion is not as directly applied as in the case of Rouse. Successive 'submolecules' are directed in sequence parallel to the x-, y- and z- axes of a rectangular co-ordinate system, thus a force applied in the x-direction extends only one-third of the submolecules. These extended submolecules behave like springs with moduli given by the Gaussian chain theory, so that Brownian motion within the submolecules is the source of the restoring forces. The whole molecule is pictured as consisting of masses of submolecules connected by identical springs. If a force is applied to such a system, a complicated set of vibrations will be executed by the springs as the model extends. Bueche then calculates the changes in positions of the masses with time when their vibrational motions are damped by a viscous medium. It is interesting that his final expression, approximated to short times (10τ) are:-

$$H(\tau) = \sqrt{2}\ H(\tau) \text{ (Rouse)} \qquad 2.111$$

$$L(\tau) = \frac{1}{\sqrt{2}}\ L(\tau) \text{ (Rouse)} \qquad 2.112$$

Activated molecular movements.

It is worthwhile to note that in all the preceding expressions for relaxation and retardation time spectra, the temperature appears only in a minor role in the rubber elasticity term. Yet the sensitivity of viscoelastic properties to changes in temperature is one of the striking features of viscoelastic behaviour. It is fairly apparent that the temperature influence must be exerted through the frictional constants invoked by all

the molecular theories.

The monomeric friction coefficient, ζ_o, as defined under Eqn. 2.110 can be related to the diffusion coefficient D by the Einstein expression (102):-

$$D = \frac{RT}{n\zeta_o} \qquad 2.113$$

Bueche (103) has obtained an expression for the diffusion coefficient by a direct walk analysis as:=

$$D = \frac{a^2 J}{2 n} \qquad 2.114$$

where a is the average distance moved by a chain atom in a single 'jump,'

J is the jump frequency

n is the number of atoms

From Eqn.2.114 and 2.114 therefore,

$$\zeta_o = \frac{2kT}{a^2 J} \qquad 2.115$$

Bueche then proceeded to estimate the average jump frequency (J) with which a polymer segment moves. This is taken as to be proportional to the probability of an enthalpy greater than some minimum activation energy being localized on neighbouring segments, the co-operation of which is necessary for rearrangement to occur. Bueche's expression for J based on Einstein's distribution function (102) is difficult to apply directly.

Fox et al (104) by analogy with Eyring's basic equation (105):-

$$J = K \frac{kT}{h} e^{-\Delta G/RT} \qquad 2.116$$

obtained Eqn.2.117 below

$$J = K\frac{kT}{h} \left(\frac{e^{\Delta H}}{\alpha g RT}\right) e^{\alpha g \, \Delta H/RT} \qquad 2.117$$

where K is the chance of the activated state passing forward into "reacted state" rather than back to the "unreacted state", and this can be taken as 0.5 in the present application. The term dg expresses the total number of degrees of freedom of the rearranging zone, as g is the number of co-operating monomers and d is the C_p/R per mole of monomer.

Combining Eqn.2115 and 2.117,

$$\zeta_o = \frac{2h}{a^2 K} \left(\frac{e^{\Delta H - \alpha g}}{\alpha g RT}\right) e^{\Delta H/RT} \qquad 2.118$$

Barrer's activated zone theory as described in Section 2.4 can be equally well applied here. Eqn. 2.75 describes the movement of a polymer segment through its surroundings.

It is seen therefore that the activated process in the diffusion of a foreign molecule, and that of the polymer chains themselves are very similar and comparable processes.

2.9. Theory of liquid scintillation counting.

In recent years a method has been developed to detect weak beta emission from isotopes like ^{14}C, or carbon-14, by dissolving or suspending the radioactive sample in a 'scintillating' liquid. This method is known as liquid scintillation counting, and it eliminates, or greatly reduces, the effects of self-absorption and window absorption (106). It has been shown to be capable of high sensitivity and to provide high efficiency for large samples in low-level counting (107). In a binary system, i.e. a liquid scintillator consisting of a fluorescent aromatic solute in a usually aromatic solvent, the passage of an ionizing particle through the solution causes ionization and excitation primarily of the solvent molecules. Subsequently the excitation energy may be transferred to the solute, the fluorescence of which represents the scintillation emission of the binary solution. The emission may be shifted in the wavelength to match the response curve of the photomultiplier tube (which is the detector), by the use of a 'secondary' solute. These processes will now be considered in more detail.

Fluorescence of aromatic compounds.

When an aromatic molecule absorbs ultraviolet radiation, its π electron system is excited from its ground singlet state S_o into one of the excited singlet states S_1, S_2, S_3 ...S_n (Fig.6), Superimposed on each of the electronic levels are vibrational sub-levels, but these are not important and are not considered. There is, however, also a sequence of excited π electron triplet states T_1, T_2, T_3... each lower in energy than the corresponding singlet state. A singlet state is one in which all spins are paired and has no net electro[illegible] magnetic moment, atriplet is formed by spin inversion of an excited singlet state - called 'intersystem crossing' - and is actually a com-

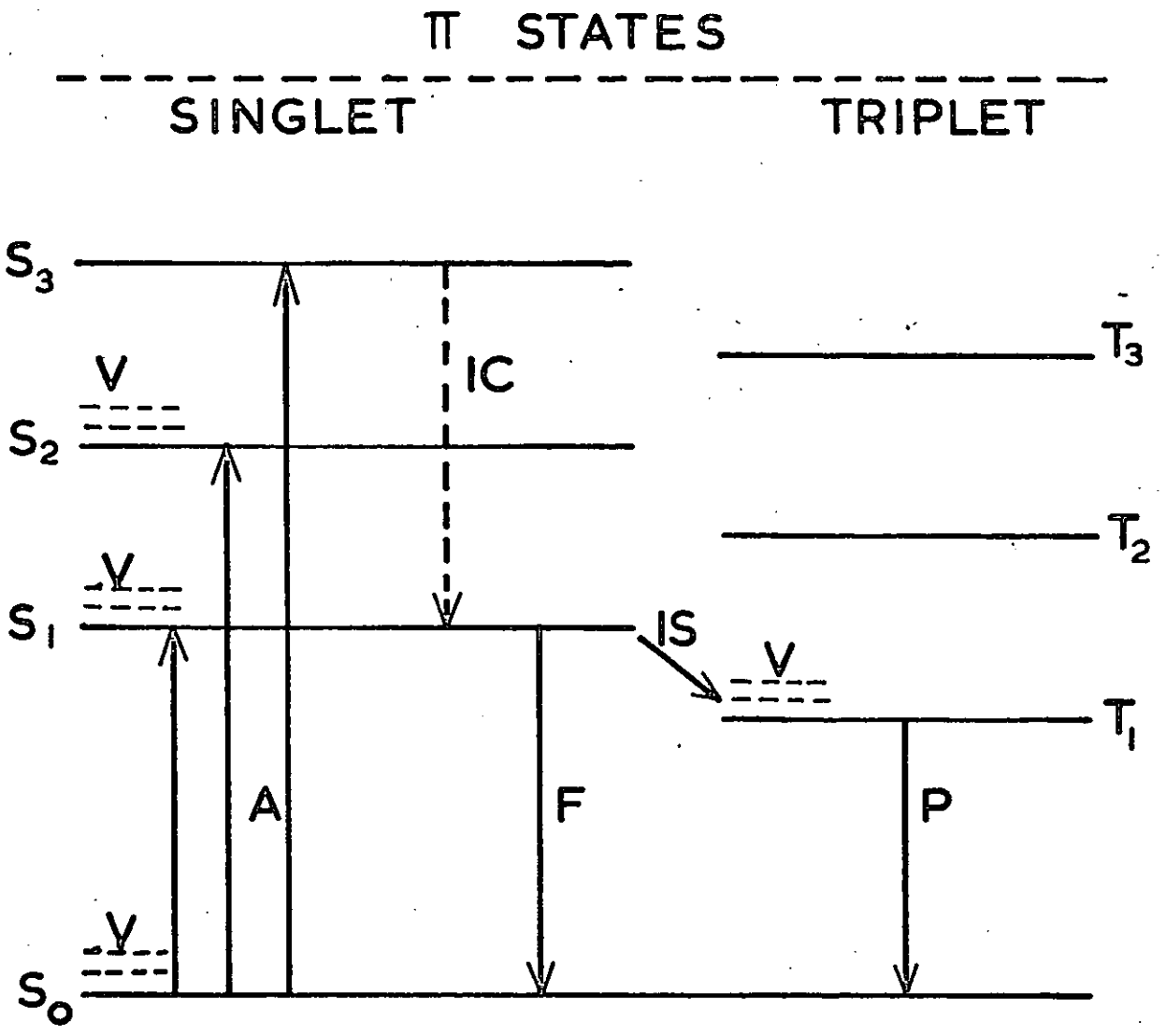

FIG. 6 THE FLUORESCENCE PROCESS

A	ABSORPTION
IC	INTERNAL CONVERSION
IS	INTERSYSTEM CROSSING
F	FLUORESCENCE
P	PHOSPHORESCENCE
V	VIBRATIONAL SUB-LEVELS

bination of three states which differ in orientation of the magnetic moment with respect to arbitrary chosen reference axes (108). At higher energies there is also a series of π-electron excited states.

The excited singlet and triplet states undergo transition to the ground state S_o by the process of fluorescence, phosphorescence, and delayed fluorescence. Fluorescence corresponds to a radiative transition from S_1 to S_o, following absorption. The radiative lifetime of S_1 is approximately 10^{-8} to 10^{-9} second, which is long compared with the period of molecular vibrations (ca. 10^{-12} sec.) so that the molecule reaches thermal equilibrium before emission, and the transition occurs from S_{10}, (the symbol o denotes ground vibrational level).

Phosphorescence is an emission at longer wavelengths than fluorescence, which decays exponentially with a much longer decay time (ca. 10^{-4} sec. or longer). This process is due to the transition of the triplet state T_1 to the ground state S_o.

Alternatively the triplet state T_1 may acquire sufficient thermal energy to return to S_1, leading to delayed emissions. The subsequent $S_1 - S_o$ luminescence has the same spectrum as the normal fluorescence, but its decay period is increased to ca. 10^{-6} sec. or longer.

The fluorescence quantum efficiency, g, of an aromatic compound is defined as the ratio of the number of fluorescent photons emitted to the number of molecules originally excited. For aromatic solvents, such as toluene, g is about 0.1, but for efficient fluorescent solutes used in liquid scintillators, g approaches unity.

The scintillation process (Fig.7)

The scintillator solution consists of a main solvent in which are dissolved a primary solute (scintillator) and in some cases a secondary solute (wavelength shifter). When ionizing radiation falls on this solution, the radiation transfers its energy to the solvent - denoted by X. The concentrations of the solutes are sufficiently small and direct excitation can be neglected. As a result of this energy transfer, the processes occurring in the molecule of X are:-

(1) Excitation into π-singlet states,

(2) π electron ionization

(3) Excitation of other electron states, and

(4) Ionization of electrons other than π electrons.

Process (1) is the cause of main fast scintillation emission. Recombination of ions as a result of process (2) also leads to singlet π excitations, and on de-excitation this also produces scintillations. About 12% of the excited molecules are in excited π-electronic singlet states, the remainder, as in process (3), dissipate their energy thermally and do not therefore contribute to the scintillation. Process (4) leads to temporary or permanent damage. Normally process (1) leads to excitation into S_2 and S_3 singlet states, and the first of the secondary processes is the de-excitation of these states to the S_1 state. This process is known as internal conversion, and is common to all types of organic scintillator systems.

The solvent excitation, S_{1X}, does not remain stationary within the solution. There is thermal diffusion (Brownian motion) of the solute and solvent molecules, and there is also excitation migration between the solvent molecules. This

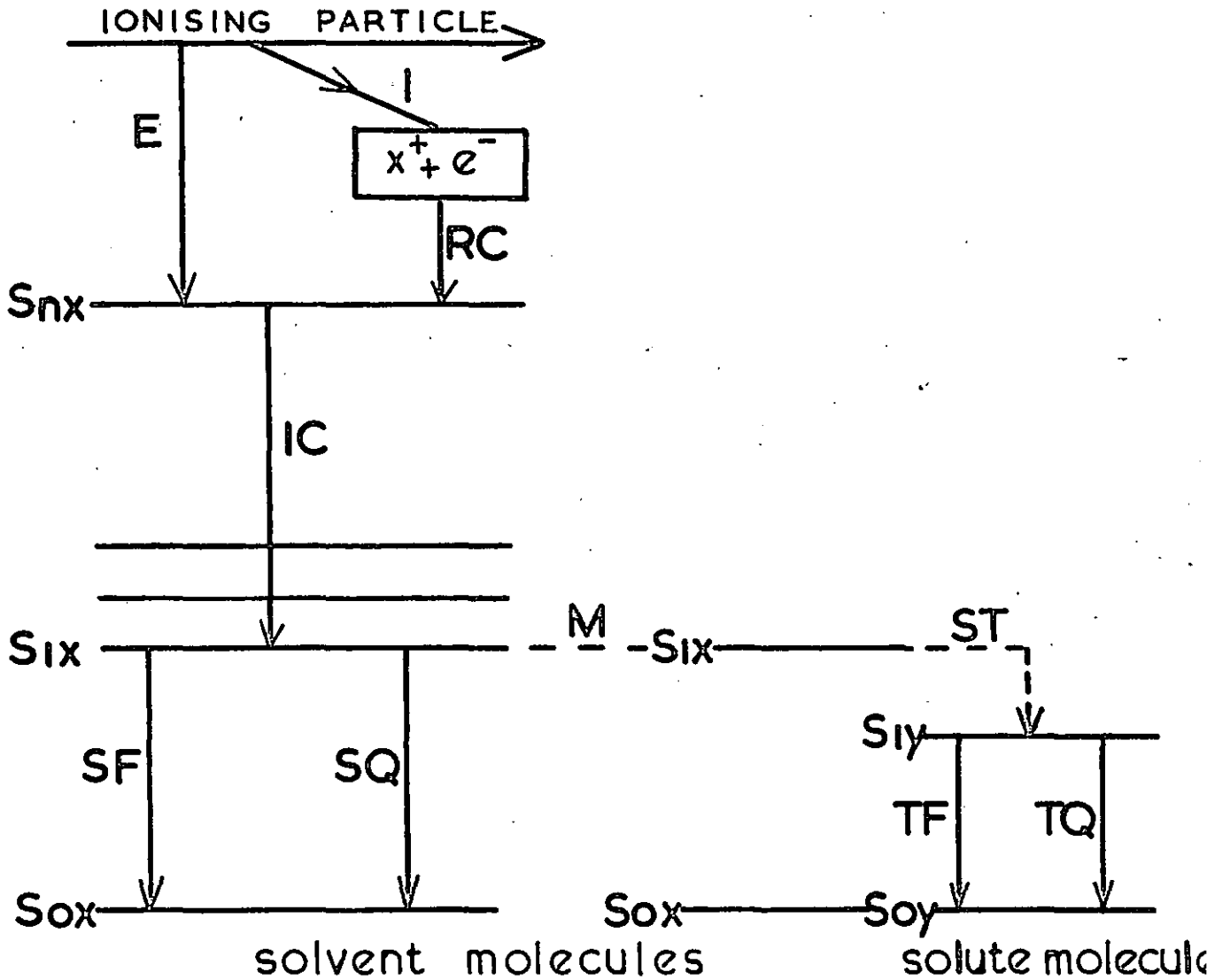

FIG. 7 SCINTILLATION PROCESS IN A BINARY SYSTEM

E	SOLVENT EXCITATION
I	SOLVENT IONISATION
RC	ION RECOMBINATION
M	SOLVENT - SOLVENT MIGRATION AND DIFFUSION
SF	SOLVENT FLUORESCENCE
SQ	SOLVENT INTERNAL QUENCHING
ST	SOLVENT - SOLUTE TRANSFER
IC	INTERNAL CONVERSION
TF	SOLUTE FLUORESCENCE
TQ	SOLUTE INTERNAL QUENCHING

migration process is due to the successive rapid formation and dissociation (in about 10^{-12} sec.) of excited dimers ("excimers") between adjacent excited (S_1) and unexcited (S_o) solvent molecules. Due to the diffusion and migration processes, the solvent excitation S_{1X} moves quickly through the solution until it comes out into the proximity of a solute molecule Y. The latter is chosen to have its lowest excited singlet energy S_{1Y} below S_{1X}. On close approach of the excited solvent molecule and Y, the excitation S_{1X} undergoes solvent-solute energy transfer to Y, where it is rapidly internally converted to S_{1Y}. If the molar concentration of Y is sufficiently high, (1-2 gl^{-1}), the energy transfer quantum efficiency is of the order of unity, so that practically all the excited solvent molecules transfer their energy to the solute, rather than dissipating it by the competing processes of solvent internal quenching or solvent fluorescence (Fig.7).

If a secondary solute (Z) is added, having an S_{1Z} state of energy less than that of Y, this would lead to an extension of the process as described in Fig.7, with further transfer etc. between Y and Z, similar to those between X and Y.

Quenching.

Any soluble material, other than the scintillator solvent and solutes, present in a liquid scintillator may cause a reduction in the scintillation efficiency. This is due to the interference of the impurity which competes with either solute Y or Z for the excitation energy of X, and absorbs this energy but does not give rise to light emission when de-excited. Dissolved oxygen is a quenching agent and does effect considerable pulse height attenuation (109). It must, therefore, be removed by, for

instance, degassing under high vacuum.

Apart from impurity quenching, the addition of highly coloured or opaque materials to the scintillator solution may be deleterious. These substances absorb some of the scintillation light flashes before it reaches the photomultiplier, therefore reducing the output pulse amplitude. Secondary solutes can be advantageous in such circumstances by shifting the spectrum of the scintillation emission to a region in which the specimen is more transparent.

A similar effect, leading to a diminution in the scintillation signal, is produced by dirt or by condensation of water vapour on the specimen vial or the photomultiplier window, and these should be avoided.

The scintillation signal is detected by a photomultiplier tube assembly, the working of which is described in detail in Chapter 4.4.

Choice of scintillator solution and solutes.

Hayes et al (110) compared the relative scintillation efficiencies of 49 carefully purified solvents, each containing 3 gl^{-1} of 2,5-diphenyloxazole (PPO). All but anisole of these solvents were alkyl benzenes. It is therefore rather interesting that n-decane, a saturated hydrocarbon, as used in this work, was found to exhibit good characteristics as a solvent with fair efficiency. It is suggested that excitation of non-π bonds must have been responsible for the excited solvent state, and this is quickly transferred to the solute molecules.

The main compounds which have been used as primary solutes fall into two groups, firstly the oxazole and oxadiazole derivatives, and secondly the substituted p-oligophenylenes.

The practical requirements of a primary solute are good solubility in the solvent, and high quantum efficiency of fluorescence.

A secondary solute does not vary in basic chemical nature from that of a primary solute, and its inclusion in the scintillator mixture to improve the emission spectrum has several advantages. Primarily, it enables more efficient matching of the photomultiplier sensitivity curve (Chapter 4.4); it also lowers the adsorption by the optical system and the walls of the counting vials. A popular secondary solute is 1,4 bis-phenyl oxazolyl benzene (POPOP), which has an emission maximum of 4320 A^{o}. This matches quite well with the sensitivity maximum of about 4000 A^{o} for most E M I photomultiplier tubes (111).

CHAPTER 3

PRELIMINARY INVESTIGATIONS INTO INSTRUMENTATION AND EXPERIMENTATION

3.1. Existing methods of measurement.

The measurement of organic vapour diffusion in polymers can be broadly classified by three methods:-

(1) Membrane permeation methods;

(2) Sorption and desorption methods;

(3) Radiotracer methods;

although some radiotracer methods may involve (1) and (2).

In the permeation method, the polymer in the form of a membrane is placed in such a position within the experimental set up so that the diffusion of the penetrant in the polymer may be followed by measuring the flux, or amount permeated per second, through the membrane. The calculation of the diffusion coefficient, D, from the flux, F, has been given in Chapter 2.2. In the simplest case,

$$F = D \frac{\Delta C}{l} \qquad 3.1$$

where ΔC is the concentration difference across the membrane, and l is the membrane thickness.

There are many methods of measuring the flux, F. One of the best known methods is the one used by Barrer (77), where the flux is measured by the increase in pressure in an initially evacuated and degassed chamber separated from the solvent vapour chamber by the polymer membrane. A sensitive Macleod gauge is used for measuring the pressure increase. Alternatively, a Bourdon gauge may be used (112). The flux may also be obtained by condensing the vapour permeated, and then transferring it

periodically to vapourise in a known space where the pressure is then measured (113). Most recently Pasternak et al (114) have devised and patented a method where the flux is measured by using a carrier gas which sweeps away the permeated vapour continuously, the amount of which is detected by a thermo-conductivity cell. Other methods include the use of mass spectrometry (115), chemical analysis (116), radiotracers (117), and gas chromatography. All these methods require a concentration gradient of the penetrant across the polymer membrane. The concentration is determined separately usually by the equilibrium uptake of the vapour by the polymer under steady conditions, in a sorption method.

The sorption method is a rapid method of determining the diffusion coefficients, as during the early stages the mass uptake of the vapour (M_t) at time t, and the equilibrium mass uptake (M_∞) are related to the diffusion coefficient D by the expression (See Eqn.2.41)

$$\frac{M_t}{M_\infty} = \frac{4}{l}\left(\frac{Dt}{\pi}\right)^{1/2} \qquad 3.2$$

where l is the thickness of the membrane.

The quantities M_t and M_∞ can be determined by a wide variety of methods. The use of a sensitive helical quartz spring from which the polymer is suspended, is probably the most common (118). The increase in weight is given by the extension of the spring, which can be measured by using a cathetometer. Other methods which have been used to determine the amount sorbed or desorbed involve the following:- dielectric measurements (119), tungsten helical spring (120-122), sensitive stress gauge (123), electrical balance (124,125), measurement of the volume change of the ambient vapour (126), use of radioisotopes (118-127), and direct weighing (39, 52).

The use of radiotracers in permeation and sorption methods have already been mentioned (117, 118, 127). In the case of permeation, the radioactive vapour permeated is transferred by a current of alcohol vapour to the measuring apparatus. In the sorption method of Park (127) the polymer is first "saturated" with a radioactive vapour, and the amount sorbed is determined by replacing the radioactive with the non-radioactive vapour, and analysing the vapour periodically by counting with a Geiger tube.

Another method of employing radiotracers to measure the diffusion coefficient at a fixed concentration level is the so-called "composite layer" method (9,10,128-131). In a typical case a very thin film of radioactive-labelled penetrant saturated polymer was applied on top of a thicker film of unlabelled penetrant saturated polymer. Assuming that the β-particle absorption follows a logarithmic law, theoretical curves of log D against I can be constructed, where I is the observed activity and D is the diffusion coefficient. By comparison of these curves with the experimental ones of log (time) against log I, values of the diffusion coefficient can be calculated (9). With soft beta emitters and thick polymer specimens, it is sometimes sufficiently accurate to assume that the measured activity is directly proportional to the concentration of the labelled compound at the surface (132).

3.2. Introduction of present method.

The permeation method described in 3.1 has the disadvantage that a concentration gradient is required. Thus besides the physical difficulties of membrane distortion due to the pressure difference, incomplete degassing which may lead to "false" pressure increases, and other complications involved with measuring vapour pressure with a delicate instrument like the Macleod gauge, the value of the diffusion coefficient obtained, (which may be concentration dependent), is the mean diffusion coefficient over the concentration range involved (see Chapter 2.2).

The sorption method has the same problem. Also if the diffusion coefficient is large, then the kinetics cannot be adequately followed.

The "composite layer" method of Moore and Ferry (132) appears to give a result for diffusion coefficient at a fixed concentration level. However the mathematics involved is complicated, and not fully justifiable, since the counting efficiency of the Geiger counter itself may vary as the labelled molecules move nearer (133). Also the efficiency of a thin end-window Geiger-Muller tube when detecting beta-emitters is very low, and a high margin of errors has been allowed in such an experiment (129).

Thus a new method has been designed which it is hoped will provide a simple, precise, and efficient way of measuring the diffusion coefficient of an organic vapour in polymers. The method involves the exchange of labelled and unlabelled solvent molecules through the polymer membrane. Schematically the method is illustrated in Fig.8. The dark dots represent the

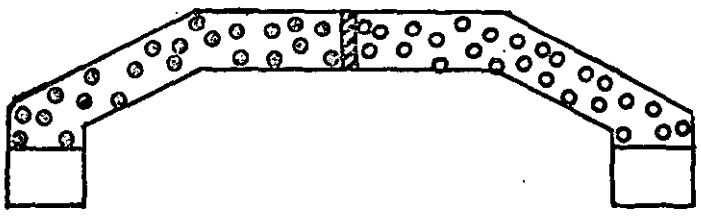

(a)

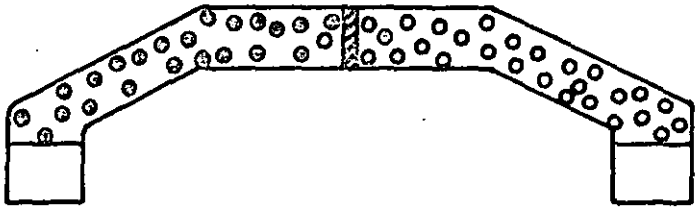

(b)

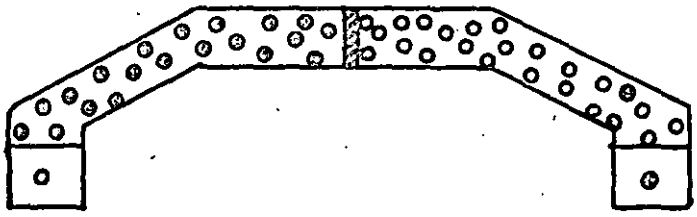

(c)

FIG. 8

radioactively labelled molecules, and the white circles represent the otherwise identical but unlabelled molecules. In Fig. 8(a) the polymer membrane separates the two types of molecules in contact with their liquid reservoirs which control their vapour pressures, i.e. concentrations in the gaseous phase. These molecules undergo random thermal motions and after a time t, some mutual exchange through the polymer will occur, the molecules first dissolving in the polymer then evaporating. This is shown in Fig. 8(b). Again by random motion, as shown in Fig. 8(c), the permeated molecule goes into solution in the opposite reservoir. Since the motion of molecules in the gaseous phase (in the absence of all other gas molecules) is many times faster than the motion of the molecules in either the liquid phase or the polymer, and provided the liquid reservoirs contain many more molecules than the ones exchanged, the rate of increase of, say, the dark molecules in the non-labelled reservoir can be taken as the rate of permeation through the polymer. This rate of increase is measured by employing a solute in the liquid reservoir which becomes fluorescent when in contact with radioactive molecules (see Chapter 2.9).

The non-radioactive molecules act as the solvent in the liquid scintillation mixture. The whole liquid scintillator reservoir is enclosed in a completely light-tight compartment which enables the photons emitted as a result of fluorescence to be counted by a photomultiplier-counter assembly.

Since there is a uniform concentration of the penetrant molecules throughout the polymer, with a concentration gradient of the radioactive molecules, the self diffusion coefficient of

the penetrant molecules at a precise concentration level can be evaluated, because the movement of the radioactive molecules can be followed.

The method involves no pressure difference, no necessity of employing complicated measuring devices, and it is rapid and accurate. The limitation of the present apparatus is the temperature range practicable (See Chapter 4), but this can be improved with further design.

3.3. The Apparatus.

The apparatus is shown diagrammatically in Fig. 9. A glass diffusion line was used, and the temperatures of the penetrant reservoir, diffusion cell, and 'collecting' cell were controlled by different water baths thermostated to $\pm$ 0.1°C.

The radioactive penetrant is placed in the container R which is joined to the main frame by a cone-and-socket connection, H_2, which is sealed by mercury. The temperature of the liquid in R is controlled by the thermostat bath A.

The diffusion cell D consists of two flatly ground glass flanges held together by three threaded bolts and nuts, as shown in Fig.10. The polymer membrane is placed between the flanges. The whole cell is immersed in a thermostat bath B.

The liquid scintillator is placed in the collecting vessel C, which is also connected to the main frame by a cone-and socket joint H_1, sealed by mercury. The temperature is controlled by circulating water from a thermostat bath through the jacket J.

The exposed parts of the diffusion line are heated by electro-thermal tapes, to prevent the existence of "cold" areas where vapours may condense.

The whole diffusion line is separated from the high vacuum line by two grease-less taps G_1 and G_2, which are made of poly (tetrafluoroethylene) (PTFE) plungers and seals fitted within glass containers (Jencons).

The 'collecting' vessel C is situated above the photo-multiplier assembly PM, which in turn is situated within the lead castle P. The whole of the vessel C is painted black, so that there is no transmission of light to the photomultiplier

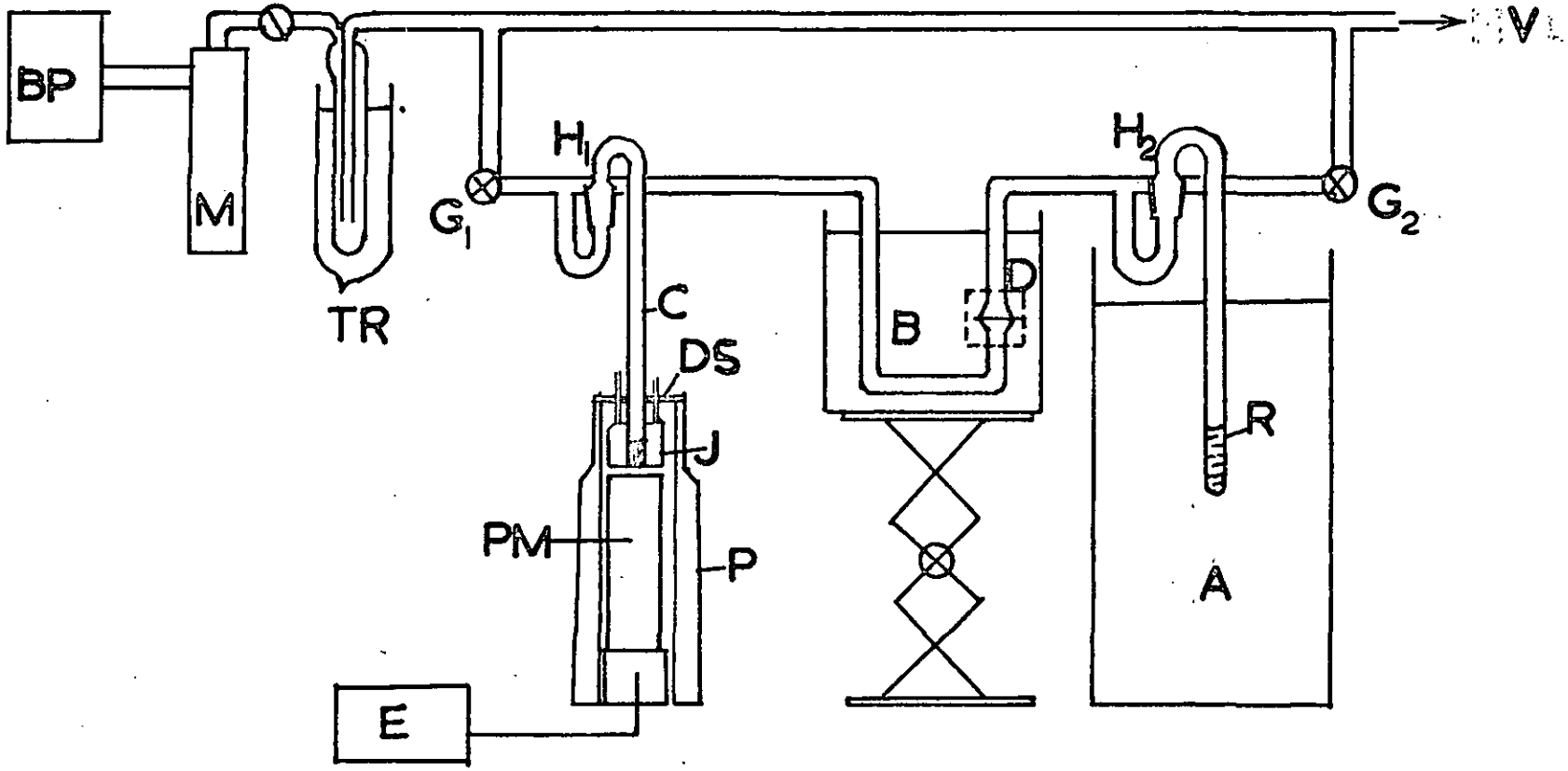

FIG. 9

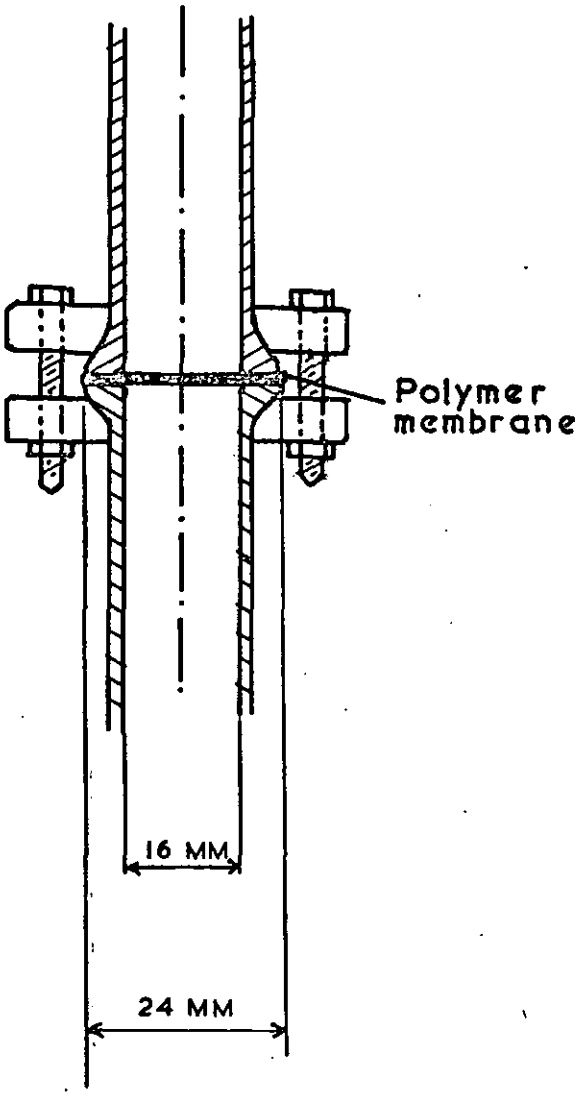

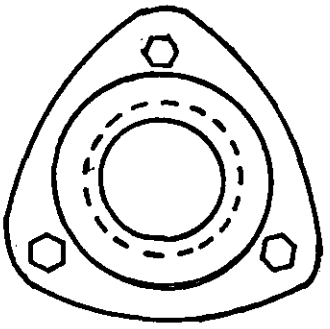

Plan

FIG. 10

tube from the surroundings. A polyester disc DS is "cemented" to the vessel C by applying a polyester resin which is then crosslinked by amines. This disc rests exactly on top of the lead castle, and black adhesive tape is wrapped round the junction to ensure no light is penetrated.

The photomultiplier tube (see Chapter 4) is connected through an emitter follower to the electronic counter E.

The high vacuum line (see Chapter 4) produces a vacuum of 10^{-3} mm Hg, and the pressure is measured by a vacuostat gauge.

3.4. Procedure.

The apparatus is assembled by first pipetting 1 ml of radioactive penetrant into the vessel R, and 6 ml of scintillator into C, which are then inserted onto the main frame line. The polymer membrane, in the form of a circular disc with a diameter equal to the outer diameter of the diffusion cell is carefully inserted between the flanges in the diffusional cell, and cautiously clamped. The penetrant and the scintillator are then frozen by methanol/solid carbon dioxide mixture ($-70^{\circ}C$), after which the system is opened to the high vacuum line whereby the air is removed. The system is then closed to the vacuum line, and the frozen liquids allowed to melt, when most of the dissolved gases will vapourise into the evacuated space. This degassing procedure is repeated four or five times until no significant increase in pressure is observed on melting of the solvents.

The three thermostat baths are brought into operation, and a short time lapse (10 minutes) is allowed for the various parts of the system to reach thermal equilibrium.

The increase in count rate with time is then noted and plotted to give a linear relationship the slope of which represents the permeation rate.

3.5. Polymer specimens and materials.

The polymer used for this part of the work was silicone rubber (polymethylvinylsiloxane) crosslinked with 2% "Perkadox" (containing 2,4 Dichlorobenzoyl peroxide in plasticizer). This rubber was moulded in a press for 7 minutes and 230°F, and the product was in the form of a membrane of uniform thickness 0.5 mm ± 0.02 mm.

The radioactive penetrant was 1 - ^{14}C labelled n-decane with an activity of 0.3 mCi/mM, diluted to about 4×10^4 times its original volume with non-active n-decane.

The scintillator was prepared in a similar way as described in Chapter 4. This consists of 0.5% by weight of 2,5 - diphenyloxazole (PPO) dissolved in redistilled n-decane. The suitability of this solution as a scintillator was tested by adding known quantities of active penetrant, as prepared above, to the scintillator, and measuring the count rate increase. A linear relationship was observed (Fig.11). The calibration was repeated with a more universal scintillator solution containing 0.5% PPO and 0.03% POPOP (1,4 bis-phenyl-oxazolyl benzene) in toluene. Evidently the n-decane scintillator was found to be less efficient. The reason for this has been explained in Section 2.9. It is satisfactory to note that there is no self-quenching which, if present, will be shown by a "tailing off" shape in the calibration curve.

The vapour pressure-temperature relationship of n-decane was calculated from Marsden's (134) experimental data using the Clausius-Clapeyron equation

$$\log P = -2336/T + 8.1228 \qquad 3.3$$

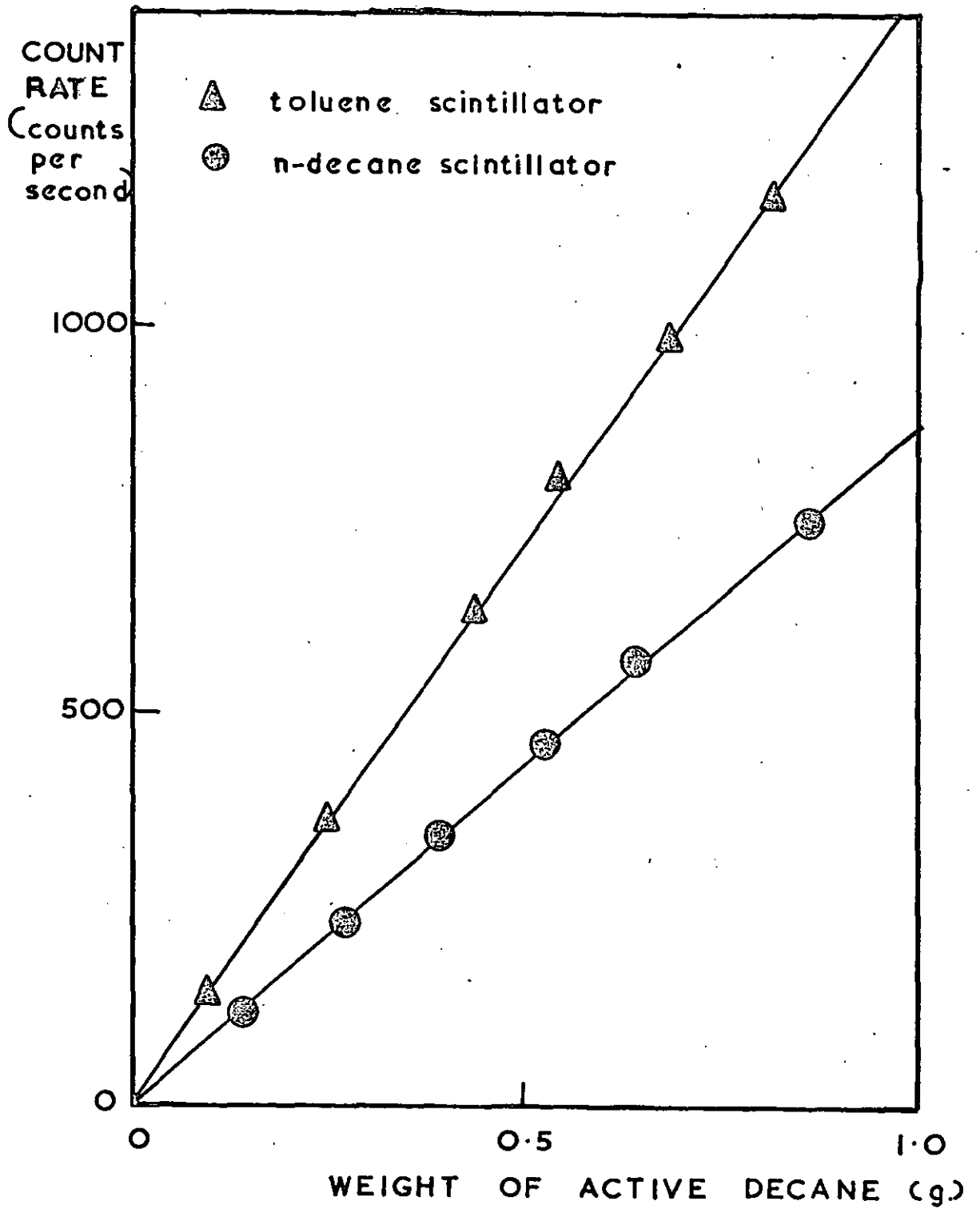
COUNT RATE (counts per second)
toluene scintillator
n-decane scintillator
1000
500
0
0
0·5
1·0
WEIGHT OF ACTIVE DECANE (g.)

FIG. 11

where P is the vapour pressure in mm. of Hg

and T is the absolute temperature.

The relationship is shown graphically in Fig.12.

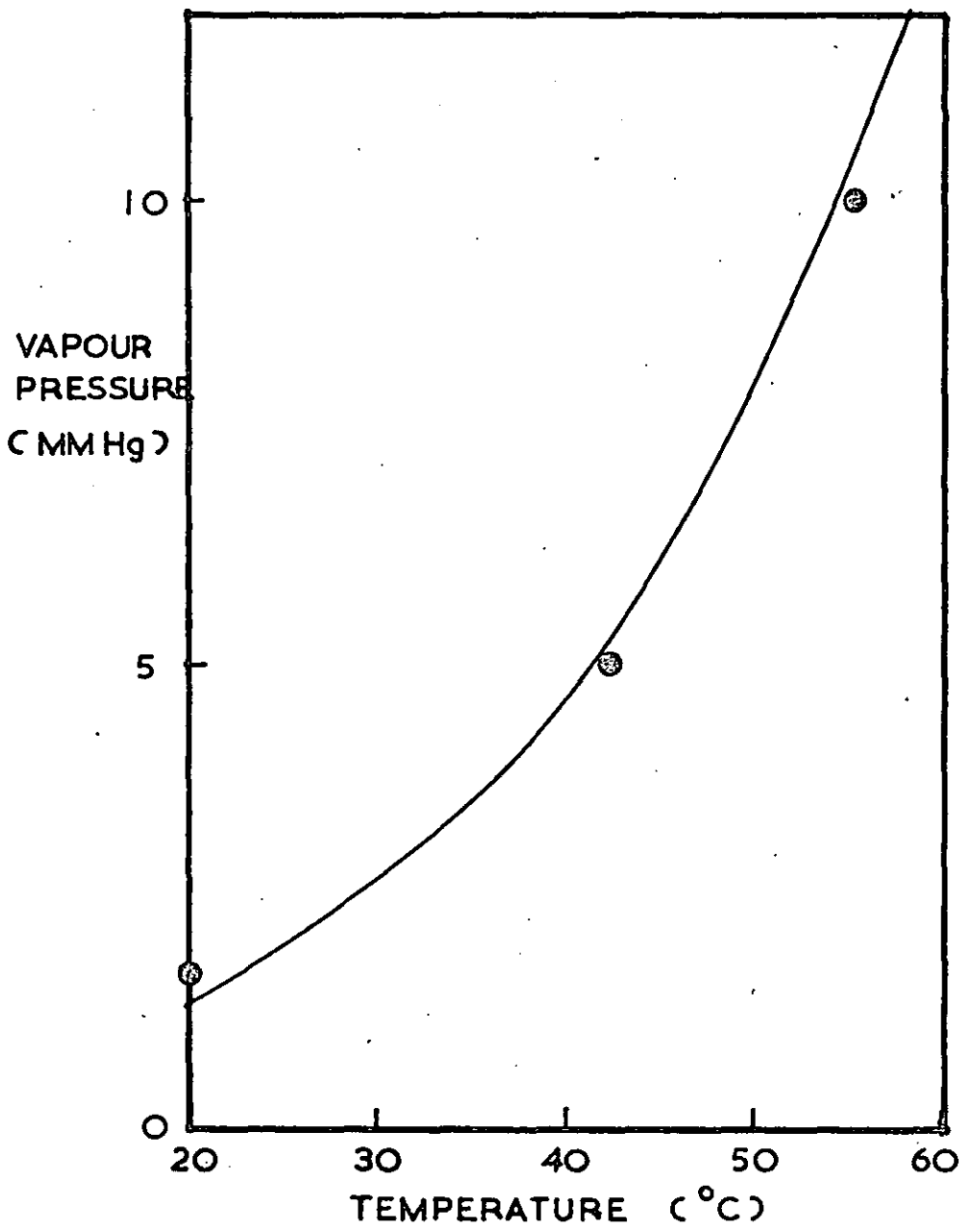

FIG. 12

line - calculated curve

⊙ - Marsden's experimental points (134)

3.6. Counter Characteristics.

The presence of noise in electronic circuits is always a source of interference and error in taking measurements. The detailed construction and working of the photomultiplier tube and the counter is given in Chapter 4, and will not be repeated here. It is sufficient to give a summary of the process of detecting photons being liberated in the liquid scintillator solution due to radioactivity.

Each radioactive disintegration will result in outgoing photons which, after striking the cathode in the photomultiplier tube, will be accelerated downwards through a series of dynodes to produce an electron current of certain strength. This electron current is then sent to the counter by an emitter follower in the form of an electronic pulse signal. The pulse height will be proportional to the number of photons which hit the cathode, and the voltage applied across the photomultiplier. The number of counts per second measured will be proportional to the number of disintegrations per second, i.e. the strength of the radioactivity. Noise in the electronics will give rise to pulses which may also be registered in the counter. But since these noise pulses usually have smaller pulse heights than the corresponding pulse heights due to radioactive disintegrations, they may be eliminated by using a discriminator or screen device which eliminates pulses below a certain set magnitude. The optimum high tension voltage (H.T.V.) and the discriminator bias setting (D.V.) may be determined as follows:

The efficiency of count (given by the ratio of counts per second measured to the actual no. of disintegrations per second) is plotted against increasing H.T.V. (Note that the source count is obtained by substracting the background count from the total

count observed). This will assume the shape shown in Fig(13). where a plateau region is reached after sufficiently high voltage is reached. The final H.T.V. chosen must lie within this region for two reasons:-

(1) The plateau region indicates that all pulses due to radioactive disintegrations are detected;

(2) A fluctuation in the H.T.V. will not cause any great change in the count rate measured.

The discriminator bias voltage is introduced, at a fixed H.T.V., and the source and background counts are measured with increasing discriminator voltage. The introduction of the discriminator bias voltage will not only eliminate most of the noise pulses, but it will also prevent some of the smaller source pulses from being detected. Thus the efficiency of count may be lowered with increasing discriminator voltage. From a plot of background count against discriminator setting, a value of D.V. is selected which eliminates most background noise (Fig.14).

The optimum H.T.V. is then selected using this discriminator setting,,by plotting (source count)^2/(Background) against increasing H.T.V. (Fig.15). A peak is shown, the position of which gives the optimum H.T.V.

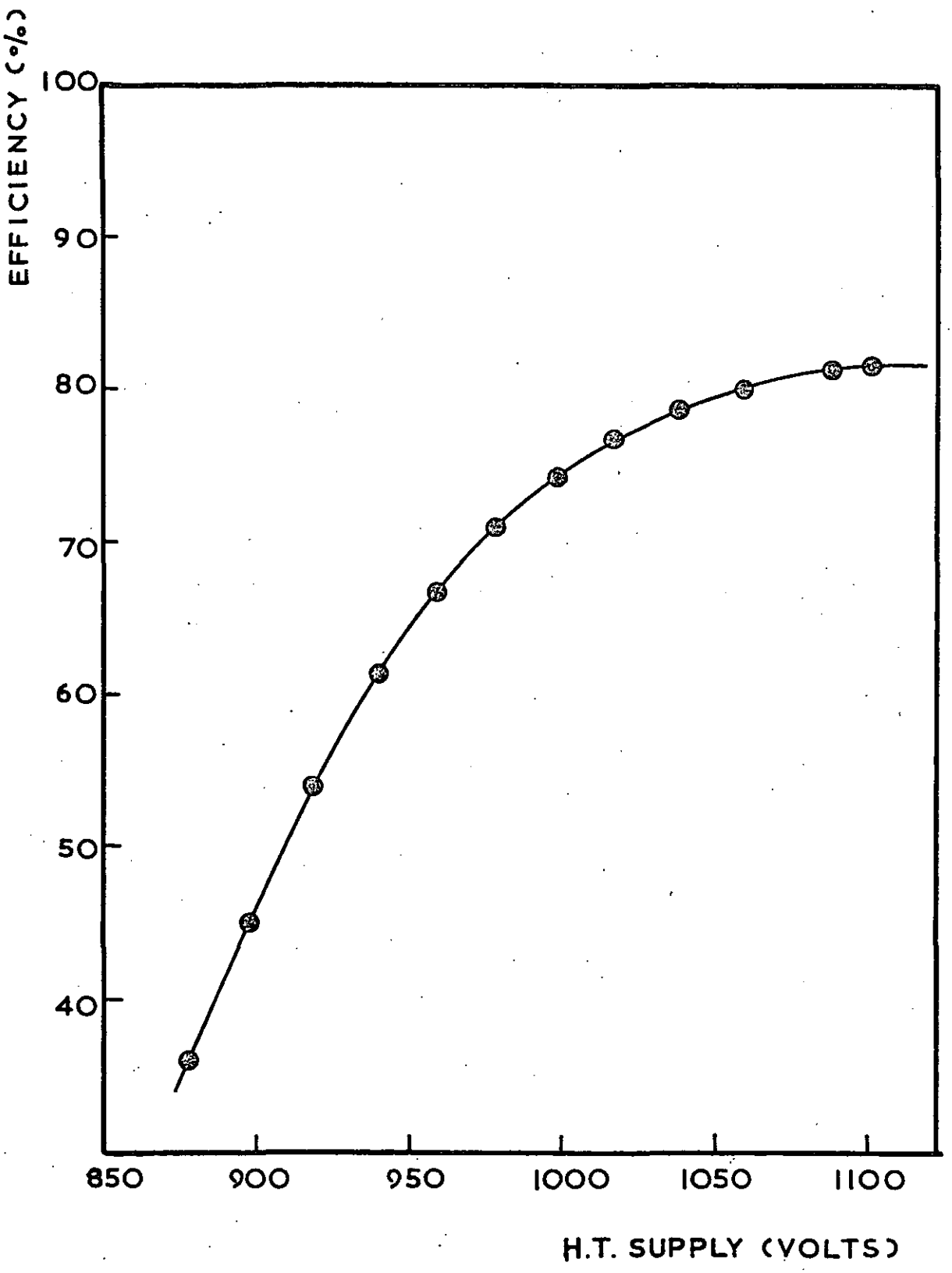
EFFICIENCY (%)
100
90
80
70
60
50
40
850
900
950
1000
1050
1100
H.T. SUPPLY (VOLTS)

FIG. 13

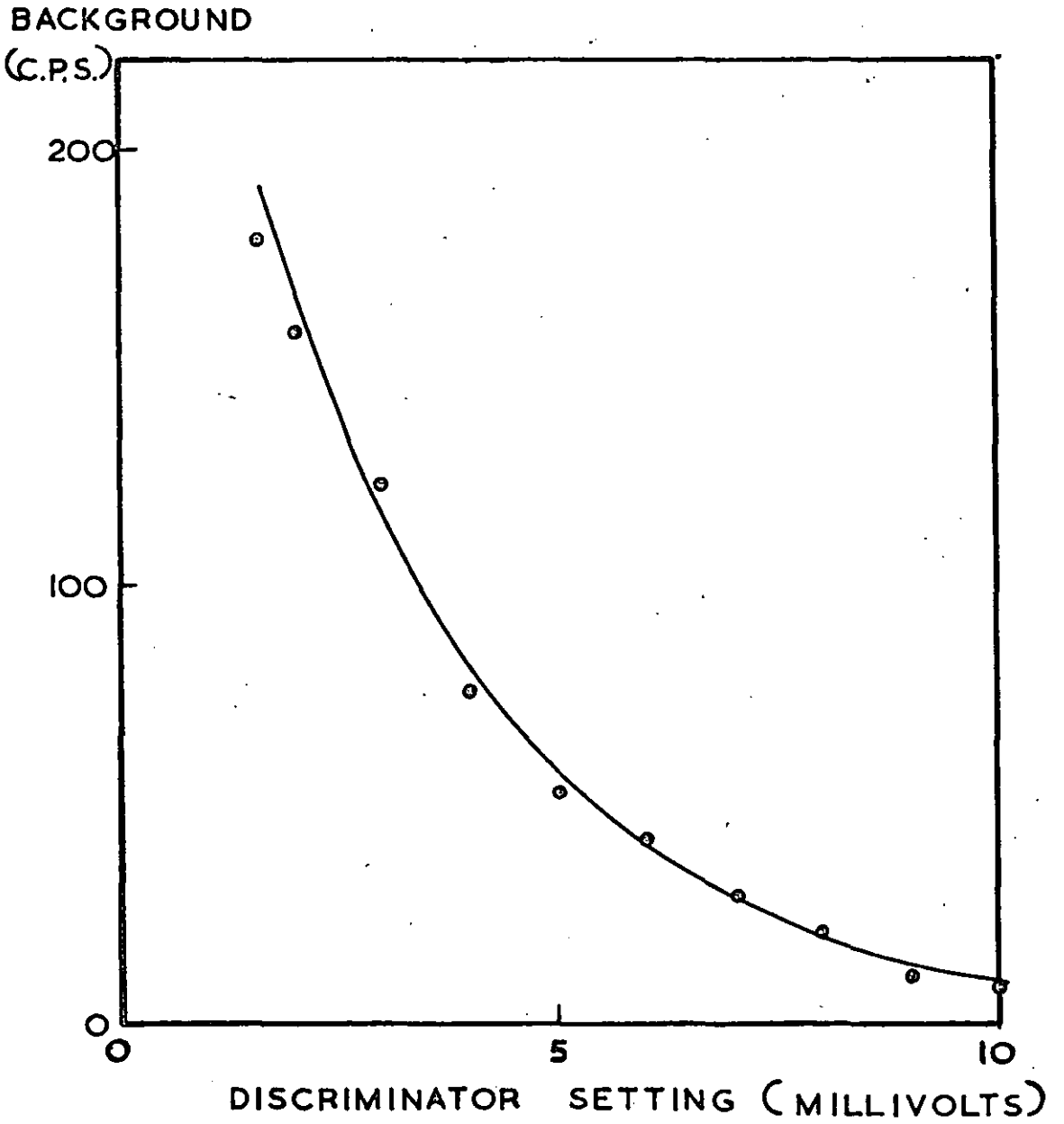
BACKGROUND
(C.P.S.)
200
100
0
0
5
10
DISCRIMINATOR SETTING (MILLIVOLTS)

FIG. 14

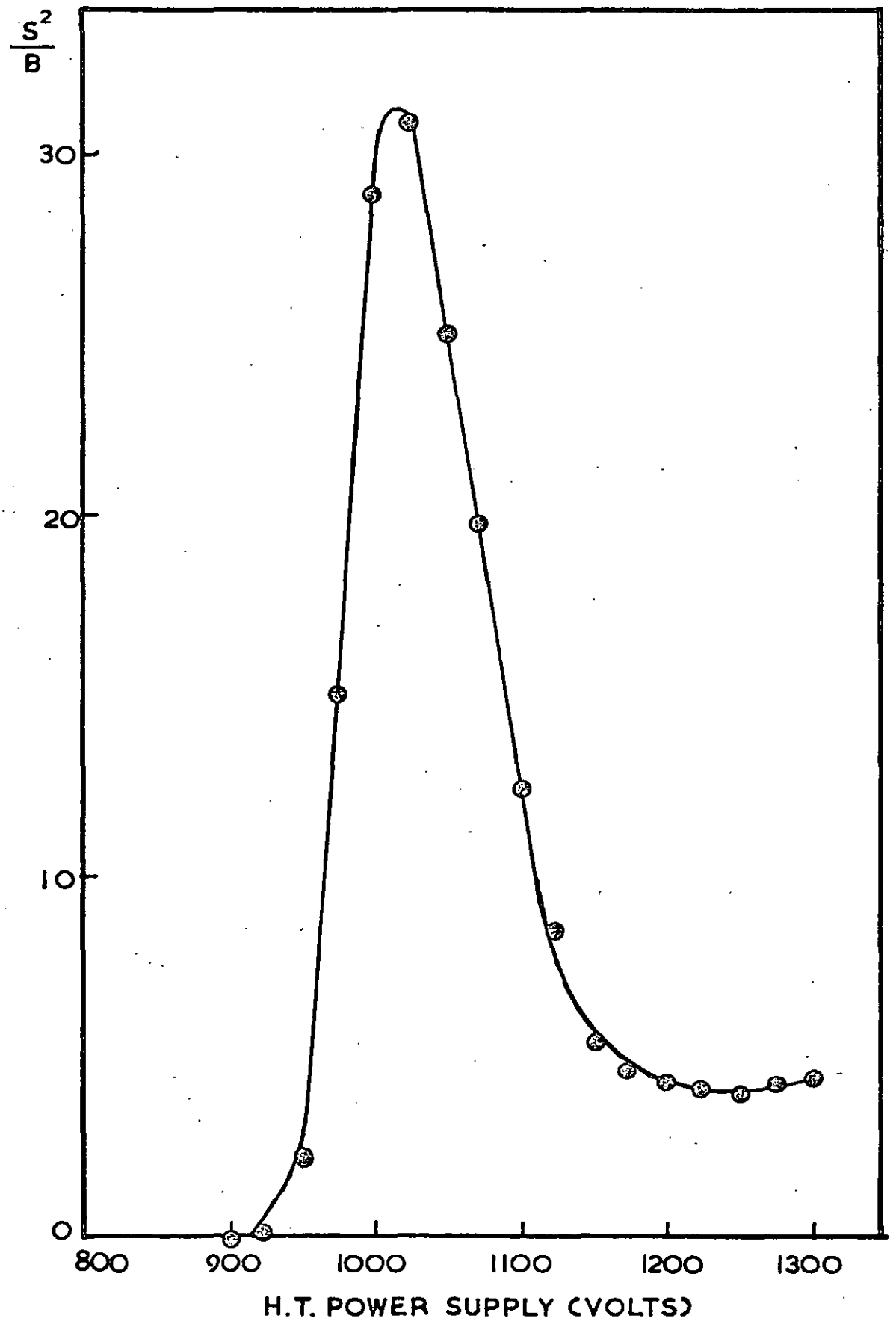
$\frac{S^2}{B}$
30
20
10
0
800
900
1000
1100
1200
1300
H.T. POWER SUPPLY (VOLTS)

FIG. 15

3.7 External factors affecting the photomultiplier tube signal.

The noise pulses inherent in the photomultiplier tube are not constant but vary with temperature primarily. If the collecting vessel C in Fig. 9 is in physical contact with the top of the photomultiplier tube, (as was originally the case to improve optical transmission), any variation in the temperature of the circulating water in the jacket J will have a drastic effect on the noise pulse level measured. This is illustrated in Fig.16.

To minimise heat transfer from the temperature jacket to the photomultiplier tube, an air gap is introduced. This reduces the number of photons reaching the cathode and so lowers the efficiency of count in the presence of a discriminator. The loss in efficiency with the bottom of the scintillator cell approximately 1.5 mm. away from the cathode face was found to be about 20% of the original efficiency. This is a necessary sacrifice. Although the conduction of heat through air is poor, a stream of cooled air was circulated in the space between the collecting vessel and the photomultiplier tube to ensure constant low noise level. This was done by drilling two holes through the polyester disk (DS in Fig. 9) and inserting two darkened rubber tubes, which acted as inlet and outlet of the cooled, dried air respectively. A compressed nitrogen gas cylinder may be used, and it may be cooled by passing through a methanol/carbon dioxide cold trap.

The use of nitrogen has another advantage. It flushes out the atmospheric air within the lead castle, so that condensation of water vapour on the collecting cell and photomultiplier tube is not a problem. Water condensation, otherwise a likely occurrence especially on freezing the scintillator, not only causes a "colour quenching" effect (see S.9), i.e. poor photo

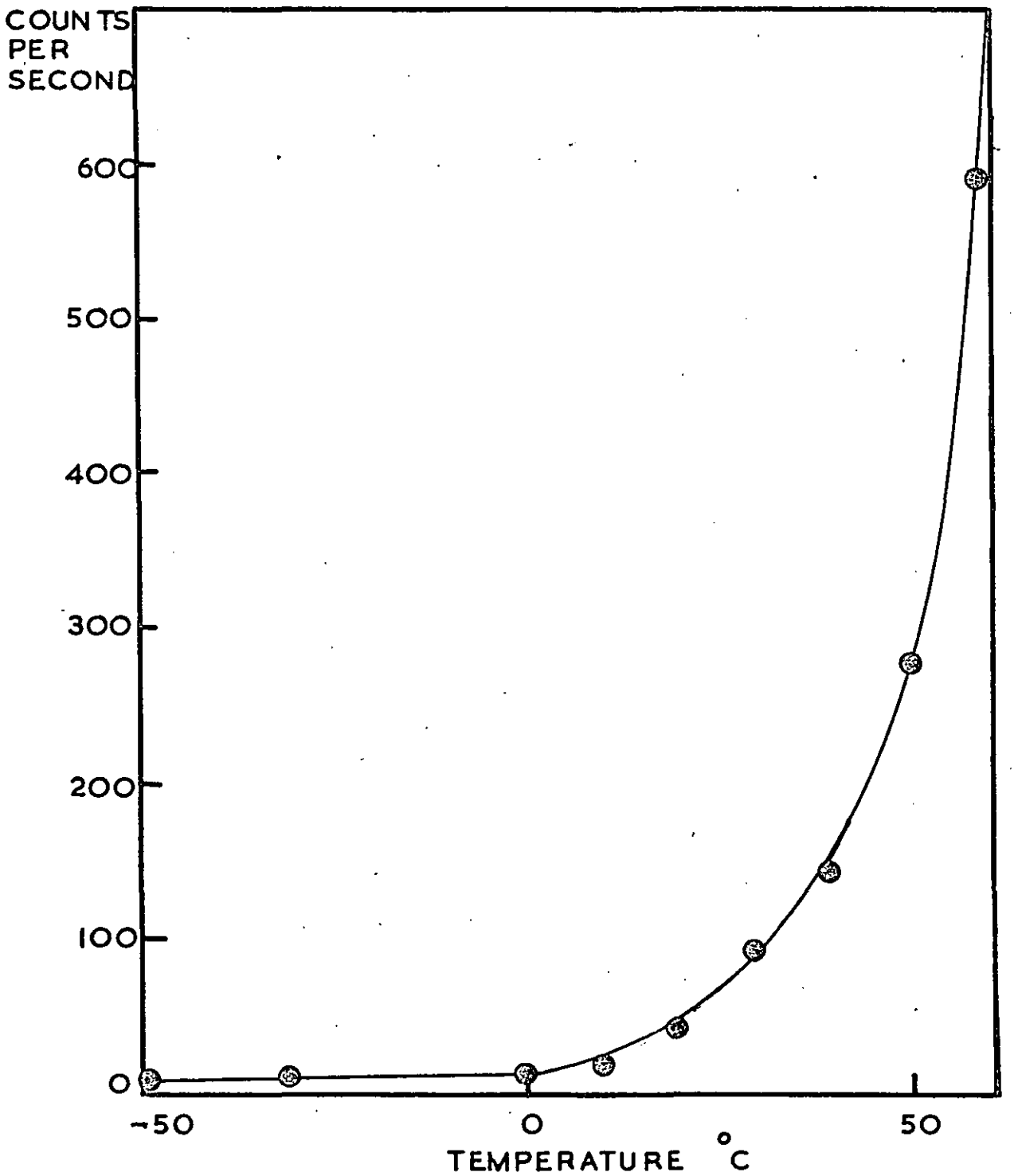

FIG. 16 NOISE VARIATION WITH TEMPERATURE

transmission, but it may also cause short contacts in the electronic circuits within the assembly.

The exposure of the photomultiplier tube to any light "leaks" will not only cause a sudden and large increase in the count rate, but it will also damage the instrument. Thus it is very important that the whole system on the collecting cell side must be perfectly light-tight.

3.8. Limitations and errors of the method.

The long and winding path which the penetrant molecules have to travel from the solvent reservoir to the collecting cell makes it difficult to assume that the time taken for this gaseous diffusion is so short compared to the diffusion in the polymer as to be insignificant, especially if the vacuum is not sufficiently high. Thus the count rate increase will measure the combined permeation of the molecules through the polymer and through the gas. In the case of mass flow where the collecting cell is kept at a lower temperature than that of the solvent reservoir, the flow of the molecules in the gaseous state will be very much faster due to a "distillation" type of behaviour, and the rate of permeation measured will correspond to the permeation rate in the polymer. But since this involves a concentration gradient of penetrant across the polymer, one of the basic aims of the experiment is not satisfied, and a new experimental design is required.

Also in this method it was a tedious process to assemble and clean the diffusion line. The greaseless taps used which employed PTFE plungers and screw threads were rather fragile and were found to distort out of alignment after a period of use. The glass apparatus makes it especially vulnerable to light penetration into the photomultiplier compartment, as light can be reflected from the inside walls of the diffusion line which is painted black. The diffusion cell, too, needs improvement, as no provision was made to fix the polymer in position, and hard clamping of the polymer may do physical damage to the polymer around the edges.

A new permeation apparatus was designed and is described in the next chapter. This apparatus is made from metal, which eliminates the light leak problem. It is geometrically compact and easy to assemble, and is fixed in position with respect to the photomultiplier tube. The diffusion path of the gas molecules is short, wide and straight, and the permeation rate measured is the permeation rate through the polymer. Metal greaseless high vacuum taps were used, which are not physically distortable. A metal grid support was inserted to prevent the polymer sagging, should there be any swelling.

CHAPTER 4

EXPERIMENTAL

4.1. Construction of the permeation cell.

The cross-section view of the assembled apparatus (to scale) is shown in Fig.17. The top section of the cell consists of two brass components which have been hollowed and shaped from solid brass cylinders on a lathe. These components (the light and heavy right-slanting shaded parts in Fig.17) were joined together by 'sweat' soldering.

The bottom section was similarly machined from a solid brass cylinder. In addition holes were drilled through the sides for vacuum, water, and nitrogen inlets. This main section was joined to the metal part of a glass-to-metal seal, MG, by soldering. The glass part of the seal was in fact fused on to a flat glass plate to form the bottom "window" of the scintillator cell, L.

The top and bottom sections are assembled by the metal collar, R. Four diagonally placed screws, A, can be tightened into the main bottom block, thus clamping the polymer specimen, P, which has been placed in position. A metal grid, G, is placed beneath the polymer, and this serves two purposes. It defines the exact area across which transfer occurs, and it keeps the polymer horizontal, i.e, prevents any "sagging."

The whole apparatus is connected to the high vacuum line via two metal high vacuum stopcocks GT1 and GT2 (Hoke 4111M2B), 1/16" copper pipings were used as the connectors, and joints were made by soft-soldering.

Three copper-constantan thermocouples T1, T2, and T3 were placed respectively in the positions shown in Fig.17. T1

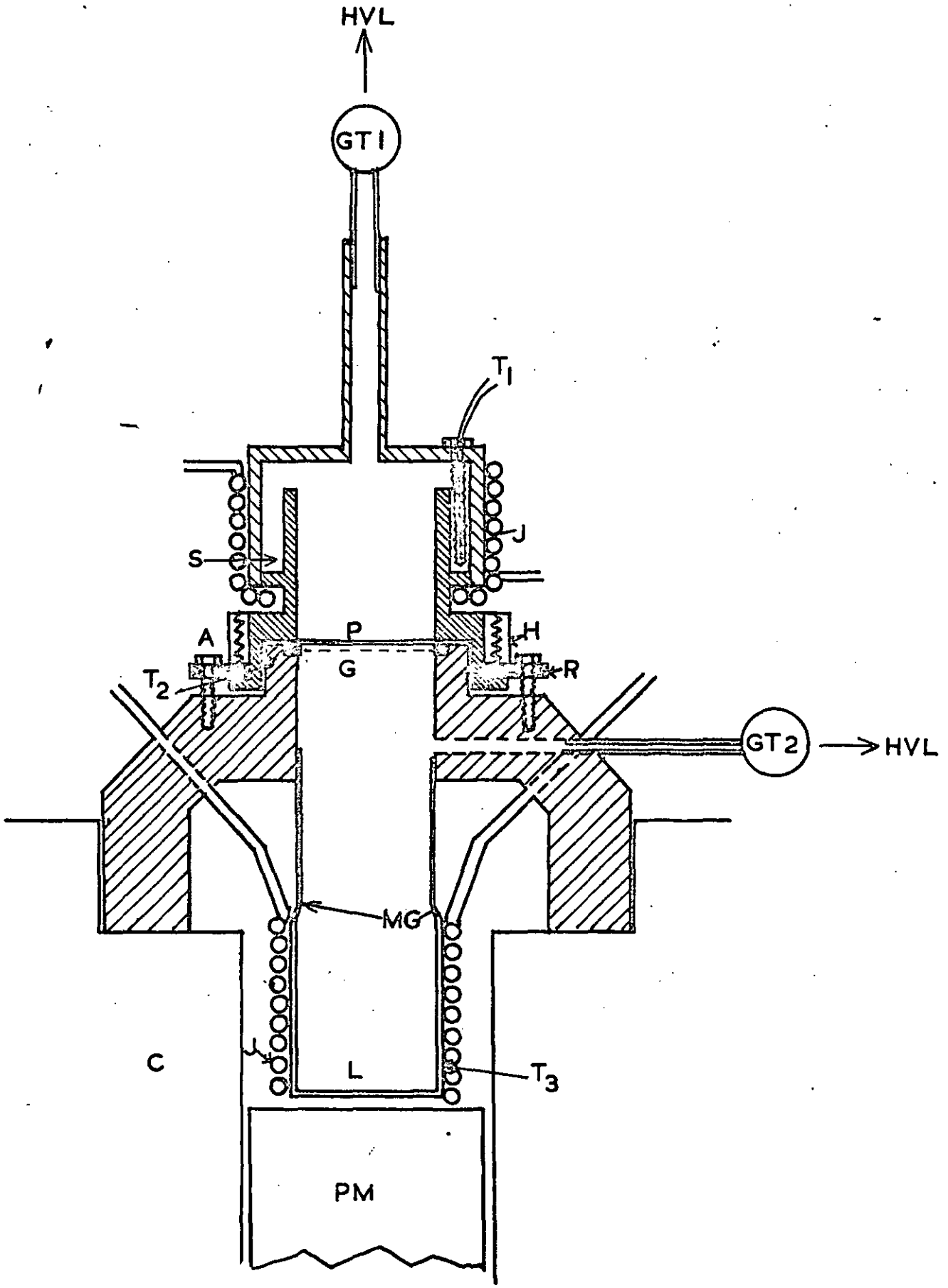

FIG. 17

was inserted in the centre of a screw, X, (This was done by carefully drilling a hole down the middle of the screw without thorough penetration, and placing T1 in this hole). X is removed when filling or emptying the solvent reservoir S. T2 was placed in a little groove by the side of the polymer specimen as shown. T3 was attached to the side of the scintillation cell L.

Thin walled copper pipings (J) were used to control the temperatures of the solvent reservoir and the scintillation cell. These pipings were coiled round the respective parts of the system, and good thermal contact made by poly (dimethyl siloxane) applied in benzene solution and cross-linked in situ with benzoyl peroxide, using a hot-air blower.

The solvent reservoir was then further thermally insulated from the surroundings by a covering of asbestos "paste." This is shown in the photograph in Fig.18.

The coiled piping around the scintillation cell was connected to the "inlets" drilled through the main brass block, by two silicone rubber tubes, as illustrated in Fig.19.

In addition, two other holes were drilled through the main bottom section to accommodate two copper tubes. One was used as inlet for the dried and cooled nitrogen gas (its use is explained in a later section), the other served both as an outlet for this gas, and as an insert for the third thermocouple, T3. Also a passage was drilled horizontally to connect the bottom compartment of the cell to the high vacuum line through the metal stopcock TC2.

The middle part of the assembly is heated electrically by the element H as shown in Fig. 17. Theelement was made by

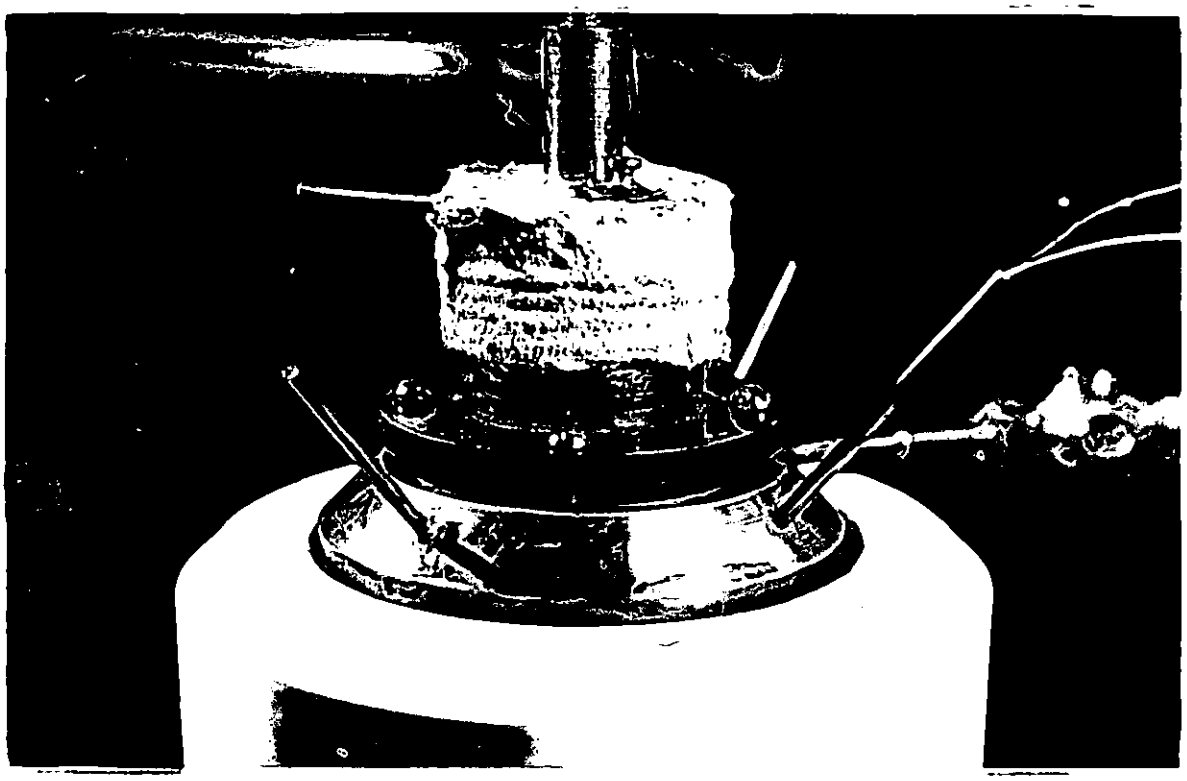

FIG. 18

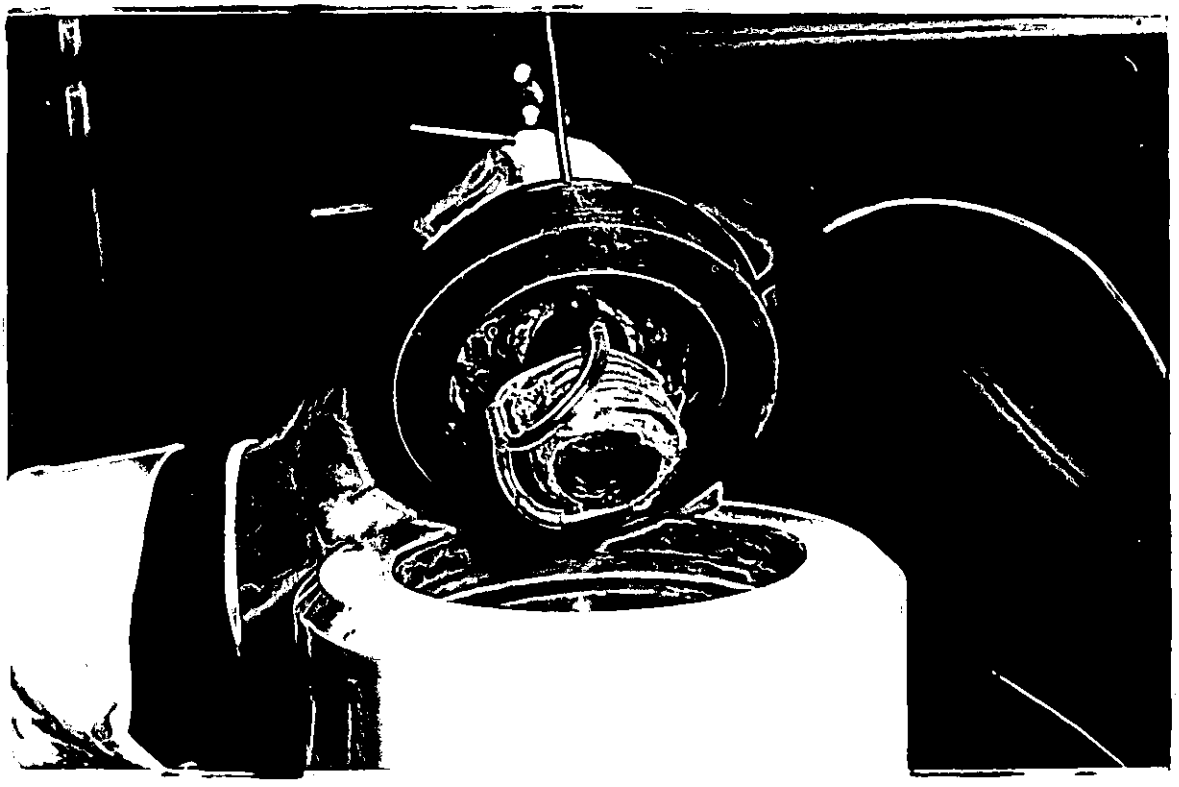

FIG. 19

wrapping 'nichrome' heating wire vertically round a former, and then insulating it with asbestos paper paste. The former was made of a thin nickel strip bent into a circle, and insulated again by asbestos paper paste. The resistance of the wire was approximately 33 ohms, and the input was controlled by a transformer variac, which stepped down the mains voltage to about 70 volts for maximum heating. This corresponds to a maximum power input of 140 watts.

A separate electrical cord was wrapped round the top of the bottom brass block to ensure the temperature of the intermediate parts of the system did not fall below that of the top or bottom reservoir, otherwise condensation problems might occur.

The whole apparatus when assembled is situated in an exact position relative to the lead castle and the photomultiplier tube as shown in Fig.17, and Fig. 18. By wrapping some dark rubber bands flat round the brass support, the cell is held firmly in place with a light tight seal between the cell and the lead castle. A small gap is left between the bottom of the scintillation cell L, and the top of the photomultiplier tube PM (Fig.17). This is constant, and is of the order of 1-2 mm; its introduction to prevent thermal conduction to the photomultiplier tube has already been mentioned previously (Chapter 3.7).

4.2. Temperature control.

Ideally the temperatures of the three main parts of the system, i.e. the active reservoir, the polymer specimen, and the liquid scintillator reservoir, should be independently adjustable. This, experimentally, is difficult to achieve because of heat conduction through the metal sides of the apparatus itself. The liquid scintillator cell is the easiest to control, as this is glass insulated, and it is possible to adjust the temperature of this part to any convenient value without affecting the rest of the system. In practice the top reservoir needs to be 'cooled' to maintain it at a temperature near to the temperature of the scintillator. The higher the polymer temperature, the greater the need for cooling, because the electrical heating element is situated adjacent to it.

The difference in temperature between the centre of the polymer membrane and the edge of the specimen (where in practice the thermocouple T 2 in Fig.17 is located) was tested by attaching thermocouples to these places and performing a "dummy" run. It was found that after an equilibrium state had been reached, the difference was only about $1^{\circ}C$.

Thermocouples were also attached to the areas near the glass-to-metal seal MS in Fig.17, in a "dummy" run to ensure that no 'cold' spots existed (i.e. colder than the solvent or scintillator reservoirs), which might cause condensation of the vapours.

The time taken for the polymer to reach the equilibrium temperature after the application of heat was also noted. This was found to vary between 10 and 30 minutes, depending on the temperature, which is well within manoeuverable limits.

The temperature of the photomultiplier tube is kept cool by a continuous stream of cooled, dry nitrogen which is applied from one of the inlets. The variation of photomultiplier noise level with temperature was discussed previously (see Fig. 16.).

4.3. High vacuum techniques.

The high vacuum line used employs a straightforward mercury diffusion pump followed by a rotary backing pump. The pressure is measured by a vacuostat gauge which is sensitive to 10^{-3}mm. of mercury. The line is illustrated in Fig.20.

High vacuum silicone grease was used for all the glass stop cocks, (but not inside the diffusion apparatus). Regreasing of the stopcocks and re-oiling of the rotary pump were carried out from time to time. The vacuum produced was $< 10^{-3}$ mm Hg.

The high vacuum line is connected to the diffusion cell by two thick-walled rubber tubes. The whole cell was tested intensively for vacuum-tightness by evacuating to 10^{-3} mm, leaving for a period of time (1-24 hours), and measuring the increase in pressure. When a leak was suspected, the whole cell was pressurised with compressed nitrogen and placed under water, and carefully observed for the escape of any tiny bubbles. It was found that the worst location for leaks (in fact the only one in the present system) was the soft solder interface in the top section of the cell. This was readily resoldered. Presently no appreciable increase in pressure was observed after 10 hours.

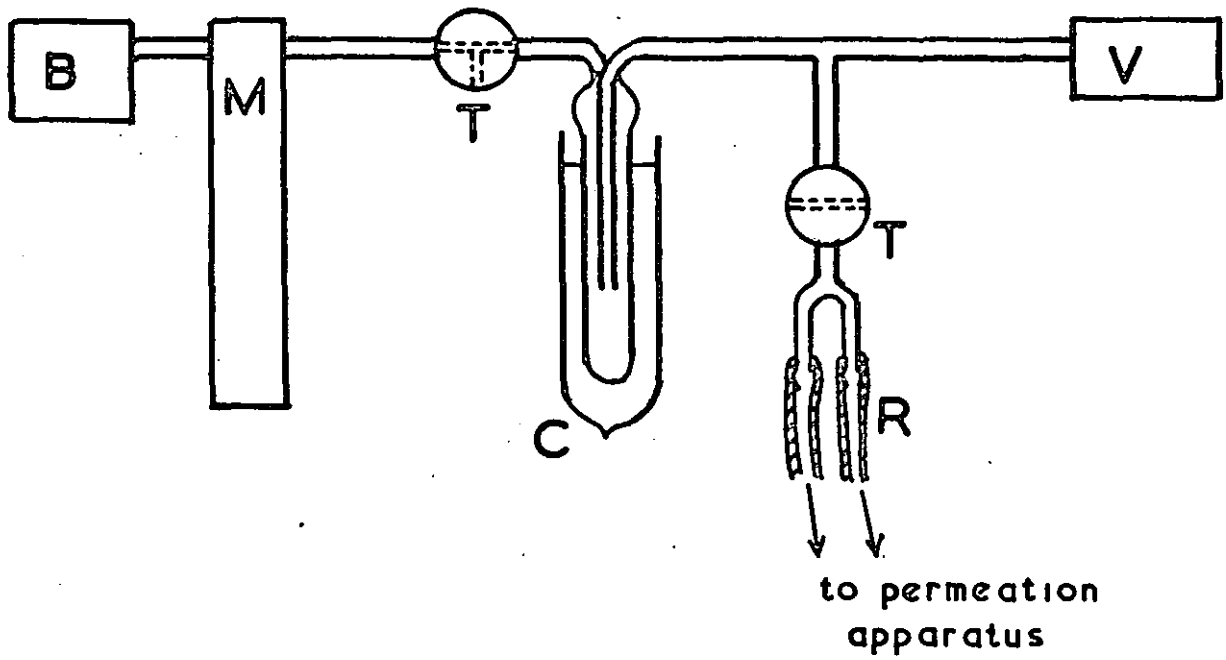

FIG. 20 High vacuum line

B rotary backing pump
M mercury diffusion pump
T high vacuum ground glass stopcock
C liquid nitrogen trap
V vacustat gauge
R thick walled rubber tubes

4.4. Photomultiplier tube and counting equipment.

The scintilation counter consists of the scintillator cell, photomultiplier tube and emitter follower, high tension voltage (H.T.V.) suppy, discriminator bias device, a timer and scaler detection unit, and a chart recorder. It is represented schematically in Fig.21.

The photomultiplier tube (E.M.I. type 60975) used has a "venetian-blind" structure where the dynodes (D), are arranged in rows as shown. The cathode (C) is made of a semi-conducting compound, in this case a caesium-antimony compound, which has good photoemissive properties. Photoelectrons impinging on the first dynode produce a number of secondary electrons which are accelerated onto the next dynode of the multiplier, where they in turn produce secondaries. The overall multiplication factor of the photomultiplier tube, or gain, is dependent on the number of dynodes and on the applied potential. The counter therefore operates as a spectrometer in which the anode current is proportional to the energy dissipated in each "scintillation." Although the pulse size of this anode current signal may be affected by geometry and other factors, the number of pulses will be equal to the number of scintillations occuring in the scintillator, provided that at least one photon for each emission is observed by the photomultiplier tube.

High gain and low dark current are two important requirements of a photomultiplier tube. (Dark current is the measure of electrons emitted from the cathode even in complete darkness due to thermionic emission, etc.) The photomultiplier tube used also has a maximum quantum efficiency at approximately 3700 A^{o}, which corresponds very well with the fluorescence quantum

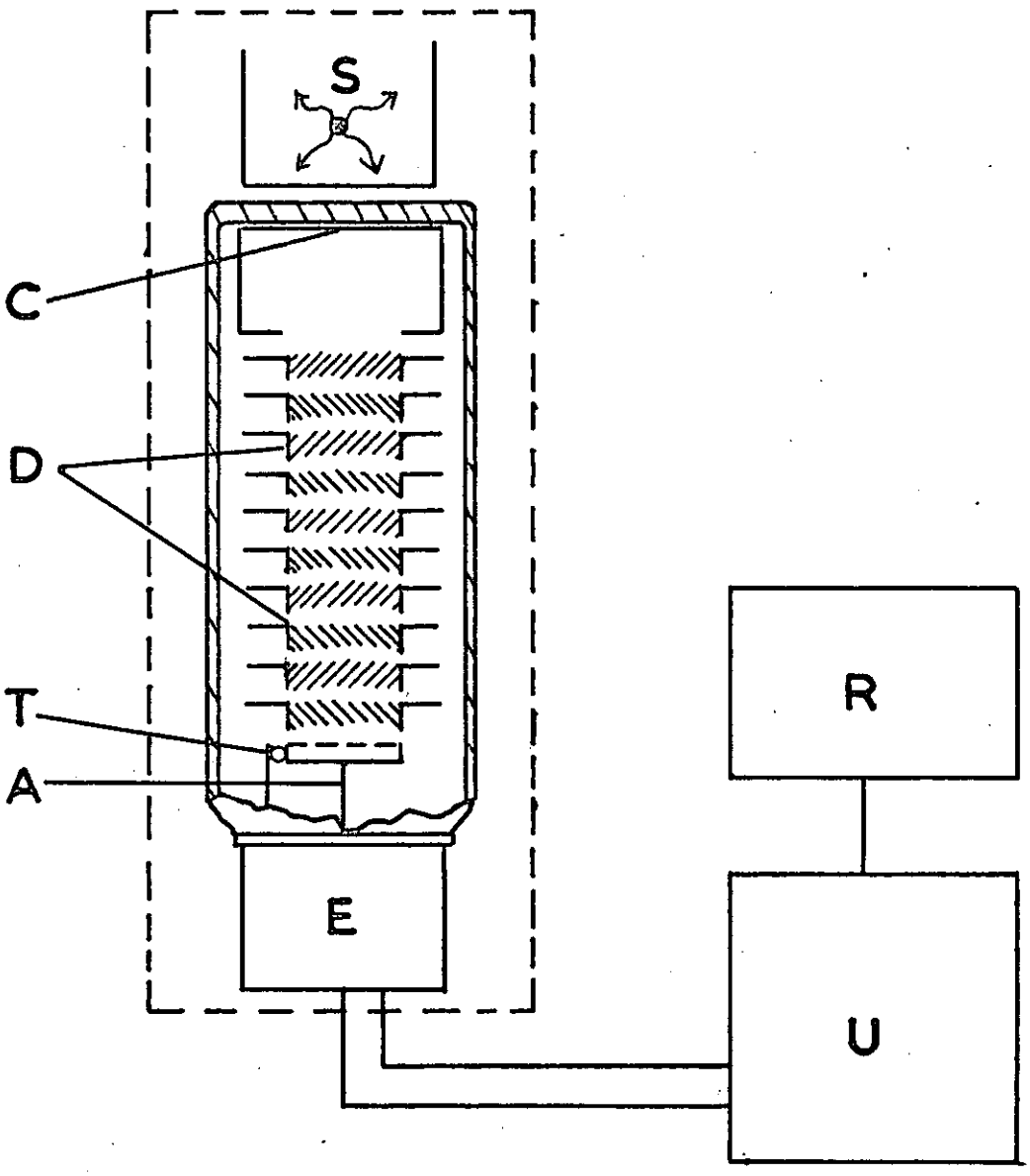

FIG.21 PHOTOMULTIPLIER TUBE AND ASSEMBLY

S radiation source
C cathode
D dynodes
A anode
T pulse collector
E emitter follower
U high tension voltage supply and counter
R recorder

emission maximum of 3650° shown by the scintillator solute 2-5-Diphenyloxazole (PPO). For more details on photomultiplier tube designs and theories, an excellent series of documents published by E.M.I. is referred (135-137).

The signal from the photomultiplier tube is sent to the counter U via an emitter follower E. A chart recorder R is used for registering automatically the increase of activity with time.

All experiments were carried out at a H.T. voltage of 1030 volts, and a discriminator voltage of 8 milli-volts. The choice of these values was based on the investigations performed in Chapter 3.

4.5. Materials.

(a) Chemicals.

1-C-14 labelled n-decane (Radiochemical centre, Amersham) of 3 mCi/mM activity was used. The amount purchased was equivalent to 0.1 mCi (0.005 ml approximately), and it was delivered in a sealed glass tube. This was frozen in liquid nitrogen before it was broken open and diluted with 2 ml. of distilled A.R. n-decane. 0.1 ml of this solution was further diluted with 20 ml of n-decane, and this was used as the diffusant.

Since the Curie (Ci) is defined as the quantity of any radioactive material in which 3.7×10^{10} disintegrations occur per second, 1 ml of the above solution, which is approximately the amount used in each run, would correspond to 9.2×10^{3} disintegrations per second.

The actual count rate of 1 ml of n-decane diffusant calibrated in situ, at 1030 volts high tension supply and 8 mV discriminator setting, was 1260 counts per second (C.P.S.) See Fig.23.

Thus the absolute counting efficiency of the system was found to be about 14%.

The efficiency was lowered by many factors, a few of which are listed as follows:-

(1) The use of a discriminator voltage to reduce background noise leads to loss in efficiency.

(2) The presence of a small air gap between the photocathode and the scintillator cell also reduces the efficiency of transmission of the photons.

(3) The chemical nature of the solvent itself (n-decane) may lead to low solvent-solute transfer of excitation (see Chapter 2.9).

However the 14% efficiency was found to be sufficient experimentally for the necessary measurements to be taken.

The scintillator consists of non-active, redistilled n-decane (British Drug Houses) as the solvent containing 0.5% by weight of 2,5-diphenyloxazole (PPO) as the primary solute. PPO has a fluorescence quantum emission maximum at 3650°A, and this matches well with the maximum sensitivity of the photo-multiplier tube used at 3700°A (See Chapter 4.4). Thus, there is no need for a secondary solute (wavelength shifter). In any case the secondary solute 1,4 bis-phenyloxazolyl benzene (POPOP) was found to be insoluble in n-decane.

(b) Polymer Specimens.

The silicone rubber used, I.C.I. low shrinkage grade, is poly (dimethyl siloxane), $\{ Si(CH_3)_2 - O \}_n$, with about 0.5 mole o/o vinyl substituted side groups introduced to promote cross-linking.

The cross-linking agent used is 2,4-dichlorobenzoyl peroxide dissolved in equivalent amount of silicone oil ("Perkadox" -50). 2% of Perkadox -50 is the amount used to vulcanize the rubber. The rubber was press moulded at 230°F for 7 minutes, and the membranes were in the form of moulded sheets 0.5 mm thick, uniform within ± 0.02 mm.

The filled samples were prepared by compounding the rubber with fine silica filler ("Aerosil 2491") in 5 parts per hundred parts of rubber (by weight) (5 phr), 10 phr, 20 phr, and 30 phr amounts. These samples were similarly vulcanized as above.

The characters of the silicone rubber (E303) used are summarised in Table 4.1 below:

TABLE 4.1

Molecular weight ($\bar{M}v$)	800,000
Density	0.98 $gm.l^{-1}$
Percentage vinyl structures (approx.)	0.5 mole %

These moulded samples of silicone rubber were extracted of all low molecular weight impurities by boiling acetone in a Soxhlet apparatus for 6-7 hours. They were then dried in a warm oven ($40^{\circ}C$)before use.

The styrene-butadine-styrene (S-B-S) block copolymer used is a commercial polymer marketed by the Shell Chemical Company under the name KRATON 1o1.

The properties of this polymer are given in Table 4.2:

TABLE 4.2

Density	0.94 gml^{-1}
Weight of styrene	28%
$\bar{M}_n$	78,000
Diene microstructure (138)	
Cis - 1,4	41%
Trans - 1,4	51%
1,2 (vinyl)	8%

The number-average molecular weight ($\bar{M}_n$) was determined with a Hewlett Parkard 502 high speed membrane osmometer, using toluene as solvent, at $25^{\circ}C$.

The weight fraction of styrene was determined using Kolthoff's method (139).

Cast Samples.

Films of uniform thickness were cast from toluene and methylene chloride. The polymer was weighed and dissolved in the solvent. The concentration of the solution was about 10%. After the polymer was dissolved, the homogeneous solution was poured onto clean mercury contained in a crystallizing dish.

The solvent was allowed to evaporate slowly at room temperature and atmospheric pressure. Complete evaporation of solvent took about a week. The films after being removed from the mercury were air dried for at least 10 days before being used.

4.6. Procedure of Measurement.

4.6.1. Assembly.

The permeation cell is thoroughly cleaned by soaking in acetone and then evacuated to 10^{-3} mm Hg. 6 ml of the prepared liquid scintillator is transferred to the bottom cell. The polymer specimen, which is cut out to size, is placed on top of the lower flange and accurately aligned. The top half of the cell is then carefully lowered on to the bottom half with the thermocouple T 2 (Fig.17) in position. The four clamping screws and the collar (R) are then slowly tightened. The top cell is then charged with about 1.5 ml of active n-decane solution by using a long drawn glass pipette through the screw hole, X in Fig.17. The screw is then replaced, and tightened onto a soft lead washer in between the bottom of the screw head and the cell, to ensure a vacuum seal. The cell is now assembled.

4.6.2. Degassing.

To degas the polymer, scintillator, and diffusant, the liquids involved must be frozen before the application of high vacuum. This is done by employing a solid CO_2/methanol mixture, which is pumped through the temperature jackets round the top and bottom reservoirs by a peristaltic pump via silicone rubber tubing. Since the freezing point of n-decane is $-29^{\circ}C$, it is sufficient to pump the methanol mixture at a temperature of $-50^{\circ}C$ in the vacuum flask. The viscosity of the methanol increases rapidly with decreasing temperature, and at -72° it becomes a slurry. The speed at which the mixture can be pumped through the system, therefore, decreases at such low temperatures, the maximum cooling efficiency being achieved at around $-50^{\circ}C$.

To prevent condensation of water vapour from the air on and around the photomultiplier tube, which could interfere with the electronics and optical properties, a continuous stream of cooled dry nitrogen from a compressed oxygen-free nitrogen cylinder is applied to the chamber to flush out atmospheric air. The coolant is thus circulated until the thermocouples T I and T 3 (Fig.17) register temperatures lower than the freezing point of n-decane. The high vacuum line is then slowly opened to both compartments of the cell, care being taken not to cause either the rupture of the membrane due to uneven pressure, or spilling of the active decane from the top reservoir due to a sudden upward motion of the air originally above it. The pressure is reduced to about 0.5 mm of Hg for the first evacuation. The cell is then isolated from the high vacuum line and the n-decane allowed to warm up. This operation is allowed about 20 minutes, by which time most of the dissolved oxygen from the decane should have left by degassing into the partial vacuum above it. The n-decane systems are then frozen again, and the cell evacuated to 10^{-3} mm Hg. This procedure is repeated four or five times until on opening the isolated system to the high vacuum line after a period of about 20 minutes, no appreciable increase in the pressure occurs.

4.6.3. Tabulation of Readings.

After degassing, temperature controls are started. The electrical heating element H (Fig.17), and the heating cord, are set at the required voltages. The bottom cell is heated directly by circulating water from a large water bath ($\pm$ 0.1°C) with the peristaltic pump, which also pumps through a separate

coil on the top cell above the active decane reservoir. For high sample temperatures, the active reservoir itself is cooled by running chilled tap water through the coiled piping (see 4.2), the temperature of the reservoir being controlled by the rate of tap water circulation. It is possible, especially at low polymer temperatures, to control the temperature of the top reservoir to within 1° of the bottom one.

The H.T. supply to the photomultiplier tube was switched on after the cell had been assembled on top of the photomultiplier. 100 second counts are taken as soon as the various thermostat devices are operating. A lapse of about 30 minutes is allowed before thermal equilibrium is reached and from then onwards the readings are tabulated as below:-

Relative Time from start (mins.)	Thermo-couple T 1 Reading (mV)	Thermo-couple T 2 Reading (mV)	Thermo-couple T 3 Reading (mV)	100 sec counts (cp 100s)	Activity (counts per sec.) c.p.s.
-	-	-	-	-	-

A straight line plot of activity against relative time represents the permeation of the active n-decane through the polymer, and the slope of this plot is proportional to the permeation rate. The rate of decane vapour transfer from and to the liquid reservoirs through the evacuated space is very much faster by comparison. A typical experimental plot with the limits of statistical error included, is shown in Fig.22.

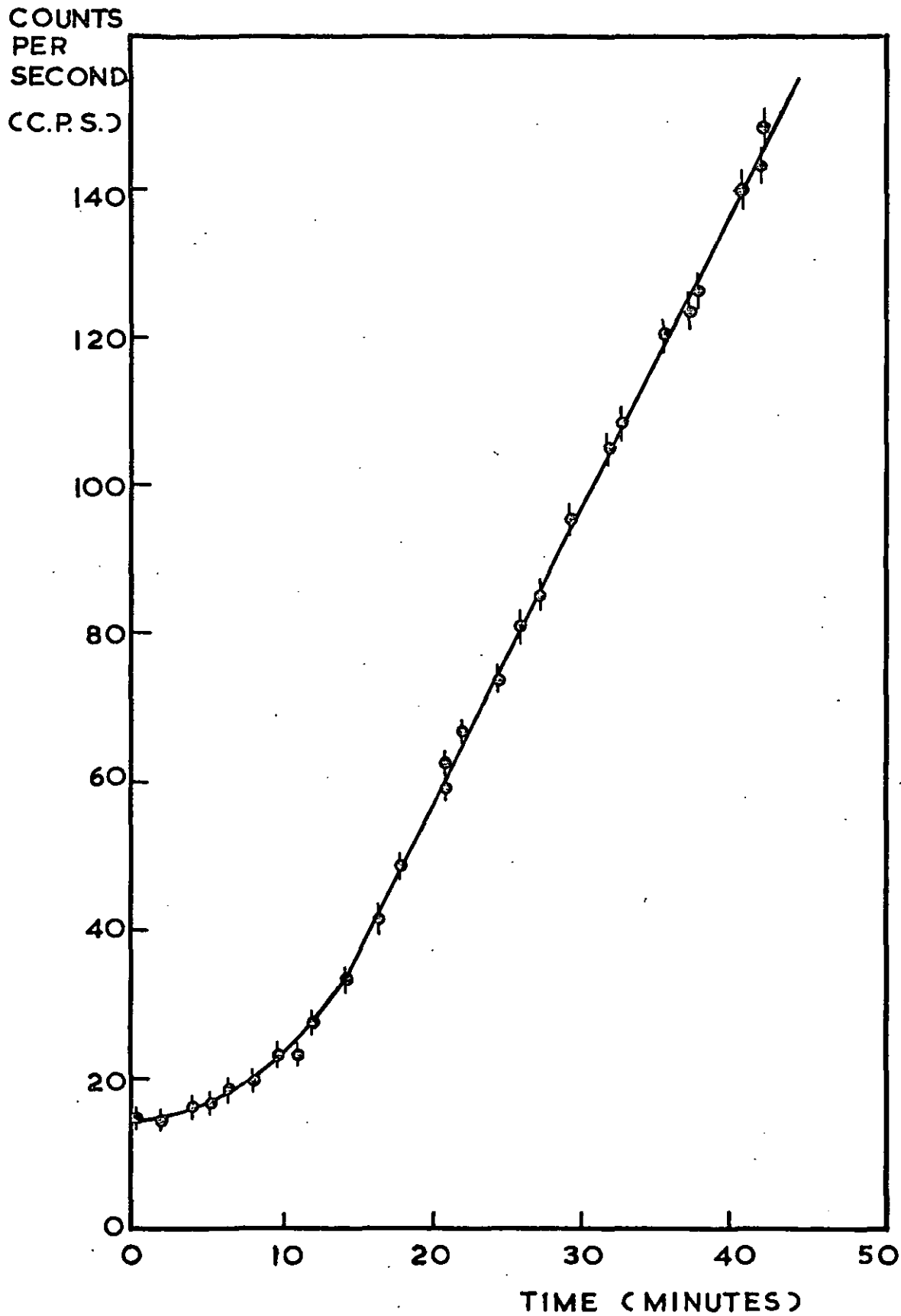

FIG. 22 A TYPICAL PERMEATION PLOT

It is important that a steady state is reached both in terms of temperature and flow for the rate to be meaningful. Occasionally the system can be opened to the vacustat gauge to check that no external gas has diffused.

After a satisfactory plot has been obtained at a certain temperature, the temperature can be raised to a new value by increasing the voltage supply to the heater. However, a corresponding increase in the top reservoir will also be observed because of heat conduction, and this is corrected, or in some cases partly reduced, by increasing the flow rate of the cooling water. The water is chilled by passing through a coil immersed in ice. In cases where it is impossible to maintain exactly equal temperatures between the top and bottom reservoirs, the respective temperatures are noted and taken into consideration in the calculation.

Thus a series of permeation rates at different specimen temperatures can be obtained with a fixed penetrant activity.

4.7. Calibration of active n-decane.

Calibration of the radioactive diffusant in air was carried out in the cell, by adding known quantities of active decane to 6 ml of liquid scintillator solution, and taking counts at the set H.T. The presence of dissolved oxygen in the scintillator reduces the efficiency of count due to quenching (2.9). Therefore, a second calibration was carried out in high vacuum. This was done by adding a certain amount of ^{14}C labelled n-decane to the cell, which was then assembled and thoroughly degassed in a manner as described in section 4.6.2. The count per sec. of the degassed scintillator was then noted. Air was then let in, and the system left for about an hour for the count rate to drop to its equilibrium value. The count per sec. of the scintillator with dissolved oxygen was then recorded, and the weight of active n-decane can be read from the first calibration. By cross-plotting the weight of n-decane thus obtained against the count rate in high vacuum, an accurate calibration curve in high vacuum was obtained. Direct attempt to weigh an exact amount of active decane into the system and counting the activity after four or five evacuations is bound to lead to innacurate results because some of the decane invariably is removed on evacuation. The two calibrations are shown in Fig.2[illegible].

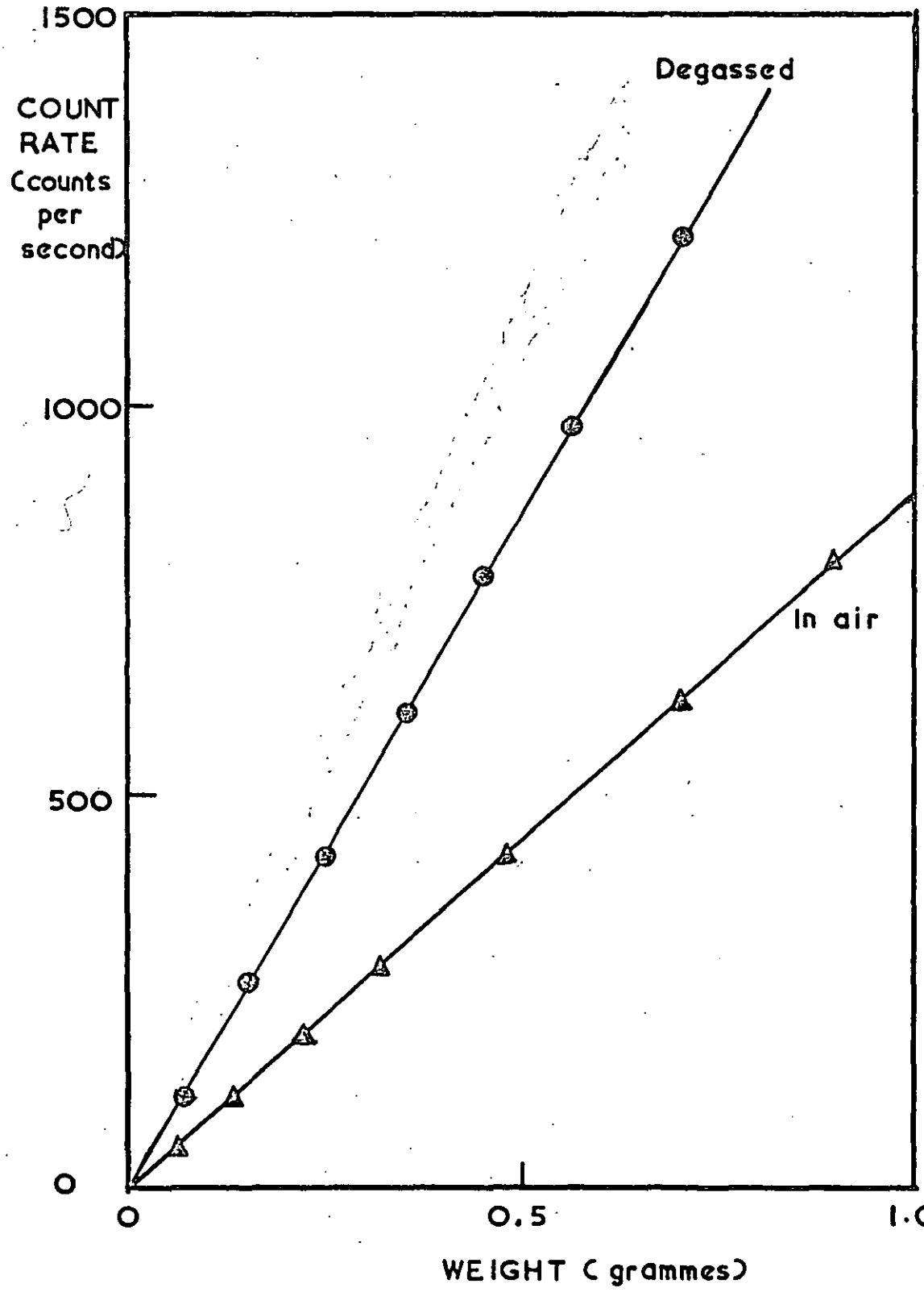

FIG.23 RADIOACTIVITY–WEIGHT CALIBRATION OF n-DECANE

4.8. Possible errors.

There are a few errors which may arise from inaccuracy of measurement or limitations of the measuring instruments, and these are listed below:-

(1) Counting error.

When a single count is taken of a radioactive source, the standard deviation from the true value will be equal to the square root of the mean count taken (140). The percentage error can be expressed as equal to $(\frac{1}{\sqrt{n}}) \times 100$, where n is the number of counts read within the period. Thus the higher the count rate, the smaller will be the percentage error. High count rate can be achieved by either having a highly radioactive source or counting for a long period of time. In an actual permeation run the count rate is actually changing with time, a long counting period is therefore not suitable, and a compromise has to be reached.

(2) Temperature error.

The thermocouple readings can be read to 0.01 mV accurately, and this represents a maximum error of about 0.5% for the temperature range 30 - 50°C, for each thermocouple reading.

(3) Error in measurement of thickness.

The thickness of the polymer membrane was measured by a micrometer screw gauge, and this is accurate up to 0.01 mm. Therefore for a film about 0.5 mm thick, the maximum error is 2%.

(4) Error in measurement of cross-section membrane area.

The radius of the circular section of the cell through which permeation occurs is measured with a pair of internal Vernier callipers, and this is accurate up to 0.1 mm. The percentage

error here has a maximum value of about 3%.

The maximum error for the whole system is estimated at about 7%.

4.9. Sorption Apparatus - electro micro-balance.

A commercial (C.1. Electronics Mark 2B Ser.No. 1412B) electro micro-balance was employed in a modified vacuum housing. This balance works on the principle of a moving vane interrupting a light beam to two photo-cells, the variation in light intensity resulting in a change in the output electric current. There are five ranges on the measuring scale viz 0 - 100 mg, 0 - 10 mg, 0 - 2.5 mg, 0 - 250 μg, and 0 - 25 μg. However, the more sensitive scales are not really useful in practice because the slightest vibration will cause a large swing of the needle on the scaler. Ranges of 0 - 10 mg and 0 - 100 mg were used.

The whole apparatus is shown in Fig.24. The balance B is situated in a glass housing with the polymer sample P suspended from one arm and a counterbalancing weight on the other arm.

The temperatures of the polymer and of the solvent reservoir were controlled by running water from a thermostat bath through the glass jackets, J.

The balance was carefully calibrated as follows. The two arms of the balance were brought into exact equilibrium by attaching small weights to the pans and using the zero adjuster on the scaler. After this had been achieved, standard weight samples which had been cleaned and dried were added to the sample pan one at a time. The needle on the scale was then adjusted to its correct value by altering the potentiometer setting on the side of the scale. The same procedure was then repeated for the other range.

After the balance had been calibrated, the polymer, in the form of a long rectangular film, was attached to the sample arm

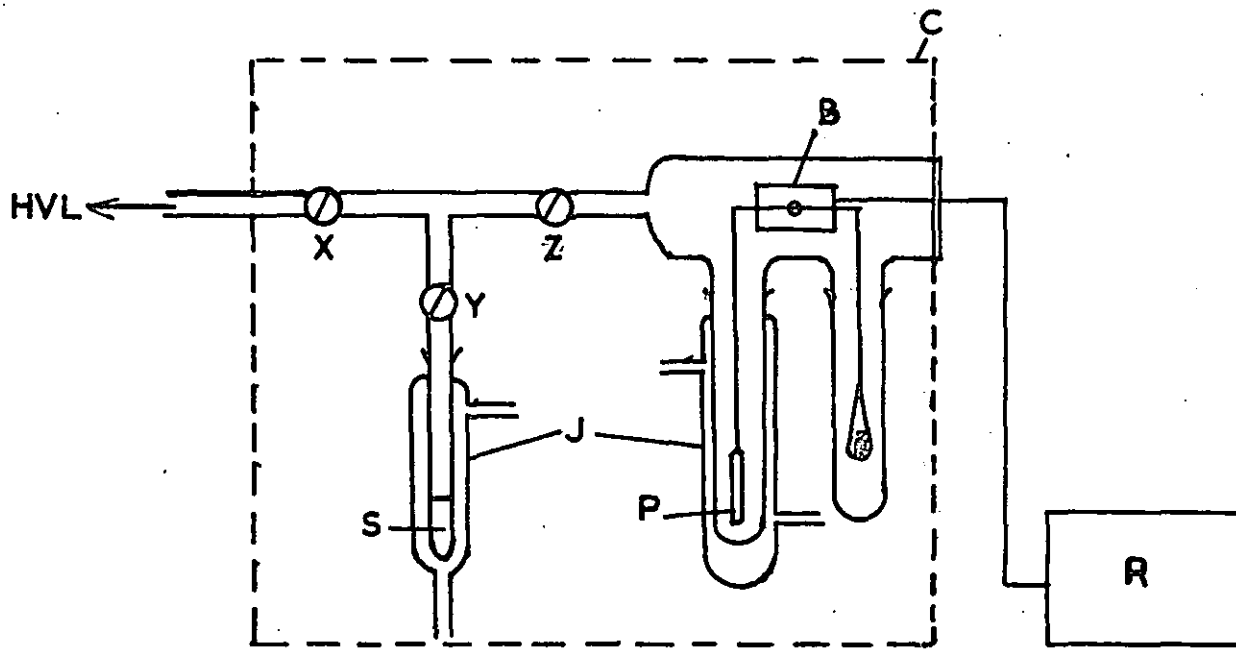

FIG.24 SORPTION EXPERIMENT EMPLOYING ELECTRO-MICROBALANCE

HVL	high vacuum line
S	solvent reservoir
J	temperature controlling water jackets
P	polymer sample
B	electro-balance
C	hot air cabinet
R	scale

of the balance by a fine wire after the sample pan was removed. Again the two arms were brought into balance by adding or removing small weights (in the form of short lengths of fine wire) on the right-hand pan. The weight of the polymer before it was inserted was measured and recorded. The thickness was also measured if the kinetics of sorption (i.e. diffusion coefficient by sorption) was required to be examined.

The temperature jacket was then fitted round the polymer, and a corresponding jacket on the right hand side of the balance. The solvent reservoir was then filled with sufficient amount of n-decane, about 10 ml, and fitted on to the vacuum line. The apparatus was then ready for the start of the experiment.

The whole system except the cold trap and the pumps was enclosed in a hard wood box with a perspex window front with holes cut out for vacuum taps, as shown by the dotted line in Fig.24. The box acted as a hot air oven, being heated by two 200 watt light bulbs. This was necessary if the solvent reservoir temperature was higher than room temperature otherwise the "exposed" parts of the system would act as cold surfaces for condensation to occur. The temperature of the chamber was controlled by a step-down transformer which controlled the potential supplied to the light bulbs.

The system was degassed by evacuating and pumping for 12 hours. This could not be applied to the solvent reservoir because of inconvenience in freezing the n-decane. The n-decane was out-gassed by pumping out most of the air above it together with some of the solvent, and isolating it for the dissolved oxygen to have time to escape the liquid phase. This was repeated several times.

After evacuating and heating the polymer and the solvent to the required temperatures, tap X was closed, and taps Y and Z opened. n-Decane vapour at a fixed pressure would then pass through the vacuum to reach the polymer. Sorption of the molecules on the polymer would then cause an increase in weight, and the readings on the scaler were taken with time until an equilibrium uptake was reached. Temperature of the solvent reservoir was then increased, and a new equilibrium uptake value obtained. Therefore at one polymer temperature, the equilibrium sorption values were obtained for various n-decane activities (vapour pressures). The whole procedure was repeated for different polymer temperatures, and a series of concentration vs vapour pressure isotherms were obtained.

From the plot of $\frac{Mt}{M_\infty}$ against $t^{1/2}$ where Mt = uptake at time t, M_∞ = equilibrium uptake, a diffusion coefficient could also be worked out. (See Chapter 2.3).

4.10. Quartz spring balance.

This experiment was performed to supplement the electromicro-balance results for high vapour activities. The maximum temperature to which the hot air chamber C (in Fig.24) could be heated in the electromicro-balance work was around 45°C. At reservoir temperatures near or higher than this value, inaccurate activity of the vapour would result, and it would not be correct to take measurements.

A diagram of the quartz-spring apparatus is shown in Fig.25, and it is sufficiently self-explanatory. The polymer is suspended at the end of a helical quartz spring Q, and its temperature is controlled by the thermostat bath A. The solvent is contained in the reservoir S, the temperature of which is controlled by bath B. R is a vapour reservoir to help the solvent vapour attain a steady pressure quickly. High vacuum stopcocks X, Y and Z, separate different parts of the system from the high vacuum line.

The working principle is simple. The uptake of the vapour is measured by the extension of the quartz spring which is measured by a cathetometer C. The extension-weight calibration of the quartz spring was previously obtained by using standard weights, and the calibration is given in Fig.26.

The exposed parts of the system are heated by electro-thermal cords (H), the temperature of which is controlled by a voltage transformer.

The experimental procedure is the same as the one described for the electromicro-balance, the only difference being the actual method of measurement of the weight increase, and also in this case the n-decane can be readily frozen by immersing the reservoir in a MeOH/CO_2 mixture.

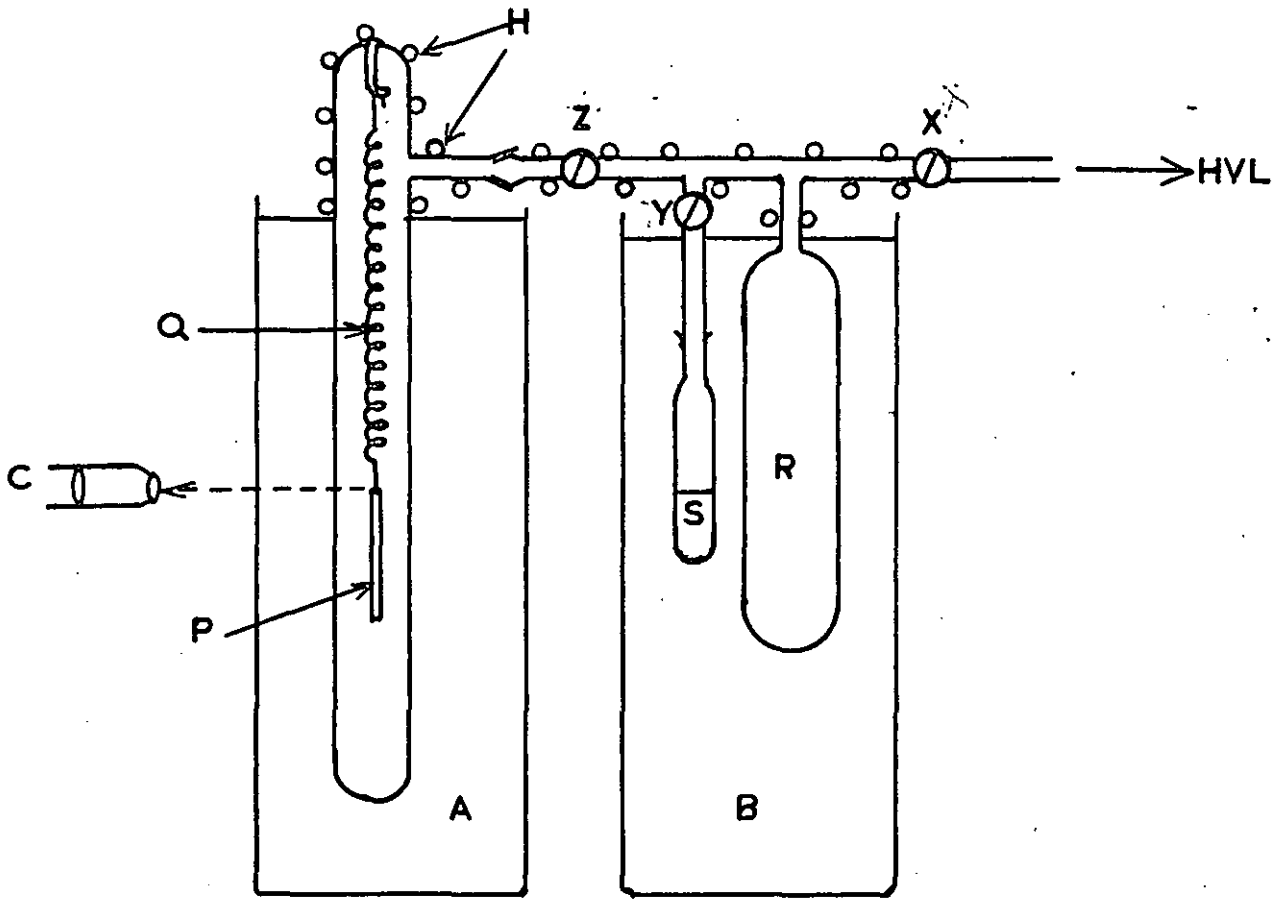

FIG.25 SORPTION EXPERIMENT EMPLOYING A QUARTZ SPRING

C	cathetometer
Q	quartz spring
P	polymer sample
H	electro heating tapes
A	thermostat bath
B	-ditto-
S	solvent reservoir
R	vapour reservoir
HVL	high vacuum line

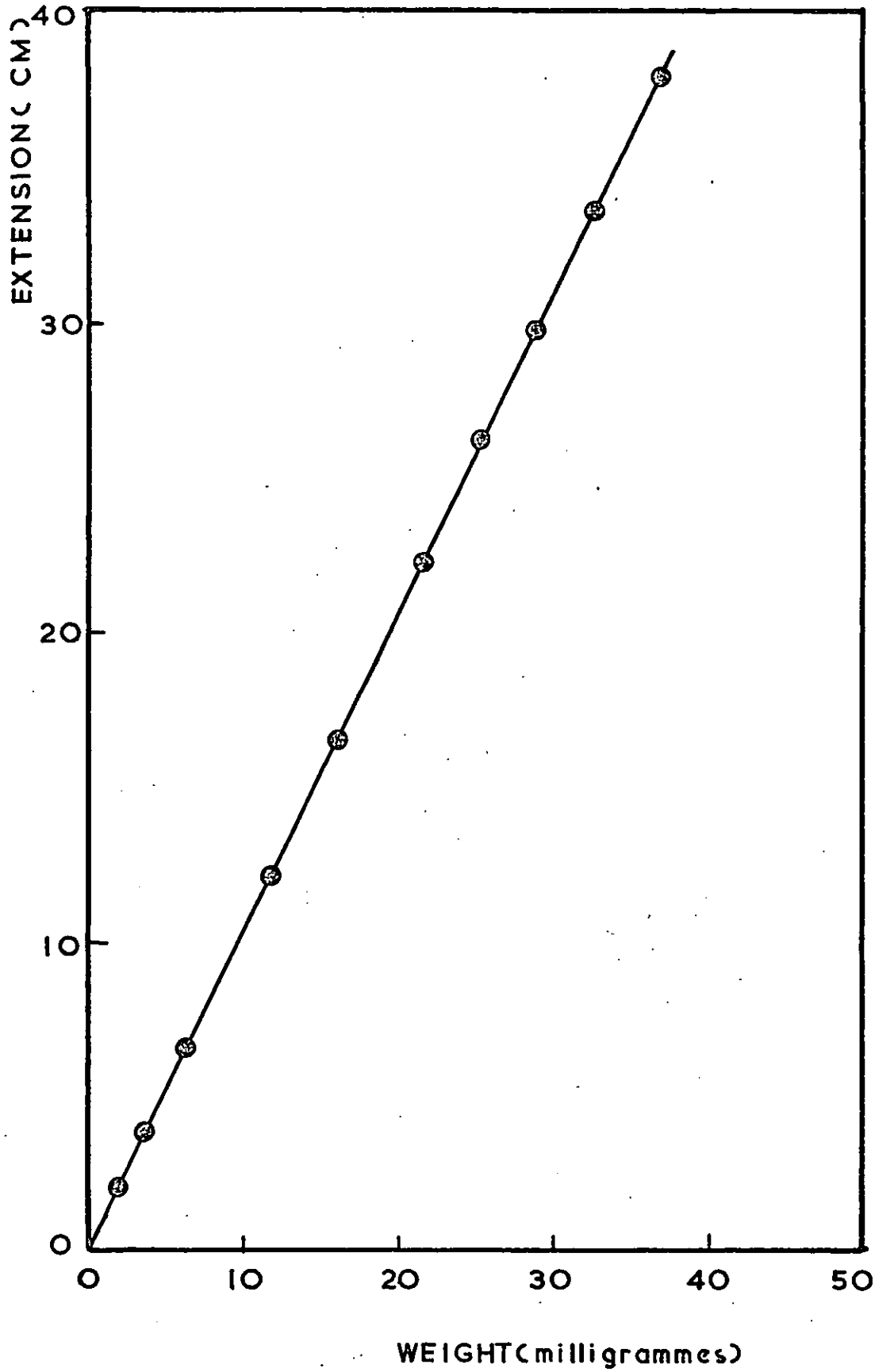

FIG. 26 QUARTZ SPRING CALIBRATION

4.11. The Dynamic Mechanical Apparatus.

The dynamic mechanical apparatus (87, 161) will not be described in detail here, and only the basic working principles are given. The polymer in the form of a rectangular beam specimen, is clamped rigidly at both ends and is oscillated in bending geometry by a central clamp. The central clamp is driven by a magnet suspended on thin wires in the centre of a coil. The force is produced by the action of a sinusoidal current in the coil of the magnet. It is resisted by the mass of the moving system, the rigidity of the specimen, and the rigidity of the suspension wire. The equation of motion for such a system may be worked out, and the resulting solution for E' and E'' at low frequencies of input current (i.e. less than one-fifth of the resonant frequency) may be simply given as:-

$$E' = \frac{1}{K} \frac{F_o}{X_o} \cos\beta \qquad 4.1$$

$$E'' = \frac{1}{K} \frac{F_o}{X_o} \sin\beta \qquad 4.2$$

where F_o is the maximum driving force

X_o is the maximum linear displacement of the driven clamp.

K is a geometric factor for the specimen given by

$$K = 2bh^3/l^3 \qquad 4.3$$

(where b is the width, h the thickness and l the length of each half of the specimen between each rigid clamp and the central clamp.)

$\beta = \tan^{-1} \frac{E''}{E'} = \delta$ (where $\tan\delta$ is the loss factor)

An essential step in the measuring process is the conversion of the linear displacement into a proportional voltage. This is done with a Bently transducer, operating in conjunction with a Bently proximator circuit and a power supply. The Bently system produces an output voltage proportional to gap and gap variation from the probe face to the observed surface. That is

$$X_o = BV \qquad 4.4$$

where X_o is the peak linear displacement

V is the RMS value of the output voltage

and B is a constant of the transducer system.

In principle, the dynamic properties of a specimen are given in terms of quantities which are measurable.

The peak driving force is proportional to the R.M.S. value of the driving current, thus:

$$F_o = N\,i \qquad 4.5$$

where N is a constant dependent on the strength of the magnet and the properties of the coil. Similarly, the peak displacement is proportional to the output voltage as given by Equation (4.4).

Combining Equations 4.1 and 4.2 with Equations 4.4 and 4.5 gives E' and E'' in terms of actual measurements.

$$E' = \frac{N}{KB}\ \frac{i}{v}\ \cos\beta \qquad 4.6$$

$$E'' = \frac{N}{KB}\ \frac{i}{v}\ \sin\beta \qquad 4.7$$

At some high frequencies, depending on the rigidity of the sample, the vibrating system will possess an amplitude resonance. The condition for a maximum in X_o with varying frequency is (161):-

$$KE' = M\,w_o^2 \qquad 4.8$$

where w_o is the resonant frequency, measurement of w_o thus gives an accurate value of E' at that frequency.

In order to convert the amplitude of the output voltage (V) to absolute values it is necessary to know the value of the constant Ni/KB. If the transducer system could be calibrated, at varying settings of transducer sensitivity, the constant B could be obtained. Then, knowing the values of N, K and i, the constant Ni/KB could be calculated.

It was not possible to calibrate the transducer as in practice it was not quite linear and it proved difficult to exactly reproduce a particular sensitivity setting. Also with change of temperature

slight distortion of the samples occurred, thus altering the transducer setting.

The results were, therefore, converted to absolute values in the following way. Equation 4.8 states that $KE' = MW_o^2$. The geometrical factor, K, is determined by direct measurement of the specimen and the mass, M, of the vibrating system by weighing. The resonant frequency may be determined accurately and thus the absolute value of E' can be obtained at this frequency.

At a given temperature the time required to take measurements over the complete frequency range is about 30 minutes. The transducer setting remains constant at a constant temperature. Thus the term Ni/KB in Equations 4.6 and 4.7 is constant for a set temperature, and it only remains to determine its absolute value. A plot of 1/V' is made against the logarithm of frequency in the region where the inertial term isnegligible. V' is the n-phase component of the output voltage and equals VCos β. This plot is extrapolated to the resonant frequency where the exact value of E' is known. Thus the 1/V' curve is calibrated, i.e. a value is given to the constant Ni/KB.

During the experiment, the apparatus was placed in a cylindrical brass container which was then sealed off by assembling the ground flange of the plate attached to the top of the apparatus, and the similar flange of the container. The apparatus was then evacuated, and placed in a temperature bath. Measurements were obtained at the resonant frequency and frequencies of 30, 10, 3, 1, 0.3 and 0.1 cycles per second, at selected constant temperatures.

CHAPTER 5

RESULTS

5.1. Sorption Results.

The equilibrium uptake of the n-decane by the polymer at fixed experimental conditions was measured by both the quartz-spring and electromicro-balance methods described in Chapter 4. The reason for using both methods, besides for checking purposes, was as mentioned in Chapter 4, i.e. that at high vapour pressures the electromicro-balance method becomes unreliable owing to the possibility of vapour condensation on the walls of the apparatus. The concentration measured was expressed as the weight of the n-decane sorbed per unit weight of the polymer (g/g). The concentration measured by the two methods was found to be the same under similar experimental conditions. The data obtained from these experiments were, therefore, tabulated together.

The vapour pressure of n-decane at a constant liquid temperature is obtained from the vapour pressure-temperature relationship as expressed in Fig.12.

The calibration graph for the quartz-spring is shown in Fig.26. This was then used to correct observed extensions into the weight increase.

The equilibrium sorption results for silicone rubber, filled and unfilled, and S-B-S block copolymer are shown in Tables 5.1 - 5.5. (Note that g represents data obtained from quartz-spring, e denotes electromicro-balance data, and b denotes data from both methods.)

TABLE 5.1. Silicone rubber (without filler)

Weight of polymer sample = 17.5 milligrammes (m.g.)

Polymer Temperature (°C)	Liquid Temperature (°C)	Vapour pressure (mmHg)	Equilibrium uptake (mg)	Concentration (g/g)	
40.0	28.0	2.3	1.93	0.110	b
	32.0	2.9	2.63	0.150	b
	34.0	3.3	3.43	0.195	b
	35.5	3.55	4.04	0.23	b
	37.0	3.9	5.45	0.31	b
46.8	29.0	2.45	1.31	0.075	g
	31.6	2.85	1.59	0.091	g
	35.2	3.50	2.50	0.142	g
	38.2	4.15	3.60	0.205	g
	42.6	5.25	5.40	0.307	g
	44.0	5.65	6.68	0.380	g
50.5	35.0	3.46	1.62	0.093	g
	36.4	3.73	1.92	0.110	g
	41.0	4.82	3.15	0.180	g
	44.0	5.68	3.35	0.218	g
	44 1	5.90	4.14	0.236	g
	45.5	6.15	4.72	0.269	g
	47.5	6.90	6.85	0.392	g
	48.8	7.35	9.36	0.534	g
53.0	36.0	3.66	1.71	0.098	g
	39.5	4.45	2.29	0.131	g
	41.8	5.00	2.85	0.163	g
	45.0	6.00	3.56	0.204	g
	47.8	7.00	4.93	0.283	g
	50.4	8.00	7.90	0.452	g
55.75	32.6	3.02	1.22	0.070	g
	36.6	3.80	1.38	0.079	g
	41.0	4.80	1.61	0.092	g
	46.5	6.50	2.65	0.154	g
	49.2	7.50	3.94	0.225	g
	51.2	8.30	5.00	0.285	g
	53.0	9.10	7.45	0.424	g
	44.5	5.82	2.13	0.121	g

TABLE 5.1 (Continued)

Polymer Temperature (°C)	Liquid Temperature (°C)	Vapour pressure (mmHg)	Equilibrium uptake (mg)	Concentration (g/g)
60.0	35.4	3.55	1.05	0.060 g
	38.2	4.15	1.26	0.074 g
	42.6	5.25	1.45	0.083 g
	46.7	6.55	2.17	0.124 g
	50.2	7.90	2.87	0.164 g
	53.5	9.30	3.78	0.216 g
	55.1	10.1	4.80	0.273 g
	56.8	11.4	5.78	0.330 g

TABLE 5.2. Silicone rubber (5 phr filler)

Weight of polymer sample = 16.90 mg.

Polymer Temperature (°C)	Vapour Temperature (°C)	Vapour pressure (mmHg)	Equilibrium uptake (mg)	Concentration (g/g)
43.0	31.4	2.80	1.37	0.081 g
	32.8	3.05	2.13	0.126 g
	34.5	3.35	3.12	0.184 g
	36.8	3.84	4.50	0.266 g
43.6	32.5	3.0	2.58	0.153 g
	35.2	3.50	3.14	0.186 g
	37.6	4.00	3.97	0.235 g
	40.6	4.70	5.92	0.350 g
47.0	33.5	3.20	2.43	0.144 g
	37.7	4.05	3.24	0.192 g
	42.0	5.10	5.55	0.327 g
	45.0	6.00	8.50	0.505 g
49.3	34.0	3.28	1.645	0.097 g
	37.0	3.90	2.43	0.144 g
	40.1	4.60	3.14	0.186 g
	43.0	5.36	4.05	0.240 g
	46.2	6.36	6.15	0.363 g
51.0	33.5	3.20	1.44	0.085 g
	37.5	4.00	2.10	0.124 g
	41.5	4.95	2.80	0.165 g
	45.4	6.10	5.45	0.322 g
	48.0	7.05	6.10	0.360 g
55.5	38.4	4.20	1.525	0.0917 g
	42.3	5.14	2.17	0.129 g
	45.0	6.00	2.60	0.154 g
	48.0	7.04	3.25	0.192 g
	51.0	8.20	5.05	0.298 g
59.8	38.5	4.20	1.14	0.067 g
	43	5.35	1.50	0.089 g
	46.8	6.60	1.69	0.100 g
	51.0	8.20	3.14	0.186 g
	56.0	10.50	5.10	0.301 g

TABLE 5.3. Silicone rubber (10 phr filler)

Weight of polymer sample = 18.00 mg

Polymer Temperature (°C)	Vapour Temperature (°C)	Vapour pressure (mmHg)	Equilibrium uptake (mg)	Concentration (g/g)	
40.0	2.7	2.20	1.83	0.102	b
	3.1	2.75	2.07	0.143	b
	35.6	3.60	4.56	0.254	b
	37.6	4.0	7.45	0.414	b
44.0	2.5	1.95	1.35	0.075	g
	27.8	2.30	1.71	0.095	g
	33.8	3.25	2.67	0.149	g
	38.4	4.20	4.53	0.252	g
	41.5	4.95	7.10	0.395	g
44.6	30.6	2.70	1.22	0.068	g
	34.5	3.35	2.17	0.121	g
	35.2	3.50	2.58	0.144	g
	36.5	3.75	3.25	0.181	g
	40.0	4.55	3.30	0.212	g
	40.8	4.75	5.20	0.289	g
	41.6	4.95	5.52	0.307	g
	42.9	5.35	8.10	0.450	g
47.0	27	2.20	1.27	0.071	g
	28.5	2.36	1.44	0.080	g
	31.1	2.76	1.80	0.100	g
	33.5	3.20	2.28	0.127	g
	34.6	3.40	2.46	0.137	g
	36.0	3.65	2.58	0.144	g
	40.6	4.72	4.33	0.241	g
	43.2	5.42	5.56	0.309	g
	46.5	6.50	13.0	0.725	g
50.0	30.0	2.60	0.521	0.029	g
	33.2	3.12	0.955	0.055	g
	37.8	4.06	1.64	0.092	g
	40.2	4.60	2.25	0.125	g
	44.0	5.68	3.25	0.181	g
	47.0	6.70	5.85	0.326	g

TABLE 5.3 Continued.

Polymer Temperature (°C)	Vapour Temperature (°C)	Vapour pressure (mmHg)	Equilibrium uptake (mg)	Concentration (g/g)
5.40	30.5	2.70	0.521	0.029 g
	34.2	3.32	0.88	0.049 g
	38.7	4.25	1.49	0.083 g
	40.8	4.76	1.91	0.106 g
	42.5	5.22	2.03	0.113 g
	43.8	5.60	2.65	0.147 g
	47	6.68	3.27	0.182 g
	50	7.80	4.85	0.269 g

TABLE 5.4 Silicone rubber (20 phr filler)

Weight of polymer sample = 20.0 mg.

Polymer Temperature (°C)	Vapour Temperature (°C)	Vapour Pressure (mmHg)	Equilibrium uptake (mg)	Concentration (g/g)	
35.0	24.5	1.9	2.60	0.130	b
	29.5	2.5	3.50	0.175	b
	32	2.9	4.50	0.225	b
	34	3.3	6.20	0.310	b
41.0	26.4	2.1	1.70	0.085	b
	30.0	2.6	2.20	0.110	b
	32.5	3.0	2.80	0.140	b
	34.6	3.4	3.80	0.190	b
	35.8	3.6	4.70	0.235	b
45.2	28.0	2.3	1.30	0.065	g
	31.0	2.75	1.66	0.083	g
	33.5	3.2	2.10	0.105	g
	35.0	3.5	2.68	0.134	g
	36.2	3.7	3.00	0.150	g
48.0	29.4	2.5	1.10	0.055	g
	33.5	3.2	1.64	0.082	g
	35.2	3.5	2.06	0.103	g
	37.5	4.0	2.70	0.135	g
	38.5	4.2	3.50	0.175	g
51.5	28.5	2.4	0.70	0.035	g
	34.0	3.3	1.20	0.060	g
	35.8	3.6	1.56	0.078	g
	37.5	4.0	1.80	0.090	g
	39.0	4.3	2.20	0.110	g

TABLE 5.5. Styrene-butadiene-styrene, 3-block copolymer

(Films cast from toluene and methylene chloride showed exactly similar results).

Weight of polymer sample = 139.2 mg.

Polymer Temperature (°C)	Vapour Temperature (°C)	Vapour Pressure (mmHg)	Equilibrium uptake (mg)	Concentration (g/g)	
35.0	26.5	2.12	14.8	0.106	e
	29.0	2.45	21.2	0.152	e
	31.0	2.76	27.8	0.200	e
	33.2	3.15	42.8	0.308	e
38.0	25.2	2.00	14.0	0.101	e
	30.0	2.60	21.0	0.151	e
	33.0	3.10	26.4	0.190	e
	36.5	3.80	48.4	0.349	e
42.0	26.5	2.12	10.4	0.075	e
	30.0	2.60	14.6	0.105	e
	36.0	3.66	26.1	0.188	e
	38.5	4.20	37.6	0.270	e
	41.0	4.80	58.6	0.421	e
45.0	25.5	2.05	8.42	0.061	e
	30.0	2.60	12.10	0.087	e
	35.0	3.48	17.60	0.127	e
	38.5	4.20	25.80	0.186	e
	42.0	5.10	38.40	0.276	e
	44.0	5.70	51.10	0.367	e
49.0	25.0	1.95	6.2	0.045	e
	29.5	2.50	7.7	0.055	e
	37.0	3.90	14.6	0.105	e
	41.5	4.92	22.6	0.162	e
	45.0	6.00	32.6	0.234	e

The results as tabulated from Tables 5.1 - 5.5 were plotted as concentration against vapour pressure of decane, and a series of isotherms were obtained. As it would be easier to check a value at a known temperature rather than at a known vapour pressure value, these curves were plotted as concentration against polymer temperature at different vapour pressure values. Thus a series of "isobars" were obtained for each polymer, and these are shown in Fig. 28 - 31. The n-decane polymer concentration was found to be related to the temperature by the relationship

$$\log C = m\left(\frac{1}{T}\right) + K \qquad 5.1$$

where C is the concentration

T is the absolute temperature

and m, K are constants

This is shown by the plot for unfilled silicone rubber shown in Fig. 27.

Determination of diffusion coefficients from absorption and desorption.

The diffusion coefficient, D, may be obtained from the rate of absorption and desorption by the relationship (see Eqn.2.41)

$$\frac{M_t}{M_\infty} = \frac{4}{l}\left(\frac{Dt}{\pi}\right)^{1/2} \qquad 5.2$$

where M_t is the mass uptake of the decane vapour at time t, M is the equilibrium uptake, and l is the thickness of the membrane. Therefore a plot of $\frac{M_t}{M_\infty}$ against $t^{1/2}$ should present a straight line, from the slope of which the diffusion coefficient may be calculated. Such plots for unfilled silicone rubber are given in Fig. 32 - 39.

*S.R. = SILICONE RUBBER

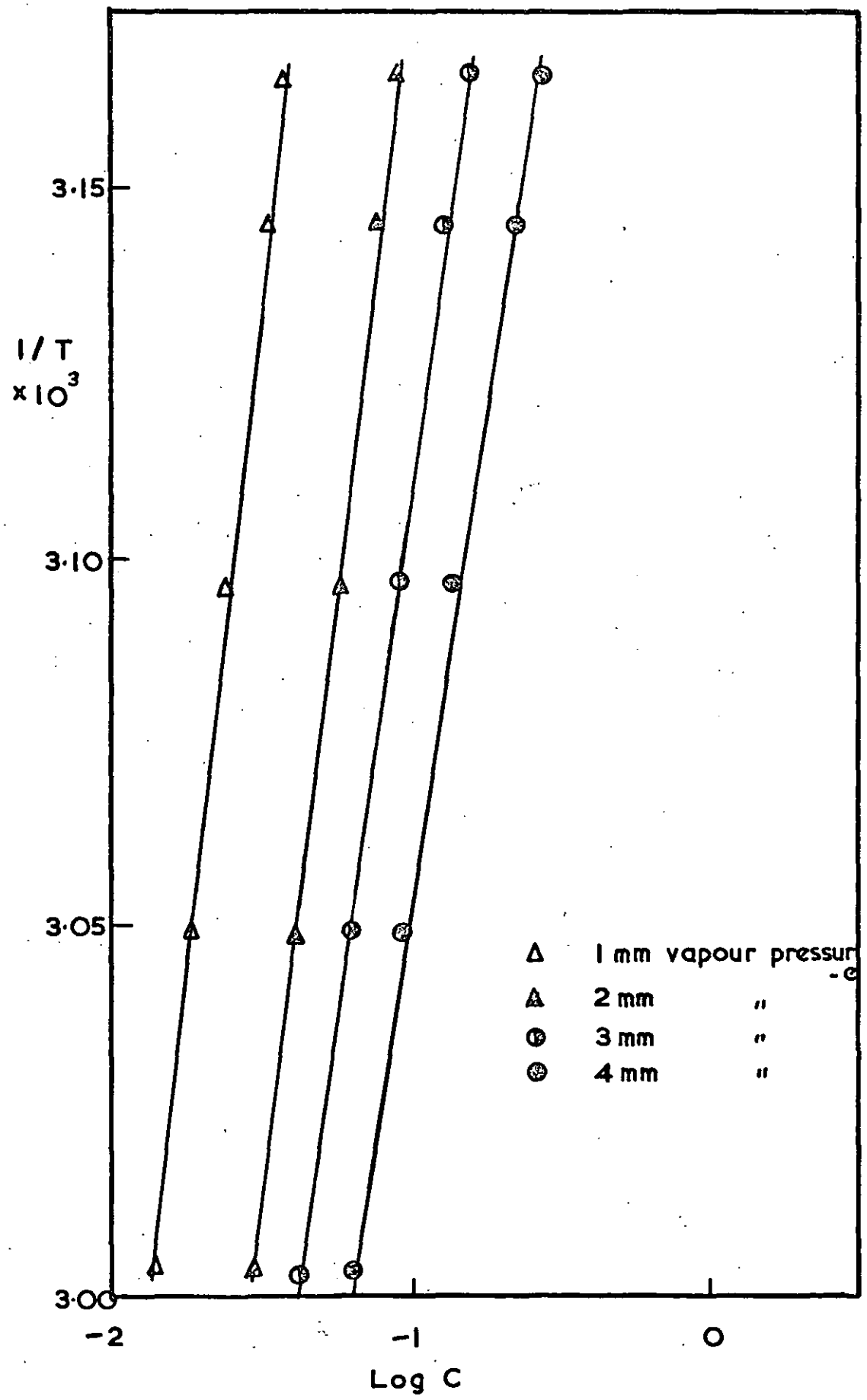

FIG. 27 n-DECANE – S.R.*

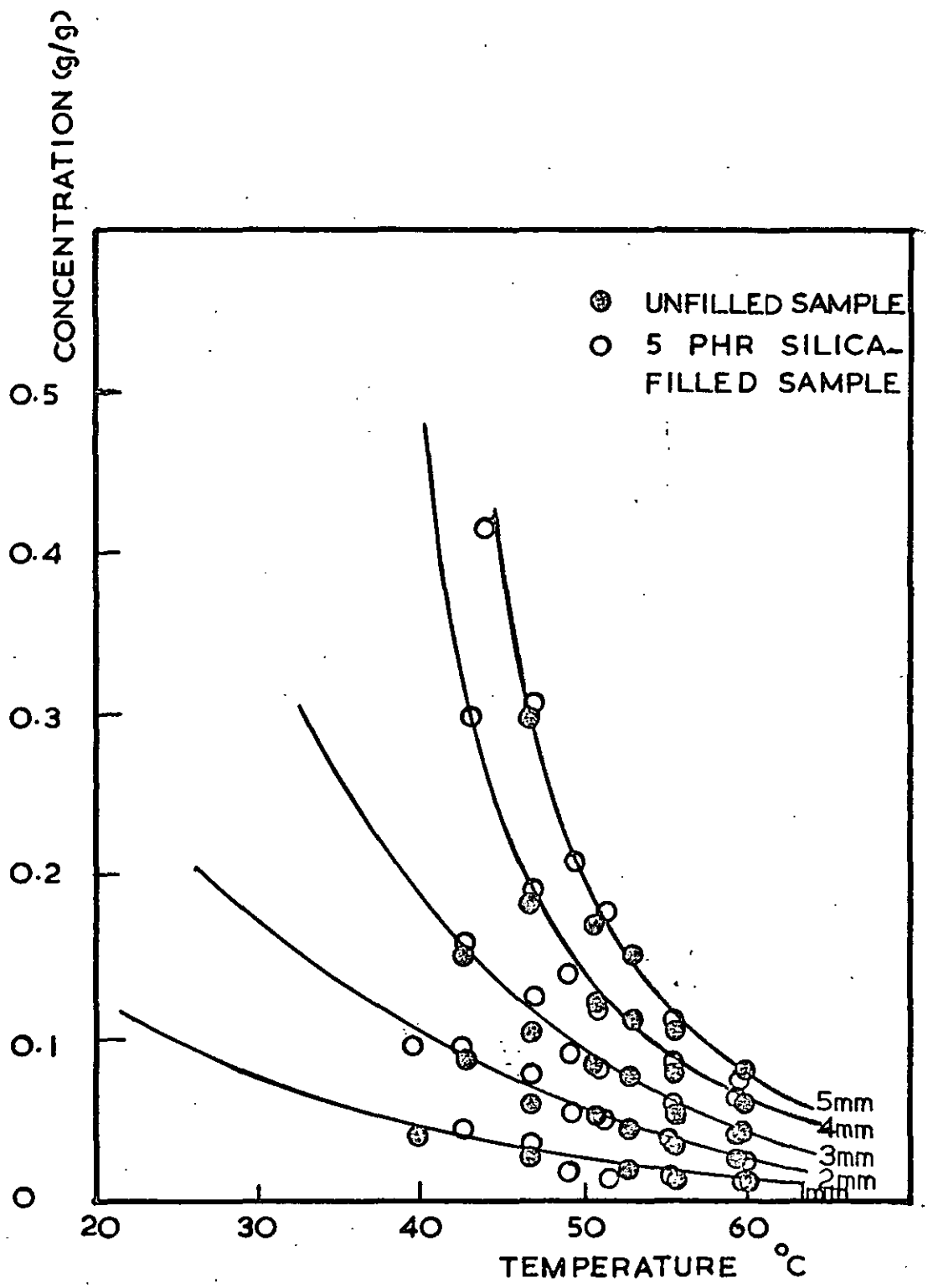

FIG. 28 n-DECANE - S.R.

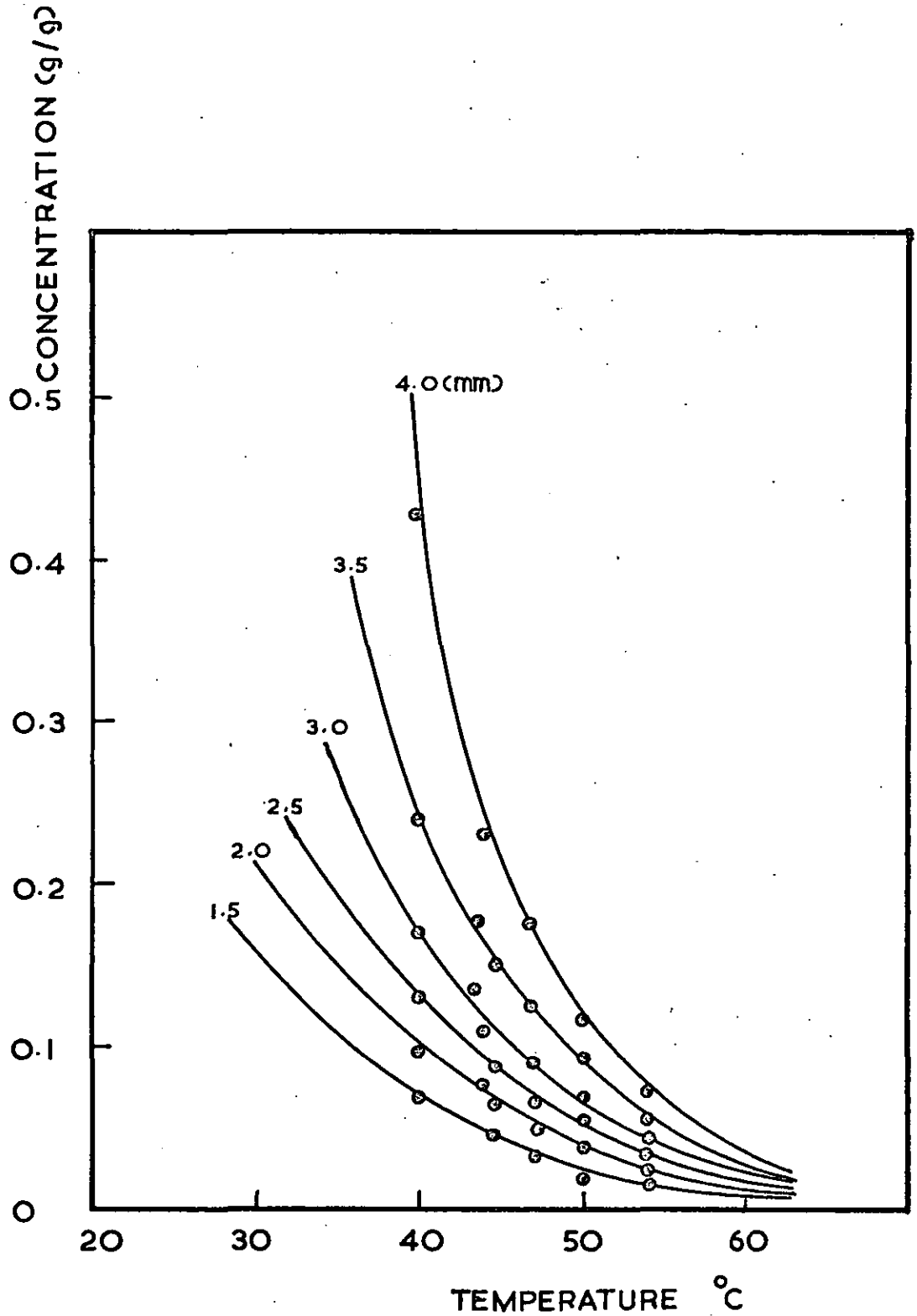

FIG. 29 Silicone - rubber.

n-DECANE - S.R. C10 phr silica filled)

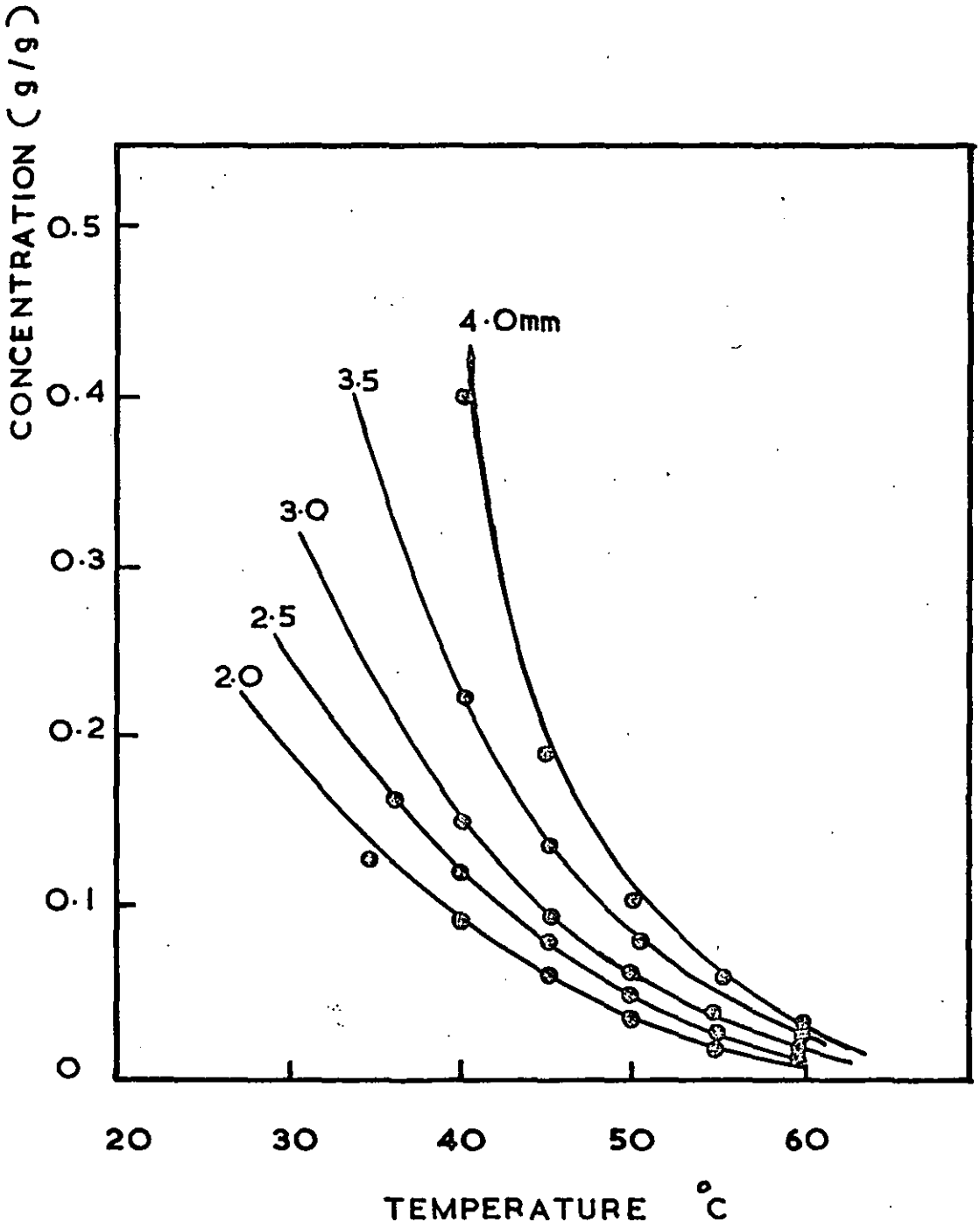

FIG. 30

n-DECANE-SR. (20 phr silica filled)

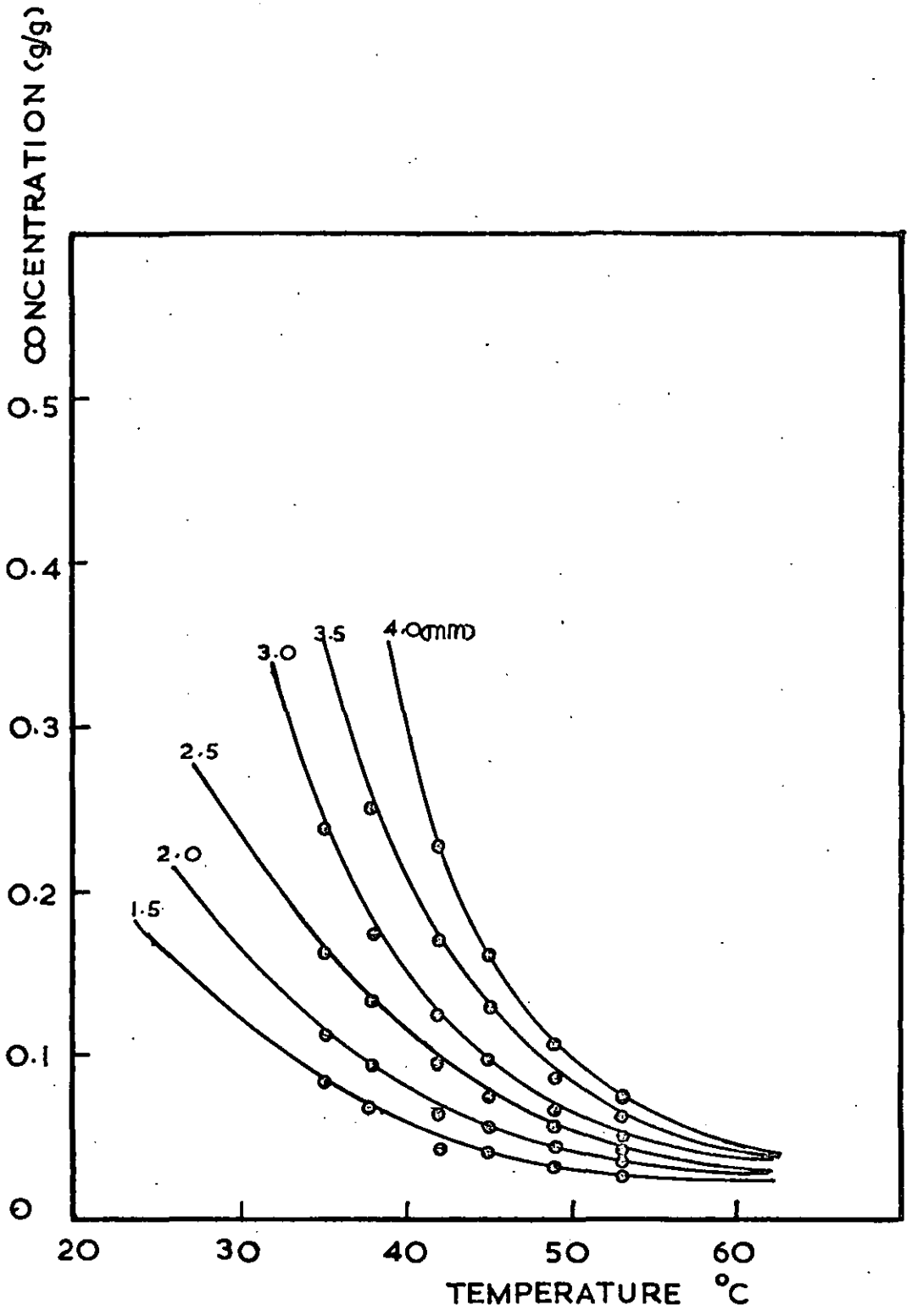

SB-5 - n-decane

FIG. 31

n-DECANE - SBS

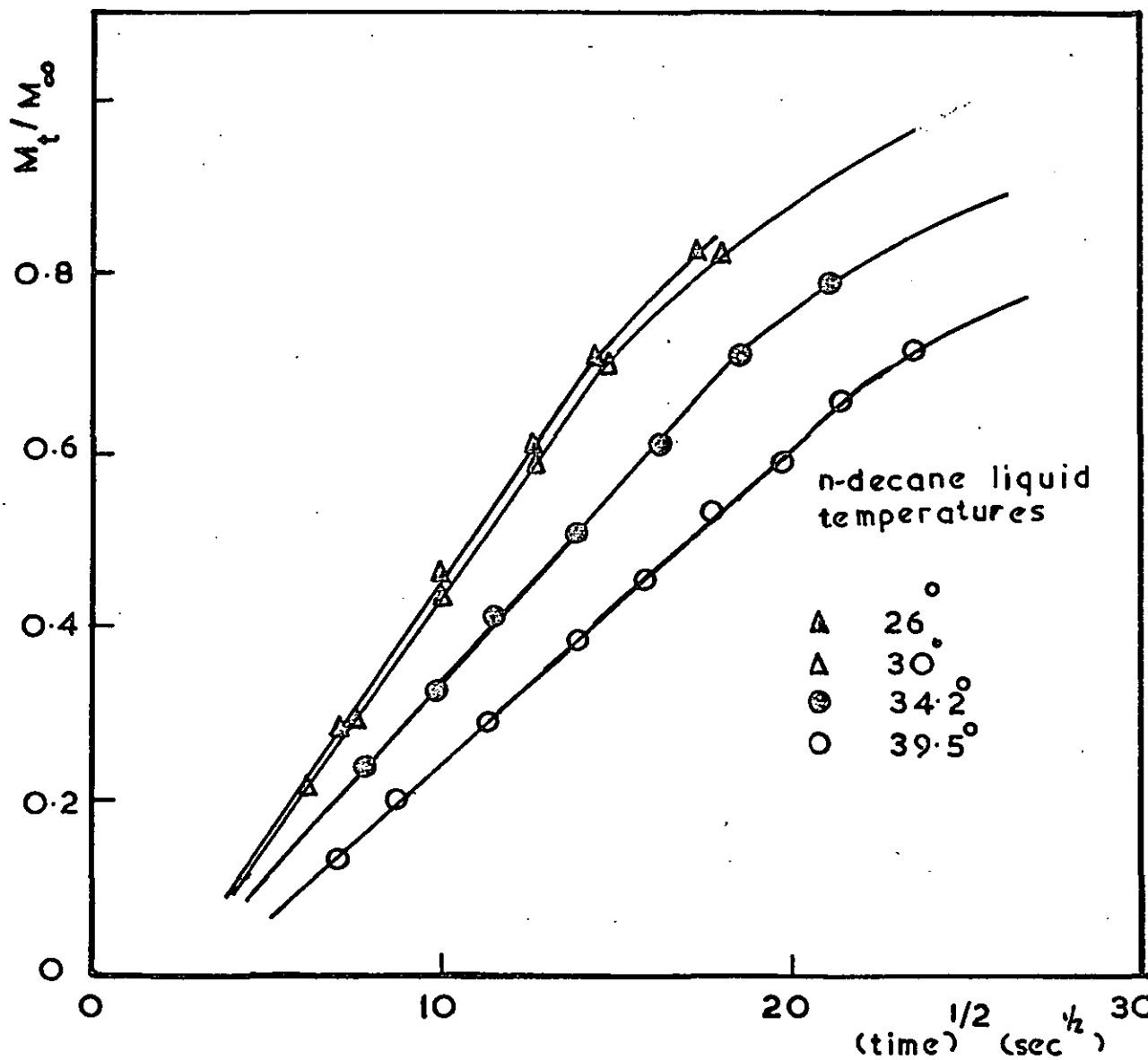

FIG. 32 ABSORPTION 43 °C

n-DECANE - S.R.

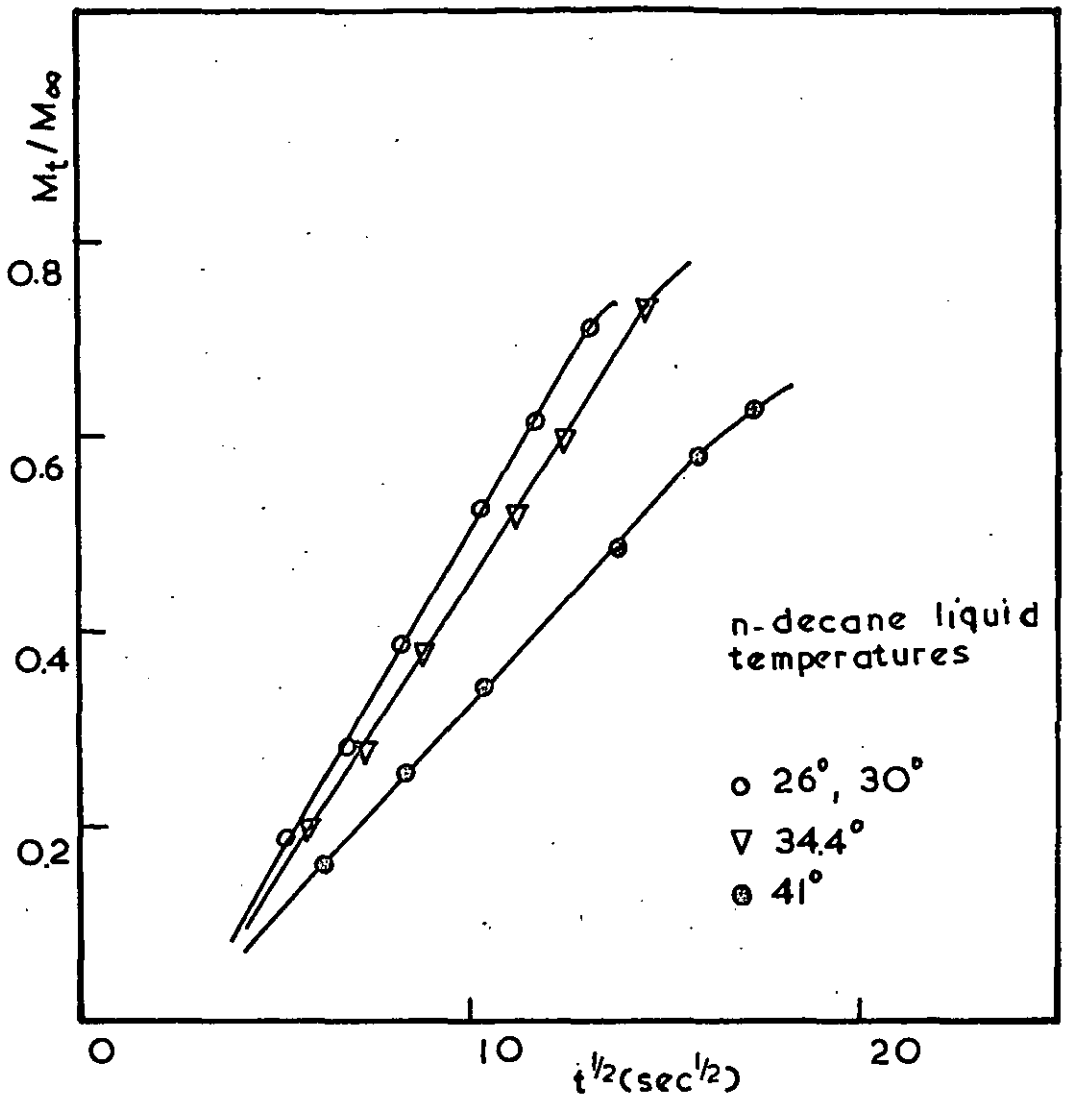

FIG. 33. ABSORPTION 47.5° C.

n-DECANE - S.R.

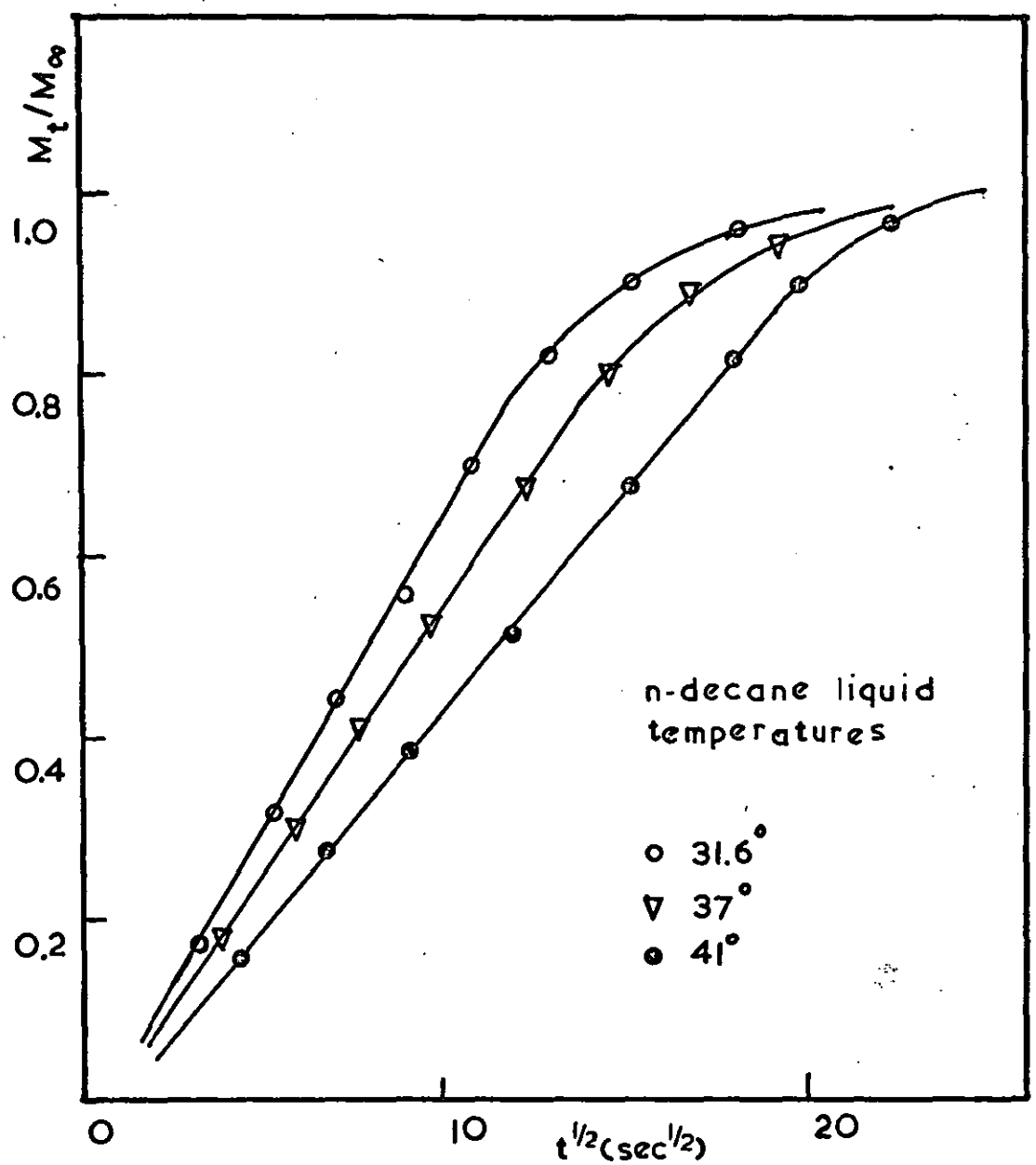

FIG. 34. ABSORPTION 50.5°C.

n-DECANE - S.R.

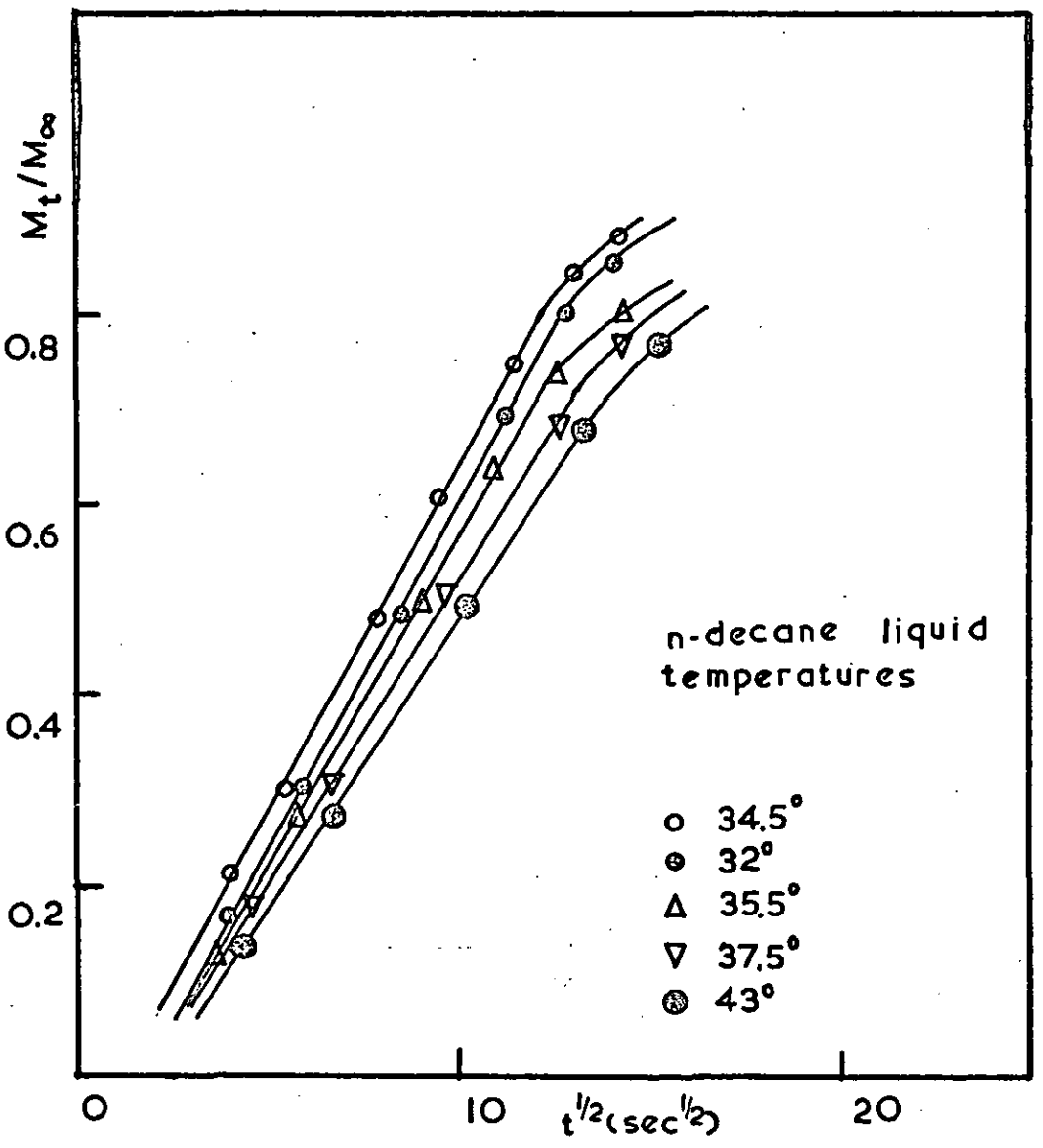

FIG. 35. ABSORPTION 57°C.
n-DECANE – S.R.

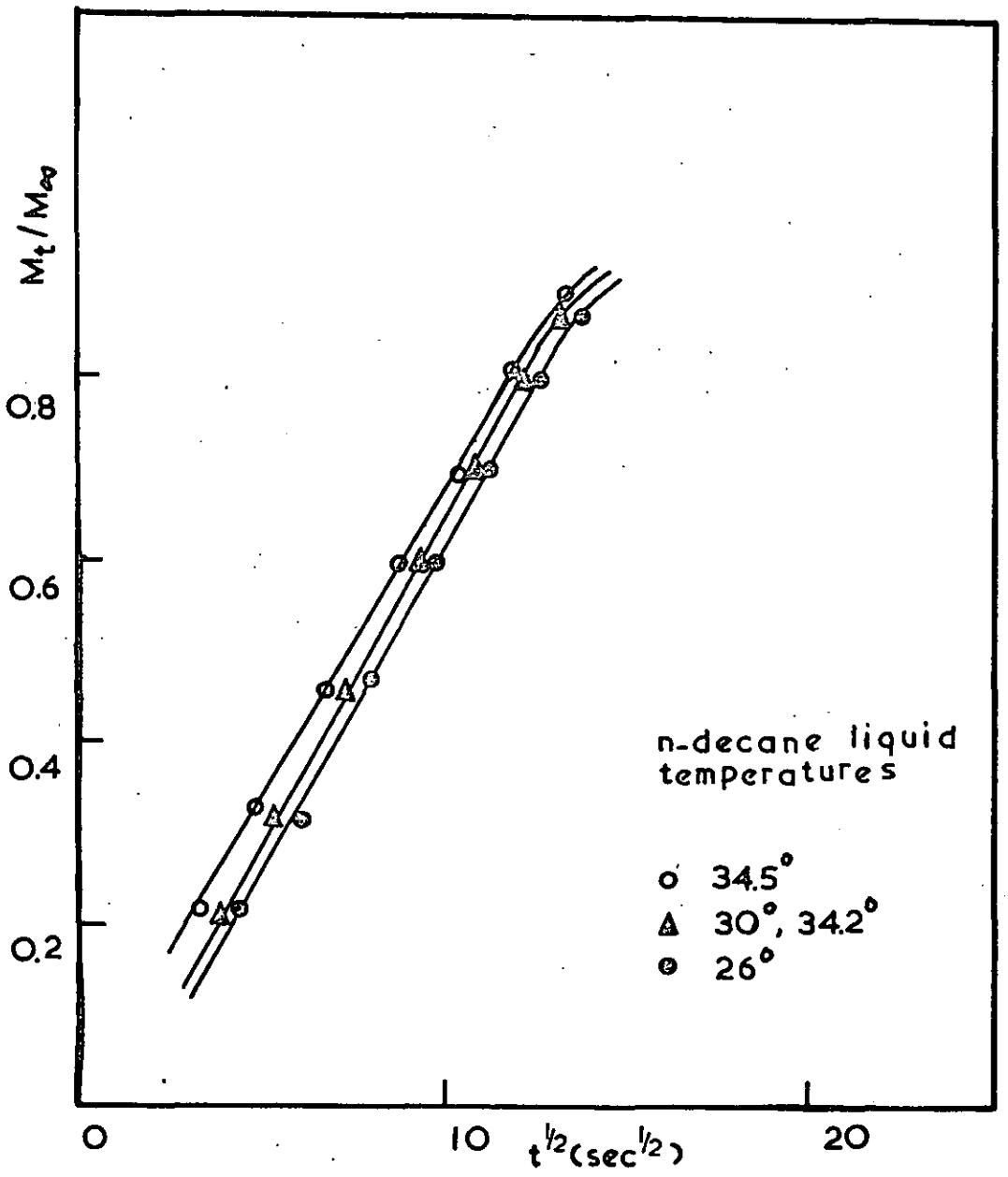

FIG. 36. DESORPTION 43°C.

n-DECANE - S.R.

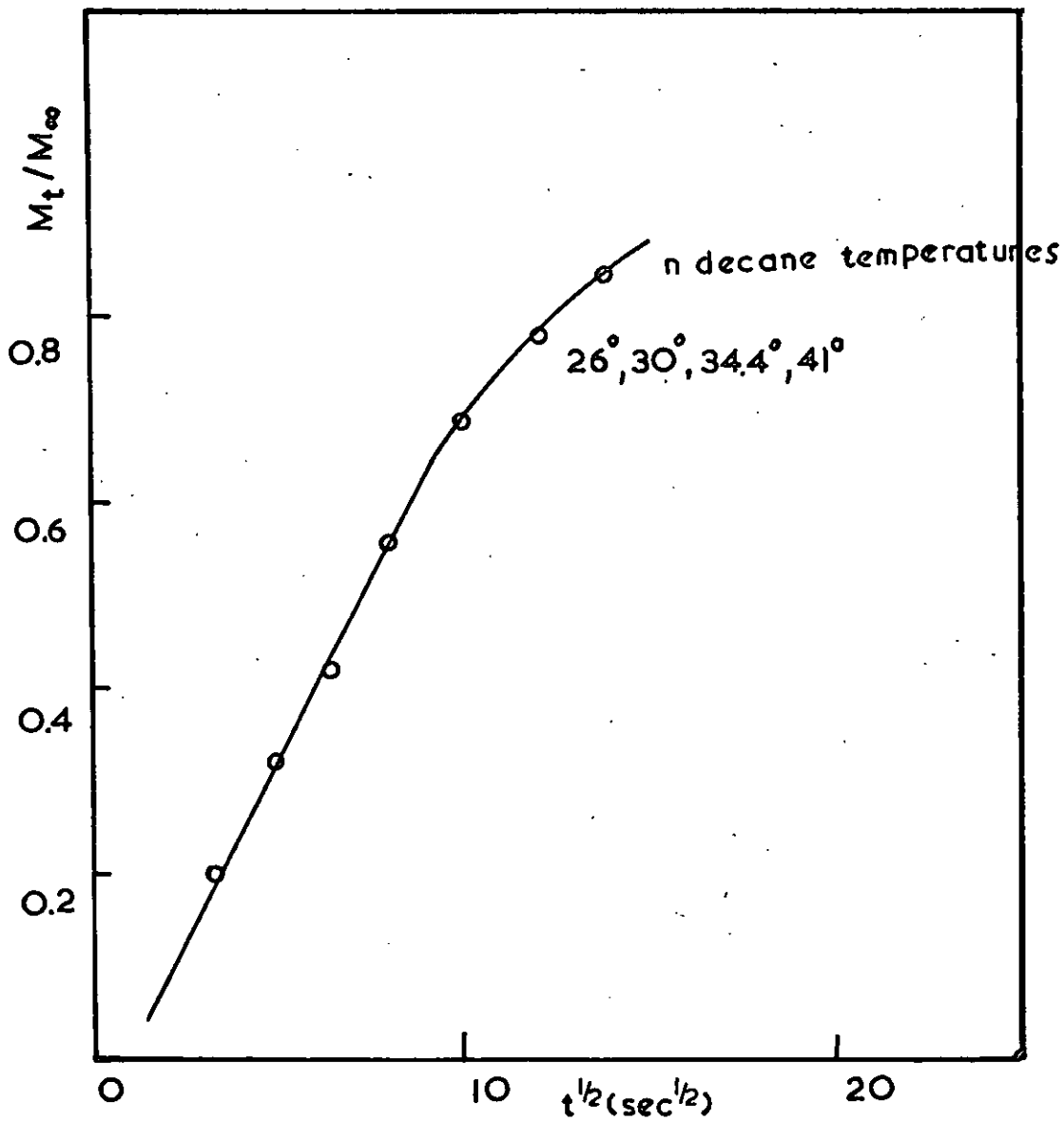

FIG. 37. DESORPTION 47.5°C.

n-DECANE - S.R.

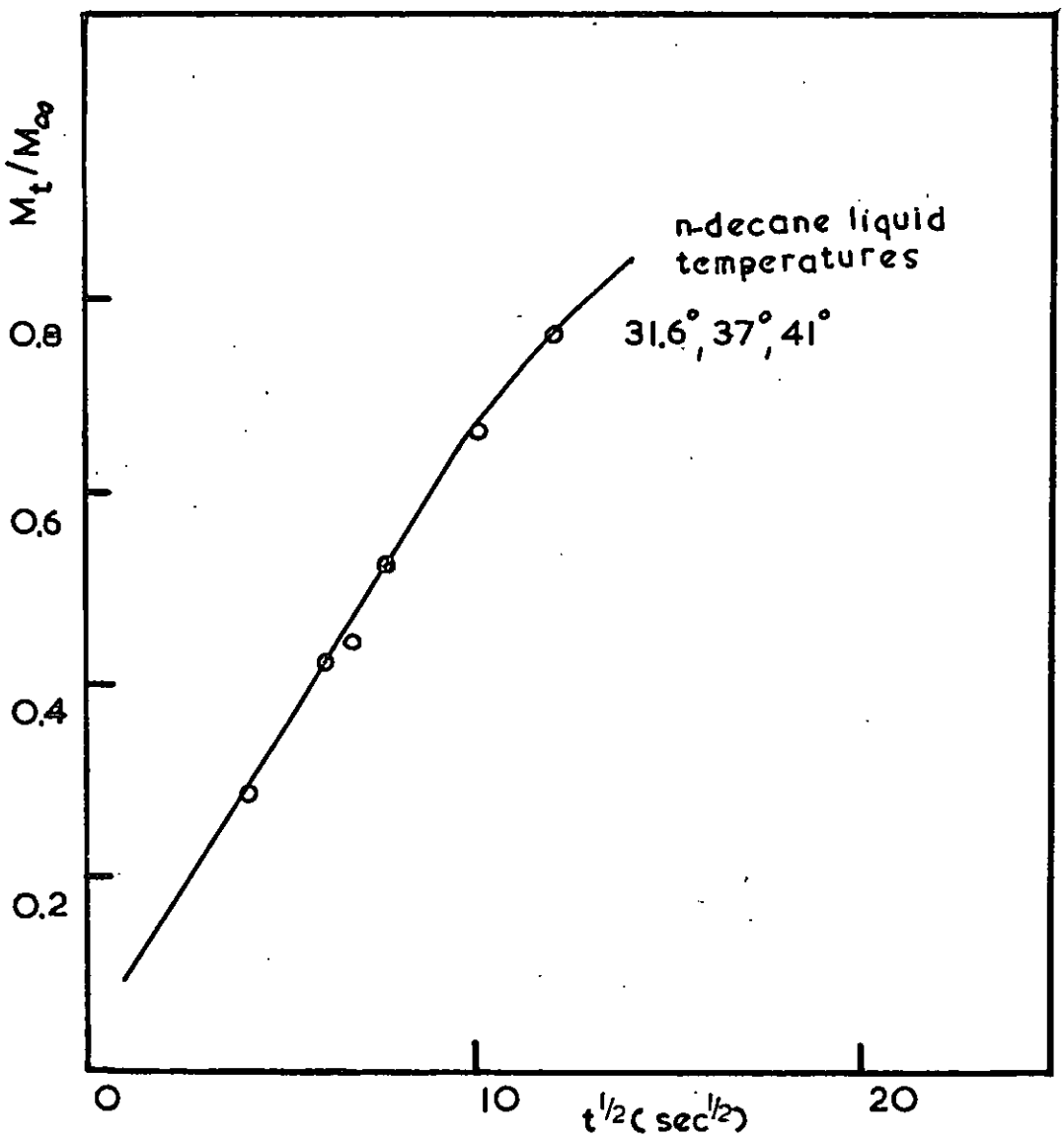

FIG. 38. DESORPTION 50.5 C°

n-DECANE - S.R.

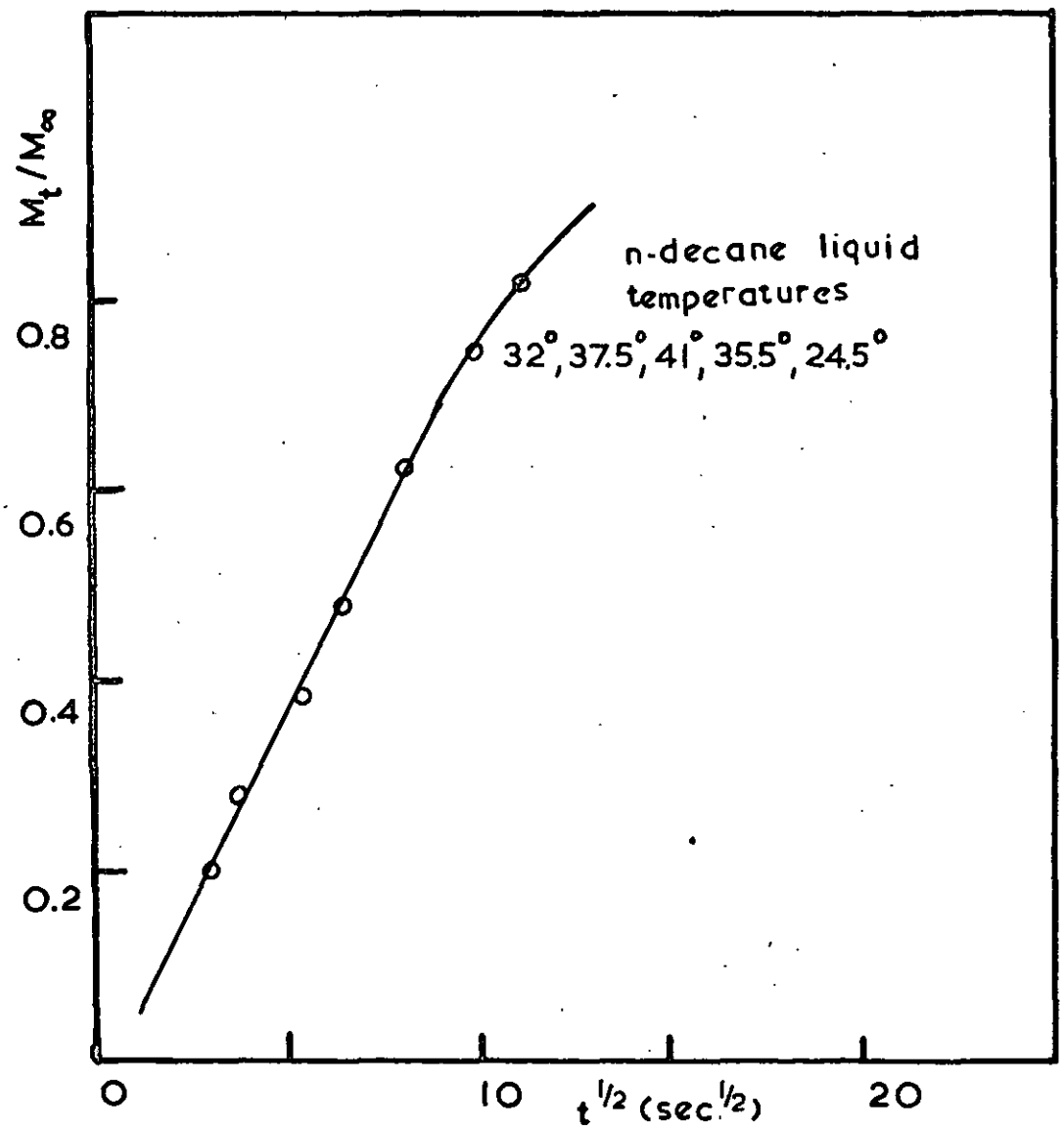

FIG. 39. DESORPTION 57.0°C

n-DECANE - S.R.

5.2. Permeation Results.

The rate of permeation, denoted as P, was measured as (counts per second) increase per minute (c.p.s. min^{-1}). The results were tabulated in four columns, viz. diffusant liquid temperature (T_1), polymer temperature (T_s), liquid scintillator temperature (T_2), and permeation rate P. From T_1, (and T_s), the concentration (C^*) of the 14C labelled decane at the radioactive face of the polymer membrane can be obtained. Similarly from T_2, the concentration (C_s) of the decane at the non-active face is known. T_1 and T_2 were kept as close in value to each other, as experimental conditions allowed. In reality T_1 was in general a little larger than T_2 (see Chapter 4.2). In the most extreme case this difference reached 8°C. The error invoked in taking the arithmetic mean of C^* and C_s as the average concentration, increases with larger differences between T_1 and T_2. Therefore in some cases it is necessary to estimate the average concentration from a graphical method as outlined in Chapter 2.2.

The permeation rate P was obtained by measuring the slope of the count rate increase versus time plot after a steady state has been reached. Some of the steady state permeation plots are shown in Fig.40 - 44, for the different polymer samples used. The polymer temperature in °C is given by the number at the end of the straight line plot, and the two figures within the bracket represent respectively T_1 and T_2.

Table 5.6 - 5.9 contain the full permeation results as well as the exact temperature measurements taken for each run.

TABLE 5.6. Silicone rubber (no filler)

Polymer Temperature (°C)	Diffusant liquid temperature T_1(°C)	Scintillator liquid temperature T_2(°C)	Permeation Rate c.p.s.min^{-1}
30.5	24.0	23.5	2.6
30.5	27.8	20.0	3.8
30.5	27.5	24.0	4.0
30.5	26.0	22.0	3.4
34.0	26.5	23.5	3.3
34.0	29.0	26.5	3.9
34.0	30.0	28.5	5.3
34.0	29.8	27.0	4.8
38.0	28.0	24.0	2.8
38.0	29.5	24.0	3.5
38.0	30.0	28.0	3.5
38.0	32.5	26.5	4.3
39.0	31.0	26.5	4.3
45.0	35.0	27.5	5.6
49.0	37.0	23.5	4.9
30.0	26.0	22.0	3.4
48.0	33.5	28.5	6.3
40.0	29.5	28.5	5.2
38.5	30.5	29.5	3.7
43.0	30.5	29.0	3.75
42.0	33.5	27.0	5.1

Thickness of polymer membrane = 0.052 cm ($\pm$ 0.002 cm).

TABLE 5.7. Silicone rubber (10 phr filler)

Polymer Temperature (°C)	Diffusant liquid temperature (°C)	Scintillator liquid temperature (°C)	Permeation Rate c.p.s.min^{-1}
24.5	21.0	19.5	3.8
28.5	27.0	22.0	5.0
30.0	27.8	22.0	4.2
32.5	30.5	23.0	6.0
41.5	36.0	26.0	7.0
42.0	38.5	30.0	15.0

Thickness of membrane = 0.062 cm ($\pm$ 0.00 2 cm).

TABLE 5.8. Silicone rubber (20 phr filler)

Polymer Temperature (°C)	Diffusant liquid temperature (°C)	Scintillator liquid temperature (°C)	Permeation rate c.p.s.min^{-1}
27.5	21.0	19.2	3.9
32.5	22.0	19.2	4.0
35.5	25.0	19.5	5.0
41.0	31.5	25.0	5.8
44.0	34.0	26.0	7.2

Thickness of membrane = 0.038 mm.

TABLE 5.9. S-B-S copolymer cast from toluene

Polymer Temperature (°C)	Liffusant liquid temperature (°C)	Scintillator liquid temperature (°C)	Permeation rate $c.p.s.min^{-1}$
32.0	28.0	28.0	1.90
32.0	24.5	20.0	1.06
32.0	24.0	18.0	1.00
32.0	27.5	26.0	1.50
32.0	25.0	25.0	1.22
26.0	21.0	19.5	1.00
36.0	29.0	21.5	1.25
36.5	29.2	21.5	1.35
38.0	32.5	21.5	1.60
39.5	32.5	26.5	1.55

Thickness of membrane = 0.0735 cm.

TABLE 5.10. S-B-S copolymer cast from methylene chloride.

Polymer Temperature (°C)	Diffusant liquid temperature (°C)	Scintillator liquid temperature (°C)	Permeation rate $c.p.s.min^{-1}$
28.0	24.5	19.5	1.20
31.0	26.5	24.0	1.40
31.0	22.5	20.0	0.85
31.0	25.5	21.0	1.1
31.0	27.5	26.0	1.60
35.5	29.5	25.5	1.55
36.5	30.0	26.0	1.60
40.0	32.5	28.0	1.75

Thickness of membrane = 0.0625cm.

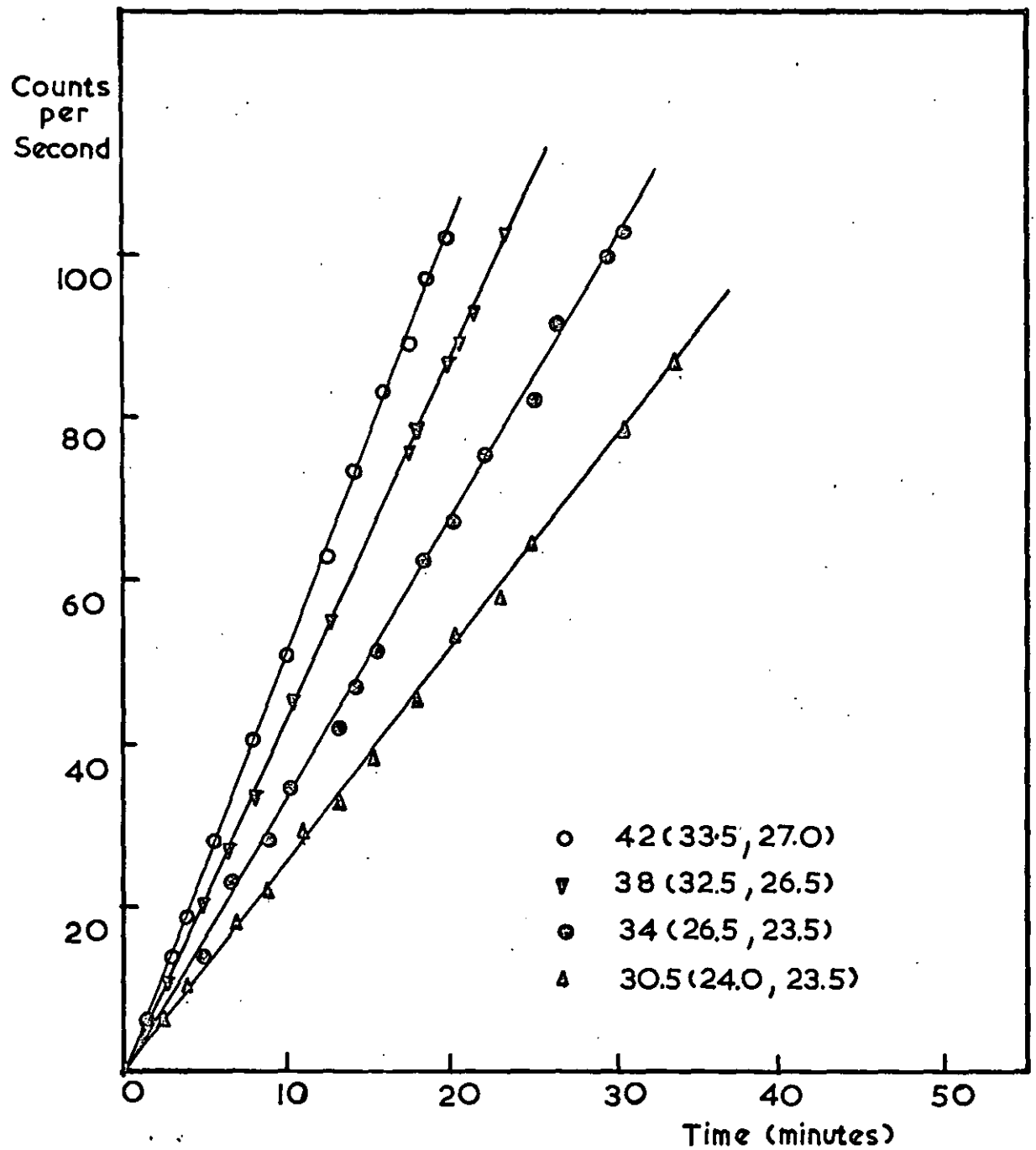

FIG.40. SOME PERMEATION PLOTS FOR UNFILLED SILICONE RUBBER.

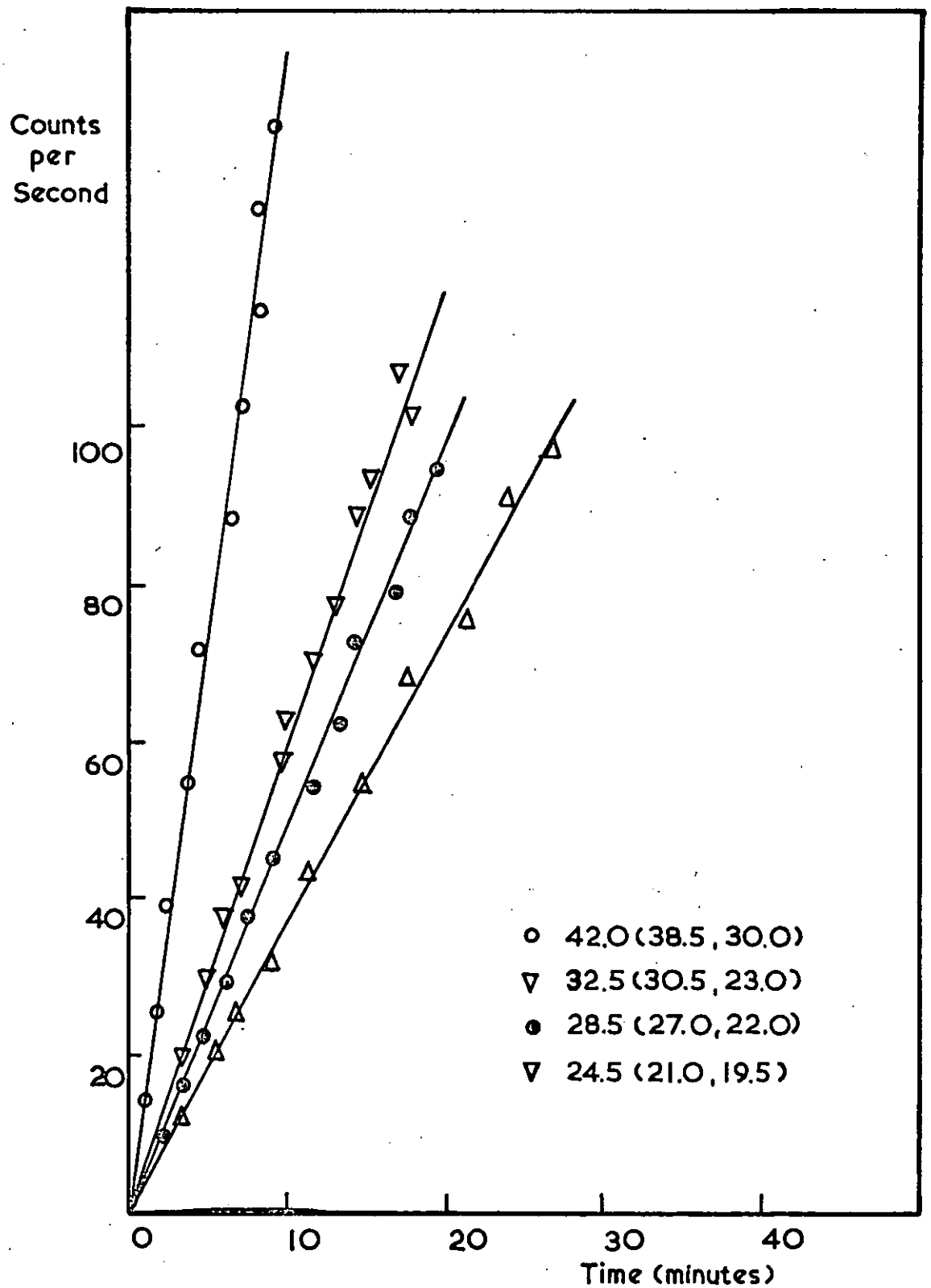

FIG. 41. SOME PERMEATION PLOTS FOR 10 phr SILICA FILLED SILICONE RUBBER.

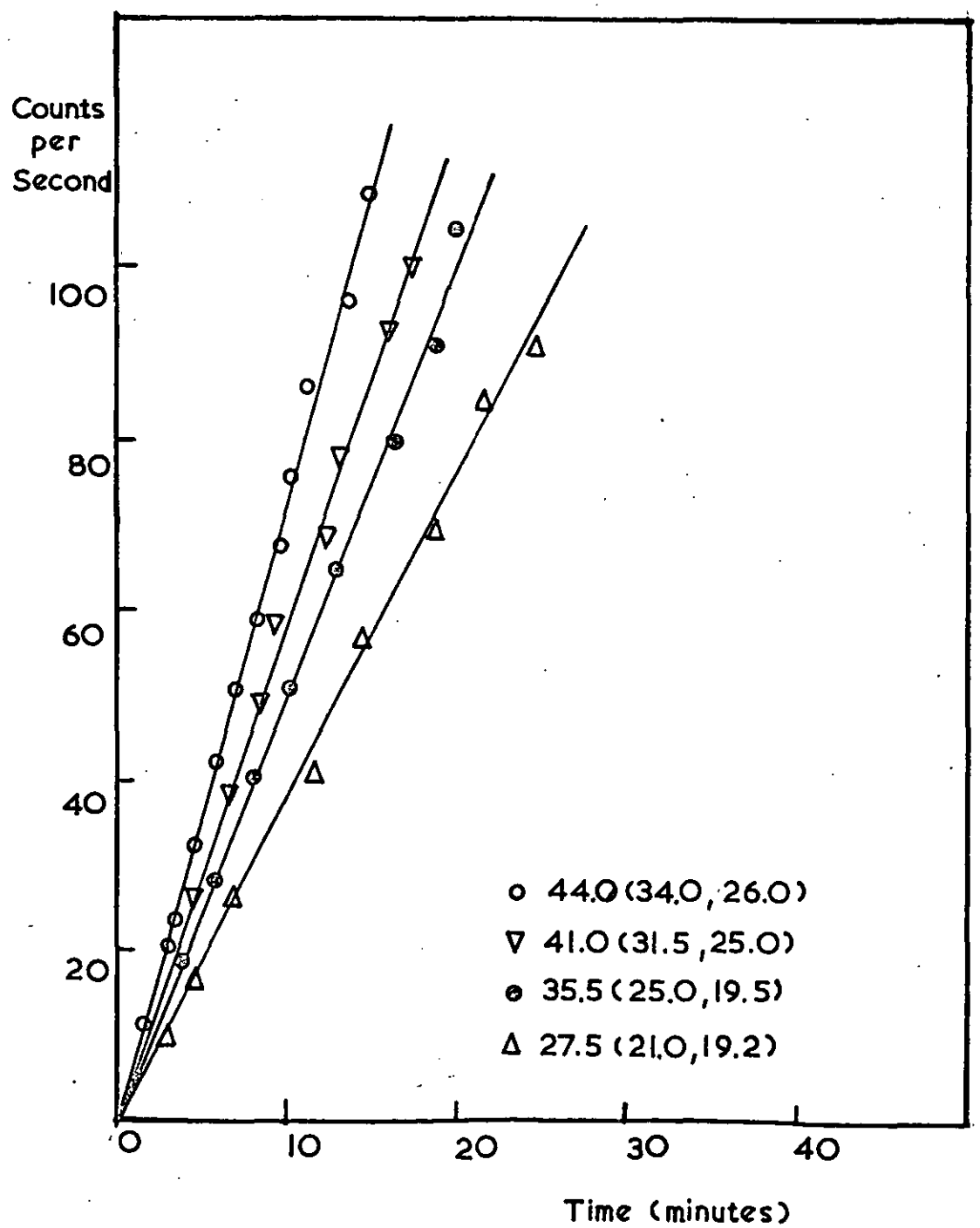

FIG. 42. SOME PERMEATION PLOTS FOR 20 phr SILICA FILLED SILICONE RUBBER.

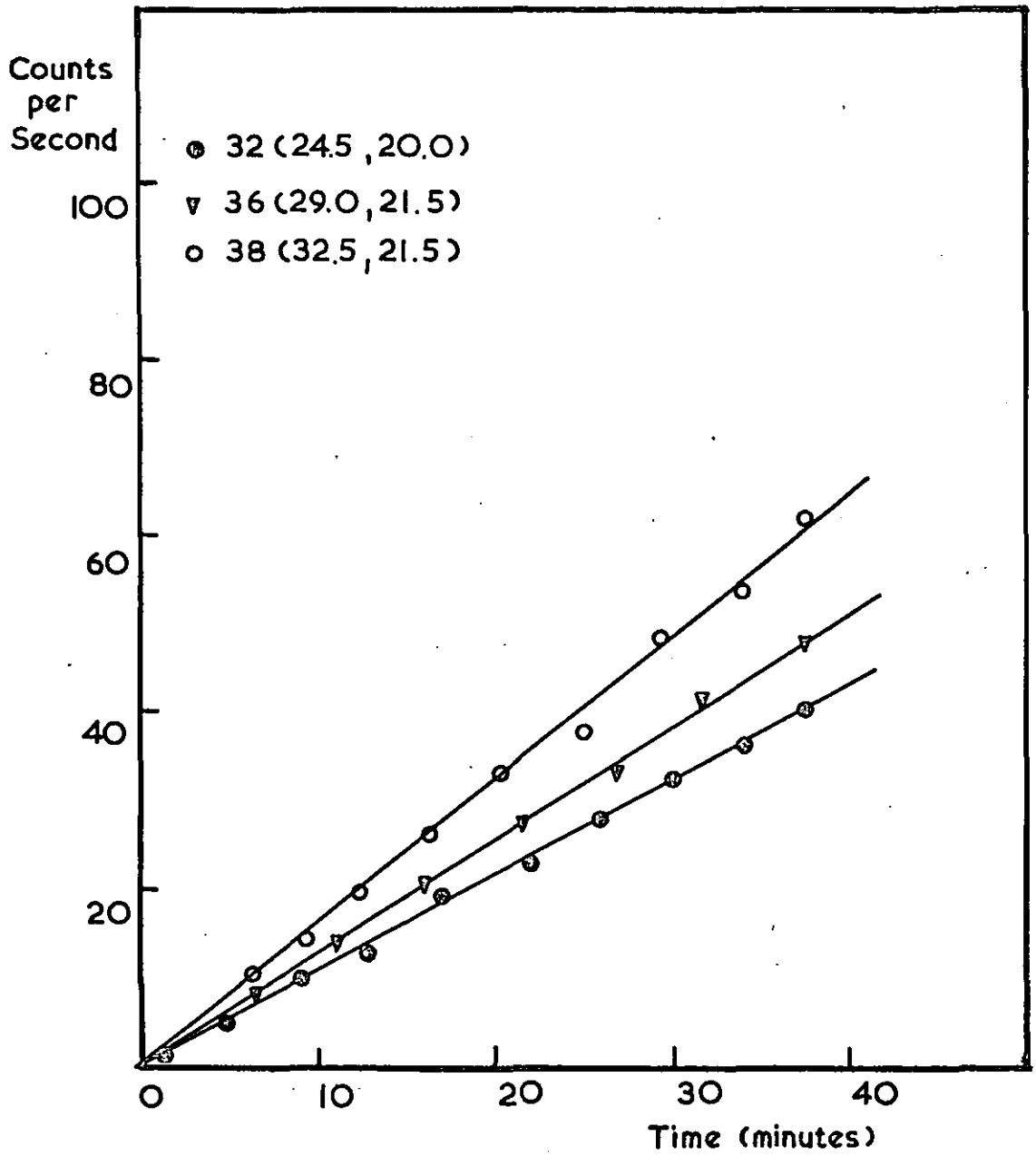

FIG. 43. SOME PERMEATION PLOTS FOR SBS SAMPLE CAST FROM TOLUENE.

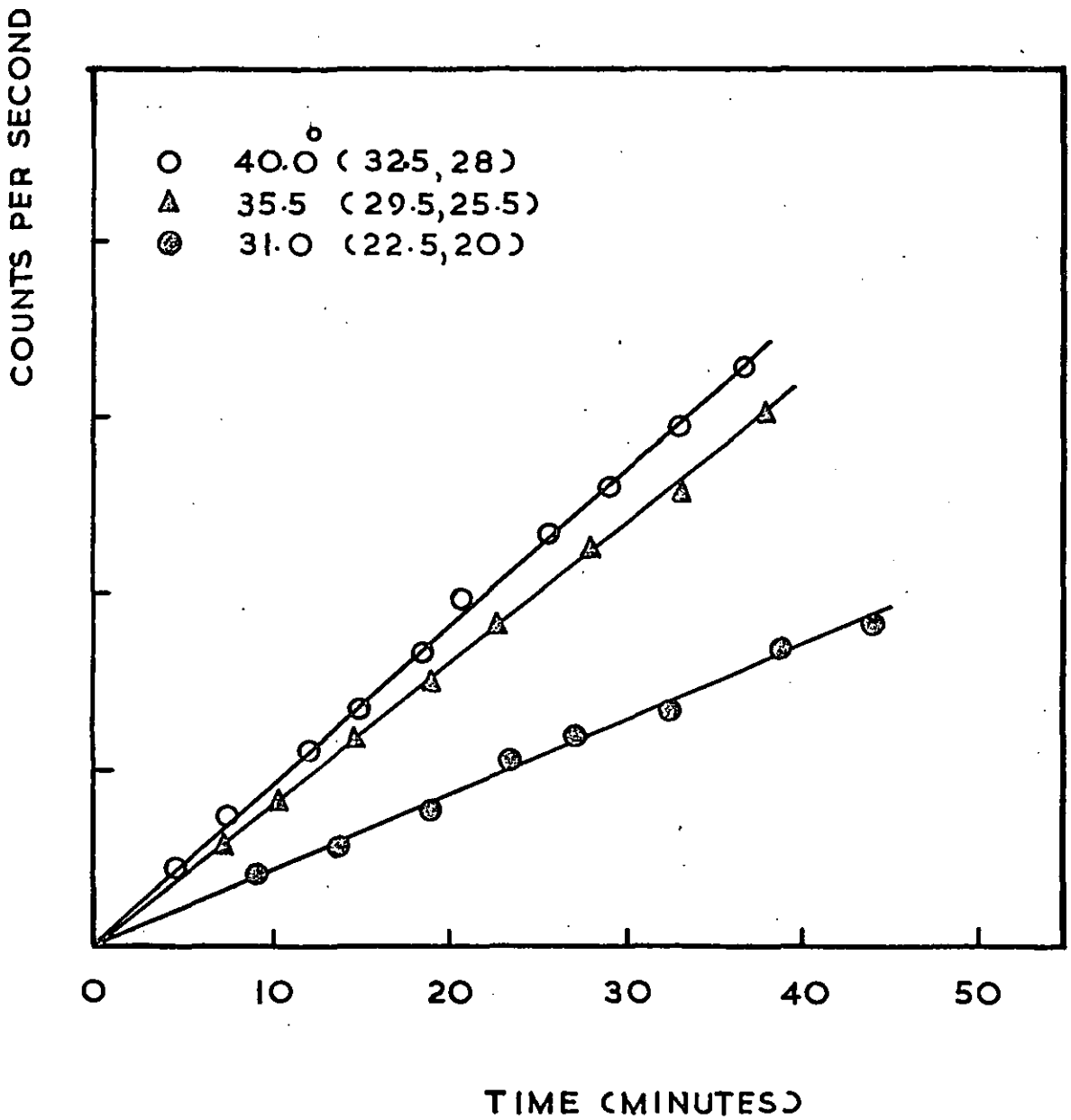

FIG. 44 SOME PERMEATION PLOTS FOR S-B-S SAMPLE CAST FROM CH_2Cl_2

Calculation of the diffusion coefficients.

Using Eqn. 2.24, the diffusion coefficient, D, is related to the flux F by the relation

$$F = - D \frac{C_1 - C_2}{l} \qquad 5.3$$

where C_1 and C_2 are the concentrations of the diffusant at the ingoing and outgoing faces respectively, and l is the thickness of the polymer membrane.

Therefore, applying Eqn. 5.3 to the permeation of the radioactive molecules, C_1 becomes the concentration of the radioactive molecules C^* at the ingoing face, and $C_2 = 0$. The actual concentration of the solvent molecules in the polymer, regardless of radioactivity, is the average of C^* and C_s measured. If C^* and C_s are close in value, then an arithmetic mean is taken to represent the average concentration, denoted by $\bar{C}$.

Thus the value of D calculated from Eqn. 5.3 is the self-diffusion coefficient of the penetrant in the polymer at concentration $\bar{C}$. This is represented as, simply

$$D_{\bar{C}} = \frac{F\,l}{C^*} \qquad 5.4$$

F is obtained from the experimentally measured permeation rate, P, as follows:-

From the weight/radioactivity calibration of n-decane (Fig.23),

1 count per second (cps) $\equiv 5.8 \times 10^{-4}$ g n-decane

Since P is expressed in cps min^{-1}

$$\therefore F = P \times \frac{5.8 \times 10^{-4}}{60} \times \frac{1}{A} \text{ g sec}^{-1} \text{ cm}^{-2} \qquad 5.5$$

where A is the cross section area of the polymer membrane across which diffusion takes place. ($A = 4.5$ cm^2.)

Expressing C^* in Eqn. 5.4 in gcm^{-3}

it becomes ρC^*, ρ being the density of the polymer.

($\rho = 0.986$)

Substituting F from Eqn.5.4 into Eqn. 5.3

$$\frac{D}{\bar{C}} = \frac{P\,l}{C^*}\ 2.18 \times 10^{-6} \quad cm^2\ sec^{-1} \qquad 5.6$$

5.3. Dynamic Mechanical Results.

The polymer measured was the unfilled silicone rubber. The results are tabulated in Table 5.11. E'_{λ} values modified by the rubber elasticity correction term $\frac{T_o \rho_o}{T \rho}$ are also tabulated. These will be required later for the William, Landel and Ferry shift procedures. The reference temperature was taken as 39°C.

The tan δ values near the glass transition point are also tabulated in Table 5.12. The modified E' and the tan δ values were plotted against log (frequency), and these are shown in Fig. 45 and Fig. 46 respectively. From these plots the activation energy terms at these temperatures can be derived.

Table 5.1I

TEMP °C.	FREQUENCY (f)	Log f	Input (volts)	E' x 10^7	E' $\frac{To\rho o}{T\rho}$ x 10^7
0	30	1.477	12.8	1.050	1.140
	10	1.000	"	1.015	1.086
	3	0.477	"	1.00	1.053
	1	0	"	0.960	1.028
	0.3	-0.523	"	0.935	1.001
22.5	30	1.477	11.05	1.04	1.091
	10	1.000	"	1.01	1.069
	3	0.477	"	0.992	1.043
	1	0	"	0.965	1.011
	0.3	-0.523	"	0.940	0.989
29.0	30	1.477	5.75	1.075	1.092
	10	1.000	"	1.032	1.066
	3	0.477	"	1.010	1.046
	1	0	"	0.99	1.011
	0.3	-0.523	"	0.955	0.978
	0.1	-1.000	"	0.940	0.961
35.0	30	1.477	7.2	1.080	1.086
	10	1,000	"	1.035	1.059
	3	0.477	"	1.02	1.031
	1	0	"	1.00	1.007
	0.3	-0.523	"	0.96	0.973
	0.1	-1.000	"	0.945	0.956
39.0	30	1.477	8.0	1.086	1.080
(To)	10	1.000	"	1.062	1.062
	3	0.477	"	1.028	1.028
	1	0	"	1.00	1.000
	0.3	-0.523	"	0.975	0.975
	0.1	-1.000	"	0.950	0.950

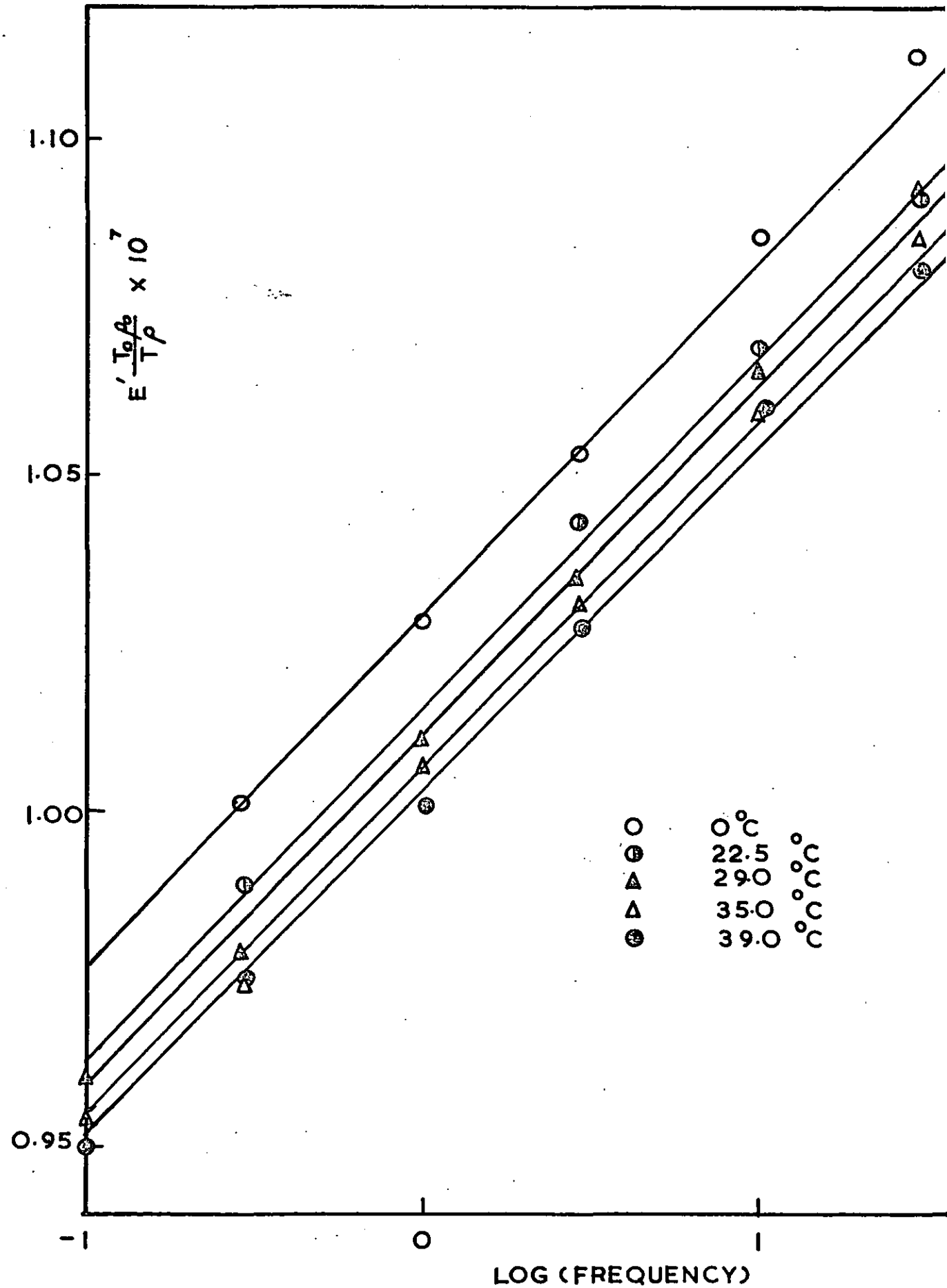
1.10
1.05
1.00
0.95
$E' \frac{T_0 \rho_0}{T \rho} \times 10^7$
-1
0
1
LOG (FREQUENCY)
0 °C
22.5 °C
29.0 °C
35.0 °C
39.0 °C

FIG. 45

Table 5.12

TEMP °C.	FREQUENCY f.	Log.f.	Input(volts)	Tan δ
-114	300	2.477	13.0	0.042
	200	2.303	"	0.039
	100	2.000	"	0.036
	30	1.477	"	0.036
	10	1.000	"	0.032
	3	0.477	"	0.028
	1	0	"	0.026
-116	300	2.477	"	0.053
	200	2.303	"	0.051
	100	2.000	"	0.047
	30	1.477	"	0.042
	10	1.000	"	0.035
	3	0.477	"	0.026
	1	0	"	0.026
-119	300	2.477	"	0.053
	200	2.303	"	0.054
	100	2.000	"	0.057
	30	1.477	"	0.056
	10	1.000	"	0.051
	3	0.477	"	0.045
	1	0	"	0.040
-124	300	2.477	"	0.036
	200	2.303	"	0.038
	100	2.000	"	0.040
	30	1.477	"	0.048
	10	1.000	"	0.054
	3	0.477	"	0.051
	1	0	"	0.045

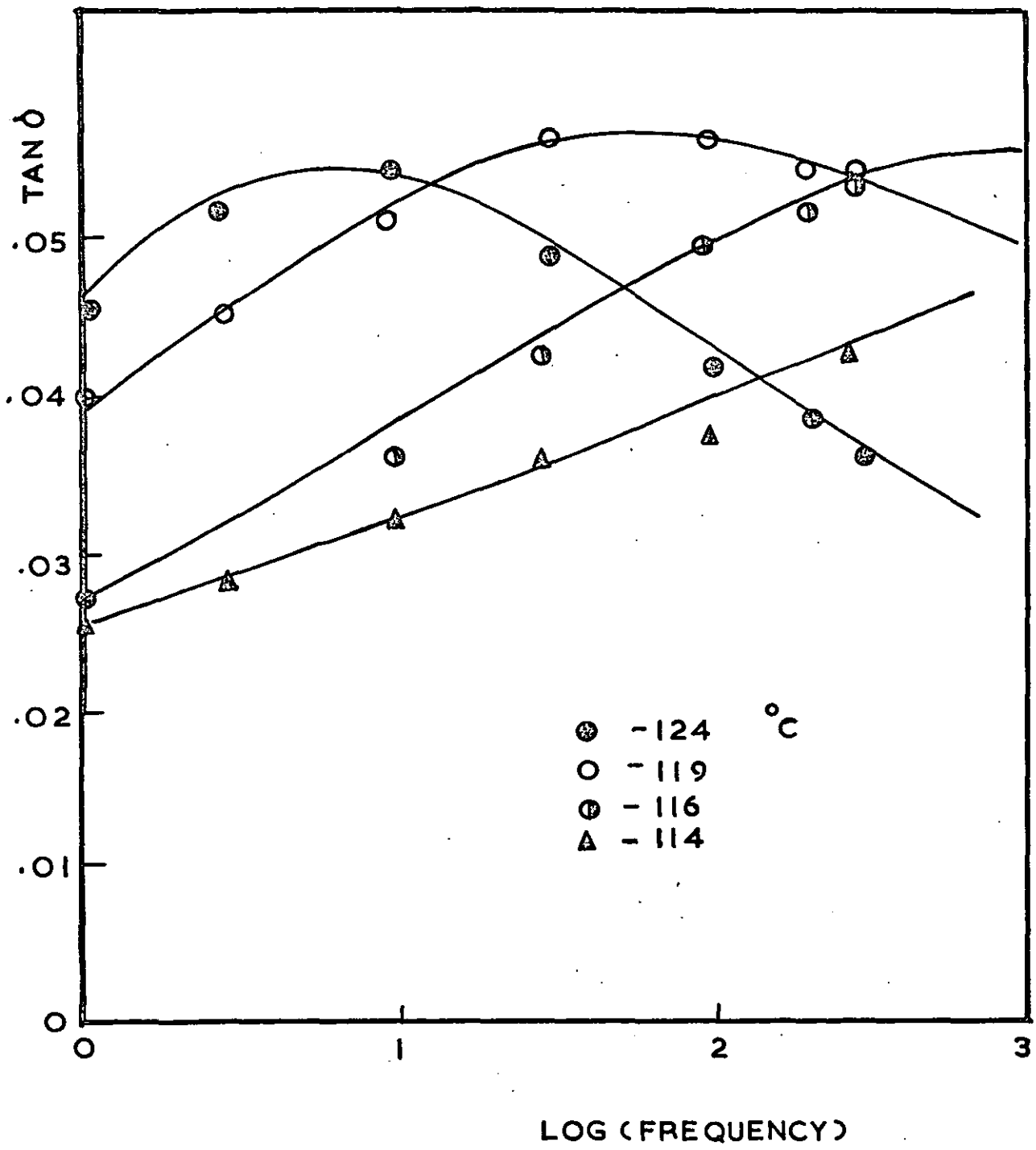

FIG. 46

CHAPTER 6

DISCUSSION

6.1. Sorption discussion.

When penetrant molecules are absorbed by a polymer sample, the amount sorbed, or solubility, will at a constant temperature, depend upon the pressure of the gas or vapour. Four principal types of solubility isotherms have been observed for polymer-penetrant systems (141). These are shown in Fig.47 and are denoted as Types I, II, III and IV.

Type I is a linear isotherm exemplified by Henry's law which is characteristic of simple solutions. This behaviour is common when no interaction occurs between the penetrant and the polymer, as in the case of a permanent gas permeating natural rubber. The Langmuir-type isotherm represented by Type II does not involve solution of penetrant but only adsorption in a single layer on any adsorption site. An example of this is the sorption of hydrogen sulphide in ethyl cellulose. Type III involves multilayer surface adsorption characterised by strong penetrant-polymer interaction as in the case of water sorption in rigid hydrophilic polymers. Type IV involves absorption into systems showing positive deviation from Henry's law. This is the case in most organic vapour-polymer systems.

Our results for n-decane sorption isotherms in filled and unfilled silicone rubber, and S-B-S block copolymer all follow the type IV behaviour. This is in agreement with the general classification of sorption behaviour described above, as decane is a solvent for these polymers.

The temperature dependence of the solubility, S, is governed by the Clausius-Clapeyron equation in the form

$$\Delta H = -R \, d \ln S / d (1/T) \qquad 6.1$$

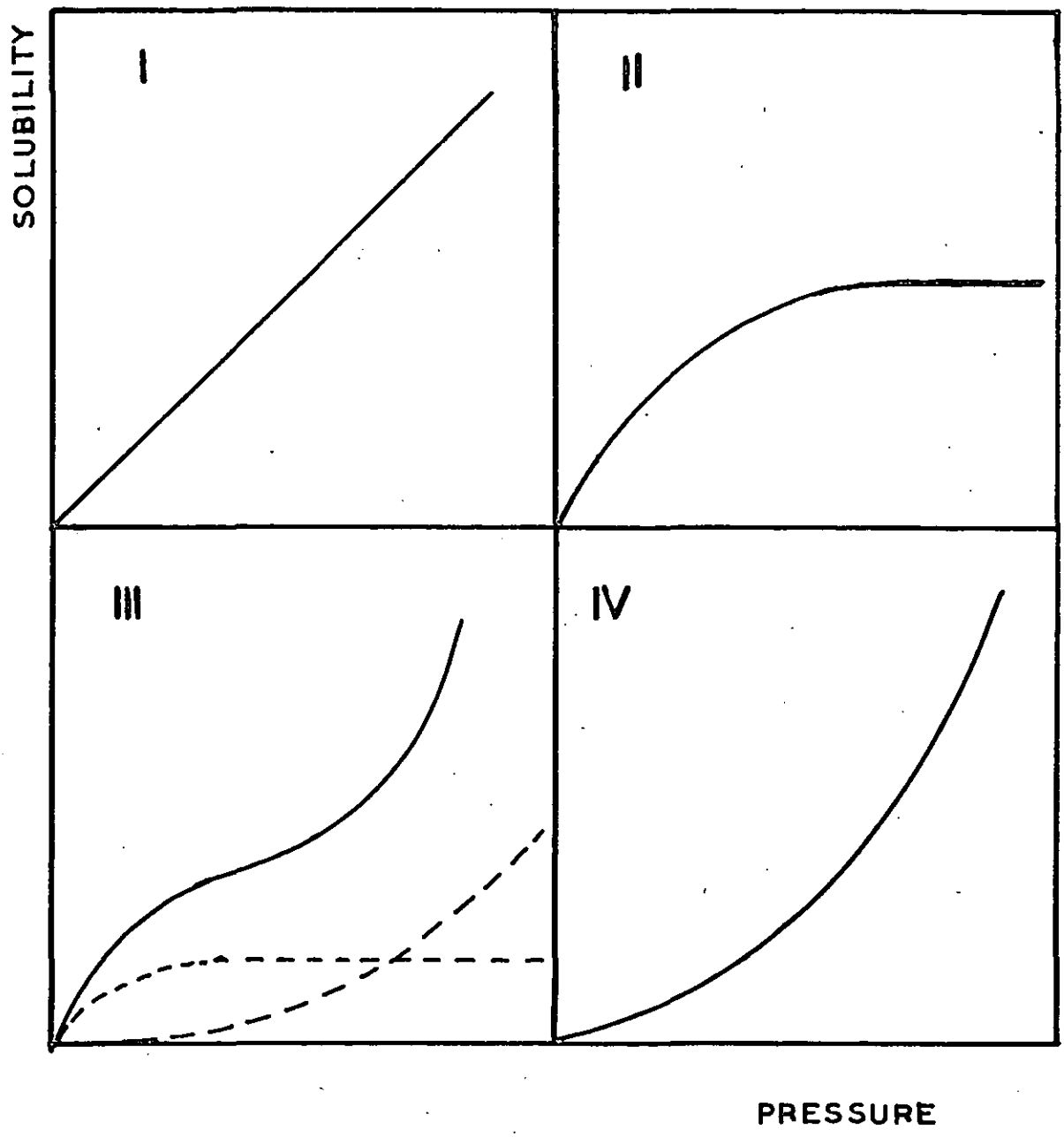

FIG. 47 TYPES OF SOLUBILITY ISOTHERMS

where ΔH, (the heat of solution), is the enthalpy change when a gramme molecule of gaseous penetrant is placed in solution. This equation allows the heat of solution to be determined.

The sorption process may be pictured in two stages: (1) the liquefaction of the penetrant from the vapour phase (an exothermic process), and (2) the mixing of the liquified penetrant with the polymer molecules (an endothermic process).

The heat of solution may be therefore written as

$$\Delta H = \Delta H_l + \Delta H_m \qquad 6.2$$

where ΔH_l is the heat of liquefaction, and ΔH_m is the heat of mixing.

For simple gases above their critical point, the heat of liquefaction is small (otherwise they would be condensible), and the heat of solution can be approximated to the heat of mixing, which, according to Hilderbrand (162), is given by

$$\Delta H_m = V (\delta_1 - \delta_2)^2 v_1 v_2 \qquad 6.3$$

where δ_1, δ_2 are the solubility parameters

V is the total volume

and v_1, v_2 are the respective volume fractions.

Therefore, for permanent gases the heat of solution is small and positive, and solubility increases with temperature.

For larger molecules, such as organic solvents, the heat of liquefaction usually outweighs the heat of mixing (given by Eqn.6.3) and the heat of solution is therefore negative, and solubility decreases with increasing temperature. This is evidenced in our results for n-decane in silicone rubber and S-B-S copolymer systems as illustrated in Fig.28-31.

The heats of solution of decane in the different samples measured as calculated from Eqn. 6.1 are tabulated in Table 6.1

TABLE 6.1

Polymer sample	ΔH (K cals/mole).
Silicone rubber (unfilled	- 13.4
Silicone rubber (5phr silica filled)	- 14.0
Silicone rubber (10 phr silica filled)	- 20.2
Silicone rubber (20 phr silica filled)	- 20.2
S-B-S block copolymer	- 14.8

Since the ΔH measured is predominantly the heat of liquefaction, it is governed by the strength of the van der Waals bond formed between penetrant molecules in the liquid state, and is not expected to be sensitive to different polymer structures. Apart from the filled samples (which will be discussed in Section 6.8), our ΔH values for silicone rubber and S-B-S are nearly the same.

Barrer et al (142) measured the heats of solution of n-butane and n-pentane in silicone rubber, and his values are tabulated in Table 6.2 with our value also inserted for comparison.

TABLE 6.2

Penetrant	ΔH (K cals/mole)	$\Delta H/_n$
n - $C_4 H_{10}$ (142)	- 5.27	- 1.41
n - $C_5 H_{12}$ (142)	- 6.26	- 1.26
n - $C_{10} H_{22}$	- 13.40	- 1.34

This shows a good linear relationship between the heat of solution and the length of a homologous molecule. The actual heat of mixing determined by Barrer (142) was found to be about 200 cals. for n - $C_4 H_{10}$ and n - $C_5 H_{12}$, and the ΔH measured must be mainly the heat of liquefaction. Barrer, however, found that the ΔH values for iso-butane and neo-pentane did not correlate so simply to their structure. He concluded that the linear addition of a CH_2 group to

a hydrocarbon will increase ΔH by a fixed amount, whereas with non-linear addition, the effective contribution to ΔH will be less as a result of screening and steric effects.

The apparently large heats of solution for the filled silicone rubber may be due to the sorption of the vapour in the pores or microstructures within the silica particles. The curious temperature dependence of this filler sorption effect observed and discussed in Section 6.8 may be a reason for the large heat of solution for the filled sample given in Table 6.2.

6.2. Permeation features.

In a penetrant-polymer system where Henry's law is not obeyed, it is inconvenient to make use of the relationship between "permeability coefficient", P, and "solubility" coefficient", S, to calculate the diffusion coefficient D as given by(Eqn. 2.33).

$$P = DS \qquad 6.4$$

This is because S is defined by (Eqn. 2.31)

$$C = Sp \qquad 6.5$$

and for a type IV sorption isotherm as mentioned in the last section, S varies with p.

Also, if D is a function of the concentration C, Eqn. 6.4 becomes unnecessarily complicated by having to "back-paddle" the S term to the concentration term.

Therefore we have left the pressure term out of our calculations, by using directly the equation (Eqn. 2.24)

$$F = \frac{D\,(C_1 - C_2)}{l} \qquad 6.6$$

where F is the flux, or rate of transfer per unit cross-section area, C_1 and C_2 are the concentrations of the penetrant at the two faces of the membrane, and l is the thickness.

Referring the flux to the transfer of the radioactive molecules, Eqn. 6.6 becomes

$$F^* = \frac{D^*\,C^*}{l} \qquad 6.7$$

The diffusion coefficient D* may be calculated from the experimentally measured values of flux and concentration, in the manner shown in the Chapter 5. By employing a non-active penetrant to make the concentration uniform throughout the polymer, a self-diffusion coefficient is measured, and may be extrapolated to zero concentration (See Section 6.3).

Increasing the polymer temperature will increase D but decrease C. This fact, plus the fact that D is actually dependent on C, will

lead to F* in Eqn. 6.7 not having a single trend in values with varying temperature and concentration. The experimentally measured permeation rates as given in Tables 5.6 - 5.10 by themselves have no significant relationship with, for instance, temperature, and these results will only be discussed in terms of the derived diffusion coefficient and its related activation energy parameter.

At high concentrations of penetrant the polymer membrane will be swollen in the direction of diffusion, because the edges are fixed by the cell. Thus the thickness, l, will increase and cause an error in the calculation of the diffusion coefficient from Eqn. 6.7, if l is taken as that for the unswollen sample. Assuming no buckling of the sample, the swollen thickness l_1 can be related to the unswollen thickness l_o by the relationship

$$l_1 = l_o \left(\frac{v_1}{v_o}\right)^{1/3} \qquad 6.8$$

where v_1 is the volume of the swollen system

v_o is the volume of the unswollen system.

Owing to the practical difficulty of keeping our polymer temperature and the active solvent liquid temperature independently constant because of thermal conduction along the permeation cell (see Section 4.2), we have covered a wide range of possible combinations of polymer temperature, "active" concentration and "inactive" concentration. Strictly a computer programme is required to process the data hence collected (shown in Tables 5.6 ~~and~~ 5.10). However, we have managed to hold the polymer temperature constant at some intermediate values, for the permeation rate at different "average" (See Section 5.2) concentration to be determined. A relationship between diffusion coefficient and concentration is derived and is assumed to hold within the narrow temperature range (30° - 50°C) used experimentally.

6.3. Diffusion coefficients.

The diffusion coefficient of a penetrant polymer system may be calculated from both sorption and permeation experimental data. It is appropriate at this point, before proceeding to discuss the derived diffusion coefficients in detail, to emphasize that the sorption method is not a suitable method for measuring fast diffusion kinetics. This is due to the temperature changes on the polymer surface caused by the heat of condensation of the vapour. Since the sorption method is not a steady state method, and the rate of uptake is determined over a very short period (~100 sec.) for a fast diffusion process, it is by no means justifiable to assume the polymer temperature is staying constant at the pre-sorption value. It is, however, interesting to consider our sorption kinetics with the view of interpreting and illustrating the significance of various diffusion coefficients defined in different manners, as shown in Section 2.1. The sorption diffusion coefficients will be treated in this context and they will be compared to the diffusion coefficients obtained from our permeation method.

The maximum possible temperature change caused by the condensation of the vapour may be estimated roughly as follows. If we assume that sorption of the vapour onto the polymer takes place instantaneously (i.e. adiabatic conditions), and the heat of solution (as calculated from section 6.1) consists almost entirely of the heat of condensation, then the temperature rise (ΔT) corresponding to sorption of 0.01 g of decane onto 0.1 g. of polymer with a specific heat of 0.5 will be given by

$$\Delta T = \left(\frac{\Delta H}{144} \times 0.01 \right) / 0.1 \times 0.5 \quad ^{\circ}C$$

$$\Delta T = 18.6^{\circ}C$$

In reality the temperature change will not be so drastic, as sorption takes place over a period of about 100 seconds, and some of

the heat evolved by vapour condensation is lost by radiation, and, to a lesser extent, convection. Crank (142) gave a full mathematical treatment on this subject, and actually plotted the variation of surface temperature with time. This has the general shape shown graphically in Fig.48.

The increase in temperature of the polymer will cause an increase in diffusion coefficient and a decrease in the solubility. Usually the increase in D has a smaller effect than the decrease in surface concentration. The diffusion coefficient calculated will thus be either higher or lower than the true value, depending partly on the concentration dependence of the diffusion coefficient.

There have been attempts to remove this heat of condensation by using forced convection methods to increase the rate of heat loss. Downes and Mackay's "Vibroscope" (143) is an example where they made use of the transverse vibration of a filament, the frequency of which varies as the square root of the mass. On the whole, however, it is not advisable to employ a sorption method to study the kinetics of a fast diffusion process, and a steady state method - where thermal equilibrium is allowed enough time to be reached - is much preferred.

Diffusion coefficient calculated from sorption data.

A diffusion coefficient may be obtained from the rate of uptake of vapour by the polymer at a fixed temperature and pressure. This diffusion coefficient, D, given in the expression (see Eqn. 2.41)

$$\frac{M_t}{M_\infty} = \frac{4}{l}\left(\frac{Dt}{\pi}\right)^{1/2} \qquad 6.9$$

can be considered as the diffusion coefficient of the penetrant with a polymer-fixed reference, defined as D_A^b in section 2.1. This is because the centre of the mass of the polymer is considered as fixed in space, so that only the mass flow of the penetrant is

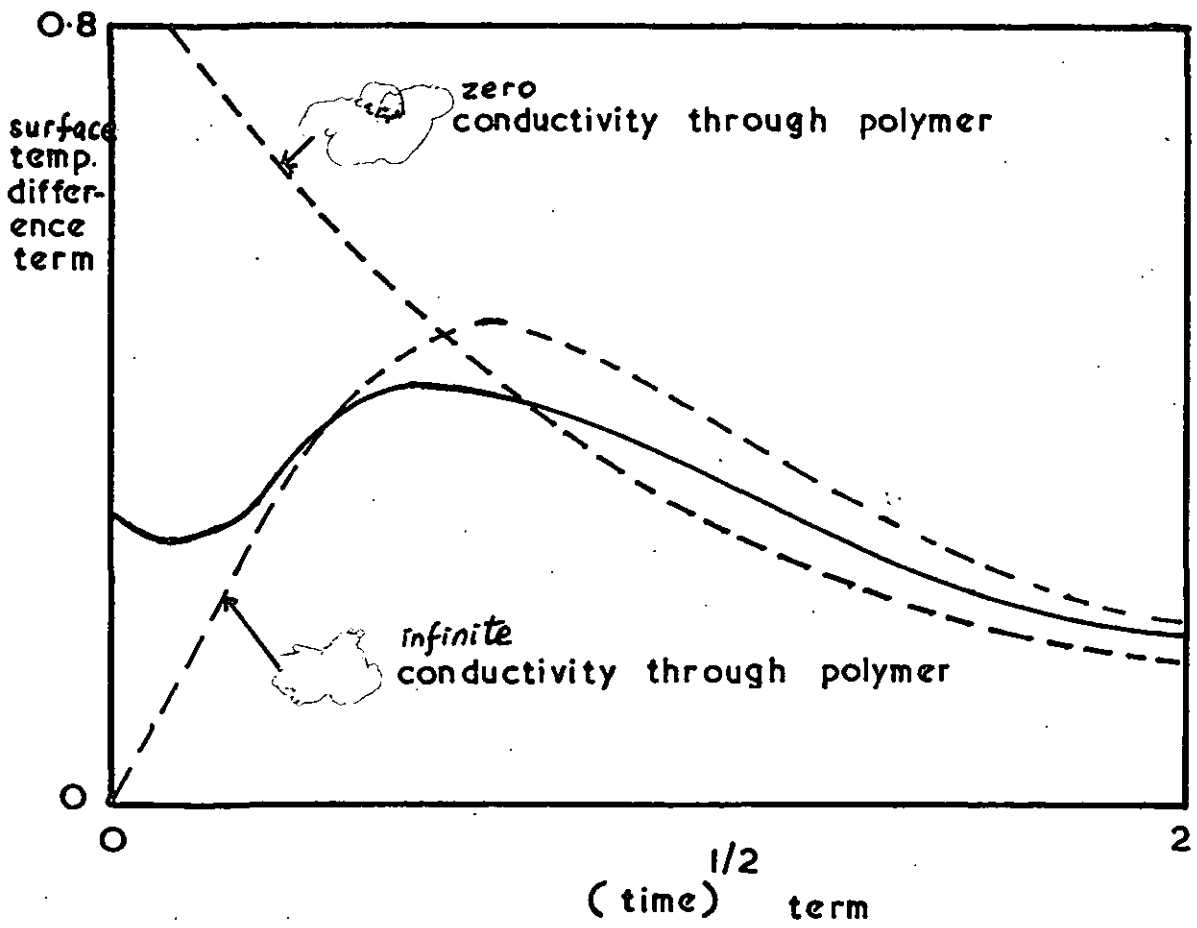

FIG. 48 VARIATION OF SURFACE TEMPERATURE WITH $(TIME)^{1/2}$

considered. To interpret the diffusion coefficient in terms of true molecular mobility, it becomes necessary to convert this polymer-fixed diffusion coefficient into the intrinsic diffusion coefficient, denoted by $\underline{D_A}$, which is defined with reference to a plane across which there is no mass flow (Section 2.1). D_A^b is related to $\underline{D_A}$ by the expression (Eqn. 2.16)

$$\underline{D_A} = D_A^b/(\text{volume fraction of polymer})^3 \qquad 6.10$$

If the diffusion coefficient is concentration dependent, it is necessary first to establish the D-C relationship. As mentioned in Section 2.3, an "integral" diffusion coefficient, $\bar{D}$, over the range O to C_o (where C_o is the equilibrium sorption concentration), is given to a good approximation by the average of the values of D obtained from absorption to and desorption from, the same equilibrium amount sorbed, C_o. Thus (Eqn. 2.43)

$$\bar{D} = \frac{1}{2}(\overline{D_a} + \overline{D_d}) \qquad 6.11$$

Using the relationship (Eqn. 2.45)

$$\bar{D} = \frac{1}{C_o} \int_0^{C_o} D \, d\, C \qquad 6.12$$

therefore, if $\bar{D}\, C_o$ is plotted against C_o, the gradient of the tangent at a point corresponding to a certain value of C_o will give a first approximation of the value of D at that concentration.

From our sorption results (Fig.32-39) it is readily observed that the rate of absorption is slower than the rate of desorption, especially at higher vapour pressure. This might be due to our D_A^b (i.e. sorption diffusion coefficient), value decreasing with increasing penetrant concentration (Table 6.3). Fujita et al (144) have observed that for a positive concentration dependence of diffusion coefficient, the rate of absorption is, in general, for an organic vapour-polymer system, larger than the rate of desorption. Thus the reverse may be true for our results. However, since in our experimental

technique (which is the electromicro-balance method described in Section 4.9), there is a high probability that the decane liquid in the reservoir in contact with the vapour may not have been completely degassed, the rate of absorption may have been retarded because of the interference of the oxygen or other dissolved gas molecules with the gaseous diffusion of decane vapour in the system. Since the desorption method involves the direct transference of the sorbed molecules from the polymer to the cold trap, no liquid decane is in contact with the vapour, and the diffusion coefficient calculated from it may be more genuine. We have, therefore, included both

$$\bar{D} = \bar{D}_a + \bar{D}_d,$$

and $\bar{D}_d$

in our calculation for the intrinsic diffusion coefficient, and they will be compared and discussed.

We have performed our sorption runs starting from a zero concentration of the penetrant in the polymer because of the rapidity of the process. It is not possible to observe the rate of uptake over a small concentration range if it takes, for instance, only 10 secs.

In Tables 6.3 and 6.4 are shown the various stages involved in determining a relationship between the intrinsic diffusion coefficient and the concentration. The average diffusion coefficients over the range 0 to C_o as calculated from Eqn. 6.9 for absorption and desorption are tabulated as $\bar{D}_a$ and $\bar{D}_d$. The mean value is denoted by $\bar{D}$. $\bar{D}C_o$ is then plotted against C_o (Fig.49), and the tangents drawn to the curve at the chosen C_o values represent the first approximation of the diffusion coefficient at concentration C_o, and this is denoted by $\bar{D}'$. More accurate approximations may be carried out by plotting $\bar{D}'C_o$ against C_o and repeating the differentiation, which will give $\bar{D}''$ (see Section 2.3). In view of the not too high accuracy of our sorption data, we have assumed the first approximation to be sufficient for our purposes.

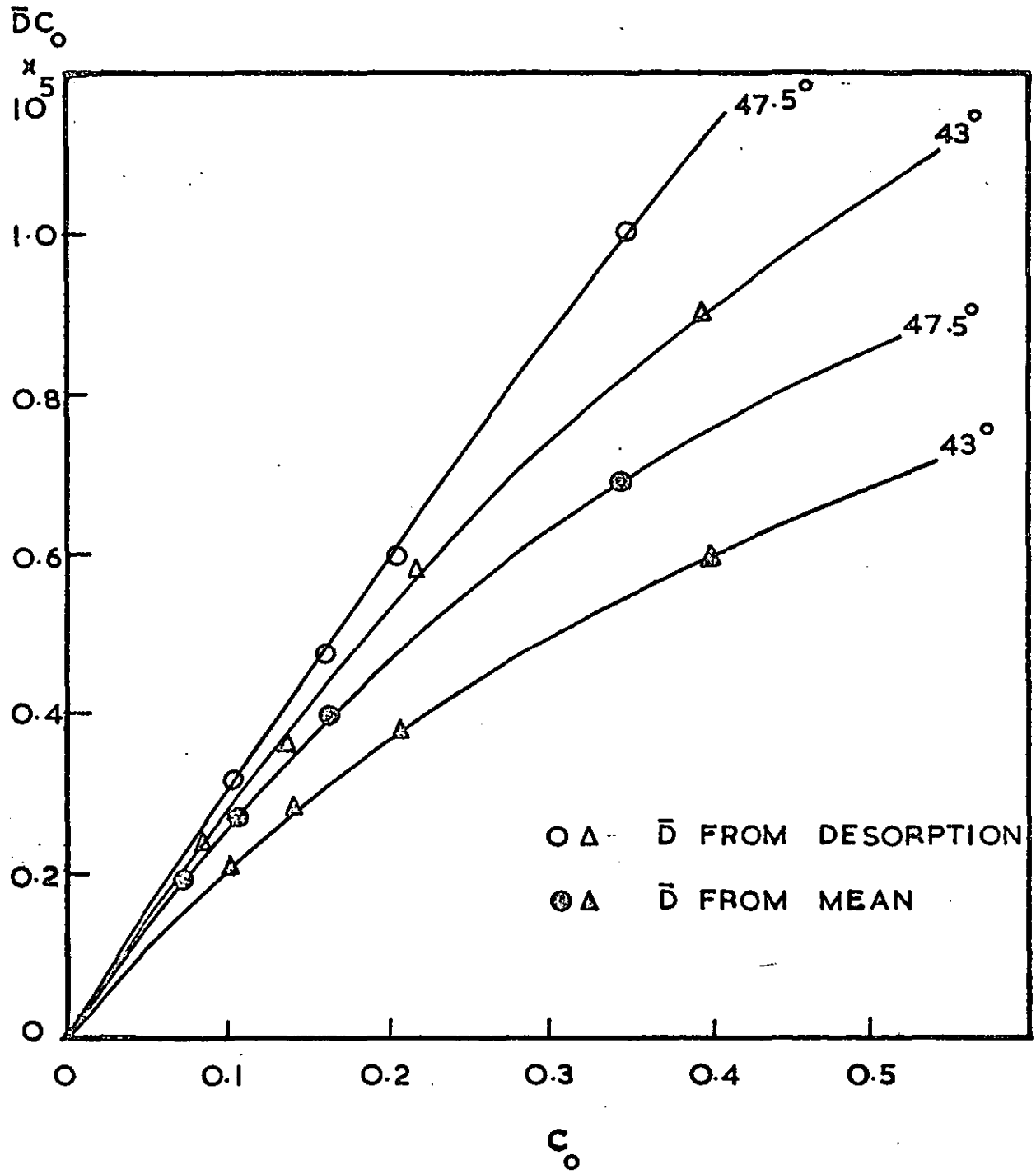
$\bar{D}C_o$
x
10^5
1·0
0·8
0·6
0·4
0·2
0
0
0·1
0·2
0·3
0·4
0·5
C_o
47·5°
43°
47·5°
43°
O Δ $\bar{D}$ FROM DESORPTION
⊛ Δ $\bar{D}$ FROM MEAN

FIG. 49

$\bar{D}'$ is then converted to the intrinsic diffusion coefficient $\underline{D_A}$ by (Eqn. 6.10).

$$\underline{D_A} = D_A^b \,/\, (\text{volume fraction of polymer})^3$$

The intrinsic diffusion coefficients based on desorption data alone are also worked out in Table 6.4.

Polymer Temp °C	Decane liquid Temp °C	Concentration (g/g)	Volume fraction C₈ pentrt.	Volume fraction polymer V_r	$\bar{D}_a \times 10^6$ slope	$\bar{D}_a \times 10^6$ $Cm^2 sec^{-1}$	$\bar{D}_d$ slope	$\bar{D}_d \times 10^6$	$\bar{D} \times 10^6$	$\bar{D} C_o \times 10^6$	$D' \times 10^6$ first approx.	$D_A \times 10^6$ cm^2 $sec.^{-1}$	
43.0	26.0	0.078	0.104	0.896	0.060	1.77	0.072	2.54	2.16	0.225	1.9	2.642	-5.578
	30.0	0.106	0.142	0.858	0.058	1.65	0.072	2.54	2.10	0.298	1.75	2.770	-5.557
	34.2	0.160	0.214	0.786	0.046	1.04	0.072	2.54	1.79	0.384	1.365	2.821	-5.549
	39.5	0.30	0.40	0.60	0.038	0.71	0.068	2.27	1.49	0.595	0.778	3.610	-5.442
47.5	26.0	0.058	0.078	0.922	0.070	2.41	0.078	2.99	2.70	0.210	2.40	3.063	-5.513
	30.0	0.080	0.107	0.893	0.070	2.41	0.078	2.99	2.70	0.289	2.30	3.228	-5.491
	34.4	0.12	0.161	0.839	0.062	1.89	0.078	2.99	2.44	0.392	1.90	3.217	-5.492
	41.0	0.26	0.350	0.650	0.044	0.95	0.078	2.99	1.97	0.69	1.35	4.089	-5.388
57.0	32.0	0.045	0.060	0.940	0.072	2.54	0.081	3.22	2.88	0.173	2.60	3.127	
	35.5	0.060	0.081	0.919	0.070	2.41	0.081	3.22	2.81	0.228	2.53	3.260	
	37.5	0.070	0.094	0.906	0.064	2.01	0.081	3.22	2.61	0.246	2.42	3.255	
	43.0	0.108	0.145	0.855	0.061	1.83	0.081	3.22	2.52	0.365	2.98	3.328	

TABLE 6.3

TABLE 6.4. Diffusion coefficient from desorption results.

Polymer Temp. °C	C_o	V_r	$\bar{\Gamma}_d \times 10^6$	$\bar{D}_d C_o \times 10^6$	$D_d' \times 10^6$	$\underline{D}_A \times 10^6$
43.0	0.104	0.896	2.54	0.255	2.60	3.615
	0.142	0.858	2.54	0.360	2.40	3.799
	0.214	0.786	2.54	0.592	2.20	4.531
	0.40	0.60	2.27	0.908	1.50	6.942
47.5	0.078	0.922	2.99	0.237	3.00	3.828
	0.107	0.893	2.99	0.320	2.95	4.141
	0.161	0.839	2.99	0.483	2.80	4.741
	0.350	0.650	2.99	1.045	2.60	9.469

These diffusion coefficients will now be compared to the self-diffusion coefficients (D*) obtained from the permeation method. D* is calculated from the expression (Eqn. 5.6)

$$D^* = \frac{Pl}{C^*} \times 2.18 \times 10^{-6} \quad cm^2 \ sec^{-1} \qquad 6.13$$

where P is the experimentally observed count rate increase

C* is the concentration of the radioactive molecules at the "ingoing" face

l is the thickness of the polymer

and the factor 2.18×10^{-6} is the radioactivity weight calibration term.

The variation of D* with the mean "overall" concentration (i.e. regardless of radioactivity) can be worked out knowing the concentration of the inactive molecules C_s. (see section 5.2).

In Fig.50 can be seen the three diffusion coefficients, viz: intrinsic from mean sorption, intrinsic from desorption, and self, plotted on the log scale against the penetrant concentration. A reasonably justifiable linear relationship is established for each case, their values will now be discussed.

The self-diffusion coefficient, D*, as measured by our permeation experiment, is a direct measure of the penetrant mobility in the polymer. It is in fact equivalent to the thermodynamic diffusion coefficient defined in section 2.4 by (Eqn. 2.50)

$$D_{th} = R \ T \ m_d \qquad 6.14$$

where m_d is the molar mobility

D* and D_{th} are related to the intrinsic diffusion coefficient by a thermodynamic function as follows (Eqn. 2.18, 2.50).

$$D^* = D_{th} = \underline{D_A} \frac{d \ln C_A}{d \ln a_A} \qquad 6.15$$

where C_A is the penetrant concentration

and a_A is the penetrant activity.

FIG. 50

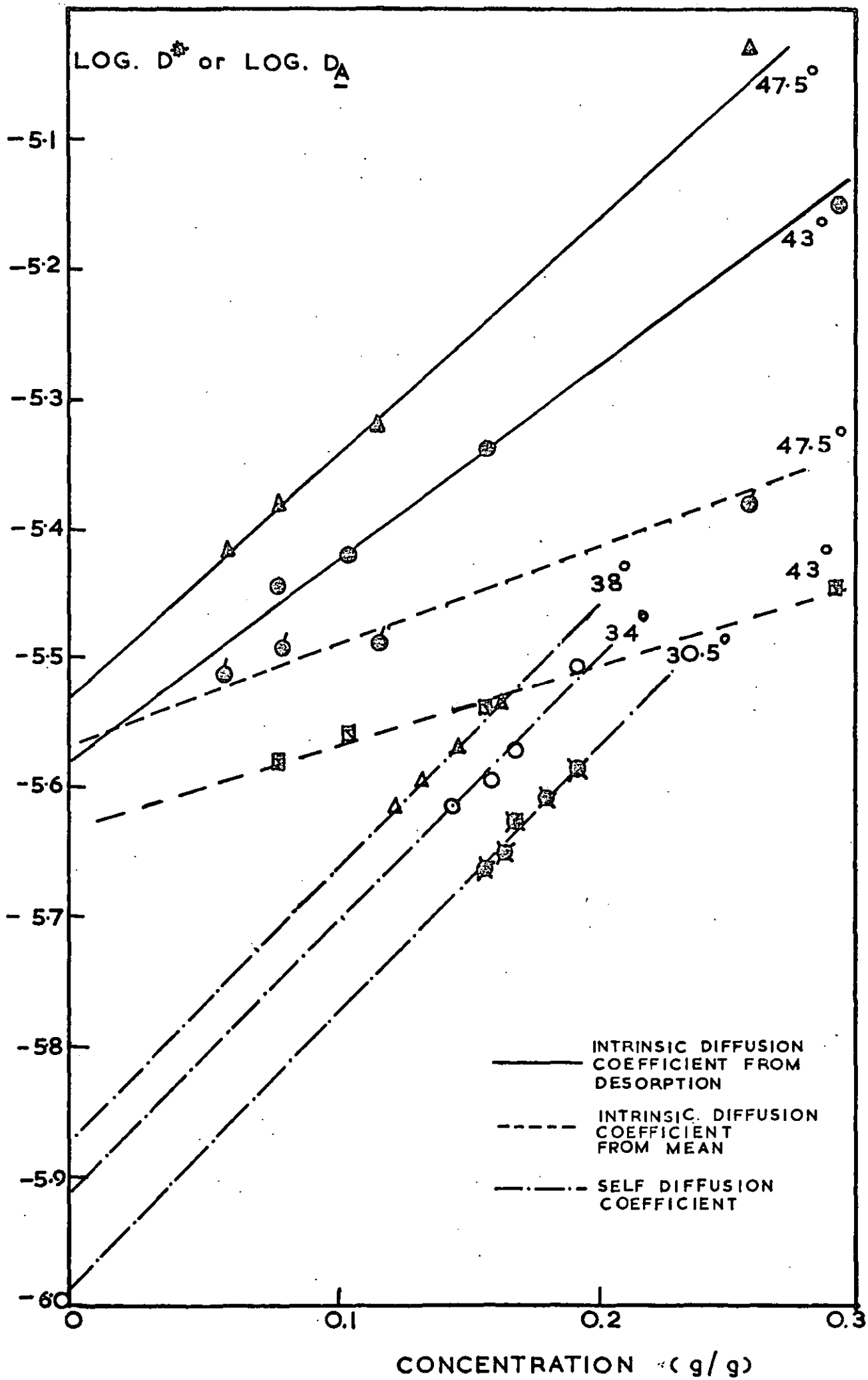
LOG. D* or LOG. D_A
-5·1
-5·2
-5·3
-5·4
-5·5
-5·6
-5·7
-5·8
-5·9
-6·0
0
0.1
0.2
0.3
CONCENTRATION (g/g)
47·5°
43°
47·5°
38°
43°
34°
30·5°
INTRINSIC DIFFUSION COEFFICIENT FROM DESORPTION
INTRINSIC. DIFFUSION COEFFICIENT FROM MEAN
SELF DIFFUSION COEFFICIENT

The term $\frac{d \ln a_A}{d \ln C_A}$ can be evaluated from an empirical relation of the form (67)

$$\frac{d \ln a_A}{d \ln C_A} = \frac{BC_A + 2CC_A^2 + 3DC_A^3}{A + BC_A + CC_A^2 + DC_A^3} \qquad 6.16$$

where A, B, C, D are empirical constants used to fit the experimental curve.

Alternatively the Flory-Huggins equation leads to

$$\frac{d \ln a_A}{d \ln C_A} = 1 - (2\chi+1)C_A V_A + 2\chi C_A^2 V_A^2 \qquad 6.17$$

at low penetrant concentration,

where χ is the interaction parameter.

The factor $\frac{d \ln a_A}{d \ln C_A}$ is normally close to unity, and will be taken as such in our discussion. This means that (self-diffusion coefficient)/(intrinsic diffusion coefficient) should also be close to unity, or these coefficients should be nearly equal to each other.

It is interesting to note that although the polymer-fixed mutual diffusion coefficient (given by D' in Table 6.3) decreases slightly with increasing penetrant concentration, the intrinsic diffusion coefficient actually increases exponentially with concentration (Fig.50). This arises as follows. At very low penetrant concentrations, mass flow results in negligible back

flow of the penetrant and so the measured diffusion coefficient is very little affected. At higher penetrant concentrations, however, an appreciable back flow of the penetrant results from the mass flow, and so the measured diffusion coefficient is reduced below the correct value given by the intrinsic diffusion coefficient.

Having dealt with mass flow, it is now appropriate to compare the various diffusion coefficients, viz: $\underline{D_A}$(mean), $\underline{D_A}$(desorption), and D which are all supposed to be related to the true mobility of the penetrant molecule in the polymer system.

Firstly we shall compare values of intrinsic diffusion coefficients derived from sorption and desorption rates. As mentioned previously it is suspected that the rate of absorption is controlled by the transport rate from the reservoir to the polymer, and it may have been retarded by dissoloved gases, which had not been completely removed, or

even by the self-diffusion process in the vapour state at high vapour pressures. The desorption experiment involved direct transfer of sorbed molecules from the polymer to the cold trap. The liquid penetrant reservoir was isolated from the polymer so that there was no possibility of interference from any other undesirable gas molecules and the whole process occurs at near zero penetrant vapour pressure. The rate of desorption would also not be affected even if adsorption onto the stopcocks or glass vessel walls did occur. As seen in Fig.50 the $\underline{D}_A$ value from the mean sorption and desorption data is lower than that from desorption data alone. In addition the dependence on concentration is much smaller than that of either the $\underline{D}_A$(desorption) or the D* values. For this reason we limit discussions here to the relationship between D* and the intrinsic diffusion coefficient obtained solely from the desorption [illegible] D*.

From Fig.50 we can see that the concentration dependence of $\underline{D}_A$ and of D* are, within experimental limitations, nearly equal. The D* value can be extrapolated to zero concentration, and applying the derived Arrhenius relation for temperature dependence (see Section 6.5) the values of $\underline{D}_A$ and D* at zero concentration and at a fixed temperature (43°C) are evaluated, the ratio $\underline{D}_A$/D* is determined and is approximately equal to 1.5. Theoretically this is considerably higher than the value of near unity predicted by our definitions (Eqn.6.15). There are a few reasons which may be forwarded to account for this difference.

The possibility of temperature variation on the polymer surface in a sorption experiment has already been discussed. Exactly how $\underline{D}_A$ is affected is not known, but we can assume this as a source of inaccuracy. In the permeation experiment the same amount of heat of condensation would be given out by the vapour but a steady state was allowed to be reached before readings were taken (Section 4.6), so this is less of a source of error.

The relation $\underline{D_A} = D_A^b$ /(volume fraction of polymer)^3 assumes that on sorption of the vapour, the polymer swells only in thickness but not in cross-section area, i.e. anisotropic swelling is assumed. This is probably true if the centre of the polymer is still in the unswollen state. As the penetrant diffuses further in the polymer, the stresses, which previously maintained anisotropic swelling, will be relaxed and swelling will become more isotropic. For pure isotropic swelling, $\underline{D_A}$ is related more accurately to D_A^b by a relation (.145).

$$\underline{D_A} = D_A^b/(\text{volume fraction of polymer})^{5/3} \qquad 6.18$$

Garrett and Park (145) have proposed that since for most systems the swelling is neither isotropic nor anisotropic, a geometric mean should be adopted, and this corresponds to

$$\underline{D_A} = D_A^b/(\text{volume fraction of polymer})^{7/3} \qquad 6.19$$

Thus the better approximated $\underline{D_A}$ would be lower than the one calculated from the previous relationship (Eqn.6.10). This could be another contributory factor in our $\underline{D_A}$ value being higher.

Strictly we can go ahead and estimate the quantity χ in the relation

$$\underline{D_A} = D_A^b/(\text{volume fraction of polymer})^{\chi} \qquad 6.20$$

if we assume

$$\text{true } D_{th} = D^* = \frac{d \ln C_A}{d \ln a_A} D_A^b/(\text{volume fraction of polymer})^{\chi} \qquad 6.21$$

The measured $\underline{D_A} = D_A^b/(\text{volume fraction of polymer})^3$

Therefore

$$\text{measured } \frac{D^*}{\underline{D_A}} = \frac{d \ln C_A}{d \ln a_A} (\text{volume fraction of polymer})^{3-\chi} \qquad 6.22$$

Since all the other terms can be determined experimentally, χ can be evaluated. Therefore, it may be possible to discover the true swelling behaviour of the polymer under the experimental conditions.

It was, however, decided not to apply Eqn. 6.22 to our data because of the larger disparity between our D* and $\underline{D_A}$ values than even 6.22 can predict.

Another possible reason for this difference could be the actual silicone rubber samples used for these experiments. For the permeation experiment, sample "E303" as characterised in Chapter 4 was used. The sorption experiment was performed earlier with "E302" with the same molecular weight and other physical characters as "E303" but is described technologically as the higher "shrinkage" grade. The term "shrinkage" refers to the physical change in size of vulcanised rubbers, due to the removal of volatile cyclic compounds from the polymer. In a "low shrinkage" sample, most of these volatile substances have been removed by the manufacturers. The molecular mobility, however, should not be affected to any significant degree by this physical effect.

A small difference in the molecular mobility between the labelled and unlabelled molecules would be caused by the "isotope" effect. This is because the mass of the nucleus in a C-14 atom is heavier than that in a C-12 atom, and the rate of movement of the former should, therefore, be fractionally slower (146). Although this effect is important to the actual gas velocity, it should not affect molecular movements which are relaxation controlled, such as diffusion in a polymer medium.

In conclusion to this section it can be said that the relationships between the mutual diffusion coefficient, intrinsic diffusion coefficient and the self-diffusion coefficient, have been quite thoroughly explored. From these relationships it is possible to gather more information on the polymer swelling and penetrant activity behaviour. The experimental disparity between $\underline{D_A}$ and D* can be partly attributed to the experimental inaccuracy in a sorption experiment, wrong assumption that swelling is entirely anisotropic, and the difference in "grades" between the polymer samples used.

6.4. Interpretation of concentration dependence of diffusion coefficient.

It is a well known phenomena that the diffusion coefficients in many organic molecule-polymer systems are clearly concentration dependent (55, 38, 69). This dependence varies from a ten-fold increase of the diffusion coefficient (in increasing the concentration from zero to 0.1 volume fraction of penetrant) for n-butane-polyisobutylene system (38), to an almost independent relationship reported by Newns and Park (69) for a benzene-silicone rubber system. Many theories or explanations have been put forward to account for these observed concentration dependences of the diffusion coefficient, a few of these will be briefly summarised before interpreting our results in terms of the free volume theory as outlined in Section 2.4 which the author feels is the most fundamental and direct approach of all the presently available theories.

Barrer and Ferguson (67) by making use of a model representation of the zone theory (Section 2.5), derived an expression for the thermodynamic mobility, m_d, in terms of the volume fraction of the penetrant, and a parameter Z defined as the number of either the polymer segments or the penetrant molecules which must be displaced outwards simultaneously for diffusion to take place. Their final expression was

$$m_d = \left(\frac{K}{kt}\right) P_B^Z \left[v_A (100)^{1/2} + (1-v_A) \right]^Z \qquad 6.23$$

where K is a proportionality constant

P_B, P_A are probability terms for A and B.

v_A is the volume fraction of A (penetrant).

By choosing a suitable value for Z, m_d can be calculated and matched with the experimental diffusion coefficients, bearing in mind that

$$\underline{D_A} = D_{th} \frac{d\ln a_A}{d\ln C_A} = R\,T\,m_d \frac{d\ln a_A}{d\ln C_A}$$

It is always difficult to justify, without fundamental reason, the choice of a parameter to fit an equation so that it may correspond with the experimental value. Barrer and Ferguson have shown that the zone theory can be used to explain the concentration dependence of D, but they

have not shown how it can be used to predict this dependence in other systems. No definitive conclusion is offered, and certainly no evidence is advanced for the chosen value of Z in Eqn. 6.23.

Prager and Long (38) in their experiment on the diffusion of hydrocarbons in polyisobutylene, found a drastic dependence of the sorption diffusion coefficient (denoted by $\bar{D}$ in the last section) on the penetrant concentration. They did not convert their $\bar{D}$ values to the intrinsic diffusion coefficient, D_A, which, if they had, would have made the concentration dependence even more pronounced. It is a pity that in their publication (38) , they have not interpreted their results quantitatively, and no numerical solution or mathematical model was forwarded to explain their findings. The explanation presented by Prager and Long for the concentration dependence of the diffusion coefficient was based on Eyring's "hole" theory (147). According to this theory there are in any liquid or solid a number of holes arising from thermal fluctuations; diffusion takes place by a molecule leaving its current position and jumping into one of these holes. In order to form a hole a certain number of van der Waals "bonds" must be broken. These "bonds" are assumed to be either between two polymer segments, a polymer segment and a molecule of the diffusing hydrocarbon, or between two molecules of the hydrocarbon. The last case is the least probable at low penetrant concentrations. Prager and Long assumed that the polymer-hydrocarbon bonds are weaker than the polymer-polymer bonds, consequently the energy required to form a hole of a certain size decreases linearly with increasing hydrocarbon concentration, and the number of such holes should therefore increase exponentially with increasing hydrocarbon concentration. The diffusion coefficient, being dependent on the "jump" frequency, is directly proportional to the number of available holes, and is, therefore, given by

$$D_C = D_o \exp (aC) \qquad 6.24$$

where D_C and D_o are diffusion coefficients at concentration C and zero respectively, and a is a constant.

The above treatment resembles, in basic assumptions, the free volume theory as given in Section 2.4. The number of "holes" big enough to allow diffusant molecule displacement, corresponds to the probability of finding a hole large enough in the vicinity of the diffusing molecules, and is given by(Eqn. 2.48)

$$P(B) = \text{exp. } (-B/f)$$

where f is the average free volume per unit volume of the system,

B is a measure of the hole size.

The thermodynamic diffusion coefficient, D_{th}, is in turn related to this probability by the expression (Eqn.2.51)

$$D_{th} = R\ T\ A_d \text{ exp. } (-B_{d/f}) \qquad 6.25$$

If the free volume increases linearly with penetrant concentration (165), then D_{th} depends exponentially on C.

Comparing the free volume theory to Prager and Long's hypothesis, it is clear that the former consists of fundamental parameters which may be derived and substituted into the main relationships, and the latter consists only of a qualitative assessment, although in both cases, an experimental dependence is predicted.

From the free volume theory, the following expression has been derived (Eqn. 2.58)

$$\frac{1}{\ln(D_{th}/D_o)} = \frac{f(o,T)}{B_d} + \frac{[f(o,T)]^2}{B_d A(T)} \frac{1}{v_1} \qquad 6.26$$

The parameters have already been defined in section 2.4.

A plot of $1/\ln(D_{th}/D_o)$ against $1/v_1$ should, if the theory is obeyed, yield a straight line, the slope and intercept will represent the obvious terms in Eqn. 6.26 respectively.

Since our data for concentration variation of the diffusion coefficient in silicone rubber do not cover a large enough temperature

range for it to show the temperature dependence, we have only plotted this relationship for one temperature (30.4°C). This is shown in Fig.52. From the slope, $[f\ (o,T)]^2 / B_d \beta(T)$ is known. The intercept when $^1/V_A = 0$ is so small that it is difficult to be evaluated graphically. However, if we assume that the linear relationship is accurate enough we may substitute the straight line by an empirical equation derived by substituting values in the equation:

$$y = mx + c$$

m, the gradient, is determined by the slope and is equal to 2,85. Table 6.5 shows the various values of c obtained by substituting the chosen values of x and y.

Table 6.5

x	y	c
0.5	1.5	.075
0.75	2.2	.070
1.0	2.92	0.070
1.5	4.36	0.078

Thus the average extrapolated y-intercept value = 0.075

From Eqn. 6.26 therefore

$$\frac{f\ (o,T)}{B_d} = 0.075 \qquad 6.27$$

and $$\frac{[f\ (o,T)]^2}{B_d\ \beta(T)} = 2.85 \qquad 6.28$$

f (o,T), the fractional free volume at temperature T, may be derived from the relation

$$f\ (o,T) = f\ (o,Tg) + \alpha_f\ (T-Tg) \qquad 6.29$$

where f (o,Tg) is the fractional free volume at Tg.

A "universal" value for f (o,Tg) may be assumed (6), and this is equal to 0.025.

α_f, which is the coefficient of thermal expansion, has a "universal" value of 4.8×10^{-4} deg.$^{-1}$

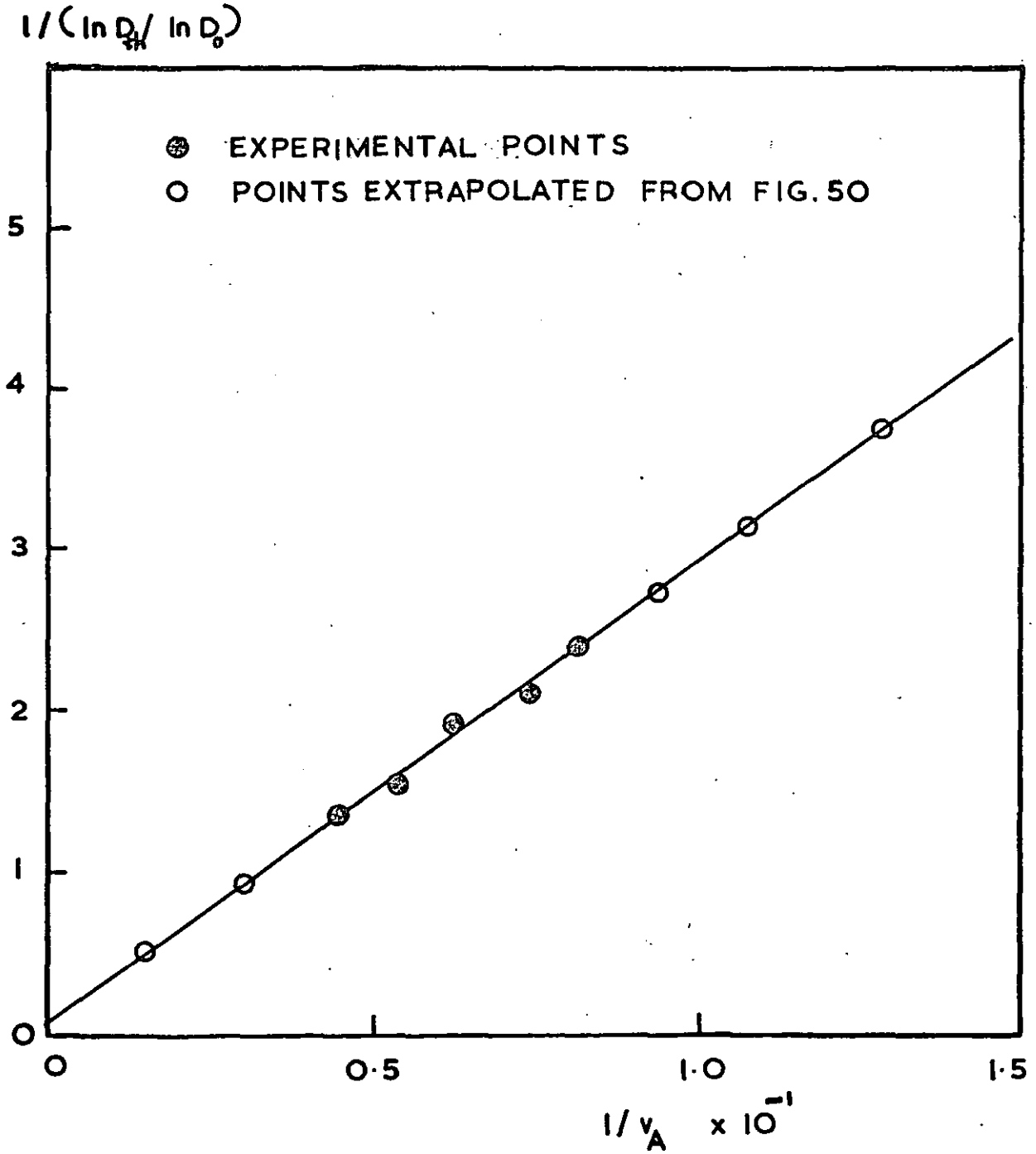
1/(ln D_th/ ln D_0)
EXPERIMENTAL POINTS
POINTS EXTRAPOLATED FROM FIG. 50
5
4
3
2
1
0
0
0·5
1·0
1·5
1/v_A x 10^-1

FIG. 52

We have, therefore, from Eqn. 6.27, 6.28 and 6.29, with "universal" values of f (o,Tg) and α_f substituted,

$$B_d = 1.39 \qquad 6.29$$

$$\beta(T) = 2.34 \times 10^{-3} \qquad 6.30$$

These values are only very rough approximations of the true value, as we have assumed the "universal" values in our calculations, and the graphical intercept obtained is only an extrapolated value. Strictly a more accurate estimation of the free volume parameters f (o,T) and α_f may be made by plotting Fig.52 at two temperatures far enough apart for the temperature dependence in these terms to become significant. From the intercepts of the two plots, the exact value of f (o,T) may be determined by substituting a known value of α_f for silicone rubber (163), and subsequent values of B_d and $\beta(T)$ may be determined from the respective slopes. In the temperature range covered by us, (30-50°C), the free volume plot (Fig.52) for all the temperatures very nearly all fall on the same straight line, this is the reason we have assumed the "universal" free volume parameters.

Since the corresponding B value for viscosity is near unity (6), it would appear, ($B_d/B > 1.$), that the minimum hole size required for diffusion is slightly larger than the minimum hole size for polymer segmented motion. B_d/B is also approximated to $e^{-RT/\Delta H_D}/e^{-RT/\Delta H_a}$, where ΔH_D and ΔH_a are the activation energies for diffusion and polymer viscoelastic relaxation respectively (see later section). We have obtained values of ΔH_D and ΔH_a at 5.75 and 5.3 K cals/mole respectively (see Section 6.5 and 6.9). Thus B_d from activation energy comparison is about 1 [illegible]. Thus from both observations B_d is near to unity. It appears, therefore, that the penetrant molecule (n-decane) is similar in size to a silicone rubber chain "segment" which is taking part in thermal motions.

$\beta(T)$ is given by the expression (Eqn.2.52)

$$f(v_1,T) = f(o,T) + \beta(T)\, v_1 \qquad 6.31$$

and is, therefore, a measurement of the concentration dependence of the free volume in silicone rubber. Its small value suggests that the effect of diluent on the free volume of silicone rubber is rather insignificant. The concentration dependence of the diffusion coefficient of n-decane in silicone rubber is small and is given to a good approximation by

$$\log D_c = \log D_o + \quad 2.0C. \qquad 6.32$$

Newns and Park (69) have in fact found no concentration dependence of the diffusion coefficient in a benzene-silicone rubber system. This point will be discussed further under section 6.6.

For extrapolation to zero concentration purposes, we have plotted the concentration dependence of D of n-decane in silicone rubber and S-B-S block copolymers as log D against C in Fig.53 and Fig.54 respectively. Within the narrow temperature range there was no noticeable change in the gradient of the linear plots, and relation like Eqn.6.32 for silicone rubber, and

$$\log D_c = \log D_o + 2.5\, C \qquad 6.33$$

for the S-B-S block copolymer may be assumed for extrapolation purposes. The diffusion behaviour of this later polymer will be discussed in Section 6.7.

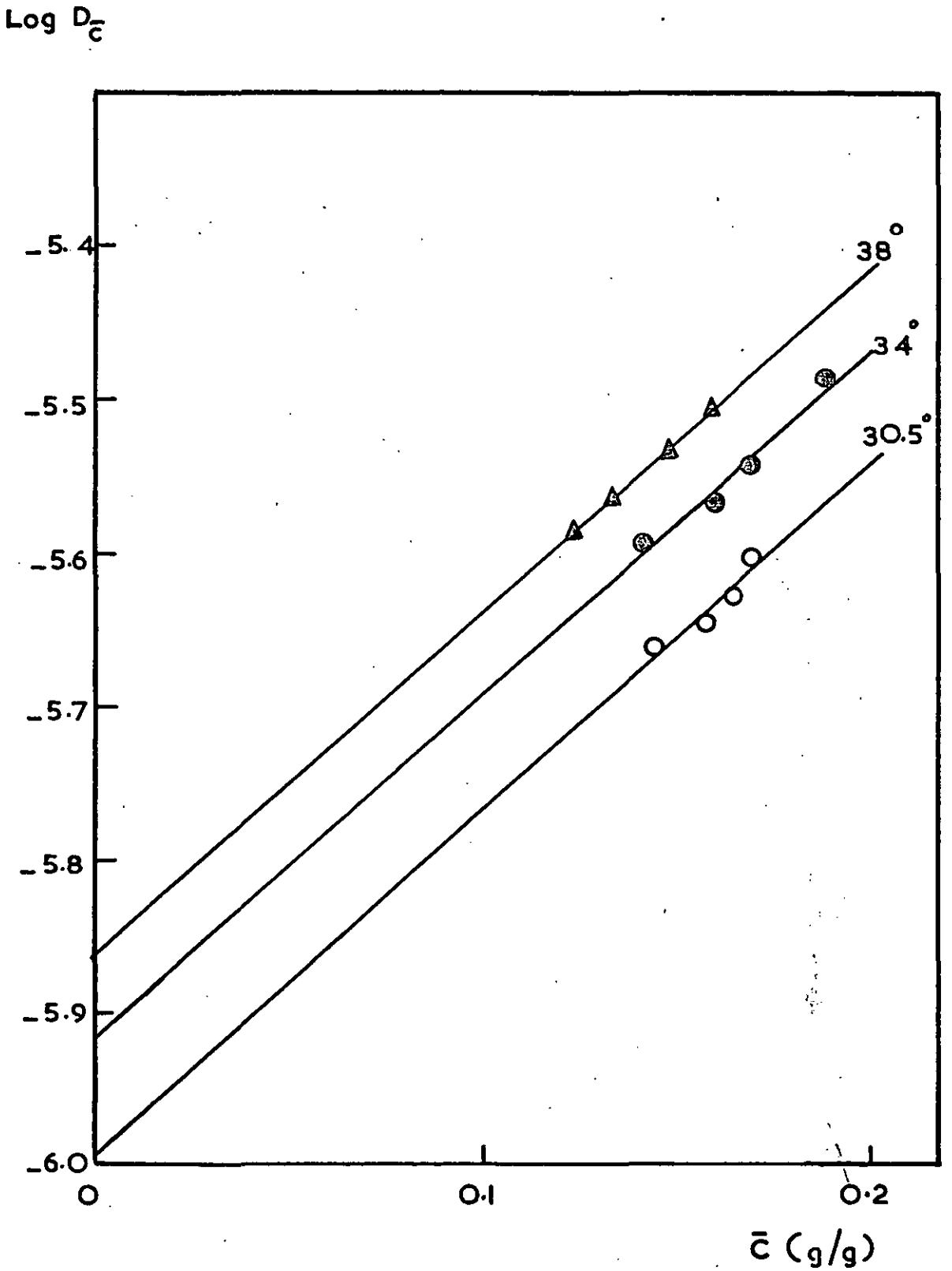

FIG. 53 CONCENTRATION DEPENDENCE OF D SILICONE RUBBER

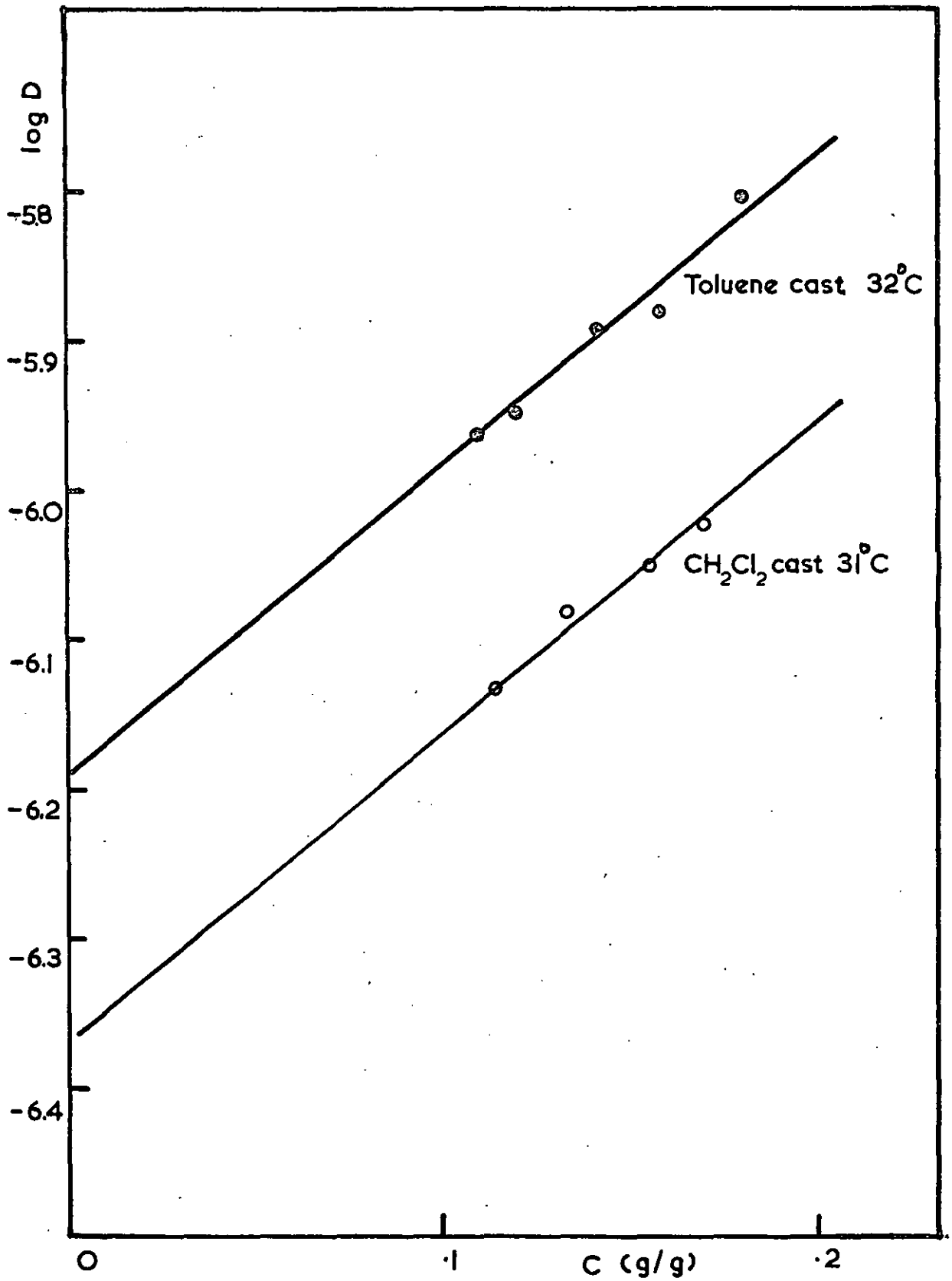

FIG. 54. SBS COPOLYMER CONCENTRATION DEPENDENCE OF D.

6.5. Temperature dependence of the diffusion coefficient.

The temperature dependence of the diffusion coefficient is one of the most valuable sources of information on the mechanism of diffusion. We have already seen how the free volume theory can be applied to account for the concentration dependence of the diffusion coefficient, by a similar argument the temperature dependence can also be illustrated by the free volume concept. In the case of concentration, the fractional free volume has been shown to increase with increasing penetrant concentration (Eqn. 2.52) in the manner

$$f(v_1,T) = f(0,T) + \beta(T)v_1 \qquad 6.34$$

Temperature also increases the fractional free volume of a polymer, and at zero penetrant concentration this is given by (Eqn. 2.60)

$$f(0,T) = f(0,0) + \alpha_f(T-T_o) \qquad 6.35$$

where $f(0,T)$ and $f(0,0)$ are the fractional free volumes at temperature T and a reference temperature T_o respectively; α_f is the coefficient of expansion of the free volume.

In section 2.4 it has been shown that the diffusion coefficient is dependent on the free volume in the manner (Eqn. 2.61)

$$D = A_d RT \exp.\left\{-B_d/\left[f(0,0) + \alpha_f(T-T_o)\right]\right\} \qquad 6.36$$

By differentiating ln D in Eqn. 6.36 with respect to (1/T),

$$\frac{d\ \ln D}{d\ (1/T)} = -T - \frac{T^2 B_d/\alpha_f}{\left[T - T_o + f(0,0)/\alpha_f\right]^2} \qquad 6.37$$

If we define the activation energy of diffusion, ΔH_D, as

$$\Delta H_D = -R\,\frac{d\ln D}{d(1/T)} \qquad 6.38$$

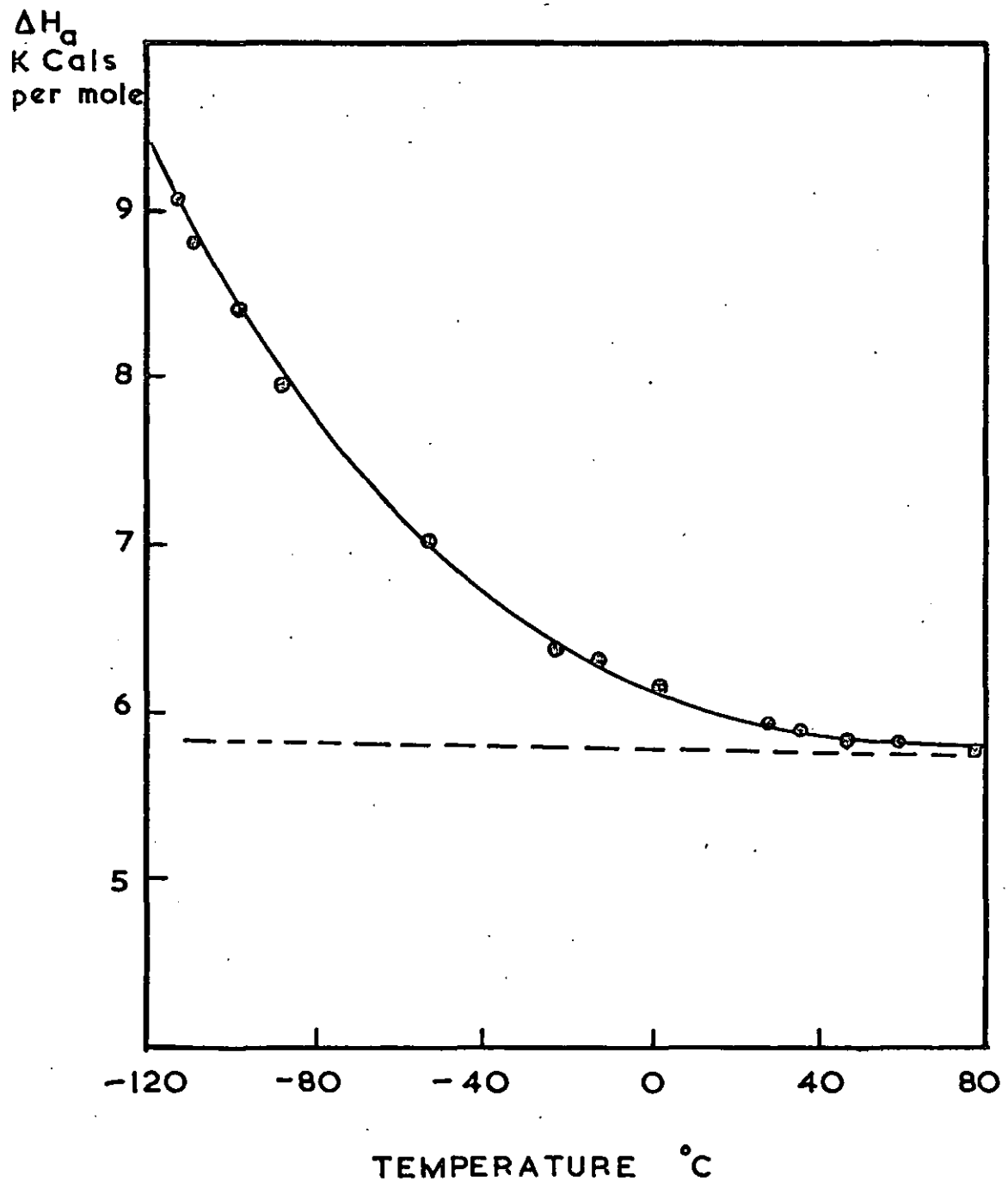

FIG. 55

then $$\Delta H_D = RT + \frac{T^2 B_d/\alpha_f}{\left[T - T_o + f(0,0)/\alpha_f\right]^2} \qquad 6.39$$

If we further define two parameters C_1^D and C_2 as

$$C_1^D = B_d/f(0,0) \qquad 6.40$$

$$C_2 = f(0,0)/\alpha_f \qquad 6.41$$

then

$$\Delta H_D = RT + \frac{RC_1^D C_2 T^2}{\left[C_2 + T - T_o\right]^2} \qquad 6.41a$$

From parallel argument Ferry(6) has derived a similar expression for the apparent activation energy of viscoelastic relaxation H_a, and this is given by

$$\Delta H_a = \frac{RC_1 C_2 T^2}{\left[C_2 + T - T_o\right]^2} \qquad 6.41b$$

where $C_1 = B/f(0,0)$

and C_2 is given by Eqn. 6.41

From Eqn. 6.41a and Eqn. 6.41b

$$\frac{\Delta H_D - RT}{\Delta H_a} = \frac{B_d}{B} \qquad 6.41c$$

Fig.55 shows the variation of theoretical ΔH_a with temperature, ΔH_a being calculated using the universal values of $f(0,0)$ and α_f. ΔH_D, as apparent from Eqn.6.41c, should also vary in a similar manner with temperature.

Over the range of temperature used in our experiments, the variation of the diffusion coefficient with temperature seems to follow an Arrhenius type of relation, and logD against 1/T is plotted for each of our polymer samples, these are shown in Figs.56-59. Table 6.6 shows the ΔH_D and D^o values hence obtained.

TABLE 6.6

	silicone r. (unfilled)	silicone r. (10phr f.)	silicone r. (20phr f.)	S-B-S (toluene)	S-B-S (CH_2Cl_2)
ΔH_D Kcals/mole	5.75	7.40	8.80	7.65	10.60
D^o $cm^2 sec^{-1}$	0.015	0.23	2.16	0.21	14.13

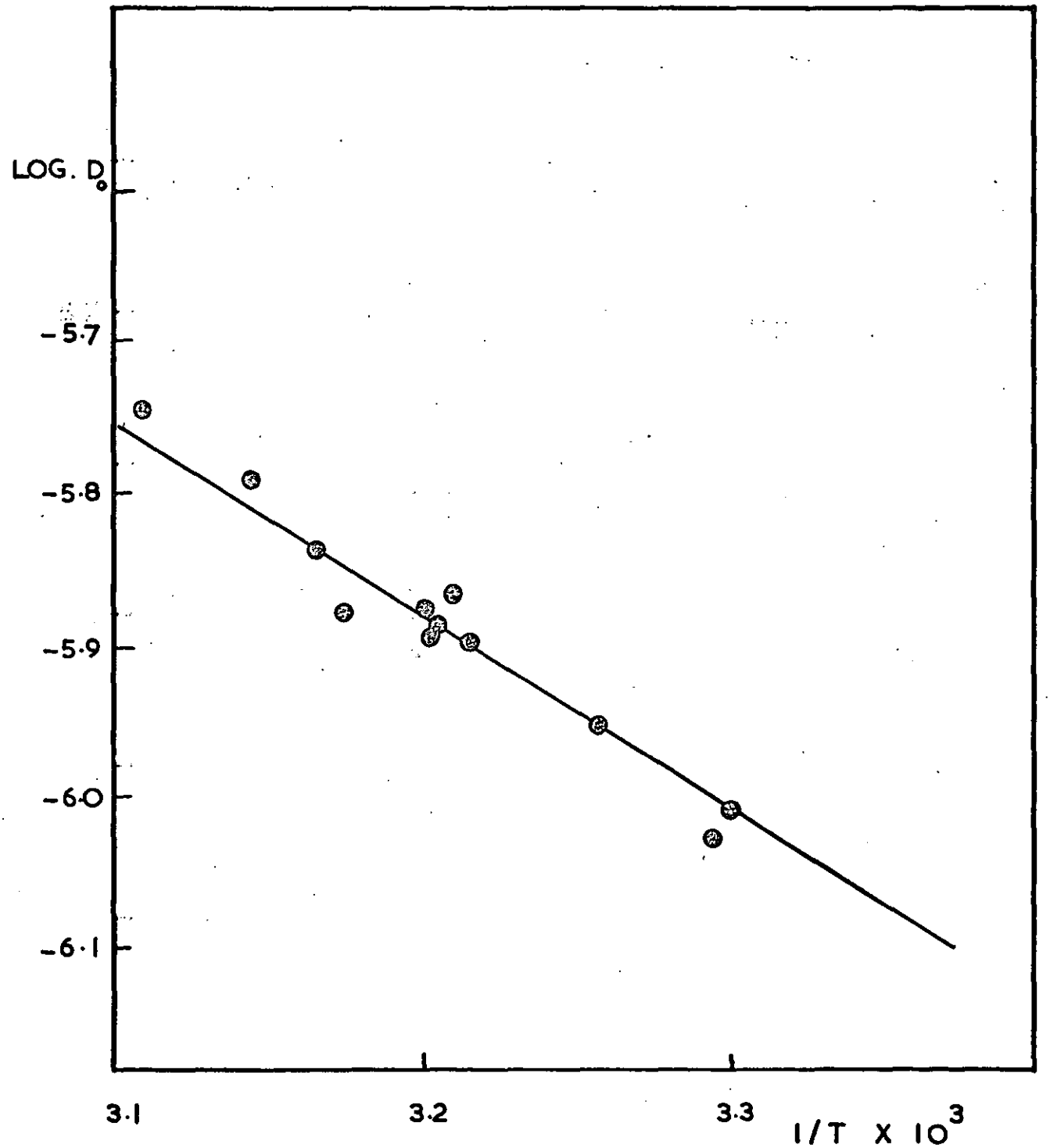

FIG. 56 ARRHENIUS PLOT
SILICONE RUBBER

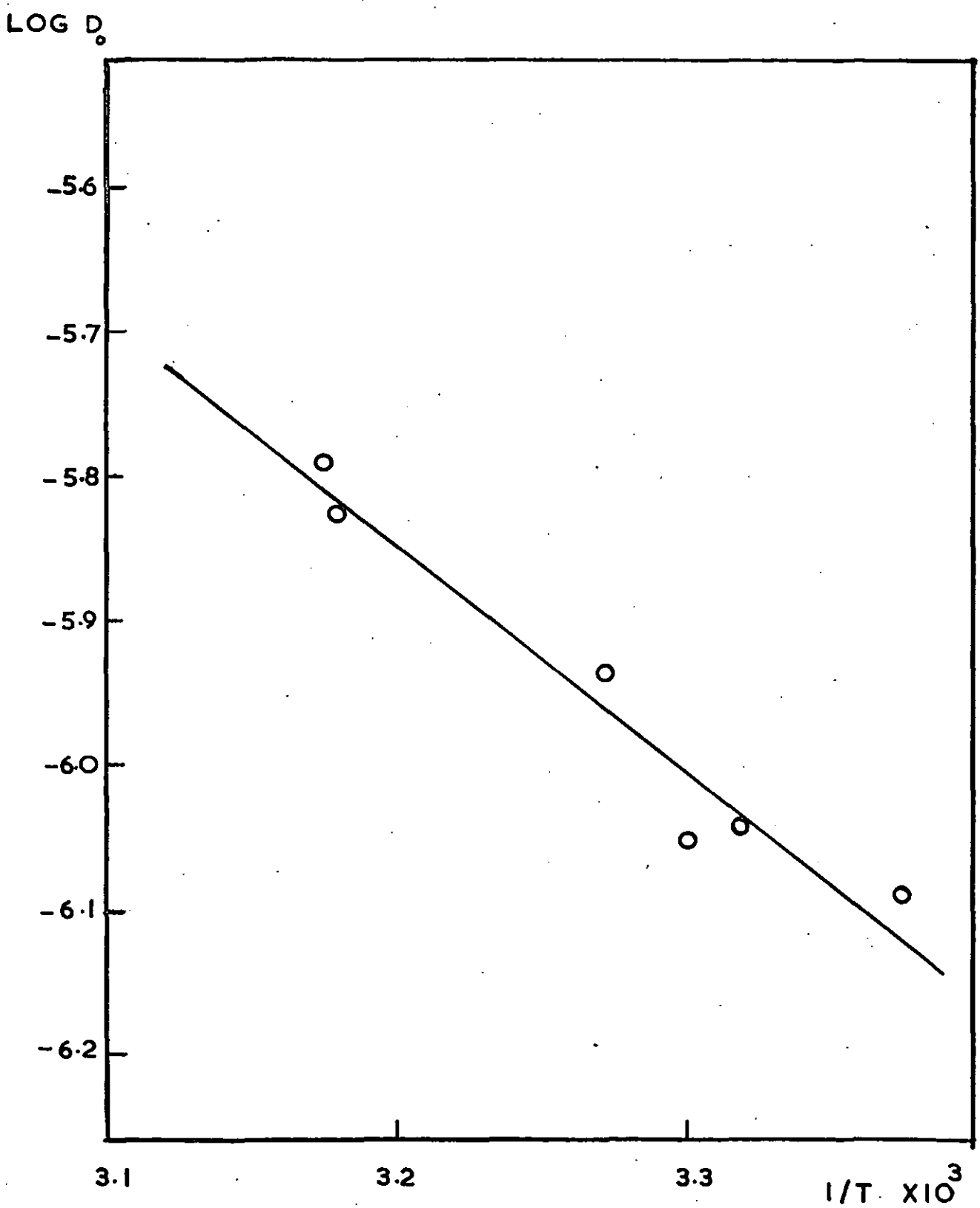

FIG. 57 ARREHENIUS PLOT SILICONE RUBBER (10 phr filler)

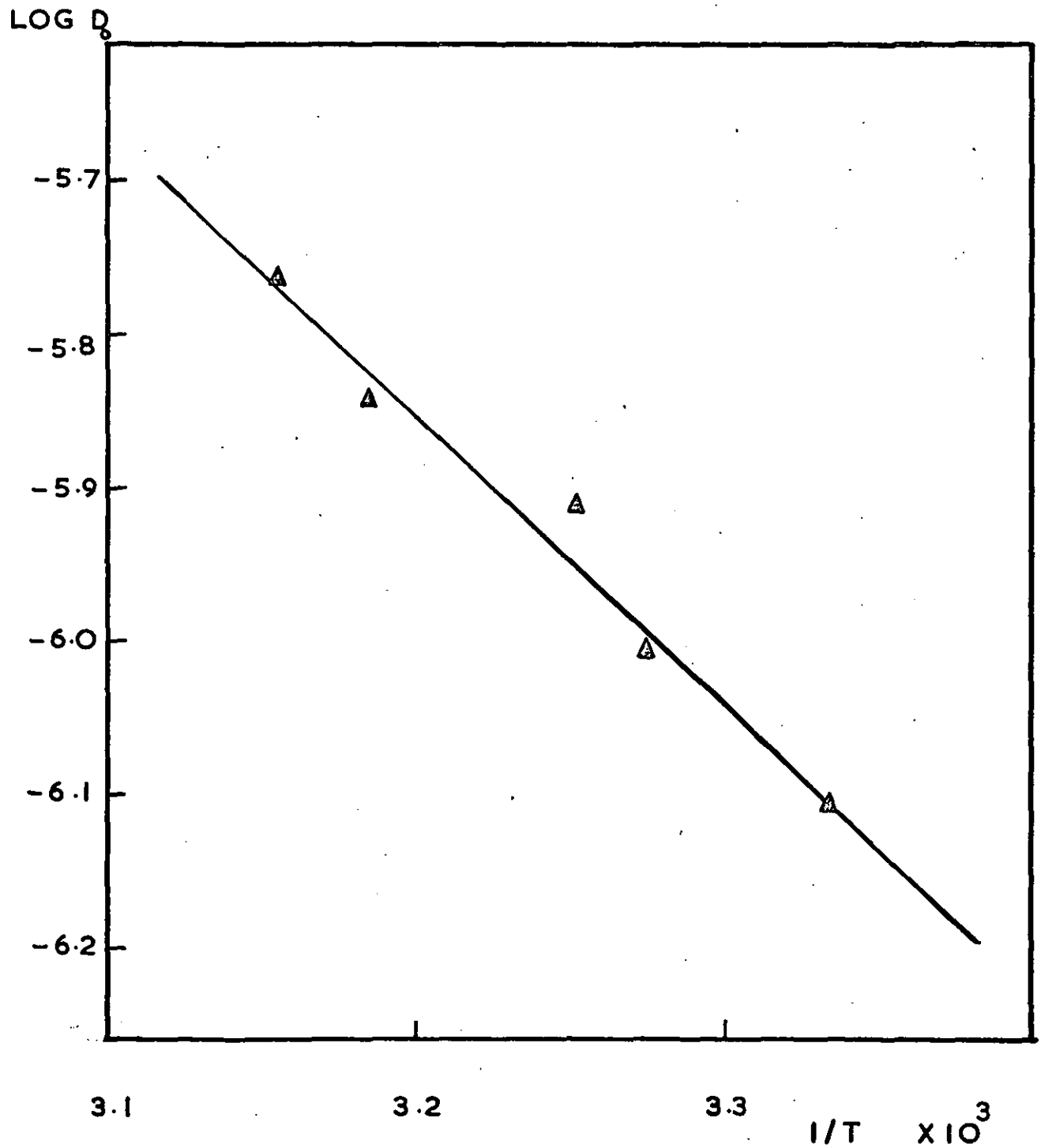

FIG. 58 ARRHENIUS PLOT SILICONE RUBBER (20 phr filler)

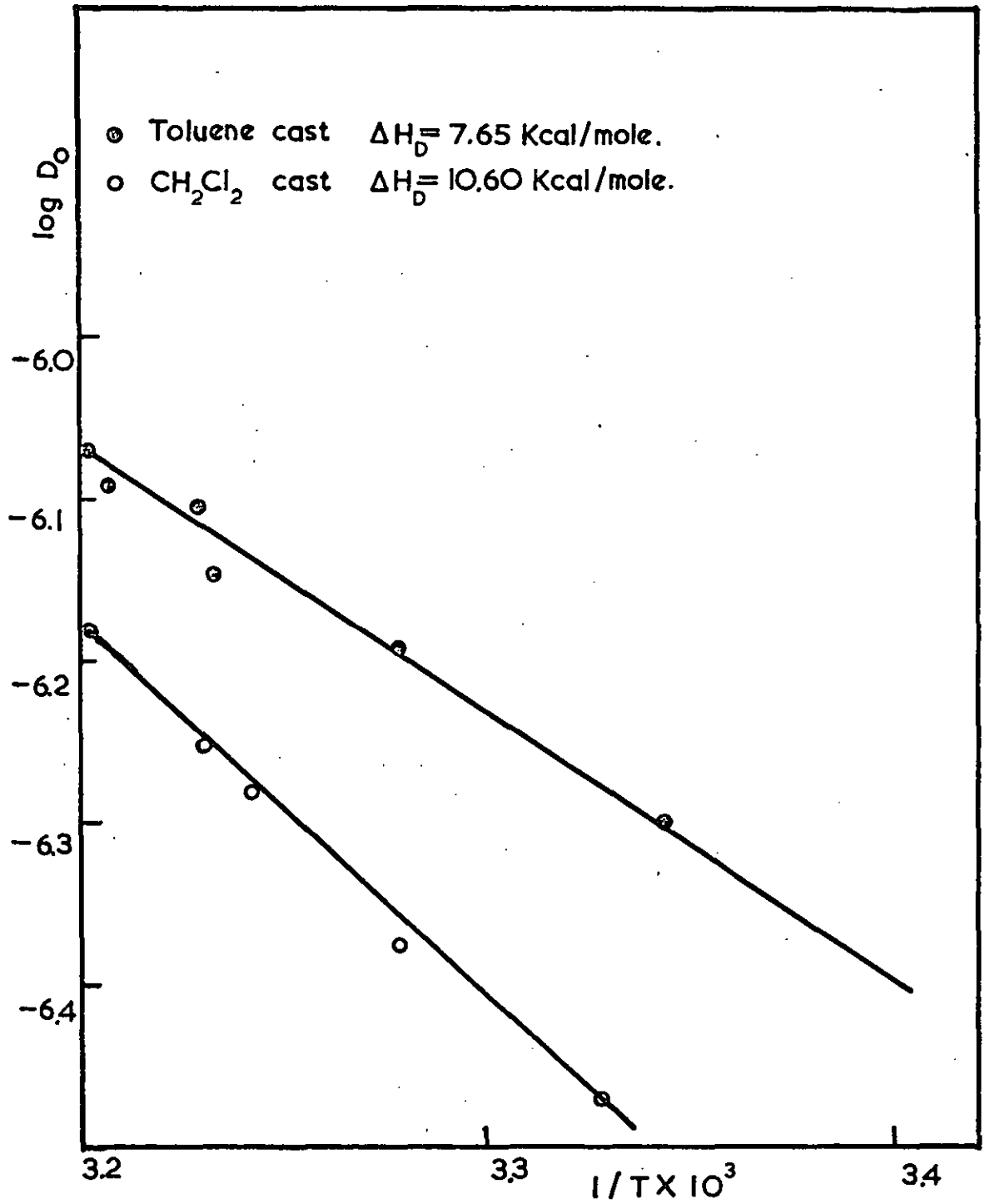

FIG.59. ARRHENIUS PLOT FOR SBS COPOLYMER.

Since the Arrhenius relationship can be represented also by

$$\log D = \log D^{\circ} - \frac{\Delta H_D}{2.303\ R\ T} \qquad 6.41$$

The value of D° which is the diffusion coefficient at "infinite temperature"can also be determined from extrapolation of the Arrhenius plots, and these values are also tabulated in Table 6.6. Both of these parameters may be interpreted as follows.

The activation energy of diffusion may be interpreted in general as the energy to be overcome for the penetrant molecule to move from one site to a new position. Brandt (section 2.5) has split this term into two contributions - viz: an intermolecular term due to the repulsion the polymer chains experience from their neighbours when displacing themselves to accommodate the penetrant molecule, and an intramolecular term due to the resistance of the chains themselves to "bending" (restricted rotation). The activation energy term therefore depends on the size of the penetrant molecule, and, more important, on the ease of segmental rotation of the polymer chains (especially for diffusion of large molecules). The activation energy for the different polymers listed in Table 6.6 will be dealt with again under the respective sections later on.

The interpretation of the constant D° is less clear. The theory of rate processes (147) relates D° to the entropy of activation for a diffusional jump ΔS^* through the equation

$$D^{\circ} = (e\delta^2 k\ T\ /\ h)\ \exp\ (\Delta S^*/R) \qquad 6.42$$

where δ is the length of a unit jump

k and h are Boltzmann and Planck constants respectively, e is a numerical constant.

Log D° has been observed by Barrer and Skirrow (77) to vary linearly with $\Delta H_D/T$ in several cases. Since the latter is also related to the number of degrees of freedom involved in a diffusion process (see Section 2.5), it would appear a linear log D° against $\Delta H_D/T$ relationship would justify the zone theory.

Barrer et al (141) in their work on the diffusion of butanes and pentanes in silicone rubber as compared to natural rubber found a linear log D° against $\Delta H_D/T$ plot for natural rubber, but the points for silicone rubber seemed to have a much higher log D° values than the linear relationship would predict. The author, however, after checking the mathematics involved in their calculation, found that this was in fact due to the omission of the factor 2.303 in Barrer's calculation for log D° in the expression

$$\log D^{\circ} - \log D + \frac{\Delta H_D}{2.303\ RT}$$

Making the due correction, a good linear relationship was established. We have also included log D° against $\Delta H_D/T$ plots for the polymers listed in Table 6.6 at 30°C, and these points fit in beautifully with Barrer's plot, forming a "master" plot involving diffusion of n-butane, neo-butane, n-pentane, iso-pentane and n-decane in natural rubber, filled and unfilled silicones, and S-B-S block copolymers cast from different solvents. This is shown in Fig.60. This plot suggests that the energy of activation is proportional to the entropy of activation in a diffusional process, and in terms of the zone theory, a greater activation of energy requires the co-operative movement of a larger number of segments. A few interesting observations are made from Fig.60 and these are listed below, and they will be discussed further in the later sections respectively:

For unfilled silicone rubber, log D° increases with larger penetrant molecules in the order

n-decane > n-pentane > n-butane,

for filled silicone rubber, log D° increases with filler content in the order

20 phr > 10 phr > unfilled.

for S-B-S block copolymer, the diffusion of n-decane has a higher log D° value in the sample with the more diffused morphology than the

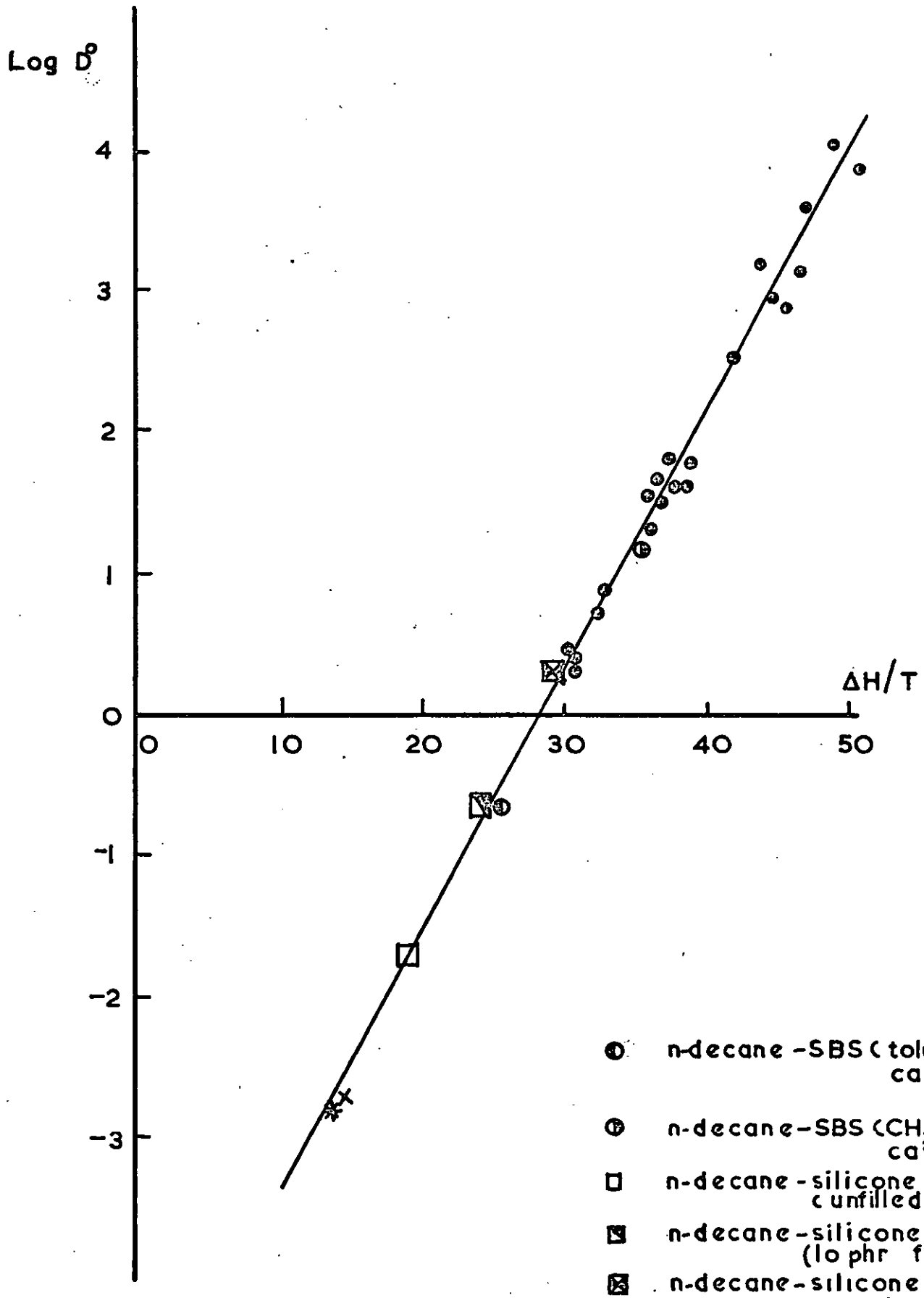
Log D°
4
3
2
1
0
-1
-2
-3
0
10
20
30
40
50
ΔH/T
n-decane-SBS (toluene cast)
n-decane-SBS (CH_2Cl_2 cast)
n-decane-silicone rubber (unfilled)
n-decane-silicone rubber (10 phr filler)
n-decane-silicone rubber (20 phr filler)
(142) X n-butane-silicone rubber
(142) * n-pentane-silicone rubber
(142) various penetrants in NR

FIG. 60

one with better phase separation (see Section 6.7),

and for similar penetrants, the log D^{o} values for silicone rubber are very much lower than those for natural rubber. This is probably due again to the segmental mobility of the former.

6.6. Silicone rubber (unfilled).

In this section we shall summarize some of the results observed in the previous sections and try to gather a complete picture on this polymer.

The first indication of the very mobile nature of the silicone chain segments is the negative concentration dependence of the mutual diffusion coefficient measured from sorption (see section 6.3). Interpreted in terms ofmass flow this has been attributed to the polymer chains being more mobile than the penetrant molecule (section 6.3, Fig.51). Later on, from free volume theory considerations we have shown that the free volume in silicone rubber is not affected to any significant extent by the presence of the penetrant (Eqn.631). This again reflects an inherent high chain mobility. Our results for the diffusion of n-decane will now be tabulated together with Barrer's results (141) for n-butane and n-pentane in the same polymer, so that a fuller discussion can be made on the various parameters involved. These data are shown in Table 6.7.

TABLE 6.7

Diffusing molecule	Concentration	Diffusion coefficient $(30^{o}C)\,cm^{2}sec^{-1}$	ΔH_D Kcals/mole	ΔH_{soln} Kcals/mole.	D^{o} $cm^{2}sec^{-1}$
n-butane (141)	small, assumed zero	5.4×10^{-6}	4.2	-5.27	0.00168*
n-pentane (141)	"	4.48×10^{-6}	4.3	-6.26	0.00185*
n-decane	extrapolated to zero	1.07×10^{-6}	5.75	-13.4	0.015

* These values are the "corrected" values from Barrer's published data (141) (see last section).

The diffusion coefficient is essentially a measurement of the velocity of translation of the penetrant through the polymer, but it is not by itself a measure of the polymer character. Since the thermodynamic

diffusion coefficient is related to the mobility term m_d, by the relation (Eqn.2.50)

$$D = RTm_d$$

and mobility is inversely proportional to the frictional force existing in the system, a Stoke-Einstein type of relation can be used to relate D to the friction coefficient , as follows

$$D = \frac{kT}{n\varepsilon} \qquad 6.43$$

where ε is the friction coefficient of a single $-CH_2-$ unit in the penetrant molecule, and n is the number of such units in a penetrant molecule. Thus in a homologous series of chemical compounds, this predicts that the friction experienc -ed by the diffusing molecule increases with its length, and the diffusion coefficient to decrease accordingly as shown by Eqn. 6.43. Therefore the ratio of the diffusion coefficient of n-butane, n-pentane, and n-decane should be 2.5:2.0:1. Table 6.7 shows a ratio of about 5:4.2:1. The value for n-decane seems to be lower than the predicted value, which indicates that n-decane diffuses by a different mechanism from that of n-butane and of n-pentane.

The activation energy of diffusion as given in Table 6.7 is best interpreted by considering the related $\log D^o$ parameter (see section 6.5). Since $\Delta H/T$ is linearly related to $\log D^o$ (Fig.60), and $\log D^o$ is related to the number of degrees of freedom(77), a greater ΔH_D means cooperation of polymer segments involving a greater number of degrees of freedom is required.

It is readily seen, therefore, that although the actual friction experienced by n-decane in the polymer is much higher compared with the lower hydrocarbons, the rearrangement process of the polymer segments needed for the penetrant translation is not appreciably more complicated. This supports the theory that diffusion of a penetrant molecule in the polymer medium occurs with the penetrant molecule participating in the thermal motion of the polymer chains themselves. Diffusion does not necessarily involve the penetration of the entire molecule into a new "hole," but possibly one portion of it followed by the rest as soon as further thermal fluctuations of the polymer segments have formed additional voids along the direction of translation. As the size of the penetrant increases the activation energy (and so the number of degrees of freedom) will increase until a certain limiting value, when the activation energy ΔH_D should become constant. The size of the penetrant molecule before this value is reached should correspond to the size of the polymer segment involved in thermal fluctuations. Flexible molecules larger in size than that of a polymer rearranging segment will diffuse by segmental motions themselves, and the energy of activation should not be higher than the energy required for polymer chain relaxation. Chen and Ferry (9) using Moore and Ferry's "composite" method (132) measured the diffusion of radioactively labelled n-hexadecane in silicone rubber, and obtained an activation energy of about 5 K cals/mole. They have stated in their publication that the error involved in their method for silicone rubber was large because of the high diffusion coefficient, so - allowing for this and our own errors, we can assume ΔH_D for n-decane and n-hexadecane in silicone rubber to be nearly equal. This suggests that at decane we are very near to this "limiting" value as mentioned above.

The variation of ΔH_D with the size of penetrant is shown in Fig.61; in section 6.9 this will be further discussed in relation to our results for dynamic mechanical data for this polymer.

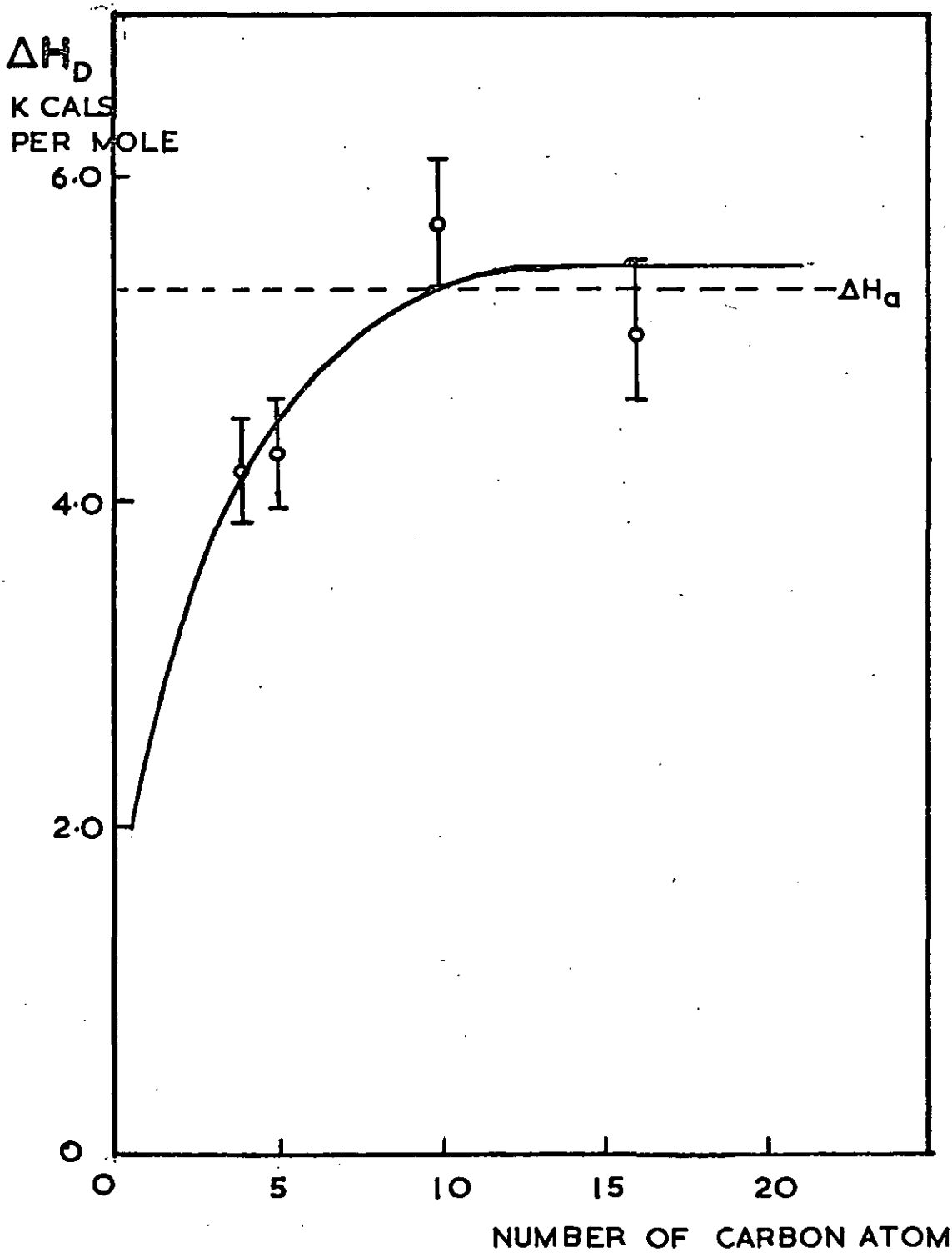
ΔH_D
K CALS
PER MOLE
6·0
4·0
2·0
0
ΔH_a
0
5
10
15
20
NUMBER OF CARBON ATOMS

FIG. 61

It is interesting to note that in Barrer's experiment (141) he compared the diffusion of n-butane and n-pentane in silicone rubber with that in natural rubber, and found that in natural rubber the diffusion coefficient of an identical hydrocarbon is about 25 times lower and the activation energy is about 3 times higher. This means that the frictional resistance encountered by the diffusing molecule in natural rubber is higher and more co-operation of the polymer segments is necessary ($g = 20$) for penetrant translation. This again emphasizes the ease of segmental rotation in silicone rubber.

The heat of solution term, ΔH_{soln}, in Table 6.7 is not important as far as molecular motions are concerned. As mentioned in Section 6.1 it is dependent essentially on the size of the penetrant molecule, when expressed per mole , since it consists mainly of the heat of liquefaction. The heat of solution per CH_2 unit from Table 6.7 in fact works out to be roughly constant, and is about - 1.3 kcals.

The D^o value in the last column of Table 6.7 has already been described primarily as an entropy of activation term. Log D^o is in fact directly related to the degrees of freedom g in the zone theory. D^o is seen to increase with larger penetrant size. This would be expected as larger penetrant molecules require greater disturbance of the surrounding molecules which have to rearrange to permit diffusion to take place.

6.7. Styrene-butadiene-styrene 3-block copolymer.

The styrene-butadiene-styrene 3-block copolymer, as the name suggests, consists of a block of polybutadiene chain terminated at each end by closely identical polystyrene blocks. This copolymer, referred to as S-B-S, exhibits the unique property of being rubbery at room temperature and thermoplastic at higher temperatures. This is due to the vast difference in the glass transition temperatures (T_g) between these respective blocks. For the polystyrene component the T_g is about 100°C, and for the polybutadiene component, about -99°C. (87). From low angle X-ray diffraction (149) and electron micrography (138)studies, a two phase structure with the polystyrene phase immobilized and distributed in some form of order (see later notes) is indicated at least at room temperature. The glassy regions can be considered as impermeable to the penetrant molecules, so that transport only takes place in the amorphous phase.

Our permeation experiments were performed on samples of S-B-S cast from two different solvents, toluene and methylene chloride. The effect of casting this polymer from different solvents on the morphology of the resulting film is discussed in detail elsewhere (87, 138), here it is sufficient to present the evidenced result, with little discussion on the mechanism of structure formation.

The solubility parameters of the various components involved in the film-casting process are given in Table 6.8.

TABLE 6.8

Component	Solubility Parameter $(cal/c.c)^{1/2}$
Polystyrene	9.1
Polybutadiene	8.6
Toluene	8.9
Methylene chloride	9.7

Since the enthalpy of mixing is expected to be proportional to the square of the difference in the solubility parameters, as given by (Eqn.6.3)

$$\Delta H_m = V(\delta_1 - \delta_2)^2 v_1 v_2$$

the closer they are the better is the mixing process.

Methylene chloride is therefore a better solvent for the polystyrene phase than the polybutadiene phase, whereas toluene is an equally good solvent for both components.

The sample cast from toluene has been observed by low angle X-ray diffraction (LAXS) to possess a discreet phase separation with spherical polystyrene phases distributed on a cubic lattice structure (149). The sample cast from methylene chloride, however, has been shown from the same evidence to possess a less ordered structure with the polystyrene domains having a more diffused pattern of distribution, with some continuous polystyrene phase. These two types of morphology are represented in Fig.62.

The diffusion results obtained for each of these samples are presented in Table 6.9.

TABLE 6.9

Sample	Diffusion coefficient extrapolated to zero penetrant concentration at 30°C. $cm^2\ sec^{-1}$	ΔH_D K cals/mole	D^o $cm^2\ sec^{-1}$
Cast from toluene	5.55×10^{-7}	7.65	0.210
Cast from $CH_2\ cl_2$	3.89×10^{-7}	10.60	14.13

The complete Arrhenius plots for the diffusion coefficients (extrapolated to zero concentration using Eqn. 6.33) for both these samples are shown in Fig.59.

To interpret these results, and the difference between the two samples varying only in morphology, it is necessary to assume that the

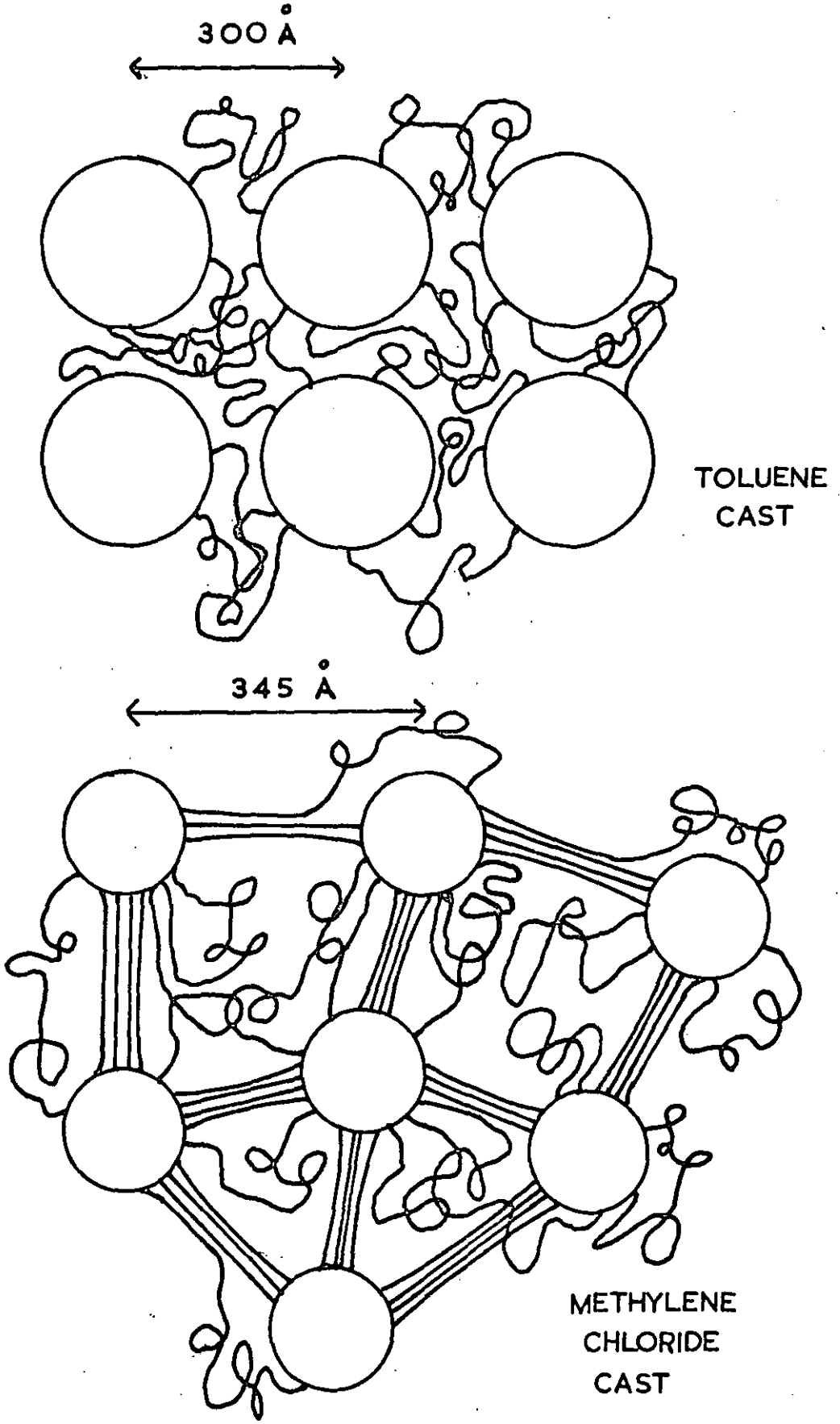

FIG. 62

polystyrene domains act as geometrical obstructions in the path of the diffusing molecules, and introducing a structure factor, k, which can be worked out quantitatively if the "filler" (polystyrene) particles are assumed to be arranged in some form of model structure.

In the case of zero sorption by the polystyrene

$$D_{(S\text{-}B\text{-}S)} = D_B\, k \qquad 6.45$$

where $D_{(S\text{-}B\text{-}S)}$ is the diffusion coefficient in the copolymer

D_B is the diffusion coefficient in the pure polybutadiene phase alone.

Various expressions derived for the analogous problem of electrical conductivity may be used to determine k. Thus Lord Rayleigh (50) and later Runge (151) considered the case of a cubic lattice of uniform spheres for obtaining an expression which may hold to high "filler" concentrations,

$$k = (1-v_A)^{-1}\left[(2-2v_A - 0.394\, v_A^{10/3}) / (2+v_A - 0.394\, v_A^{10/3})\right] \qquad 6.46$$

whereas it was derived by Thirion (152, 153) that

$$k = (1-v_A)^{-1}\left[1 + v_A/(1-v_A^{2/3})\right] \qquad 6.47$$

Many other expressions, often more complicated, are known either for spheres (154), for cylinders (151), or for oblate or prolate ellipsoids, the former approaching the lamellae type of filler (155).

Evidence (87, 149) has shown that our toluene cast S-B-S film sample has a cubic lattice structure of spherical polystyrene domains. It would, therefore, be appropriate to apply the Rayleigh and Runge model, and determine a value for the structure factor k.

The volume fraction for the polystyrene in the S-B-S sample used is 0.28 (see section 4.5), substituting this in Eqn. 6.46, we obtain

$$k = 0.78$$

Now the diffusion coefficient of n-decane in the pure polybutadiene has not been obtained by us, but a good approximation may be derived from Newns and Park's "master plot" relating diffusion coefficients of a fixed

penetrant in various polymers to the T_g values of these polymers (69). They derived a relationship (Eqn. 2.67) (D_o = Diffusion coefficient extrapolate to zero concentration at 25°C)

$$T_g = C_1 + \frac{C_2}{(\log D_o + C_3)} \qquad 6.48$$

where C_3 has a small value of about 0.53 and therefore does not affect log D_o to any large extent. T_g therefore is related linearly to $(\log D_o + C_3)^{-1}$. Assuming T_g of pure poly-butadiene (PBD) to be -99°C quoted earlier, and that of silicone rubber (PDMS) to be -123°C (69), the ratio of D_o in PBN/D_o in PDMS can be worked out from Newns and Parks' linear plot. This was in fact found to be 0.58. Since we know the diffusion coefficient of n-decane in silicone rubber (1.07×10^{-6} cm^2 sec^{-1} at 30°C - see section 6.6), it can be reasonably assumed that the diffusion coefficient of n-decane in PBN = $0.58 \times 1.07 \times 10^{-6}$ cm^2 sec^{-1} at 30°C, which is 6.22×10^{-7} cm^2 sec^{-1}.

Thus $D_B = 6.22 \times 10^{-7}$ cm^2 sec^{-1}

Applying Eqn. 6.45 therefore

$$D_{(S-B-S)} = 0.78 \times 6.22 \times 10^{-7} \text{ cm}^2 \text{ sec}^{-1}$$
$$= 4.85 \times 10^{-7} \text{ cm}^2 \text{ sec}^{-1}$$

From Table 6.9, the measured experimental value = 5.55×10^{-7} cm^2 sec^{-1}. The comparison is good considering the approximations taken, and this seems further justification of the cubic lattice structure in the toluene cast sample, and of the non-sorption by the polystyrene phase.

The result for the methylene chloride cast sample seems best approximated by Bottcher's model of suspended ellipsoids (156). We have not actually calculated the value of $D_{(S-B-S)}$ directly from his model, but since the ratio of the D/D_B value for Rayleigh's model and Bottcher's model is 0.38/0.25 (157), therefore

$$\text{Predicted } \frac{D\ CH_2Cl_2 \text{ cast}}{D \text{ toluene cast}} = \frac{0.25}{0.38} = 0.66.$$

The experimental ratio as given by Table 6.9 $= \frac{3.89}{5.55} = 0.70$

A reasonable comparison can, therefore, be made.

We have thus shown that the two phase structure in S-B-S can be represented reasonably well by assuming a cubic-lattice distribution of the spherical polystyrene domains in the toluene-cast sample, and a suspended ellipsoid polystyrene structure in the methylene-chloride sample. Fig. 59 seems to indicate either the collapse of the cubic lattice structure or the conversion of the ellipsoid structure to the cubic with increasing temperature. LAXS investigations of the sample at higher temperatures under the same physical conditions may reveal more about this phenomena.

The activation energy, ΔH_D, is observed to be higher in the more randomly distributed sample (Table 6.9.) This again suggests that the structure may be changing slightly with temperature.

6.8. Filled Systems.

The use of silicone rubber industrially invariably includes the compounding of a filler, as the gum rubber is so weak in mechanical strength as to be useless in most applications. The interaction between fine silica fillers and silicone rubber is chemically and structurally a complicated process. It is not well understood despite much work done in this field (see for example, 4, 142, 158, 159). The sorption and diffusion data obtained in this work are discussed in the light of current theories (4,142) and it is hoped a few conclusions may be drawn from this.

There are two main considerations in discussing the role of a rigid filler in the polymer in a vapour permeation experiment. Firstly the actual solubility of the vapour in the filled system will be affected in a manner depending on:

A. The preferential adsorption of either the polymer molecules or the vapour molecules onto the filler surface.

B. The existence of vacuoles or porosity in the filler particles which may absorb the vapour.

Secondly, the diffusion coefficient is dependent on a structural factor (see last section), which allows for the fact that the average diffusion path is increased by the presence of the filler particles because the localized direction of flow is not always normal to the geometrical cross-section of the membrane (159). This structural factor can be estimated from analagous solutions of conductivity in a hetereogeneous medium as discussed in Section 6.7.

Sorption considerations.

When fine silica such as "Aerosil 2419" (particle diameter approx. 180A°) is mixed with silicone rubber on the mill, the filler particles

may experience two or perhaps three types of interactions with the silicone rubber. They may be attached "chemically" to the polymer chains, thus forming additional "cross-link" points, or the polymer can be physically absorbed on the filler surface, forming "coated silicas." (4). In addition it is conceivable that the filler particles themselves may form "clusters."

For "cross-linked" silicas, the filler particles can be considered as an independent phase from the rubber phase, and the equilibrium sorption of a vapour by the whole system can be written

$$S = V_r S_r + V_f S_f \qquad 6.49$$

where S_r and S_f are the equilibrium sorption coefficient of the vapour in rubber and the filler. V_r and V_f are the respective volume fractions.

If the polymer completely "wets" the filler surface, i.e. for "coated silicas," the filler particles may preferentially absorb the polymer rather than the penetrant, and Eqn. 6.49 then reduces to

$$S = S_r V_r \qquad 6.50$$

However, it is conceivable that absorption of the decane vapour may still take place in the internal pores of the filler, which are not accessible to the siloxane but may be to the penetrant molecules, which have smaller cross section areas.

In our data, as expressed by Fig.63, a curious behaviour is observed which may be related to the porous sorption effect as mentioned above. At low temperatures (below 40°) there is little difference in the amount sorbed between the filled and unfilled samples. As the temperature is raised, the second model (Eqn. 6.50) is progressively more obeyed until ultimately the sorption of the vapour is expected to become proportional to the volume fraction of the rubber. If we envisage most of the silica as being "wetted" by the polymer, and only a small portion in the cross-linked form, the total sorption will be equal to the sorption by the

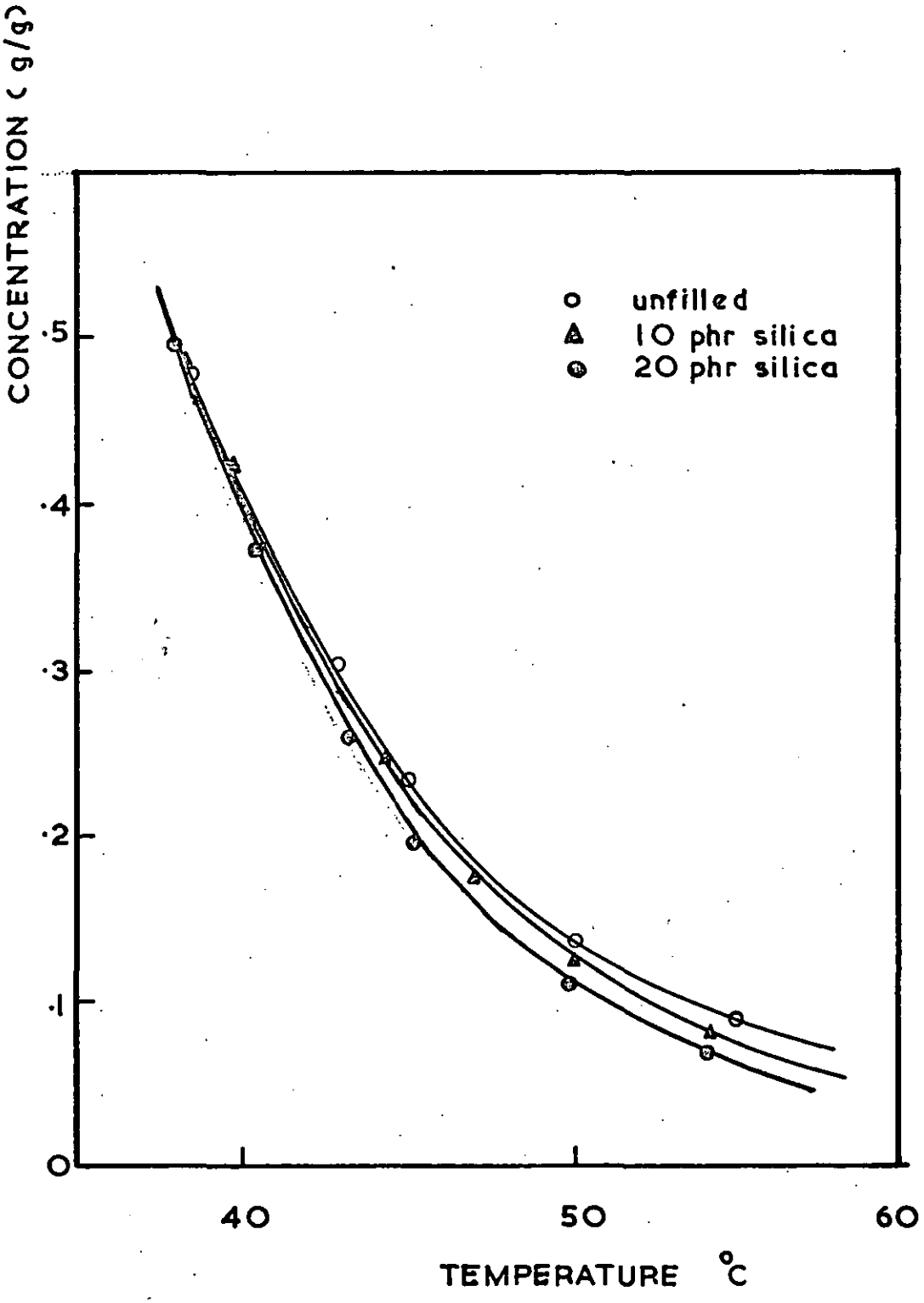
CONCENTRATION (g/g)
·5
·4
·3
·2
·1
0
40
50
60
TEMPERATURE °C
unfilled
10 phr silica
20 phr silica

FIG. 63

rubber, the sorption by the small amount of "non-wetted" silica, and the sorption in the pores of the filler. If the sorption by the silica is strongly temperature dependent, and this is evidenced by the high heat of solution in the filled sample (see section 6.1), then Fig.63 can be explained if the adsorption on the "free" filler varies from a value higher than the rubber sorption coefficient at low temperatures, to a value approaching zero at temperatures higher than 50°C.

Diffusion parameters.

The Arrhenius relationship is found to be reasonably obeyed in the filled samples (Fig. 57-58). From the Arrhenius plots, the usual parameters are derived and these are tabulated below (the unfilled sample is inserted for reference.)

TABLE 6.10

Silicone rubber sample	ΔH_{soln} (Kcals/mole)	ΔH_D (Kcals/mole)	D_2^0 $cm^2 sec^{-1}$	Diffusion coefficient (30°C) $cm^2 sec^{-1}$
Unfilled	- 13.4	5.75	0.015	1.12×10^{-6}
10 phr. filled (V_r=0.955)	- 20.2	7.4	0.229	1.12×10^{-6}
20 phr. (V_r=0.91)	- 20.2	8.8	2.158	1.04×10^{-6}

It is quite significant that the diffusion coefficient of the filled sample is not reduced as would be predicted from structural considerations. On closer examination, however, we discover that the structure factor, k, (as defined in section 6.7), assuming a Rayleigh model (150), would work out to about 0.98 and 0.93 for the 10 phr and 20 phr filled samples respectively. Thus the diffusion coefficient should not be greatly reduced anyway. It is also possible that some filler particles may have "through" porous holes, which may shorten the diffusion path of the diffusing molecule. The "clustering" of the filler particles may

also create microstructures between particles equivalent to pores.

The larger heat of solution in the filled systems is obviously linked to the sorption by the "free"silica as described above. That there is no difference between the 10 phr and 20 phr samples may be further evidence of the "clustering" behaviour of the silica particles as mentioned previously.

The D^{o} value describes the entropy of activation, and since it is seen to increase with filler content, it seems likely that the polymer segments become more restricted with increasingly filled samples, and this in turn is reflected by the higher activation energy of diffusion observed, (i.e. higher number of degrees of freedom is involved).

There may have been an error in the evaluation for the activation energy of diffusion in the filled samples because of the "free" silica sorption effect described previously. At low temperatures some of the sorbed vapour which is sorbed onto these silicas may not participate in the diffusion, and the diffusion coefficient obtained thus gives some mean value between the diffusivity in the polymer phase and the zero diffusivity of the vapour absorbed on the filler. The overall measured diffusion coefficient would be therefore smaller than the real value. Since this absorption on the silica is shown to gradually disappear at higher temperatures, the diffusion coefficient then approaches the true value. The activation energy should, therefore, be lower than the measured value. This problem is, however, deemed not too serious, and the general picture of diffusion of n-decane in silica-filled silicone rubber remains as described.

6.9. Comparison of diffusion and viscoelastic relaxation parameters.

Two parameters can be meaningfully used to correlate diffusion behaviour of a penetrant molecule in a polymer to the thermal chain mobility behaviour of polymer chains themselves. These are the friction coefficient, ζ, and the related activation energy term.

The monomeric friction coefficient, $\hat{\zeta}_o$, is defined as the measure of frictional resistance per monomer unit encountered by a chain segment in translatory motions.

The friction coefficient, ζ_1, of the penetrant molecule in the polymer matrix, is given by the expression (Eqn. 1.1)

$$\zeta_1 = kT/D_o \qquad 6.50$$

where D_o is the diffusion coefficient at vanishing concentration of penetrant, and k is the Boltzmann constant.

Therefore, if a penetrant similar in size to the monomer unit is used, ζ_1 should be very near to $\hat{\zeta}_o$. Ferry (160) has in fact tabulated ζ_1 values for various penetrants in the size range near to that of the monomer unit, and compared them favourably with $\hat{\zeta}_o$. Thus he confirmed that the force experienced by a monomer unit in the "relaxing" polymer segment is almost exactly the same as that experienced by a penetrant molecule in pushing its way through the polymer medium. ζ_o can, therefore, be estimated from a knowledge of ζ_1, and diffusion may therefore be used to predict the time scale of transition zone of viscoelastic properties.

From the free-volume theory, ζ_o may be expressed in the following manner:

Since $\zeta_o \propto \frac{1}{m}$

(where m is the mobility)

and $m = A \exp(-B/f)$ Eqn. 2.49

therefore, $\log \zeta_o = \text{const.} + B/f$ 6.51

where B, f have been defined previously (Section 2.4).

A similar expression may be derived for diffusion (49,55)

$$\log \mathcal{E}_1 = \text{const.} + B_d/f \qquad 6.52$$

The ratio B/B_d can be determined from the measurement of the activation energies of relaxation and diffusion, since (6)

$$\Delta H_a = \frac{d \ln a_T}{d(1/T)} \qquad 6.53$$

where a_T is a shift factor and can be defined as

$$\ln a_T = B\left(\frac{1}{f} - \frac{1}{f_o}\right) \qquad 6.54$$

Over a narrow temperature range

$$\frac{B_d}{B} = \frac{(\Delta H_D - RT)}{\Delta H_a} \qquad 6.55$$

B_d is found to be usually smaller than B, and this means that the minimum hole size required for the translation of a penetrant molecule is smaller than that required for a polymer segment. Thus if $\mathcal{E}_1 = \mathcal{E}_o$ and $\Delta H_D < \Delta H_a$, this suggests that more than one monomer unit isinvolved in a polymer relaxing segment. Hypothetically if we can increase the size in a homologous series of penetrant until $\Delta H_D - RT = \Delta H_a$, then the ratio of $\mathcal{E}_1/\mathcal{E}_o$ should approximate to the number of monomer units involved in one rearranging segment.

In our data for silicone rubber the activation energy of viscoelastic relaxation was found to be 5.30 K cals/mole from the WLF shift procedure (Fig.64). The activation energy of diffusion of n-decane was found to be 5.15 K cals/mole.

$$B_d/B \doteq 1$$

If we assume that this is near enough for unity, and further taking $\mathcal{E}_o$ to be 8.9×10^{-9} (160), then $\mathcal{E}_1/\mathcal{E}_o$ at 25°C works out to be about 7. Each rearanging segment in silicone rubber consists therefore of seven monomer units. The above assumptions need to be substituted by more data for hydrocarbons in between C_5 and C_{10} and even higher ones, so

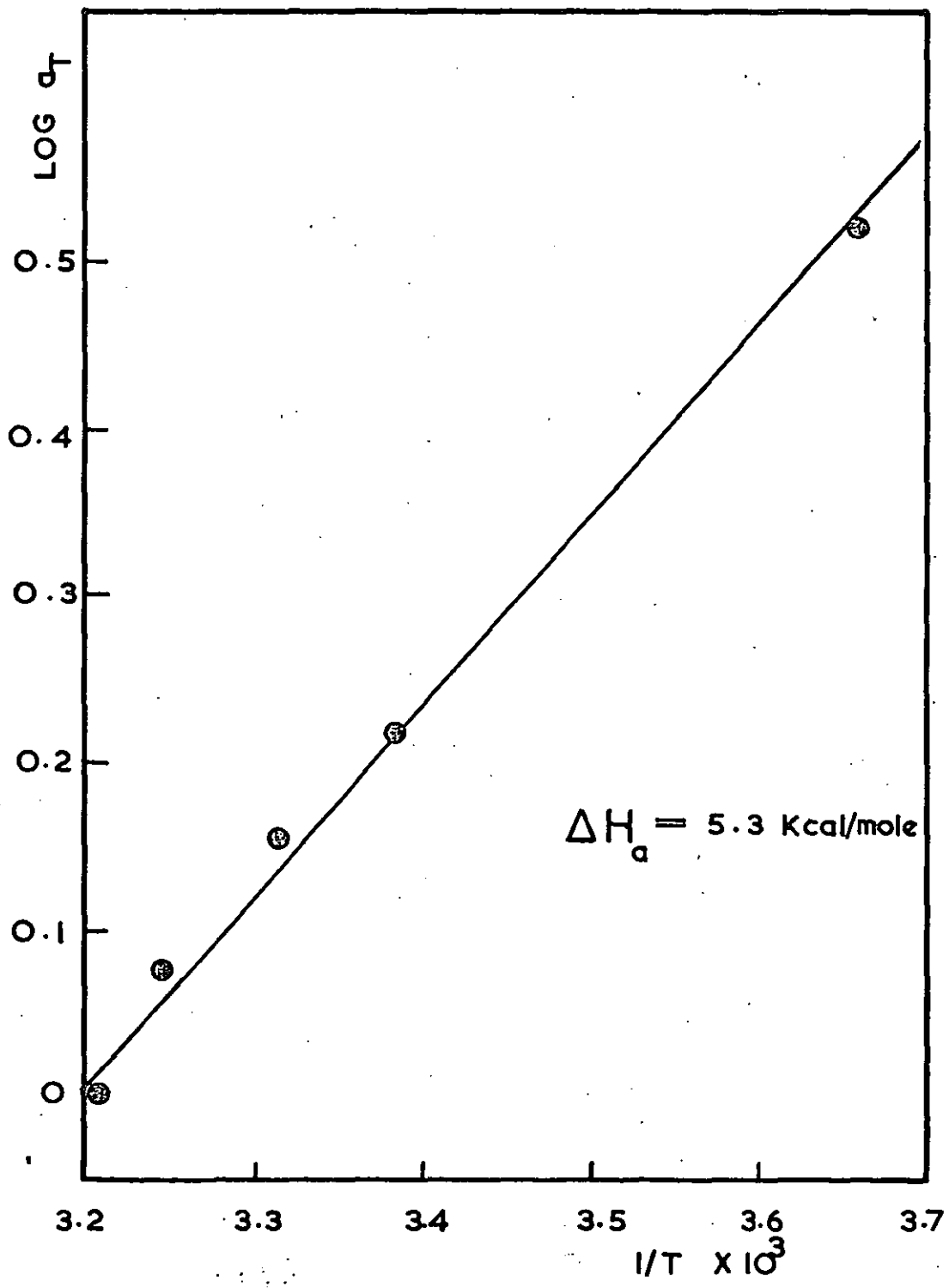
LOG d_T
0.5
0.4
0.3
0.2
0.1
0
3.2
3.3
3.4
3.5
3.6
3.7
1/T X 10^3
ΔH_a = 5.3 Kcal/mole

FIG. 64

that a value of ε_1 can be chosen which gives a ΔH_D value which is a good match to the ΔH_a value. Nevertheless it is shown that from a combination of diffusion and mechanical data, an estimation of the size of the very popularly referred to "polymer segment" can be made.

For the S-B-S polymer, the ΔH_a value was found to be 12 K cals/mole (87). Since our diffusion value for n-decane is 7.65 K cals/mole (Table 6.9), B_d/B is about 0.6. The polymer segment involved in thermal motions appears to be therefore larger in size than the penetrant (n-decane) molecule. At 25° the ratio $\varepsilon_1/\varepsilon_o$ works out to be about unity. This seems to indicate that the polybutadiene segment involved in its own relaxation is about 1 - 2 monomer units in size. The value of ε_o used to estimate the above ratio is the one quoted for 1,4 - polybutadiene with a cis:trans:vinyl ratio 43:50:7 (160), this value may not be completely true when applied to our polymer, and some errors may have been incurred.

The activation energy (about 18 K cals/mole) measured from the loss peak at and near the glass-transition temperature (Fig.46, Chapter 5), of silicone rubber may be interpreted as follows. It is much higher than the Arrhenius activation energy measured at ambient temperature, due to restricted segmental motions (Section 6.5), and to a lesser degree the crystallisation of the silicone rubber at -50°C (163). The quantity corresponds in magnitude to that predicted by the free volume theory (Fig.55), the fact that it is larger may be due to the deviation of the true free volume parameters from the "universal" values, and the effect of crystallization.

6.10. Development of the Apparatus.

The main problems facing the design of a permeation apparatus with the principles described for our method can be listed under the following headings:

1. Light (photomultiplier)
2. Temperature control
3. Good vacuum
4. Efficient transfer of penetrant
5. Non-interference with electronics of counting instrument

In our glass diffusion line (Chapter 3), we initially concentrated on 2 and 5, with the result that the apparatus performed well on 2, fair on 5 and 3, but poor on 1 and 4 (reasons given in Chapter 3).

To improve 4, and 1, we designed the metal permeation cell (Chapter 4). This we achieved with some success, with 3 and 5 remaining good. However, we underestimated the rate of heat conduction along the metal walls of the cell, with the inevitable consequence that our temperature control became less precise, the temperature of one part of the system being affected by heat changes in another part (see Chapter 4, Section 2). Therefore, a third design (based on our metal cell design) becomes desirable which concerns mainly the elimination of problem 2 listed above.

Since our major problem is the heat conducted between the active reservoir and the polymer membrane (See Fig. 17 and 65), with the scintillator cell reasonably well thermally insulated by the metal-to-glass seal, the solution lies in the search of a way to insulate the top part of the system thermally from the middle part. This must be done without affecting conditions 1, 3, 4, 5 listed above. One way in which this can be done would be to use a tough thin stainless steel tube to separate the top and middle parts of the cell, as shown in Fig.65. Since

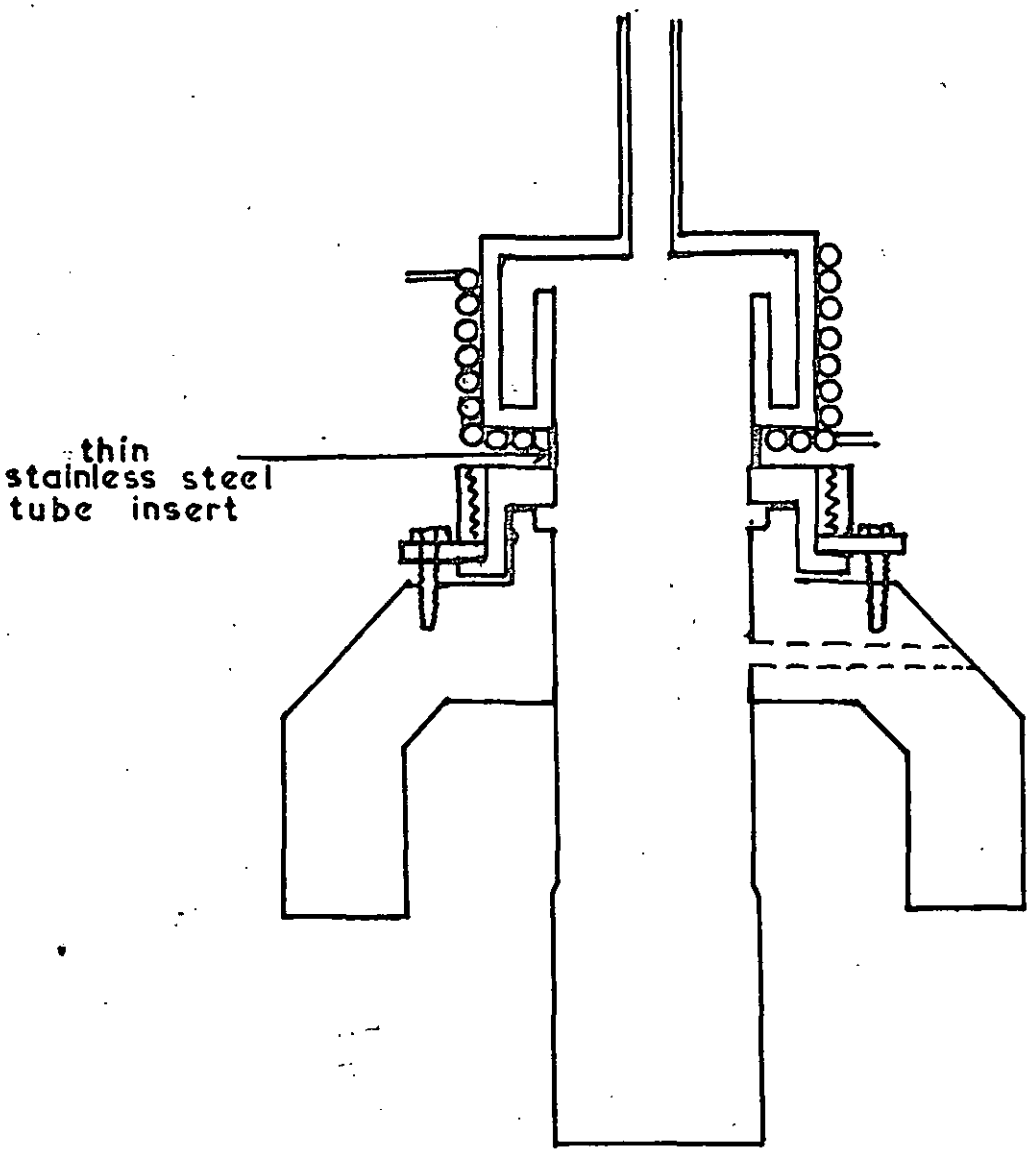

FIG. 65

the amount of heat conducted is proportional to the cross-section area, this will be reduced greatly, and the remaining small amount of heat which may still manage to be conducted should be eliminated by efficient thermostating.

It must be pointed out that the problem of membrane distortion due to uneven pressure applied on two sides of the membrane in a "normal" permeation experiment, should not be one in our method, where there should be no pressure gradient whatsoever across the membrane.

Conclusions.

We have shown that a simple, rapid and accurate method can be used to determine directly the self-diffusion coefficient D* of a penetrant in the polymer matrix; the design of the apparatus is to date not perfect but it can be readily further improved. The working of the method depends on the penetrant being also functionable as the solvent medium in a liquid scintillator mixture. This should impose no great limitation as many organic molecules can act as primary solvents for liquid scintillation counting (106).

Theoretical definitions of various diffusion coefficients have been illustrated by comparing diffusion coefficients we obtained from sorption methods and our permeation experiment. From these comparisons it is possible to gather more information on the manner of swelling (i.e. isotropic or uni-directional), and the thermodynamic behaviour regarding penetrant activity etc.

The concentration dependence of the diffusion coefficient was explained by the free volume concept, and a few "free volume parameters" have been estimated and interpreted accordingly. Barrer's zone theory was found to be a convenient way of describing the activation energy variation among different polymers, and a linear log D° versus $\Delta H_D/T$ relation was found to hold for all our data.

The morphology of S-B-S block copolymers was looked at from the diffusion coefficient variation, and from the assumptions of Rayleigh's and other hetereogeneous models used for conductivity, good comparisons were observed regarding the structural distributions of the styrene phases between our study and low angle X-ray diffraction evidences.

Silica filler-silicone rubber interaction, an up-to-date not fully comprehensible subject, was looked at from the sorption and diffusion data. The data could only be explained if sorption of decane

into the silica (pores) was assumed large at ambient temperatures and low at high temperatures.

The free volume theory can be used to correlate diffusion data with dynamic-mechanically obtained data to yield new information on polymer chain mobility. The length of the motional segment in the polymer can be estimated, and for silicone rubber this was estimated at 7 monomer units. Further work in this and other fields mentioned above should provide more fruitful contributions to present-day knowledge of molecular motion in and morphology of polymer systems.

REFERENCES

1. G. J. Van Amerongen. Rubber Chem. Technol. 28. 821 (1955)
2. J. H. Fielding. Ind.Eng.Chem. 29. 880 (1937)
3. W. F. Watson. Ind.Eng.Chem. 47 1281 (1955)
4. D. W. Southwart. M.Sc. Thesis, Manchester University (1969)
5. P. E. Rouse. J.Chem.Phys. 22 603 (1954)
6. J. D. Ferry. "Viscoelastic Properties of Polymers. John Wiley & Son. 2nd Ed. P.361 (1969)
7. F. Bueche, W. M. Cashin & P. Debye T.Chem. Phys 20 1956 (1952)
8. B. D. Boss, E. O. Stejskal & J. D. Ferry J.Phys.Chem. 71 1501 (1967)
9. S. P. Chen and J. D. Ferry Macromolecules 1, 270 (1968)
10. I. Auerbach, S. D. Gehman, W. R. Miller & W. C. Kurzla J. Polymer Sci. 28 129 (1958)
11. S. D. Morton & J. D. Ferry J. Phys. Chem. 63 1335 (1959)
12. A. Aitken & R. M. Barrer Trans. Faraday Soc. 51 116 (1955)
13. Ref. 6. p.372.
14. W. L. Robb Annals, N.Y. Acad. Sci. 146 119 (1968)
15. J. F. Beecher Polymer Reprints 8 1532 (1967)
16. A. Fick Ann. Phys Lpz 170, 59 (1855)
17. J. B. Fourier Theorie analytique de la chaleur) Euvres de Fourier (1822)
18. J. Crank "Mathematics of Diffusion" Chapter 1, p.3 Oxford University Press (1964)
19. ibid, p.224.
20. G. S. Hartley Trans. Faraday Soc. 42 B 6 (1946)
21. C. Robinson Trans. Faraday Soc. 42 B 12 (1946)
22. Ref. 18, p.226
23. W. A. Johnson Trans. Amer.Inst. Mining Met.Engrs. 47, 331 (1942)
24. R. M. Barrer J.Phys.Chem. 61, 178 (1957)

25. J. Crank & G. S. Park — "Diffusion in Polymers." Academic Press p.4. (1968)

26. R. M. Barrer — Proc.Phys.Soc. 58 321 (1946)

27. W. A. Rogers, R.S.Buritz and D. Alpert — J.Appl.Phys. 25 868 (1954)

28. C.C.Lieby Jnr. & C.L.Chen — J.Appl.Phys. 31 268 (1960)

29. V. O. Alternose — J.Appl.Phys. 32 1309 (1961)

30. P. Meares — J.Appl.Polymer Sci. 9 917 (1965)

31. Ref. 18, p.48.

32. H. Daynes — Proc.Roy.Soc. 97 A 286 (1920)

33. R. M. Barrer — "Diffusion in and through solids." Cambridge p.19 (1941)

34. H. L. Frisch — J.Phys.Chem. 61 93 (1957)

35. H. L. Frisch — J.Phys.Chem. 62 401 (1958)

36. R. M. Barrer & H.T.Chio — J.Polymer Sci.Pt.C 10 111 (1965)

37. Ref.18, p.45.

38. S. Prager & F. A. Long — J.Amer.Chem. Soc.73 4072 (1957)

39. J. Crank & G. S. Park — Trans. Faraday Soc. 45, 240 (1949)

40. R. J. Kokes, F. A. Long and J. L. Hoard — J.Chem. Phys. 20 1711 (1952)

41. R. M. Barrer & D. W. Brook — Trans.Faraday Soc. 49 1049 (1953)

42. S. Prager — J. Chem.Phys. 19 537 (1951)

43. H. Fujita & A.Kishimoto — Text Res. J. 22 94 (1952)

44. L. J. Huang — J. Chem.Phys. 20 1320 (1952)

45. Ref. 18, p.256.

46. S. Prager & F. A. Long — J.Amer.Chem.Soc. 73 4072 (1951)

47. R. J. Kokes, F. A. Long and J. C. Hoard — J.Amer.Chem.Soc. 75 6142, 6319 (1953)

48. A. Kishimoto and K. Matsumoto — J.Phys,Chem.63 1529 (1953)

49. H.Fujita, A. Kishimoto and K. Matsumoto — Trans.Faraday Soc. 56 424 (1960)

50. A. Kishimoto & Y. Enda — J.Polymer Science AI 1799 (1963)

51. P. Meares — J.Polymer Sci.27 391 (1958)

52. G. S. Park — Trans.Faraday Soc. 46 684 (1950)

53. H. Fujita — J.Phys.Soc. Japan 8 271 (1953)

54. W. W. Brandt — J. Phys.Chem.Washington 63 1080 (1959)

55. H. Fujita — Adv. in Polymer Sci. 3 1 (1961)

56. J. B. Wilkens & F. A. Long — Trans.Faraday Soc. 53, 1146 (1957)

57. A. K. Doolittle — J.Appl.Phys 22 1471 (1951)

58. A. K. Doolittle — Ibid 23, 236 (1952)

59. T.G.Fox & P.J.Flory — J.Polymer Sci.14 315 (1954)

60. S.S.Rogers & L.Mandelkern — J.Phys.Chem.61 985 (1957)

61. M.L.Williams, R.F.Landell and J. D. Ferry — J.Amer.Chem.Soc. 77 3701 (1955)

62. H.Fujita & A,Kishimoto — J.Polymer Sci.28 547 (1958)

63. J. D. Ferry & R.A.Stratton — Kolloid Z 171 107 (1960)

64. M.H.Cohen & D.Turnbull — J.Chem.Phys. 31 1164 (1959)

65. H.Fujita & A.Kishimoto — J.Chem.Phys. 34 393 (1961)

66. M.J.Hayes & G.S.Park — Trans.Faraday Soc.52 949 (1956)

67. R.M.Barrer & R.R.Ferguson — Trans.Faraday Soc.54 989 (1958)

68. Ref.6, p.307

69. A.C.Newns & G.S.Park — J.Polymer Sci.Pt.C 22 927 (1969)

70. T.A.Garett & G.S.Park — J.Polymer Sci.C, 16 601 (1965)

71. R.M.Barrer — Trans.Faraday Soc.38 322 (1942)

72. R.M.Barrer — ibid 35, 644 (1939)

73. R. M. Barrer — ibid 39, 48, 59 (1943)

74. R. M. Barrer — ibid 35, 628 (1939)

75. R. M. Barrer — ibid 36, 645 (1940)

76. R. M. Barrer — Koll.Z. 120 177 (1950)

77. R.M.Barrer & G.Skirrow — J.Polymer Sci.3 549, 564, (1948)

78. Ref.33.

79. Ref.54 Appendix

80. D. R. Paul & A.T.Di Benedetto J. Polymer Sci.Pt.C 10 17 (1965)

81. A.T. Di Benedetto — J.Polymer Sci. A 1 3477 (1963)

82. P. Meares — Trans.Faraday Soc. 53, 101 (1957)

83. A. T. Di Benedetto & D. R. Paul — J.Polymer Sci. A2 1001 (1964)

84. B. Gross — "Mathematical Structures of the theories of Viscoelasticity" Paris, Herman & Cie (1953)

85. K.W.Scott & R.S.Stein — J.Chem.Phys. 21 1281 (1953)

86. F.R.Eirich (Editor) — "Rheology, Theory and Applications" Vol.I,II,III New York Academic Press (1956)

87. A. S. Tan — Ph.D. Thesis, Loughborough University, England (1970).

88. P. Meares — "Polymers, Structure and Properties. D Van Nostrand p.277 (1965)

89. A.V.Tobolsky & R.D.Andrews — J.Chem.Phys.11 125 (1943) J.Polymer Sci. 3 669 (1948)

90. H.Leaderman — "Elastic and creep properties of filamentous materials and other high polymers" The Textile Foundation, Washington, p.171 (1943)

91. J. D. Ferry — Amer.Chem.Soc. 72 3746 (1950)

92. J. D. Ferry, E.R.Fitzgerald, M.F. Johnson and L. D. Grandine — J.Appl.Phys. 22 717 (1951)

93. W.Dannhauser, W.C.Child Jnr. and J. D. Ferry — J.Colloid.Sci.13 103 (1958)

94. P.Flory — "Principles of polymer chemistry". Cornell University Press, N.Y. Chapter 10, (1953).

95. F. Bueche, — J.Chem.Phys. 22 603 (1954)

96. J.G.Kirkwood — J.Chem.Phys. 14 51 (1946)

97. D. James & H.M.E.Guth — J.Chem.Phys. 11 455 (1943)

98. J.G.Kirkwood & F.M.Fuoss — J.Chem.Phys. 2 329 (1934)

99. P.E.Rouse — J.Chem.Phys. 21 1272 (1953)

100. J.D.Ferry & R.F.Landell — Kolloid Z. 148 (1956)

101. Ref. 6, p.185.

102. A.Einstein — Ann.Physik 17 549 1905)
ibid 19 371 (1905)
Z.Elektrochem 14 235 (1908)

103. F. Bueche — J.Chem.Phys. 20 1959 (1952)

104. T.G.Fox, Serge Gratch and S.Loshack — "Rheology" Vol.I. (Ed.Eirich) p.479

105. H.Eyring — J.Chem.Phys 4 283 (1936)

106. J.B.Birks — "Theory and Practice of Scintillation Counting" Pergamon (1964)

107. E.C.Anderson & F.N.Hayes — Ann.Rev.Nuclear Sci. Vol.6 p.303 (1956)

108. D.J.Gram & G.S.Hammond — "Organic Chemistry" McGraw-Hill, N.Y. p.743, (1964)

109. S.B.Garfinkel, W.B.Mann, R.W.Medlock & O.Yura — Int.J.Appl.Radiation & Isotopes, 15 133 (1964)

110. F.N.Hayes, B.S.Rogers and P.C.Saunders — Nucleonics 13 No. 1 46 (1955)

111. EMI Publication — Photomultiplier Tubes. Brochure Ref. 30M/6-67 (PMT) Issue 1.

112. G.King. — Trans.Faraday Soc. 41 479 (1945)

113. G.S.Park — Trans.Faraday Soc. 48 11 (1952)

114. R.A.Pasternak, J.F.Schimscheimer & J. Heller — J.Polymer Sci.A.2 8 467 (1970)

115. F. J. Norton — J.Appl.Polymer Sci. 7 1649 (1963)

116. I. Phillips & D.V.Bartlett — British Plastics 34 533 (1961)

117. U.S.S.R. Pat.150 682 (R.A.P.R.A. Trans. No. 1083)

118. A. W. Myers, J. A. Meyer, C. E. Rogers, V. Stannet and M. Szwarc — Tappi 44, 58 (1961)

119. D. W. McCall and W. P. Slichter — J.Amer.Chem.Soc. 80 1861 (1958)

120. P.M.Hauser & A.D.Maclaren — Ind.Eng.Chem. 40 112 (1948)

121. S. L. Madorsky — Rev.Sci.Instr.21 393 (1950)

122. P. E. Rouse — J.Amer.Chem.Soc. 69 1068 (1947)

123. W.W.Wendlandt — J.Chem.Edu. 38 566 (1961)

124. S. J. Gregg — J.Chem.Soc. 561 563 (1943)

125. F.H.Muller & E.Hellmuth — Kolloid Z. 144 125 (1955)

126. B. Rosen — J.Polymer Sci. 35 335 (1959)

127. G. S. Park — Trans.Faraday Soc. 57 2314 (1961)

128. A.Gromov, V.B.Miller M.B.Neiman and Y. A. Shlyapni Kov — Internat.J.Appl.Radiation Isotopes 13 281 (1962)

129. M.Dubini, O.Cichetti, G.P.Vicario & E.Ena — European Polymer J. 3 473 (1967)

130. G. S. Park — "Radioisotope Conference" 2 11 (1954)

131. R.E.Pattle, P.J.A.Smith and R. M. Hill. — Trans.Faraday Soc. 63 2389 (1967)

132. R.S.Moore & J.D.Ferry — J.Phys.Chem. 66 2699 (1962)

133. A. R. Ware — Personal communication, Loughborough University.

134. C. Marsden — "Solvents Guide", 2nd Ed. Cleaver Hume (1963)

135. V. A. Stanley — E.M.I.Document Ref. R/P031.

136. E.M.Worster — EMI Symposium and Exhibition "Recent Advances in Photomultiplier Tubes" (1965)

137. J. Sharp — EMI Ref. R/P021.

138. J.F.Beecher, L.Marker, R.D.Bradford, S.L.Aggarwal — J.Polymer Sci. C-26 117 (1969)

139. Z.M.Kolthoff, T.S.Lee, C.W.Carr. — J.Polymer Sci. 1, 429 (1946)

140. R.T.Overman and H.Clark — "Radioisotope Techniques." McGraw-Hill N.Y. p.98 (1960).

141. R.N.Rickles — Ind.Eng.Chem. 58 6 19 (1966)

142. R. M. Barrer, J. A. Barrie and N. K. Raman. — Polymer 3 595 (1962)

142* Ref.18, p.319.

143. J.G.Downes & B.H.MacKay — Proc.1st Int. Wool.Text. Res.Conf. Australia Paper D, 203 (1955).

144. Ref.25 p.76

145. T.A.Garett & G.S.Park — J.Polymer Sci. C 16 601 (1966) T.A Garett M.Sc thesis u. of wales.

146. Ref. 140, p.405.

147. S.Glasstone, K.J.Laidler and H. Eyring. — "The theory of rate processes." McGraw-Hill, Chapter IX.

148. Ref. 88, p.326.

149. K. U. Fulcher — Ph.D. Thesis, Loughborough University, England. (1970)

150. Lord Rayleigh — Phil. Mag. (5) 34 481 (1892)

151. I. Runge — Z.Tech. Phys. 6 61 (1925)

152. P.Thirion, G.J. van Amerongen and R. Chasset. — Rev.Gen.Caoutchouc 28 684 (1951)

153. P.Thirion — Proc.3rd Rubber Technol.Conf.London, p.334 (1954)

154. R. E. Meredith and C.W.Tobias. — J.Appl.Phys. 31 1270 (1960)

155. M. Fricke — Physics 1, 106 (1931)

156. C.J.F.Böttcher — Recl.Trav.Chim.Pays.Bas Belg. 64 47 (1945)

157. Ref.25, p.186.

158. A.S.Michaels & R.B.Parker — J.Polymer Dir. 41 53 (1959)

159. R.M.Barrer, J.A.Barrie and M. G. Rogers. — J.Polymer Sci. A1 2565 (1963)

160. Ref. 6, p.372.

161. I. Bowman — Ph.D.Thesis, Loughborough University (1967).

162. J. Hilderbrand & R.Scott — "The solubility of non-electrolytes" Reinhold N.Y. 3rd Edn. (1949).

163. F. Bueche — "Physical properties of polymers" Interscience p.110 (1962).